

### Comments from Referee #1

Interactive comment on "Direct or indirect recharge on groundwater in the middle-latitude desert of Otindag, China?" by Bing-Qi Zhu and Xiao-Zong Ren, Anonymous Referee #1, Received and published: 22 May 2018.

The manuscript describes interesting results about the recharge mechanisms of arid zones in China, especially considering the importance of the topic. Despite the multidisciplinary approach, which is very useful in groundwater recharge studies, there are many weak points which have to be improved for a publication in HESS. The main points are listed below: 1) The datasets belong to sampling campaigns carried out in different moments (years) and seasons and for this reason in my opinion cannot be discussed together, without a clear distinction between the different phases. 2) A reconstruction of the piezometric morphology as well as a stratigraphy of the considered study areas should be reported. This could help also the discussion of the groundwater preferential pathways. 3) The organization of the paper is still at a draft level, since there is not a clear distinction between the results and discussion paragraphs. Many paragraphs need to be summarized and better explained. 4) The number of figures should be reduced (probably putting together some and deleting others). 5) The English is very poor and there are many typo errors. The reported delta notation is wrong. Due to the consideration of these main points the manuscript can be accepted only if major revision will be reported.

Interactive comment on Hydrol. Earth Syst. Sci. Discuss., <https://doi.org/10.5194/hess-2018-71>, 2018.

### The authors' responses to the comments from Referee #1

Dear Dr/Professor Referee #1:

On behalf of my co-authors, we thank you very much for giving us an opportunity to revise our manuscript. We appreciate you very much for your positive and constructive comments and suggestions on our manuscript (hess-2018-71). We have studied your comments carefully and have made revision which marked in red in the revised manuscript. We tried our best to revise our manuscript according to the comments point by point. Attached please find the revised version, which we would like to submit for your kind consideration. Thank you and best regards.

1) The datasets belong to sampling campaigns carried out in different moments (years) and seasons and for this reason in my opinion cannot be discussed together, without a clear distinction between the different phases.

Our response: AGREE AND NO CHANGES MADE.

Firstly, we thank you very much for this comment from you and we truly agree this point that water samples collected in different moments (years) and seasons cannot be discussed together without a clear distinction between the different water phases. In fact, although we stated in the manuscript that our fieldwork had taken place during the summer season of 2011 and the spring season of 2012, we collected the natural water samples at the same time for the same phases in the study area. For example, (1) all the groundwater samples discussed in this paper were collected during the 2011 summer in five days in the Otindag Desert. For other natural water samples discussed in this study, the detailed sampling methods are as follow: (2) all the spring water samples and (3) the precipitation water sample (p1) discussed in this paper were also collected during the 2011 summer in five days in the study area, and (4) all the river water samples and (5) lake water samples were collected during the spring season of 2012 in three days in the study area. This is to say that the water samples within the same phase are discussed together in the paper.

2) A reconstruction of the piezometric morphology as well as a stratigraphy of the considered study areas should be reported. This could help also the discussion of the groundwater preferential pathways.

Our response: AGREE AND CHANGES MADE.

We thank you very much for this comment. And yes, according to this comment, we revised the

manuscript and focused on reporting the geological (tectonic, lithological, sedimentological and structural), geomorphological, hydrogeological and stratigraphical settings of the study area. Please see the section 2 "Regional setting" of the revised manuscript in its pages 2-4 lines 103-188.

3) The organization of the paper is still at a draft level, since there is not a clear distinction between the results and discussion paragraphs. Many paragraphs need to be summarized and better explained.

**Our response: AGREE AND CHANGES MADE.**

We thank the you very much for this comment. And yes, we have revised the manuscript accordingly. The structure and content of the paper has been thoroughly reorganized in the revised manuscript, especially for the results and discussion sections, to make the content and context of the paper being more logic, coherent and readable. And yes, almost all of the paragraphs in the paper are newly summarized and explained. The detailed changes can be easily observed in the revised manuscript by reading one of the two resubmitted MS-Word files with the "changes marked" version (in contrast, another version is "clear copy").

4) The number of figures should be reduced (probably putting together some and deleting others).

**Our response: AGREE AND CHANGES MADE.**

We thank you very much for this comment. And yes, we have revised the manuscript accordingly. We reduced the number of figures in the revised manuscript by putting some figures together and deleting several figures. At last the revised manuscript has 11 figures compared with the original manuscript that including 15 figures. For example, the Figs. 5, 11, 13, 14a in the original manuscript are deleted in the revised manuscript, and the Figs. 7 and 8, the Figs. 10, 12 and 14a are combined, respectively. In addition, two newly-built figures are added into the revised manuscript according to the second comment from you (the detailed content of this comment can be seen above). The specific changes and the final results of these figures can be seen in the newly submitted revised manuscript.

5) The English is very poor and there are many typo errors. The reported delta notation is wrong.

**Our response: AGREE AND CHANGES MADE.**

We thank you very much for this comment. We are very sorry for our poor and incorrect English writing in the original manuscript. For the shortcomings of the English presentation and the grammatical edit in the first paper, we have checked and revised the whole manuscript carefully to avoid language errors, and finally we have got the help of a native English speaking professional to check and improve the English quality of the revised manuscript. We believe that the language is now acceptable for the publishing purpose.

In addition, the wrong use of the dalta notation in the original manuscript, such as  $\delta^2H$ , has been corrected as " $\delta D$ " in the revised manuscript.

6) Due to the consideration of these main points the manuscript can be accepted only if major revision will be reported.

**Our response: AGREE AND CHANGES MADE.**

Special thanks to you for your good comments. We have tried our best to improve the manuscript and made specific changes in the revised manuscript according to the comments from you one by one. These changes will not influence the content and framework of the paper. And here we did not list the changes but marked in red in the revised paper. We hope that the correction will meet with approval. Once again, thank you very much for your comments and suggestions.

1 **Direct or indirect recharge on groundwater in the  
2 middle-latitude desert of Otindag, China?**

3 Bing-Qi Zhu<sup>1\*</sup>, Xiao-Zong Ren<sup>2</sup>, Patrick Rioual<sup>3</sup>

4 <sup>1</sup>KLWCRESP, IGSNRR, CAS, Beijing, China

5 <sup>2</sup>SGS, TYNU, Jinzhong, China

6 <sup>3</sup>KLCGE, IGGCAS, Beijing, China

7 *Correspondence to:* Bing-Qi Zhu ([zhubingqi@sina.com](mailto:zhubingqi@sina.com))

8 **Abstract.** The Otindag Desert is essential to livestock-economy and ecoenvironment of northern China.  
9 Although surface water is the traditional source for China's socio-economy in arid areas, the  
10 groundwater resources underlying the desert are increasingly burdened by groundwater pumping,  
11 which increases interest in the status of the groundwater resources. Widespread fresh groundwater deep  
12 to 60 m was found at the eastern part of the Otindag Desert. The occurrence of this massive fresh  
13 groundwater raises doubts on the often-made assumption in the literature that regional atmospheric  
14 precipitation or palaeowater, namely the direct recharge, is the source of water in the middle-latitude  
15 desert aquifers of northern China and makes further investigation necessary. Knowledge on the origin  
16 and recharge of this fresh groundwater is key in assessing the possibility of groundwater exploitation  
17 and utilization. In this study we conducted hydrogeochemical and isotopical analyses to assess possible  
18 origin and recharge of these groundwaters. It is concluded that the fresh groundwater can neither  
19 originate from regional atmospheric precipitation derived from the Asian Summer Monsoon system,  
20 nor from palaeowater that formed during the last glacial period. Our results indicate that with  
21 groundwater dating it is possible to originate from remote mountain areas via the faults of the Solonker  
22 Suture zone, including the Daxing'Anlin and Yinshan Mountains. Furthermore, it is deduced that the  
23 hydrological connection between desert aquifers and mountain systems through the suturezone is  
24 crucial to the hydrogeological functioning of the Otindag aquifer. This suggests that the modern indirect  
25 recharge mechanism, instead of the direct recharge and the palaeo-water recharge, is the most  
26 significant for groundwater recharge in the Otindag Desert. This study provides a new perspective into  
27 the origin and evolution of groundwater resources in the middle-latitude desert zone of Asian continent.

28

29 **Keywords:** fresh groundwater recharge; atmospheric precipitation; direct recharge; indirect recharge;  
30 palaeowater recharge; fault hydrology; middle-latitude desert; Otindag Desert.

31

32 **1. Introduction**

33 In a semi-arid to arid region where rainfall is insufficient to supply the needs of a growing  
34 population and a higher standard of living, the deficit is normally made up by extracting groundwater.  
35 Many areas in the middle-latitude desert zone of northern China such as the Badanjilin Desert, the Mu  
36 US sandy Land and the Hobq Desert (Chen et al., 2012a; Chen et al., 2012b), are unexpectedly rich

37 with large groundwater resources although they have been under arid or hyper-arid climate for a long  
38 time (Sun et al., 2010). How these groundwaters originated and how they are recharged in these deserts  
39 are thus fundamental scientific questions. Until now, however, no consensus has been achieved in  
40 academic circles.

41 The Otindag Desert is one of the largest sandy lands located at the monsoon margin of northern  
42 China and is the geographical centre of the northeastern Asian Continent (Fig. 1), which can be  
43 regarded as a significant repository of information relating to the groundwater recharge in the arid  
44 Inner Asia. At present, the eastern Otindag is also a typical case for its unexpected groundwater  
45 resources, because there is abundant groundwater in this desert land and even rivers originate there due  
46 to the spillover of spring water, such as the tributaries of Xilamulun River in its north and the Shandian  
47 River in its south (Fig. 1). Climatically, the monsoon margin of northern China refers to a strip along  
48 the present East Asian Summer Monsoon (EASM) limits and is considered to be sensitive to climate  
49 change (Wang and Feng, 2013). Geologically, the Otindag Desert lies in a tectonic depression of the  
50 central Solonker suture zone with a few faults stretching east and west (Fig. 2), with its northern  
51 margin along a fault marked by a series of lake basins. Thus, the large-scale hydrogeological conditions  
52 of the Otindag Desert belong to a fault zone under the influence of the EASM climate.

53 Until now, however, whether the climate or other factors affected the groundwater recharge in the  
54 Otindag are still not known. Little data about the groundwater and its origin is available in the literature,  
55 and knowledge and reliable data on various hydrogeological characteristics of the desert such as the  
56 catchment extent, input/output, the hysteretic hydraulic functions, the transient hydraulic conditions,  
57 in-homogeneities, and on transfer functions to overcome scale problems are also missing. Under such  
58 conditions, conventional methods such as water balance and hydraulic methods sometimes fail in  
59 determining groundwater recharge, particularly in extreme environments (arid, semi-arid, or cold)  
60 (Drever, 1997). Because pristine aquatic conditions may significantly differ from managed conditions  
61 in arid environment, and thus groundwater recharge is not a fixed number, but may vary with the  
62 boundary conditions of the recharge system (Seiler and Gat, 2007).

63 Groundwater recharge can be broadly classified into two categories: the direct recharge by native  
64 water resources and the indirect recharge by external water resources (Herczeg and Leaney, 2011).  
65 Water infiltration of atmospheric precipitation through the unsaturated zone to the groundwater is  
66 hydrologically defined as the direct recharge, and the indirect recharge is defined as recharge from  
67 mappable features such as rivers, canals, lakes and originates from remote areas (Scanlon et al., 2006;  
68 Healy, 2010). It is well known that groundwater recharge can be influenced by environmental factors,  
69 including climate change, underlying soil and geology, land cover and the growth in human population  
70 that affects withdrawal and economic development (Zhu et al., 2015, 2017). Among these  
71 environmental factors, climate and land cover largely determine precipitation and evapotranspiration,  
72 whereas the underlying soil and geology dictate whether a water surplus (precipitation minus  
73 evapotranspiration) can be transmitted and stored in the subsurface (Doll, 2008, 2009; Giordano, 2009).

74 For some earth scientists, the direct recharge is thought to be very important for groundwaters in  
75 the wide desert lands of north China due to the lack of surface runoffs (Yang et al., 2010; Yang and  
76 Williams, 2003; Zhao et al., 2017). They argued that although the amount of atmospheric precipitation

77 is small, the vast catchment area in the desert region could concentrate the rainfall into large inland  
78 basins, creating an aquifer with large storage capacity and great thickness. However, some hydrologists  
79 estimated by the chloride mass balance method that the direct recharge was 1.4 mm/year, which  
80 represents approximately only 1.7% of the mean annual precipitation in a cold large desert (Badanjilin)  
81 in northern China (Gates et al., 2008). A similar estimation of 1 mm/year was given for Gobi deserts  
82 from the Hexi Corridor to the Inner Mongolia Plateau in northwestern China (Ma et al., 2008).  
83 Consequently, they thought that heavy potential evaporation and little precipitation make it difficult for  
84 direct recharge to meet the supply of groundwater in these desert areas. Thus, the indirect recharge is  
85 considered to be an important mechanism for groundwater recharge in these desert areas. For example,  
86 Zhao et al. (2012) suggested that little precipitation had recharged into groundwaters in the Badain  
87 Jaran Desert. Chen et al. (2004) argued that the groundwaters in the Badanjilin Desert were recharged  
88 by palaeo-glacial melt water through faults and deep carbonate layers far away from the local desert.  
89 Many studies also suggested that palaeowaters stored in an aquifer during wetter climate periods could  
90 recharge to groundwater under certain conditions in arid lands (Edmunds et al., 2006; Ma and Edmunds,  
91 2006). Other kinds of indirect recharge, such as mountain front recharge from adjacent mountain  
92 blocks, are also proposed to offer an important inflow to aquifers within arid to semiarid catchments  
93 (Blasch and Bryson, 2007).

94 In this paper, we focus to answer the question that whether groundwater recharge in Otindag is  
95 mainly direct or indirect, using hydrochemical and isotopic indicators as tracers to offer a valuable  
96 support for identifying the contributions of precipitation recharge on groundwater, since these  
97 indicators reflect the composition of water molecules and are sensitive to physical processes such as  
98 mixing and evaporation (Sultan et al., 2000; Guendouz et al., 2003; Petrides et al., 2006; Scanlon et al.,  
99 2006; Zhu et al., 2007, 2008; Jobbágé et al., 2011). The detailed objectives are: (1) to recognize the  
100 major sources of groundwater in the area, and (2) to identify the key mechanism of groundwater  
101 recharge in the desert.

102

## 103 **2. Regional settings**

104 Geographic setting. The Otindag Desert lies between latitudes 42° and 44°N and longitudes 112°  
105 and 118° E (Fig. 1). It forms a part of the great middle-latitude desert belt in northern China which  
106 stretches from the Taklamakan Desert of northwestern China to the Kelqin Desert of northeastern  
107 China, near the west coast of the Pacific Ocean. The desert has an area of approximately 21,400 square  
108 kilometers located in the eastern Inner Mongolia and at the monsoon margin of northern China (Fig. 1).  
109 It is the fourth largest sandy lands in China (Yang et al., 2012) and is bordered by a flat steppe terrain  
110 of Dali Basin to the north, the Yinshan Mountains and mountainous loess landscape to the south, and  
111 the the Greater Khingan (Daxing'Anling) Mountains to the east (Fig. 1). The Otindag Desert is  
112 essential to livestock-economy and ecoenvironment of northern China. Settlements in this desert are  
113 restricted to areas to permanent springs, shallow groundwater and oases to areas where irrigation is  
114 possible. Some nomads continue to eke out a precarious existence grazing livestock in the desert.

115 Topography and geomorphology. The Otindag Desert has a varied relief, combining extensive  
116 dune fields with rugged mountains along the eastern, southern and southeastern rims. In the east, the

117 Daxing'Anling Mountains stretch from the Heilong River Valley into the upper reach valleys of the  
118 Xilumulun River from northeast to southwest, gradually increasing in height northwards from about  
119 180 m near Huma to Huanggangliang, where the highest peaks reach 2,029 m with an average  
120 elevation range from 1,100 to 1,400 m. In the south and southeast, the Yinshan Mountains decline  
121 gradually near Duolun and Zhenglanqi, and in some areas leave wide alluvial plains. The terrain of the  
122 Otindag Desert is less rough and elevations decrease from ca. 1300 m in the southeast to ca. 1000 m in  
123 the northwest. Over the greater part of this desert the ground cover consists of fixed and semi-fixed  
124 sandy dunes, with a few mobile dunes in area of little vegetation. The dominated dune types are  
125 represented from parabolic to barchans, linear and grid-formed types, ranging from a few meters to  
126 over 40 m in height (Zhu et al., 1980; Yang et al., 2008).

127 Climate, vegetation and soil. The climate of the Otindag Desert was not uniform in geological  
128 period, with much sand movement, occasional rainy years, and several wetter intervals during the  
129 Holocene (Yang et al., 2015; Tian et al., 2017). At present the whole desert belongs to the arid and  
130 semi-arid temperate zone, with a meanannual temperature of 2 °C in the north and 4°Cin the south (Liu  
131 and Yang, 2013). At the regional scale, the climate of the desert is typically controlled by the East  
132 Asian Monsoon system, characterized by a warm summer, with precipitation transported by the EASM,  
133 and by a cold and dry winter under the influence of the East Asian Winter Monsoon (EAWM). The  
134 rainfall in the desert exhibits a wide variation in space and time. Influence of the EASM changes from  
135 southeast to northwest in the desert, and varies with latitude and distance from the Pacific Ocean,  
136 leading to the mean annual rainfall decreasing from ~450 mm in the southeast to ~150 mm in the  
137 northwest (Yang et al., 2013). This uneven distribution of precipitation has a major influence on the  
138 availability of near-surface moisture, consequently on the distribution of vegetation, soil and the animal  
139 husbandry potential of local communities. The basic soil cover consists of grey desert soil in the west  
140 and changes to sierozems and chernozem or chestnut soil in the east. Through the desert, vegetation is  
141 sparse in the west and relatively abundant in the east. The natural vegetation is characteristic of desert  
142 or semi-deserts, with scrub woodland in the east and steppe in the west. Due to the scarcity of surface  
143 water, the growing season is affected by temperature, rainfall and elevation, and hence cultivation is  
144 restricted mainly to flood plains.

145 Geology. The Otindag Desert is located in a tectonic depression of the Solonker Suture Zone (Jian  
146 et al., 2010) bounded by the Northern Early to Mid-Paleozoic Orogen Zone and the Hatug Uul Block to  
147 the north, the Southern Early to Mid-Paleozoic Orogen Zone and the North China Craton system to the  
148 south (Fig. 2). A few faults such as the Xar Moron Fault and Chifeng-Bayan Obo Fault stretch east and  
149 west, with its northern margin along the Solonker Suture Zone marked by a series of lake basins (Figs.  
150 1 and 2). The tectonostratigraphic units and overall structural trends are mainly oriented NE–SW (Fig.  
151 2), which may be interpreted as resulting from overall compressive stresses oriented principally in the  
152 NW–SE quadrants during orogenesis (Jian et al., 2010; Zhang et al., 2015). Diverse rock types from  
153 unlithified and lithified clastic sediments through to carbonate, crystalline, and volcanic rocks are  
154 distributed in and around the Otindag Desert (Zhang et al., 2015) (Figs. 2 and 3). Tertiary and  
155 Quaternary sandstones and mudstones are the common basement rocks under the dunes of the Otindag,  
156 and extensive volcanic basalts forming flat terrains are to the north (Zhu et al., 1980; Li et al., 1995).

157 Hydrology and hydrogeology. The Otindag Desert originated during the Late Quaternary (Yang  
158 et al., 2015) and various alluvial fans formed at the margins of this desert during the early to middle  
159 Holocene. These are composed of conglomerate and sand deposits, where major periodic steams or  
160 wadis debouched into the Otindag. At present two rivers run through the eastern margin of the Otindag  
161 Desert, i.e. the Xilamulun River in the north and the Shandian River and its two tributaries, the Shepi  
162 River and Tuligen River in the south. Both stem from the eastern and southeastern parts of the Otindag  
163 (Fig. 1). The Xilamulun River, 380 km in length and  $32.54 \times 10^3 \text{ km}^2$  in area, is a neighboring river both  
164 to the northeastern Otindag and the southeastern Dali Basin, the northern catchment of the Otindag  
165 Desert. The Xilamulun River flows to the east and finally goes into the Xiliao River, with an annual  
166 mean runoff of  $6.58 \times 10^8 \text{ m}^3$  (Wu et al., 2014). The Shandian River is the upper reach of the Luan  
167 River, with a length of 254 km and a catchment area of  $4.11 \times 10^3 \text{ km}^2$  (Yao et al., 2013). Along the low,  
168 flat and sandy shorelines of some lakes in the Otindag, salt flats or sabkhas have formed in shallow  
169 depressions. Due to the high rate of evaporation, salt crusts develop which have been locally exploited  
170 where the salt is relatively free from sand. During rainy season, some rain and floodwaters (generally  
171 coming from the Yinshan piedmonts) are retained in low-lying areas, which may temporarily recharge  
172 shallow aquifers. Under storm conditions, occasional heavy, short rainstorms cause floods in soil-rich  
173 wadi channels. Under other conditions, sand dunes and sand sheets bury the ground and sabkhas.

174 The Otindag Desert can depend on several water-bearing formations and units (aquifers) for their  
175 groundwater resources (Fig. 3). Coarse- to fine-grained sedimentary rocks, magmatic rocks and  
176 metamorphic rocks of the Inner Mongolia-Daxing'Anling Orogenic Belt (Zhang et al., 2015) form the  
177 major regional aquifer unit (Fig. 3). They are composed mainly of alluvial sediments (mid-Permian  
178 Zhesi Formation), melange (Solonker suture zone), A-type granite (early Permian), bimodal volcanic  
179 rocks with sedimentary intercalations (early Permian Dashizhai Formation), diorite-quartz  
180 diorite-granodiorite rocks (Carboniferous-Permian) and metamorphic complex (predominantly gneiss,  
181 early Paleozoic) (Fig. 2). The aquifer is generally unconfined in dune fields of the Otindag Desert,  
182 unconfined to semi-confined in the Yinshan Mountains' piedmont, and semi-confined to confined in the  
183 Daxing'Anling uplands (Fig. 3). Water-level measurement in June 2010 indicated that the general depth  
184 of unconfined groundwater level ranges between 10 to 70 m in the Otindag Desert (Fig. 3). Local  
185 granular aquifers in the central desert are composed of coarse fluvial, lacustrine and aeolian sediments,  
186 but their extent and thickness vary throughout the watershed (Zhu et al., 1980; Li et al., 1995). The  
187 generally coarse-grained texture of the unconsolidated rock formations provides primary porosity in  
188 terms of groundwater flow in the desert.

189

### 190 **3.Methods**

191 The hydrochemistry of natural water in the Otindag Desert, as related to the prevailing EASM  
192 climate, as well as, the dominant topographical, geological (tectonic) and hydrogeological conditions,  
193 are discussed here and interpreted, using chemical and isotope analyses of water samples from rain,  
194 springs, shallow aquifers and deep aquifers, rivers and lakes, and are represented on relevant graphs  
195 and diagrams. Fieldworks took place during the summer season of 2011 and the spring season of 2012.  
196 Water samples were mainly retrieved from shallow and deep wells located over a wide area in dune

197 fields of the study regions. The detailed locations of the sampling sites are shown in Fig. 4.

198 Two groups of parameters are measured to characterize the chemistry of any water analysis:  
199 field-measured parameters and lab-measured parameters. The filed-measured parameters include  
200 temperature (°C), hydrogen-ion concentration (pH), electrical conductivity (EC in micro-Siemens per  
201 centimeter or  $\mu\text{S}/\text{cm}$ ) and total dissolved solid (TDS, mg/L). The values of these parameters change  
202 when they are not directly measured in the field. The number lab-measured parameters depend on the  
203 purpose of study. However, the measurement of major cations ( $\text{F}^-$ ,  $\text{Cl}^-$ ,  $\text{NO}_2^-$ ,  $\text{NO}_3^-$ ,  $\text{SO}_4^{2-}\text{HCO}_3^-$ ,  
204  $\text{CO}_3^{2-}$  and  $\text{H}_2\text{PO}_4^-$ ) and anions ( $\text{Li}^+$ ,  $\text{Na}^+$ ,  $\text{NH}_4^+$ ,  $\text{K}^+$ ,  $\text{Mg}^{2+}$  and  $\text{Ca}^{2+}$ ) are determined in most chemical  
205 analyses. Analysis for stable ( $^2\text{H}$  and  $^{18}\text{O}$ ) and radioactive isotopes ( $^3\text{H}$ ) in rain and groundwater are  
206 also included. The analytical data of the physiochemical parameters and the stable and radioactive  
207 isotopes of the water samples collected in this study are listed in Tables 1, 2 and 3, respectively.

208

#### 209 **4. Results and Discussions**

210

##### 211 **4.1. Hydrochemical characteristics of natural waters**

212 The natural water samples collected in this study are generally neutral to slightly alkaline, with the  
213 pH values varying between 6.26 and 9.44 (except the precipitation sample p1, 4.61) (Table 1) and a  
214 median value of 7.27. The TDS values range between 67 and 660 mg/L (average 211 mg/L) (Table 1),  
215 all belonging to fresh water (TDS < 1000 mg/L) in the salination classification of natural water  
216 (Meybeck, 2004). The variations in ion concentrations of the major cations and anions in the studied  
217 water samples were displayed in a fingerprint diagram with a semi-logarithm y-axis (Fig. 5). The rain  
218 water sample is the most depleted in ions among these samples. The groundwater samples have the  
219 highest concentrations of cations and anions and the lake, river and spring waters had intermediate  
220 values. The calcium concentration is the highest among cations in almost all of the water samples, and  
221 the  $\text{HCO}_3^-+\text{CO}_3^-$  concentration (bicarbonate + carbonate, alkalinity) is the highest among anions in most  
222 of the water samples. For several groundwater samples (g3, g4, g5, g6 and g11), spring sample (s1) and  
223 precipitation sample (p1), they have higher  $\text{SO}_4^{2-}$  concentrations than alkalinity (Fig. 5).

224 Two chemically distinct water types are recognized for the studied waters via a Piper diagram (Fig.  
225 6), calcium bicarbonate and calcium sulphate. No Chloride-type and sodium-type waters occur in the  
226 study area (Fig. 6). Based on more than 10,000 chemical analyses of groundwater samples from the  
227 world, Chebotarev (1955) observed that the global groundwater tends to evolve chemically towards the  
228 composition of seawater. He also observed that this evolution is associated with regional changes in  
229 dominant anions but not cations, as the concentration of cations may exhibit a wide range of  
230 fluctuations in groundwater and is not as steady as the changes in anion dominance. Freeze and Cherry  
231 (1979) illustrated the Chebotarev's (1955) general evolution of groundwater as a anion evolution line:  
232  $\text{HCO}_3^- \rightarrow \text{HCO}_3^- + \text{SO}_4^{2-} \rightarrow \text{SO}_4^{2-} + \text{HCO}_3^- \rightarrow \text{SO}_4^{2-} + \text{Cl}^- \rightarrow \text{Cl}^- + \text{SO}_4^{2-} \rightarrow \text{Cl}^-$ , which travels  
233 along the flow paths and increasing ages. On this evolution line, bicarbonate water is generally  
234 characteristic of low salinity, renewable water resources and low residence time, while sulphate waters  
235 predominate in groundwater passing through gypsum and anhydrite aquifers, and is usually associated  
236 with intermediate salinity in unconfined aquifers (Clark, 2015). The distribution pattern of water

237 chemical types occurred in the studied area indicates a primary stage of groundwater evolution in the  
238 Otindag Desert.

239 The  $\delta D$  values of the groundwater samples collected in this study varied from -63.42‰ to -75.92‰  
240 (Table 3), with an average -69.53‰. The  $\delta^{18}\text{O}$  values ranged between -8.64‰ and -11.26‰ (Table 3),  
241 with an average -10.17‰. The spring water samples were relatively concentrated in  $\delta D$  and  $\delta^{18}\text{O}$  and  
242 were greatly similar to those of the groundwater samples (Fig. 7). The  $\delta D$  and  $\delta^{18}\text{O}$  values in the river  
243 water samples were slightly more variable and were also similar to those of the groundwater (Fig. 7).  
244 The lake water samples were enriched in  $\delta D$  and  $\delta^{18}\text{O}$  by comparison to the groundwater samples (Fig.  
245 6). The precipitation sample p1 was also enriched in  $\delta D$  and  $\delta^{18}\text{O}$  by comparison to the groundwater  
246 samples (Fig. 7). The content of radioactive isotope of tritium ( $^3\text{H}$ ) measured in seven well  
247 groundwater samples with 6-60 m depth ranged from 1.86 to 24.35 TU (Table 3), with an average  
248 14.95 TU, higher than the mean tritium concentration (9.8 TU) of groundwater in the Vienna Basin,  
249 Austria (Stolp et al., 2010), the seat of the International Atomic Energy Agency (IAEA).

250 If we plot the relationships between oxygen and hydrogen isotopes of groundwater, spring, river  
251 and lake water samples, we observed that the regression line that fits all data points can be described by  
252 the equation:  $\delta D = 4.09\delta^{18}\text{O} - 28.31$  ( $R^2=0.93$ ,  $n=24$ ) (EL1 in Fig. 7). This local groundwater line  
253 (LGWL) is different from the Global Meteoric Water Line (GMWL,  $\delta D = 8\delta^{18}\text{O} + 10$ ) and the  
254 Mediterranean Meteoric Water Line (MMWL,  $\delta D = 8\delta^{18}\text{O} + 20$ ) estimated by Craig (1961), but it is  
255 similar to the local groundwater lines established for other deserts in northern China and central Asia  
256 with a same slope but different Y-intercepts, such as  $\delta D = 4.17\delta^{18}\text{O} - 31.3$  for the Badanjilin Desert (Jin  
257 et al., 2018),  $\delta D = 4.8\delta^{18}\text{O} - 15.2$  for the Ejina Desert in China (Wang et al., 2013), and  $\delta D = 4.26\delta^{18}\text{O}$   
258 + 9.23 for the Rub Al Khal Desert in the United Arab Emirates (Rizk and El-Etr, 1997). The scatter of  
259 stable isotope data points for the lake water samples (Fig. 7) in the Otindag suggests that the lake  
260 waters are affected by evaporation, but the other waters in the desert are not so.

261

#### 262 **4.2. Local precipitation recharge on groundwater in the Otindag**

263 To incorporate the isotopic analysis of precipitation with similar areas in the studied area, local  
264 data (p1) was plotted with those of Baotou (Fig. 7). The isotopic composition of rainfall in Baotou, the  
265 nearest long-term station to the Otindag Desert, was monitored for the period 1986-2001 within the  
266 scope of the International Atomic Energy Agency/World Meteorological Organization (IAEA/WMO)  
267 global survey. The stable isotope data available from this station was used to provide basic  
268 characteristics of the stable isotopic composition of the present-day meteoric water, especially in the  
269 westward inland areas of the Otindag Desert (Fig. 1). Stable isotope data of the Tianjin station was also  
270 used to characterize precipitation of the eastern coastal areas of the Otindag Desert (Fig. 1).

271 Based on the isotopic data from the Baotou station, the local meteoric water lines can be  
272 statistically expressed as the isotopic regression equation of  $\delta D = 6.36\delta^{18}\text{O} - 5.21$  (LMWL-B). It can  
273 also be expressed as  $\delta D = 6.57\delta^{18}\text{O} + 0.31$  (LWML-T), based on the data from the Tianjin station (Fig.  
274 7). The precipitation sample p1 collected in this study fell onto the GMWL (Fig. 7). It also showed  
275 similar  $\delta D$  and  $\delta^{18}\text{O}$  values to those of the precipitation collected in the GNIP stations of Baotou and  
276 Tianjin (Fig. 7).

277       Compared to the precipitation data from the GNIP stations and from the local precipitation (p1),  
278       the groundwater, spring, and river water samples were evidently depleted in heavy stable isotopes in  
279       the Otindag (Fig. 7). Except for the lake water samples, most of the groundwater, river water and  
280       spring water samples in the Otindag fall on or lay between the LMWL-B and the LMWL-T lines, and  
281       are located at the lower left area of the precipitation points (Fig. 7).

282       Because the isotopic evolution of  $\delta D$  and  $\delta^{18}O$  in water illustrated in the Craig line represents a  
283       one-way and irreversible process, the water bodies distributed at the upper right area of the Craig line  
284       can not be recharge sources for the water bodies distributed at the lower left area of the line. Such  
285       results indicate that the groundwater, river water and spring water in the Otindag are not recharged by  
286       the regional precipitation, namely no significant modern direct recharge has taken place for  
287       groundwater in the Otindag.

288       Dogramaci et al. (2012) documented that only intense and remarkable rainfall events  $>20$  mm  
289       could recharge groundwater in the semi-arid Hamersley Basin of northwest Australia, while the rainfall  
290       events  $<20$  mm had limited influences on groundwater recharge. Chen et al. (2014) described that  
291       rainfall events  $\leq 5$  mm in the arid and semi-arid region of northern China would be evaporated into  
292       the atmosphere rapidly before it is infiltrated into the groundwater system. Based on the analysis on the  
293       data records from two meteorological stations around the Otindag, i.e. the Duolun and Xilinhaote  
294       stations (see Fig. 1a), we observed that rainfall events  $>20$  mm on average only occur 2.5-3.4 times per  
295       year (Table 4). In some years (e.g. from 2005 to 2007 at the Xilinhaote Station), no rainfall events  $>20$   
296       mm even occurred. It further indicated the limited contribution of regional precipitation on  
297       groundwater recharge in the Otindag.

298       In addition to groundwater, the river and spring water samples from the Otindag also deviated  
299       from the local precipitation in the Craig diagram (Fig. 7). These water samples came from the  
300       Xilamulun, Shepi and Tuligen rivers. They shared the same evaporation line (EL1) with the  
301       groundwater and lake water samples (Fig. 7). Generally speaking, natural waters that have a same  
302       recharge source are distributed on a same line of evaporation in the  $\delta^2$  and  $\delta^{18}O$  diagram (Chen et al.,  
303       2012b). This indicates that the recharge sources of groundwater, river water, spring water and lake  
304       water in the Otindag are genetically associated each other and differ from the local precipitation.

### 306       **4.3. Winter precipitation and palaeowater recharge on groundwater in the Otindag**

307       Since the groundwater samples in the Otindag are depleted in their  $\delta D$  and  $\delta^{18}O$  values even more  
308       than those of the local rainfall (Fig. 7), they must be sourced from other waters characterized by similar  
309       or more depleted signals in their stable isotopes compositions. Due to the temperature effect (such as  
310       evaporation) on isotopic fractionation, only the waters issued from colder environments can be more  
311       depleted in their  $\delta D$  and  $\delta^{18}O$  values even more than those of the local rainfall.

312       Because the Otindag Desert is under the control of the EASM climate (Fig. 1), the local rainfall in  
313       the desert is mainly sourced from summer precipitation. This can also be illustrated by the seasonal  
314       distributions in annual mean precipitation (Fig. 8a), in annual mean air temperature (Fig. 8b) and in  
315       annual mean water vapor pressure (Fig. 8c) over the last forty years at the two surrounding GNIP  
316       weather stations in Baotou and Tianjin. The seasonal distributions of stable isotopes in the two stations

317 (Fig. 8d-e) show that the summer rainfall is evidently positive in its signals of  $\delta D$  and  $\delta^{18}O$  by  
318 comparison with those of the winter rainfall, further suggesting that the waters issued from cold  
319 environments can be more depleted in their  $\delta D$  and  $\delta^{18}O$  values than those of the summer rainfall. Thus  
320 we speculate that groundwater in the Otindag can be potentially derived from (1) modern precipitation  
321 in winter, (2) palaeowater formed in the past glacial period, or (3) remote/mountains waters that  
322 emanate in colder and wetter conditions.

323 The annual mean values of  $\delta D$  and  $\delta^{18}O$  over the last forty years are more depleted in winter  
324 precipitation than in summer precipitation at the Baotou and Tianjin stations (Fig. 8d-e). This isotopic  
325 signal qualifies the regional winter precipitation to be a potential source of groundwaters in the Otindag.  
326 However, the precipitation amounts and the water vapor pressures (effective moisture) in winter  
327 months are much lower than those in the summer months at both the Baotou and Tianjin stations (Fig.  
328 8a and 8c). It indicates that the winter seasons in these regions are relatively colder and drier but not  
329 colder and wetter. A colder-wetter winter season is a necessary condition for winter precipitation to be a  
330 water source for the formation of groundwater under a summer monsoon climate. This is because the  
331 bigger amounts of summer precipitation will easily remove or weaken the depleted isotopic signals of  
332 winter precipitation in groundwater. In this regard, modern winter precipitation is unlikely to be an  
333 important source of groundwater in the Otindag.

334 As to the palaeowaters formed in colder and wetter periods such as the last glacial, it has been  
335 proposed to be a potential water source for groundwaters in the wide arid lands of the world. The  
336 depleted signals of stable isotopes ( $\delta D$  and  $\delta^{18}O$ ) in groundwater have been recognized in global arid  
337 and semi-arid regions, such as the Sinai Desert in Egypt (Gat and Issar, 1974), Israel (Gat, 1983), South  
338 Australia (Love et al., 1994, 2000), northern China (Ma et al., 2010), Saudi Arabia (Bazuhair and Wood,  
339 1996) and North Africa (Guendouz et al., 2003). These signals are very often explained as  
340 palaeo-groundwater that recharged by precipitation during past wetter and colder periods (Love et al.,  
341 1994, 2000; Herczeg and Leaney, 2011).

342 Here we use the tritium data as a environmental tracer to estimate the groundwater age in the  
343 Otindag. The tritium data at the GNIP stations of the Baotou and Tianjin are also referenced as the  
344 background values in precipitation of recent years. The residence time of groundwater in aquifer and  
345 the residual tritium of a water body can be calculated by  $N = N_0 e^{-\lambda t}$  (Yang and Williams, 2003). Where  
346  $N$  = content of residual tritium in water sample,  $\lambda = 0.0565$ , the radioactive decay constant,  $N_0$  =  
347 content of tritium at the time of rainfall and  $t$  = years after precipitation. Based on this equation, the  
348 residual tritium was theoretically calculated and the standard for tritium dating was established for  
349 seven groundwater samples in the Otindag Desert (Table 3). As a result, ages of 0-60 years were  
350 obtained for these groundwater samples (Table 5). This indicates that recent recharge took place several  
351 decades after the peak in global nuclear tests. We thus conclude that groundwater is generally not older  
352 than 70 years in the study area. It means that groundwater in the Otindag are not palaeowater  
353 recharged.

354 Both the modern summer and winter precipitation recharge and the palaeowater recharge can be  
355 refuted, indicating that direct recharge is not a major mechanism controlling the groundwater recharge  
356 in the Otindag.

357

358 **4. 4. Remote water recharge on groundwater in the Otindag: Dali Basin**

359 The third hypothesis that “remote/mountains waters emanate under colder and wetter conditions”  
360 is further considered here. In essence, it is an indirect recharge mechanismas as water originates from  
361 remote areas (Healy, 2010; Herczeg and Leaney, 2011).

362 It is worth noting that the values of deuterium and oxygen-18 for groundwater in the north part of  
363 the study area are more depleted in  $\delta\text{D}$  and  $\delta^{18}\text{O}$  than those in the south part (Table 3). It suggests that  
364 the Otindag groundwater might be potentially recharged by water resouces coming from the northern  
365 neighboring catchment, such as the Dali Basin.

366 Recently published data of  $\delta\text{D}$  and  $\delta^{18}\text{O}$  in groundwater, lake water, river water and spring water  
367 sampled from the Dali Basin (e.g., Chen et al., 2008; Zhen et al., 2014) were compiled in this study and  
368 were co-analyzed with the data from the Otindag. About 70 natural water samples from the Dali and  
369 Otindag with  $\delta\text{D}$  and  $\delta^{18}\text{O}$  values are shown in a Craig diagram (Fig. 9). All of these samples fell on or  
370 lied near the evaporation line EL2 in the Craig diragram (Fig. 9), with a regression equation of  $\delta\text{D} =$   
371  $4.81\delta^{18}\text{O} - 21.55$  and a high correlation coefficient ( $R^2=0.98$ ,  $n=70$ ). Compared to the groundwater  
372 samples in the Otindag, water samples from the groundwaters, rivers and springs from the Dali Basin  
373 are more depleted in  $\delta^{18}\text{O}$  and  $\delta\text{D}$  (Fig. 9). Such results further indicate that, in terms of itsisotopic  
374 signature, the groundwater in the Otindag has a close relationship with the natural waters in the Dali  
375 Basin.

376 The similar signals of  $\delta\text{D}$  and  $\delta^{18}\text{O}$  between the groundwater in the Otindag and the river water in  
377 the Dali (Fig. 9) point towards the idea that the groundwater in the Otindag might be sourced from the  
378 river water in the Dali Basin, since the Dali has more depleted isotopic signals in water than the  
379 Otindag (Fig. 9). Considering the topographical gradient of elevations between the two regions,  
380 however, river water in the Dali Basin cannot flow into the eastern Otindag, because the terrain  
381 elevation of the Dali Basin is lower than that of the Otindag (Fig. 1). This is also the reason why the  
382 huge Dali Lake that lies in the Dali Basin has no equivalent in the Otindag (Fig. 1). If there is a  
383 hydraulic linkage between the two regions, water should flow from the Otindag into the the Dali, but  
384 not conversely.

385 In view of the hydraulic gradient, river water in the Dali Basin could not be a recharge source for  
386 groundwater in the Otindag. However, in view of the isotopic gradients, groundwater in the Otindag  
387 could not conversely be the source of river water in the Dali (Fig. 9). Thus, the similar isotopic signals  
388 between the river water in Dali and the groundwater in Otindag indicate that these waters might be  
389 recharged from a common source.

390 Similar isotopic signals also occurred in the groundwaters between the Otindag and the Dali Basin  
391 (Fig. 9). In order to understand the linkage of groundwaters between the two regions, the potential  
392 movement of groundwater in the transition zone of the two regions need to be known. In this study, a  
393 groundwater-sampling project was designed in the field along a N-S section of a palaeo-channel  
394 located at the transition zone between the Dali and Otindag (Figs. 1, 2). The channel was named  
395 “PCSX” in this study, with its north part named “NPCSX” and the south part named “SPCSX”.

396 The GPS elevation of the northernmost sampling site in the NPCSX (g11, about 1317 m a.s.l.) was

397 much lower than that of the southernmost site in the SPCSX (g1, 1396 m.a.s.l.) (Fig. 2 and Table 1).  
398 Regarding to the topographical gradient in the channel, there is a drop of about 80 m between the  
399 NPCSX and the SPCSX. Under such slope, the underground hydraulic gradient for groundwater flow  
400 can be roughly parallel with that of the surface water flow, namely that the groundwaterflow should  
401 move downwards from the SPCSX area into the NPCSX area. Thus we can speculate that groundwater  
402 in the NPCSX would have higher salinity than those in the SPCSX under such flowing direction. In  
403 order to verify this speculation, actual variations of water salinity (chloride and TDS) were detected  
404 along the PCSX section. The sampling site g1 was defined as the initial point and the distances between  
405 g1 and other sampling sites along the PCSX section were calculated, based on their GPS geographical  
406 coordinates measured in the field. The results are shown in Fig. 10a-b. It is clear that the variations of  
407 chloride and TDS concentrations in groundwater do not increase along the palaeo-channel from south  
408 to north (Fig. 10a-b). On the contrary, both the values of chloride and TDS are lower in the NPCSX  
409 area than those in the SPCSX area. Such kind of spatial variations in the chloride and TDS values  
410 contradict the speculated patterns abovementioned, suggesting that the hydraulic gradient of  
411 groundwater flowing path in this region is not controlled by the topographical gradient between the  
412 NPCSX and SPCSX areas.

413 Compared between the NPCSX and SPCSX regions, the stable isotopic values ( $\delta^{18}\text{O}$  and  $\delta\text{D}$ ) of  
414 groundwaters in the SPCSX region vary greatly with a large amplitude, while those in the NPCSX are  
415 relatively constant (Fig. 10c-d). The constant variations indicate that the recharge source of  
416 groundwater in the NPCSX is relatively unitary. The isotopic values in the SPCSX are much lighter  
417 than those in the NPCSX along the distance section from south to north (Fig. 10c-d). The heaviest  
418 values occurred in the sample g11 collected from the NPCSX (Fig. 10c-d), indicating a water being  
419 earlier recharged. The spring water sample s2, a representation of discharge water, is characterized by  
420 medium values of  $\delta\text{D}$  and  $\delta^{18}\text{O}$ . These results indicate that the groundwaters in the SPCSX area, with  
421 relatively enriched isotopic signals in  $\delta\text{D}$  and  $\delta^{18}\text{O}$  by comparison with those in the NPCSX area, are  
422 composed of a mixture of the groundwaters in the NPCSX with other waters.

423 The tritium contents were broadly and positively related to the values of deuterium excess in the  
424 groundwater samples in the PCSX (Fig. 10e). For water that experiences an evaporation process, the  
425 d-excess value will increase in the evaporated water vapor, but will decrease in the residual water body  
426 (Dansgaard, 1964; Merlivat and Jouzel, 1979). In this study, except for sample g11 (a sample very  
427 close to the riverhead area), the positive relationship between the tritium and the deuterium excess  
428 generally shows that the d-excess values are higher in the groundwaters collected from the NPCSX, but  
429 are lower in those from the SPCSX (Fig. 10e). This distribution pattern indicates that the groundwaters  
430 in the NPCSX are relatively younger and experienced a lower degree of evaporation than those in the  
431 SPCSX. The d-excess gradient, increasing from south to north in the PCSX, further suggests that  
432 groundwater does not flow from the SPCSX area to the NPCSX area, namely out of the topographical  
433 control.

434 Many studies (e.g., Boronina et al., 2005; Kazemi et al., 2006) have demonstrated that  
435 groundwater flows in the direction in which it gets older. In view of this point, groundwaters in the  
436 PCSX region should flow from the NPCSX area to the SPCSX area, in opposition to the S-N

437 topographical gradient between the Otindag and Dali regions. Thus groundwater in the Dali are not the  
438 source of groundwater in the Otindag. The similar isotopic signals between groundwaters in the two  
439 regions indicate that these waters might be recharged from a common source in other place.

440

#### 441 **4. 5. Remote water recharge on groundwater in the Otindag: mountains waters**

442 The discussions above revealed that both the groundwaters in the Otindag and Dali Basin might be  
443 recharged from a common source derived from another place. Considering the third hypothesis  
444 abovementioned that “remote/mountains waters emanate under colder and wetter conditions”, we  
445 propose that this “common source” of the two regions are from mountain areas surrounding the  
446 Otindag and Dali Basin.

447 There are two large permanent rivers and lots of small intermittent streams entering the Dali Basin  
448 (Xiao et al., 2008), including the Xilamulun River to the south and the Gongger River to the north, both  
449 of which are stemming from the Greater Khingan Mountains (Daxing’Anling Mountains in Chinese  
450 pinyin, 1,100-1,400 m above seal level) (Fig. 1). The Xilamulun River carries a large amount of water  
451 (about  $6.58 \times 10^8 \text{ m}^3/\text{y}$ ) from the Daxing’Anling Mountains flowing through the east margins of the Dali  
452 and Otindag (Wu et al., 2014). This is an important clue linking natural waters between the Otindag  
453 and Dali Basin.

454 Variation in the elevation from the Dali Lake to the riverhead of the Xilamulun River can be  
455 clearly found along a land surface topographical section (Fig. 11). The channel of the Xilamulun River  
456 is located in the Xar Moron Fault (Fig. 1), which is a part of the Solonker Suture Zone (Eizenhöfer et  
457 al., 2014) or the Xilamulun-Changchun-Yanji plate suture zone (Sun et al., 2004) in the regional  
458 tectonical settings (Fig. 2). Outcrop observations indicate that fault zones commonly have a  
459 permeability structure suggesting they should act as complex conduit-barrier systems in which  
460 along-fault flow is encouraged and across-fault flow is impeded (Bense et al., 2013). Thus the  
461 hydraulic gradient of groundwater flow in the Eastern margins of the Otindag and Dali Basin must be  
462 controlled by the fault zone hydrogeology. This may be the reason why the hydraulic gradient of  
463 groundwater represented by the isotopic and hydrogeochemical gradients of groundwater samples in  
464 this study is not consistent with the local topographical gradient in the Otindag Desert. On the other  
465 hand, the regional aquifer is generally unconfined in dune fields of the Otindag Desert but  
466 semi-confined to confined in the Daxing’Anling uplands (Fig. 3), thus the thick unconsolidated  
467 aquifers in the study area (Figs. 3 and 11) will be favourable conditions for groundwater storage and  
468 transportation along the Solonker Suture Zone. When rivers stem from the Daxing’Anling  
469 Mountains and flow downward to the marginal areas of the Dali and Otindag, leakage water from these  
470 rivers can recharge the desert land through thick unconsolidated aquifers. A strong isotopic evidence is  
471 that the lake and river waters in the Dali Basin share the same evaporation line (EL2) with the  
472 groundwaters in the PCSX area.

473 Although groundwaters in the SPCSX area are different from those in the NPCSX area, their  
474 isotopic data points still fell onto the EL2 (Fig. 9), which further indicates that the groundwaters in the  
475 SPCSX are a mixture of waters from the Daxing’Anling Mountain and other sources. Another source  
476 for groundwater recharge in the SPCSX could be represented by remote water such as flash floods

477 coming from the north Yinshan Mountains, because it can be clearly observed from digital maps that  
478 many transient rivers or streams originated from the Yinshan Mountains flow into the south and  
479 southeastern Otindag (Fig. 1). Supportive evidence for this idea can also be observed in the summer  
480 rainy season. During rainy days or under storm conditions, occasional heavy, short rainstorms cause  
481 floods in soil-rich wadi channels and low-lying depressions in the unconfined to semi-confined areas of  
482 the Yinshan Mountains' piedmont. These waters may temporarily recharge shallow aquifers in the  
483 SPCSX area.

484

## 485 **5. Conclusions**

486 In the middle-latitude desert zone of northern China, many deserts such as the Otindag and  
487 Badanjilin Deserts, are unexpectedly rich in groundwater resources, although they have no surface  
488 runoff and have been under an arid or hyper-arid climate for a long period of time. How groundwaters  
489 originated and recharged in these deserts are thus key questions that are still under debate. For some  
490 earth scientists, the direct recharge is thought to be very important for groundwaters in the wide desert  
491 lands of northern China, due to the lack of surface runoffs. However, groundwater availability is very  
492 much a function of the local- and regional-scale geological and climatic settings. To achieve an  
493 integrated understanding of the groundwater recharge and its controlling mechanisms is of great  
494 significance. In this study, groundwater recharge was explored using multiple environmental tracers in  
495 the Otindag Desert of northern China, a region that is under the influence of the East Asian Summer  
496 Monsoon (EASM) climate. Compared to modern summer precipitation, the groundwaters, river waters  
497 and spring waters are depleted in  $\delta D$  and  $\delta^{18}O$ . All these waters shared a same Craig line, indicating a  
498 genetic relationship on their recharge sources. The stable isotopic signals of the groundwaters is more  
499 depleted than those of the modern summer precipitation and this suggests that the groundwaters studied  
500 could only be sourced from cold water different from the EASM precipitation. In general, the analyses  
501 revealed that the highland remote water resources from the Daxing'anling and Yinshan Mountains  
502 were isotopically and geochemically traced to be a major source for the groundwater in the Otindag. It  
503 suggests that the modern indirect recharge mechanism, instead of the direct recharge and the  
504 palaeo-water recharge, is the most significant for groundwater recharge in the eastern Otindag. This  
505 study provides a new perspective into the origin and evolution of groundwater resources in the  
506 middle-latitude desert zone of northern China.

507

## 508 **Acknowledgements**

509 This study was financially supported by the National Natural Science Foundation of China  
510 (41771014 and 41602196) and the National Key Research and Development Program of China  
511 (2016YFA0601900). We thank the China Meteorological Data Sharing Service system for providing  
512 the weather data. Sincere thanks are also extended to Profs. Xiaoping Yang, Xunming Wang, Jule Xiao  
513 and other workmates, e.g., Ziting Liu, Hongwei Li, and Deguo Zhang for their generous help in the  
514 research work.

515

## 516 **References:**

- 517 Bazuhair, A.S., and Wood, W.W.: Chloride mass-balance method for estimating ground water recharge  
518 in arid areas: examples from western Saudi Arabia. *Journal of Hydorlogy*, 186, 153-159, 1996.
- 519 Bense, V.F., Gleeson, T., Loveless, S.E., Bour, O., and Scibek, J.: Fault zone hydrogeology.  
520 *Earth-Science Reviews*, 127, 171-192, 2013.
- 521 Blasch, K.W., and Bryson, J.R.: Distinguishing sources of ground water recharge by using  $\delta^{2\text{H}}$  and  
522  $\delta^{18\text{O}}$ . *Ground Water*, 45, 294-308, 2007.
- 523 Boronina, A., Renard, P., Balderer, W., and Stichler, W.: Application of tritium in precipitation and in  
524 groundwater of the Kouris catchment (Cyprus) for description of the regional groundwater flow.  
525 *Applied Geochemistry*, 20, 1292-1308, 2005.
- 526 Chebotarev, I.I.: Metamorphism of natural waters in the crust of weathering. *Geochimica et &*  
527 *Cosmochimica Acta*, 8, 22-32, 1955.
- 528 Chen, F., Chen, J., Holmes, J., Boomer, I., Austin, P., Gates, J.B., Wang, N., Brooks, S.J., and Zhang, J.:  
529 Moisture changes over the last millennium in arid central Asia: a review, synthesis and  
530 comparison with monsoon region. *Quaternary Science Reviews*, 29, 1055-1068, 2010.
- 531 Chen, J., Chen, X., and Wang, T.: Isotopes tracer research of wet sand layer water sources in Alxa  
532 Desert. *Advances in Water Science*, 25, 196-206, 2014 (in Chinese).
- 533 Chen, J., Li, L., Wang, J., Barry, D.A., Sheng, X., Gu, W., Zhao, X., and Chen, L.: Water resources:  
534 groundwater maintains dune landscape. *Nature*, 432, 459-460, 2004.
- 535 Chen, J., Liu, X., Wang, C., Rao, W., Tan, H., Dong, H., Sun, X., Wang, Y., and Su, Z.: Isotopic  
536 constraints on the origin of groundwater in the Ordos Basin of northern China. *Environmental*  
537 *Earth Sciences*, 66, 505-517, 2012a.
- 538 Chen, J., Sun, X., Gu, W., Tan, H., Rao, W., Dong, H., Liu, X., and Su, Z.: Isotopic and hydrochemical  
539 data to restrict the origin of the groundwater in the Badain Jaran Desert, Northern China.  
540 *Geochemistry International* 50, 455-465, 2012b.
- 541 Chen, J., Yang, Q., and Hao, G.: Using hydrochemical and environmental isotopical data to analyse  
542 groundwater recharge in the Hunshandake Sandy Land. *Inner Mongolia Science Technology &*  
543 *Economy*, 17, 9-12, 2008 (in Chinese).
- 544 Clark, I.D.: *Groundwater Geochemistry and Isotopes*. CRC Press, Boca Raton, 2015.
- 545 Craig, H.: Isotopic Variations in Meteoric Waters. *Science*, 133, 1702-1703, 1961.
- 546 Dansgaard, W.: Stable isotopes in precipitation. *Tellus*, 16, 436-468, 1964.
- 547 Dogramaci, S., Skrzypek, G., Dodson, W., and Grierson, P.F.: Stable isotope and hydrochemical  
548 evolution of groundwater in the semi-arid Hamersley Basin of subtropical northwest Australia.  
549 *Journal of hydrology*, 475, 281-293, 2012.
- 550 Doll, P., and Fiedler, K.: Global-scale modeling of groundwater recharge. *Hydrology and Earth System*  
551 *Sciences*, 12, 863-885, 2008.
- 552 Doll, P.: Vulnerability to the impact of climate change on renewable groundwater resources: a  
553 global-scale assessment. *Environmental Research Letters*, 4, 035006,  
554 doi:10.1088/1748-9326/4/3/035006, 2009.
- 555 Drever, J.I.: Catchment mass balance. In: Saether, O.M., and de Caritat, P. (Eds.), *Geochemical*  
556 *Processes, Weathering and Groundwater Recharge in Catchments*. A.A, Balkema, Rotterdam, pp.

- 557 241-261, 1997.
- 558 Edmunds, W.M., Ma, J., Aeschbach-Hertig, W., Kipfer, R., and Darbyshire, D.P.F.: Groundwater  
559 recharge history and hydrogeochemical evolution in the Minqin Basin, North West China. *Applied  
560 Geochemistry*, 21, 2148-2170, 2006.
- 561 Eizenhöfer, P.R., Zhao, G., Zhang, J., and Sun, M.: Final closure of the Paleo-Asian Ocean along the  
562 Solonker Suture Zone: Constraints from geochronological and geochemical data of Permian  
563 volcanic and sedimentary rocks. *Tectonics*, 33, 441-463, 2014.
- 564 Freeze, R.A., and Cherry, J.A.: *Groundwater*. Prentice-Hall, Inc, New Jersey, 1979.
- 565 Gat, J.R.: Precipitation, groundwater and surface waters: control of climate parameters on their isotopic  
566 composition and their utilization as palaeoclimatological tools. In: *Palaeoclimates and  
567 palaeowaters: a collection of environmental isotope studies*. Proc. Adv. Gp. Meeting, Vienna,  
568 25–28 Nov 1980, pp 3–12, IAEA, Vienna, 1983.
- 569 Gat, J.R., and Issar, A.: Desert isotope hydrology: water sources of the Sinai Desert. *Geochimica et &  
570 Cosmochimica Acta*, 38, 1117-1131, 1974.
- 571 Gates, J., Edmunds, W.M., Ma, J., and Scanlon, B.: Estimating groundwater recharge in a cold desert  
572 environment in northern China using chloride. *Hydrogeology Journal*, 16, 893-910, 2008.
- 573 Giordano, M.: Global groundwater? Issues and solutions. *Annual Review of Environment and  
574 Resources*, 34, 153-178, 2009.
- 575 Guendouz, A., Moulla, A.S., Edmunds, W.M., Zouari, K., Shand, P., and Mamou, A.:  
576 Hydrogeochemical and isotopic evolution of water in the Complexe Terminal aquifer in the  
577 Algerian Sahara. *Hydrogeology Journal*, 11, 483-495, 2003.
- 578 Healy, R.W.: *Estimating groundwater recharge*. Cambridge University Press, New York, 2010.
- 579 Herczeg, A.L., and Leaney, F.: Review: environmental tracers in arid-zone hydrology. *Hydrogeology  
580 Journal*, 19, 17-29, 2011.
- 581 Jahn, B.M.: The Central Asian Orogenic Belt and growth of the continental crust in the Phanerozoic.  
582 Geological Society London Special Publications, 226, 73-100, 2004.
- 583 Jian, P., Liu, D., Kroner, A., Windley, B.F., Shi, Y., Zhang, W., Zhang, F., Miao, L., Zhang, L., and  
584 Tomurhuu, D.: Evolution of a Permian intraoceanic arc-trench system in the Solonker suture zone,  
585 Central Asian Orogenic Belt, China and Mongolia. *Lithos*, 118, 169-190, 2010.
- 586 Jin, K., Rao, W., Tan, H., Song, Y., Yong, B., Zheng, Y., Chen, T., and Han, L.: H-O isotopic and  
587 chemical characteristics of a precipitation-lake water-groundwater system in a desert area. *Journal  
588 of Hydrology*, 559, 848-860, 2018.
- 589 Jobbágy, E., Nusetto, M., Villagra, P., and Jackson, R.: Water subsidies from mountains to deserts: their  
590 role in sustaining groundwater-fed oases in a sandy landscape. *Ecological Applications*, 21,  
591 678-694, 2011.
- 592 Kazemi, G.A., Lehr, J.H., and Perrochet, P.: *Groundwater age*. John Wiley & Sons, Hoboken, 2006.
- 593 Li, J.: Permian geodynamic settings of Northeast China and adjacent regions: closure of the Paleo-Asian  
594 Ocean and subduction of the Paleo-Pacific Plate. *Journal of Asian Earth Sciences*, 26, 207-224.
- 595 Li, S., Sun, W., Li, X., and Zhang, B.: Sedimentary characteristics and environmental evolution of  
596 Otindag sandy land in Holocene. *Journal of Desert Research*, 15, 323-331, 1995 (in Chinese).

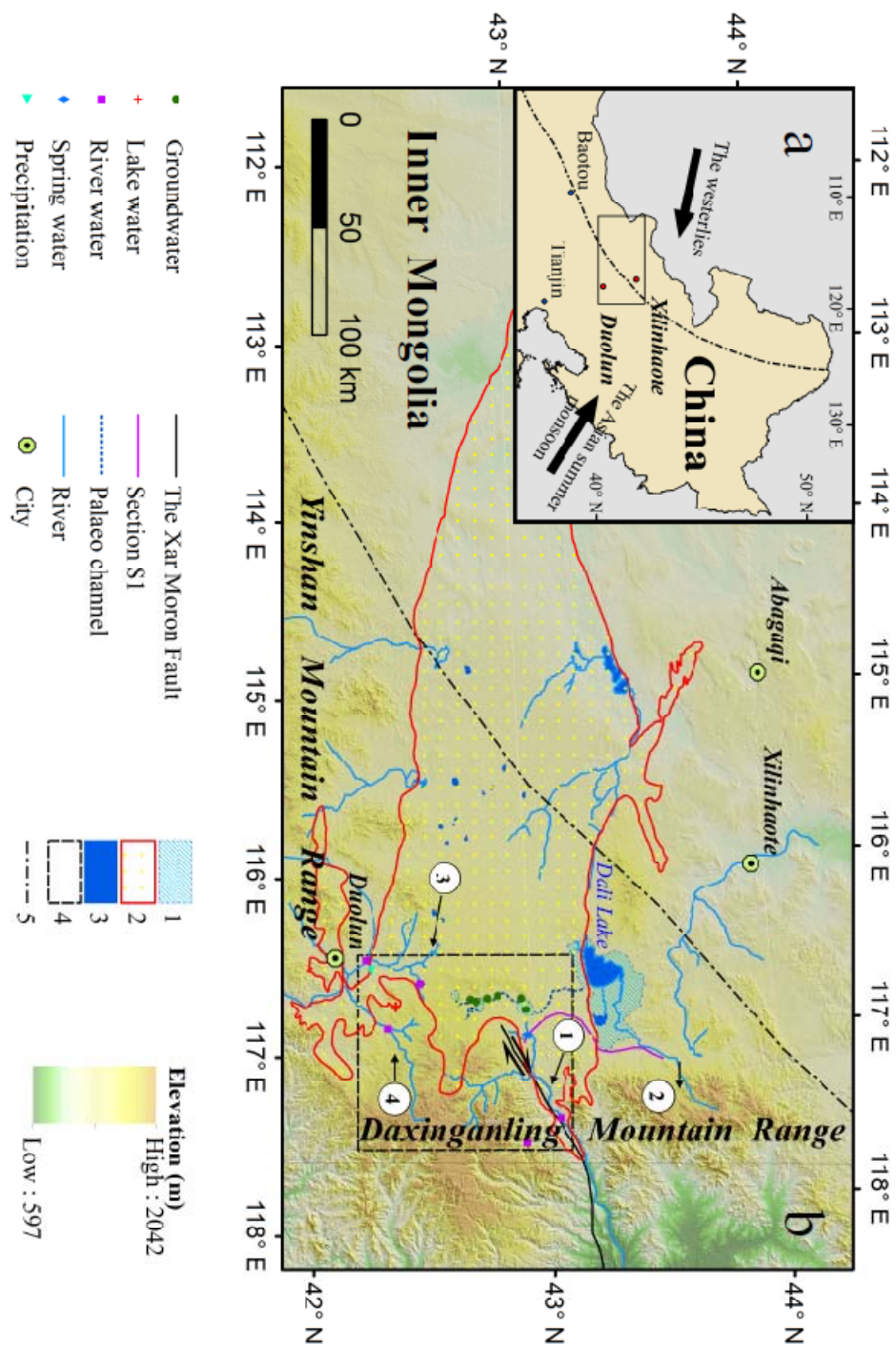
- 597 Liu, Z., and Yang, X.: Geochemical-geomorphological evidence for the provenance of aeolian sands  
598 and sedimentary environments in the Hunshandake Sandy Land, eastern Inner Mongolia, China.  
599 *Acta Geologica Sinica* (English Edition), 87, 871-884, 2013.
- 600 Love, A.J., Herczeg, A.L., Leaney, F.W., Stadter, M.H., Dighton, J.C., and Armstrong, D.: Groundwater  
601 residence time and palaeohydrology in the Otway Basin, South Australia. *Journal of Hydrology*,  
602 153, 157-187, 1994.
- 603 Love, A.J., Herczeg, A.L., Sampson, L., Cresswell, R.G., and Fifield, L.K.: Sources of chloride and  
604 implications for  $^{36}\text{Cl}$  dating of old groundwater, south-western Great Artesian basin, Australia.  
605 *Water Resources Research*, 36(6), 1561-1574, 2000.
- 606 Ma, J., Ding, Z., Gates, J.B., and Su, Y.: Chloride and the environmental isotopes as the indicators of  
607 the groundwater recharge in the Gobi Desert, northwest China. *Environmental Geology*, 55,  
608 1407-1419, 2008.
- 609 Ma, J., and Edmunds, W.M.: Groundwater and lake evolution in the BadainJaran Desert ecosystem,  
610 Inner Mongolia. *Hydrogeology Journal*, 14, 1231-1243, 2006.
- 611 Ma, J., Pan, F., Chen, L., Edmunds, W.M., Ding, Z., He, J., Zhou, K., and Huang, T.: Isotopic and  
612 geochemical evidence of recharge sources and water quality in the Quaternary aquifer beneath  
613 Jinchang city, NW China. *Applied Geochemistry*, 25, 996-1007, 2010.
- 614 Merlivat, L., and Jouzel, J.: Global climatic interpretation of the deuterium-oxygen 18 relationship for  
615 precipitation. *Journal of Geophysical Research*, 84, 5029-5033, 1979.
- 616 Meybeck, M.: Global occurrence of major elements in rivers. In: Drever, J.I. (Ed.), *Surface and Ground*  
617 *Water, Weathering, and Soils*. Holland, H.D., and Turekian, K.K. (Exec. Eds), *Treatise on*  
618 *Geochemistry*, vol. 5. Elsevier-Pergamon, Oxford, pp. 207-223, 2004.
- 619 Petrides, B., Cartwright, I., and Weaver, T.R.: The evolution of groundwater in the Tyrrell catchment,  
620 south-central Murray Basin, Victoria, Australia. *Hydrogeology Journal*, 14, 1522-1543, 2006.
- 621 Rizk, Z.S., and El-Etr, H.A.: Hydrogeology and hydrogeochemistry of some springs in the United Arab  
622 Emirates. *Arabian Journal for Science and Engineering*, 22, 95-111, 1997.
- 623 Scanlon, B.R., Keese, K.E., Flint, A.L., Flint, L.E., Gaye, C.B., Edmunds, W.M., and Simmers, I.:  
624 Global synthesis of groundwater recharge in semiarid and arid regions. *Hydrological Processes*, 20,  
625 3335-3370, 2006.
- 626 Seiler, K.P., and Gat, J.R.: *Groundwater Recharge From Run-Off, Infiltration and Percolation*. Springer,  
627 The Netherlands, 2007.
- 628 Stolp, B.J., Solomon, D.K., Suckow, A., Vitvar, T., Rank, D., Aggarwal, P.K., and Han, L.F.: Age dating  
629 base flow at springs and gaining streams using helium - 3 and tritium: Fischa - Dagnitz system,  
630 southern Vienna Basin, Austria. *Water Resources Research*, 46, W07503,  
631 doi:10.1029/2009WR008006, 2010.
- 632 Sultan, M., Sturchio, N., Gheith, H., Hady, Y.A., and Anbeawy, M.: Chemical and Isotopic Constraints  
633 on the Origin of Wadi EliTarfa Ground Water, Eastern Desert, Egypt. *Ground Water*, 38, 743-751,  
634 2000.
- 635 Sun, D., Wu, F., Zhang, Y., and Gao, S.: The final closing time of the west Lamulun  
636 River-Changchun-Yanji plate suture zone-Evidence from the Dayushan granitic pluton, Jilin

- 637 Province. *Journal of Jilin University (Earth Science Edition)*, 34, 174-181, 2004 (in Chinese).
- 638 Sun, J., Ye, J., Wu, W., Ni, X., Bi, S., Zhang, Z., Liu, W., and Meng, J.: Late Oligocene-Miocene  
639 mid-latitude aridification and wind patterns in the Asian interior. *Geology*, 38, 515–518, 2010.
- 640 Tian, F., Wang, Y., Liu, J., Tang, W., and Jiang, N.: Late Holocene climate change inferred from a  
641 lacustrine sedimentary sequence in southern Inner Mongolia, China. *Quaternary International*, 452,  
642 22-32, 2017.
- 643 Wang, P., Yu, J., Zhang, Y., and Liu, C.: Groundwater recharge and hydrogeochemical evolution in the  
644 Ejina Basin, northwest China. *Journal of Hydrology*, 476, 72-86, 2013.
- 645 Wang, Q., and Liu, X.Y.: Paleoplate tectonics between Cathaysia and Angaraland in Inner Mongolia of  
646 China. *Tectonics*, 5, 1073-1088, 1986.
- 647 Wang, W., and Feng, Z.D.: Holocene moisture evolution across the Mongolian Plateau and its  
648 surrounding areas: a synthesis of climatic records. *Earth-Science Reviews* 122, 38-57, 2013.
- 649 Wu, J., An, N., Ji, Y., and Wei, X.: Analysis on Characteristics of Precipitation and Runoff in Silas  
650 MuLun River Basin. *Meteorology Journal of Inner Mongolia*, 23-25, 2014 (in Chinese).
- 651 Xiao, J., Si, B., Zhai, D., Itoh, S., and Lomtadze, Z.: Hydrology of Dali Lake in central-eastern Inner  
652 Mongolia and Holocene East Asian monsoon variability. *Journal of Paleolimnology*, 40, 519-528,  
653 2008.
- 654 Yang, X., Li, H., and Conacher, A.: Large-scale controls on the development of sand seas in northern  
655 China. *Quaternary International*, 250, 74-83, 2012.
- 656 Yang, X., Ma, N., Dong, J., Zhu, B., Xu, B., Ma, Z., and Liu, J.: Recharge to the inter-dune lakes and  
657 Holocene climatic changes in the BadainJaran Desert, western China. *Quaternary Research*, 73,  
658 10-19, 2010.
- 659 Yang, X., Scuderi, L.A., Wang, X., Scuderi, L.J., Zhang, D., Li, H., Forman, S., Xu, Q., Wang, R.,  
660 Huang, W., and Yang, S.: Groundwater sapping as the cause of irreversible desertification of  
661 Hunshandake Sandy Lands, Inner Mongolia, northern China. *PNAS*, 112, 702-706, 2015.
- 662 Yang, X., Wang, X., Liu, Z., Li, H., Ren, X., Zhang, D., Ma, Z., Rioual, P., Jin, X., and Scuderi, L.:  
663 Initiation and variation of the dune fields in semi-arid China – with a special reference to the  
664 Hunshandake Sandy Land, Inner Mongolia. *Quaternary Science Reviews*, 78, 369-380, 2013.
- 665 Yang, X., and Williams, M.A.J.: The ion chemistry of lakes and late Holocene desiccation in the  
666 BadainJaran Desert, Inner Mongolia, China. *Catena*, 51, 45-60, 2003.
- 667 Yang, X., Zhu, B., Wang, X., Li, C., Zhou, Z., Chen, J., Yin, J., and Lu, Y.: Late Quaternary  
668 environmental changes and organic carbon density in the Hunshandake Sandy Land, eastern Inner  
669 Mongolia, China. *Global and Planetary Change*, 61, 70-78, 2008.
- 670 Yao, S., Zhu, Z., Zhang, S., Zhang, S., and Li, Y.: Using SWAT model to simulate the discharge of the  
671 river Shandianhe in Inner Mongolia. *Journal of Arid Land Resources and Environment*, 27,  
672 175-180, 2013 (in Chinese).
- 673 Zhang, Z., Li, K., Li, J., Tang, W., Chen, Y., and Luo, Z.: Geochronology and geochemistry of the  
674 Eastern Erenhot ophiolitic complex: implications for the tectonic evolution of the Inner  
675 Mongolia-Daxinganling Orogenic Belt. *Journal of Asian Earth Sciences*, 97, 279-293, 2015.
- 676 Zhao, J., Ma, Y., Luo, X., Yue, D., Shao, T., and Dong, Z.: The discovery of surface runoff in the

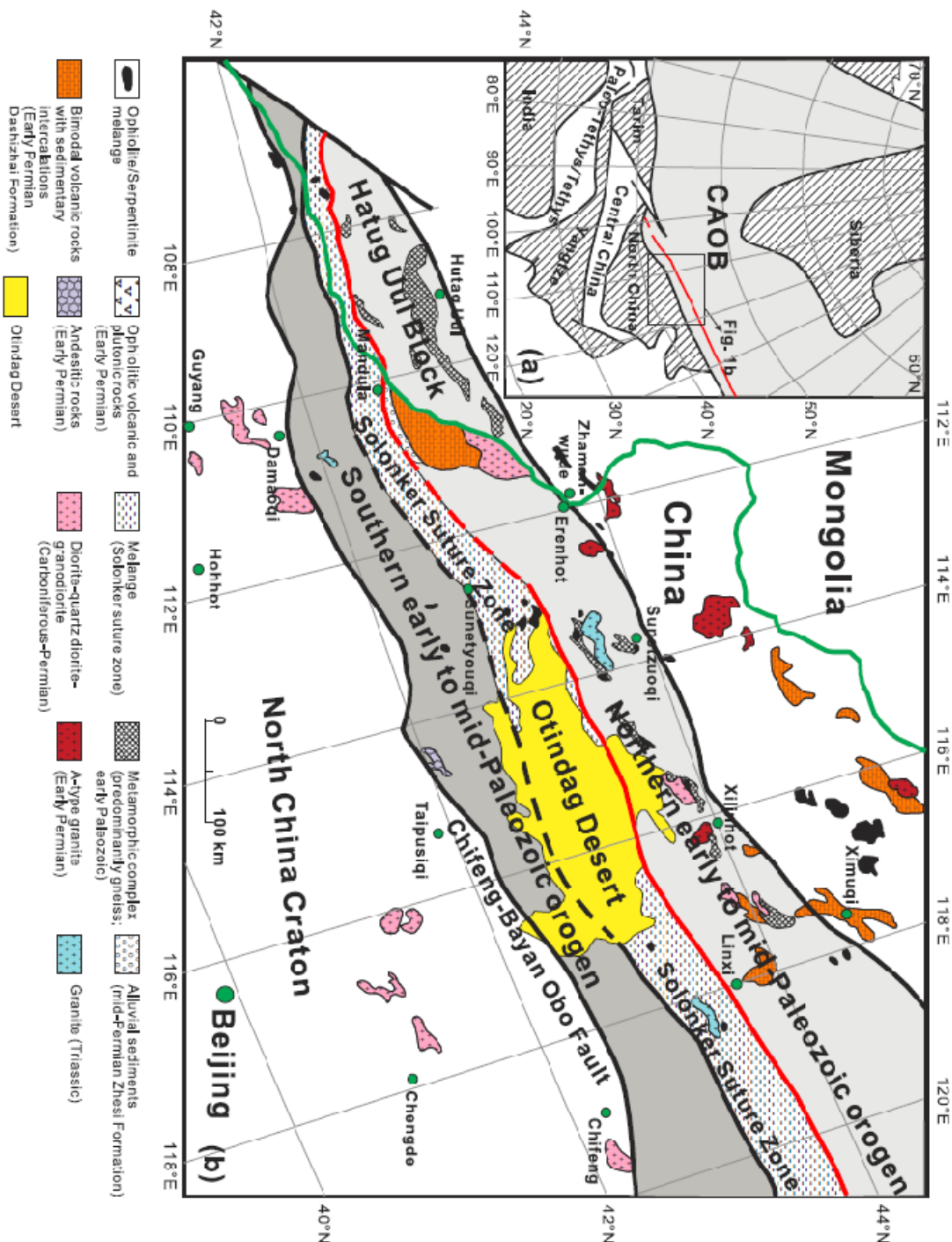
- 677        megadunes of BadainJaran Desert, China, and its significance. *Science China Earth Sciences*, 60,  
678        707-719, 2017.
- 679        Zhao, L., Xiao, H., Dong, Z., Xiao, S., Zhou, M., Cheng, G., Yin, L., and Yin, Z.: Origins of  
680        groundwater inferred from isotopic patterns of the Badain Jaran Desert, Northwestern China.  
681        *Ground Water*, 50, 715-725, 2012.
- 682        Zhen, Z., Li, C., Li, W., Hu, Q., Liu, X., Liu, Z., and Yu, R.: Characteristics of environmental isotopes  
683        of surface water and groundwater and their recharge relationships in Lake Dali basin. *Journal of*  
684        *Lake Sciences*, 26, 916-922, 2014 (in Chinese).
- 685        Zhu, B.Q., Yu, J.J., Rioual, P., Gao, Y., Zhang, Y.C., and Xiong, H.G.: Climate effects on recharge and  
686        evolution of natural water resources in middle-latitude watersheds under arid climate. In:  
687        Ramkumar, M. U., Kumaraswamy, K, and Mohanraj, R. (Eds.), *Environmental Management of*  
688        *River Basin Ecosystems*. Springer Earth System Sciences, Springer-Verlag, Heidelberg, pp.  
689        91-109, 2015.
- 690        Zhu, B.Q., Wang, X.M., and Rioual, P.: Multivariate indications between environment and ground  
691        water recharge in a sedimentary drainage basin in northwestern China. *Journal of Hydrology*, 2017,  
692        549, 92-113, 2017.
- 693        Zhu, G.F., Li, Z.Z., Su, Y.H., Ma, J.Z., and Zhang, Y.Y.: Hydrogeochemical and isotope evidence of  
694        groundwater evolution and recharge in Minqin Basin, Northwest China. *Journal of Hydrology*,  
695        333, 239-251, 2007.
- 696        Zhu, G.F., Su, Y.H., and Feng, Q.: The hydrochemical characteristics and evolution of groundwater and  
697        surface water in the Heihe River Basin, northwest China. *Hydrogeology Journal*, 16, 167-182,  
698        2008.
- 699        Zhu, Z., Wu, Z., Liu, S., and Di, X.: *An Outline of Chinese Deserts*. Science Press, Beijing, 1980 (in  
700        Chinese).
- 701
- 702

703  
704 **Figure Captions:**  
705

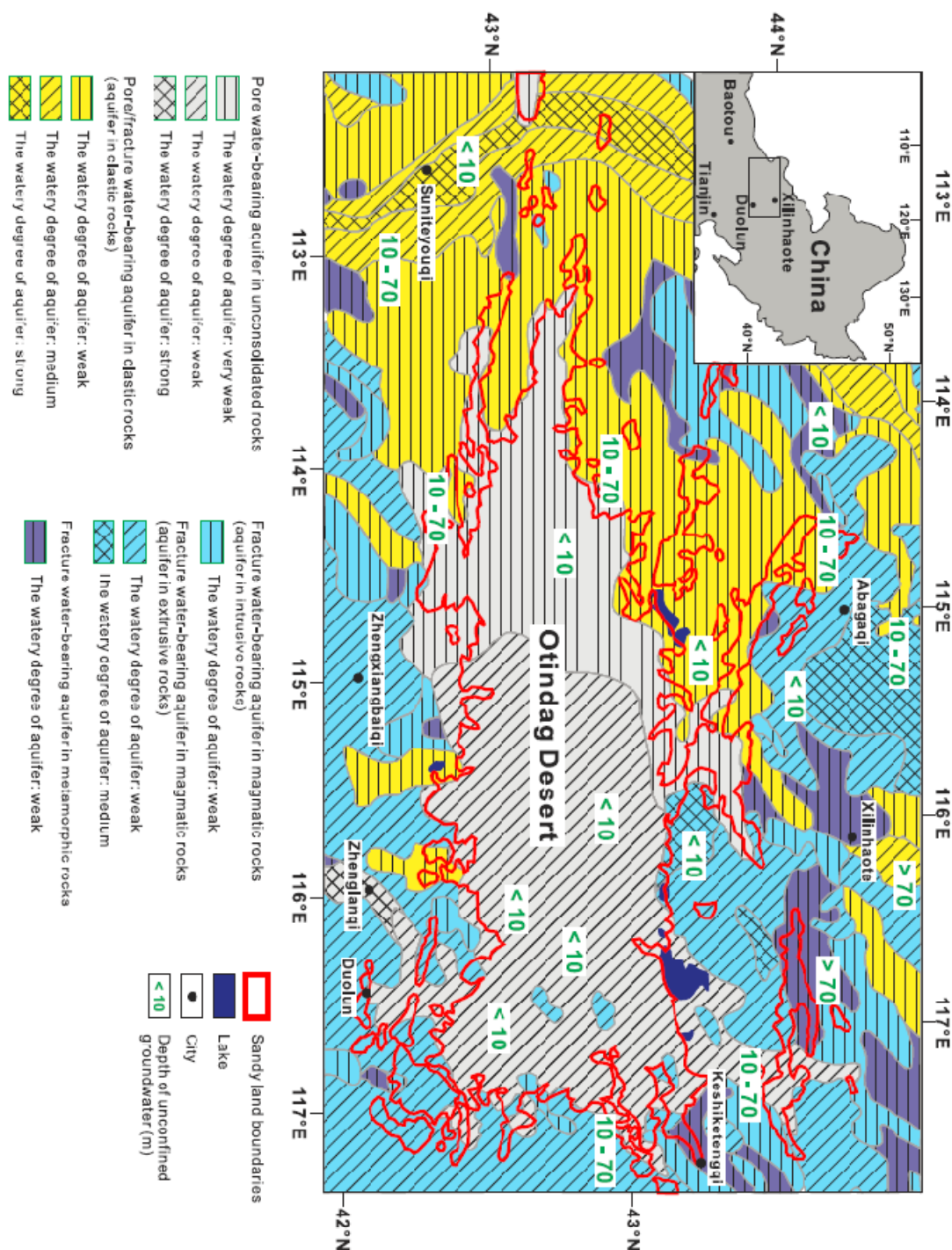
706 **Fig. 1.** The Geographical location of the Otindag Desert in northern China. (a) The study area shown at  
707 a large scale, and (b) the study area shown at a smaller scale, with detailed information about the  
708 boundary and tectonic settings of the desert land. 1, the palaeo lake area of the megalake Dali; 2, the  
709 boundary of the Otindag; 3, the modern lake area; 4, the boundary of Fig. 2; 5, the boundary between  
710 the westerlies and the East Asian Summer Monsoon (EASM) climate systems. ①, the Xilamulun River;  
711 ②, the Gonggeer River. ③, the Shepi River. ④, the Tuligen River. The boundary between the  
712 westerlies and the EASMin (a) and (b) is modified from Chen et al. (2010). The palaeo lake area of the  
713 megalake Dali and the palaeo channel in (b) is modified from Yang et al. (2015). The location of the  
714 Xar Moron Fault is referenced from Eizenhöfer et al. (2014). Section S1 is an elevation section starting  
from the upstream of the Dali Lake and ending with a spring sample (s2) in the riverhead of Xilamulun  
River.

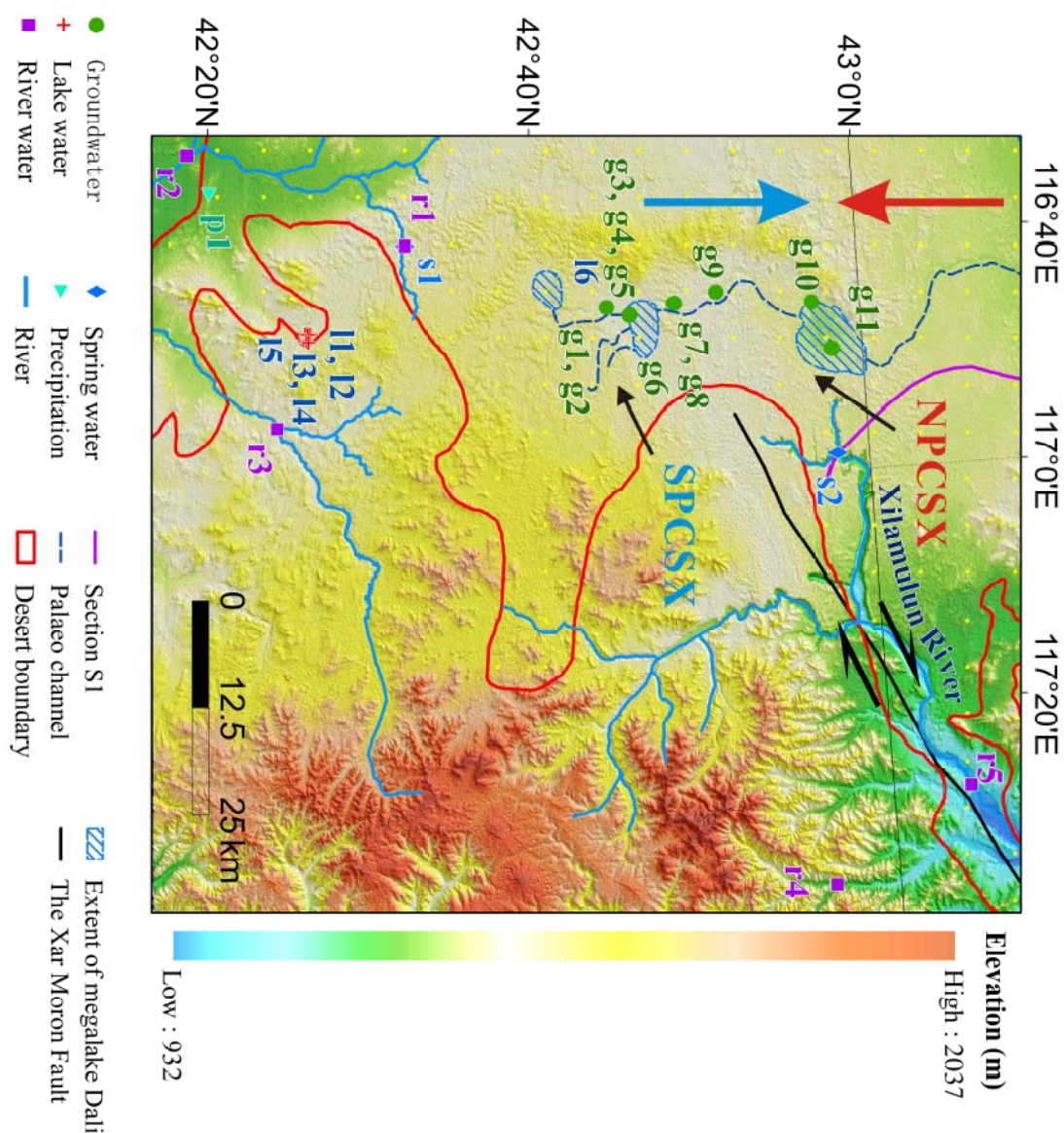


**Fig. 2.** (a) Tectonic framework of the north China-Mongolian segment of the Central Asian Orogenic Belt (modified after Jahn, 2004). (b) Geological sketch map of the northern China-Mongolia tract (modified after Jian et al., 2010). The Solonker suture zone represents the tectonic boundary between the northern (Hutag Uul Block-Northern orogen) and the southern (southern orogen-Northern margin of North China craton) continental blocks. Note that the red line marks the early Permian paleobiogeographical boundary (Wang and Liu, 1986; Li, 2006), which coincides with the northern boundary of the suture zone.

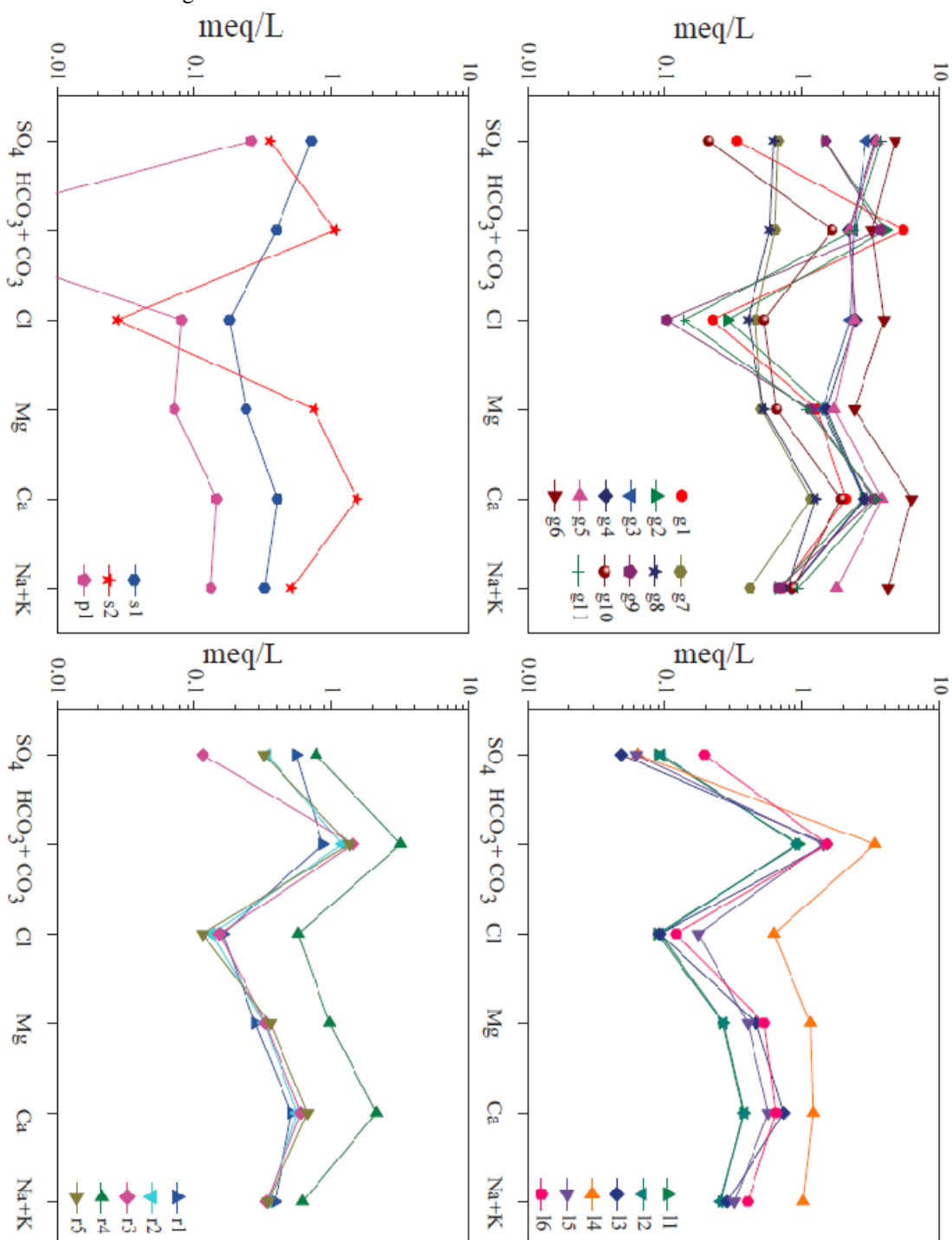


723  
724  
725  
726  
727  
728  
729  
730

**Fig. 3.** The hydrogeological division map of the Otindag Desert.

**Fig. 4.** The locations of the water sampling sites in this study.

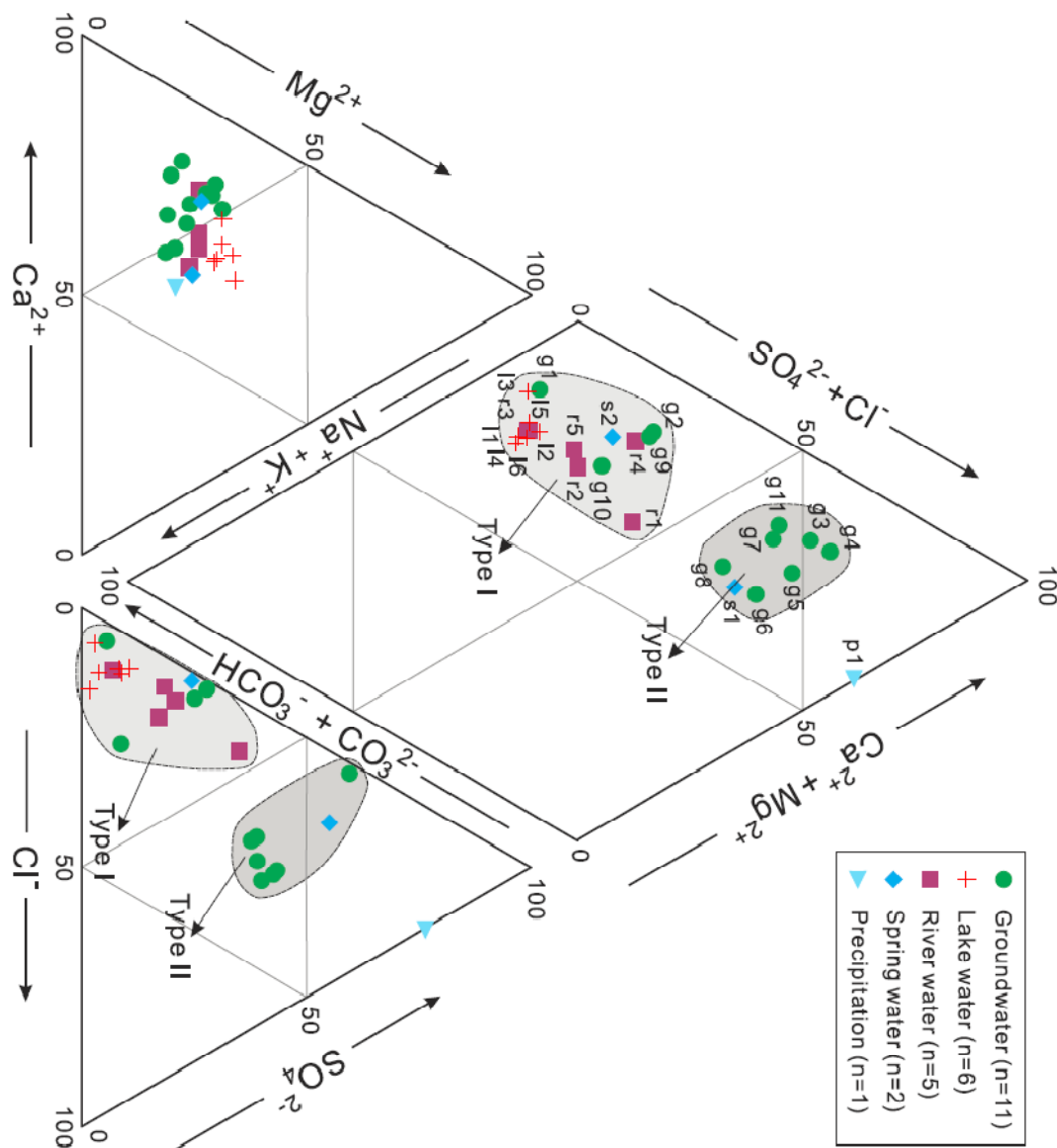
767  
768  
769 **Fig. 5.** The fingerprint diagram showing the variations of multiple ions' concentrations in the studied  
769 water samples in an equivalent unit. The  $\text{HCO}_3 + \text{CO}_3$  concentration in the sample p1 was not shown,  
769 due to its value being lower than the detection limit.



770  
771  
772  
773  
774  
775  
776  
777  
778  
779  
780

781  
782

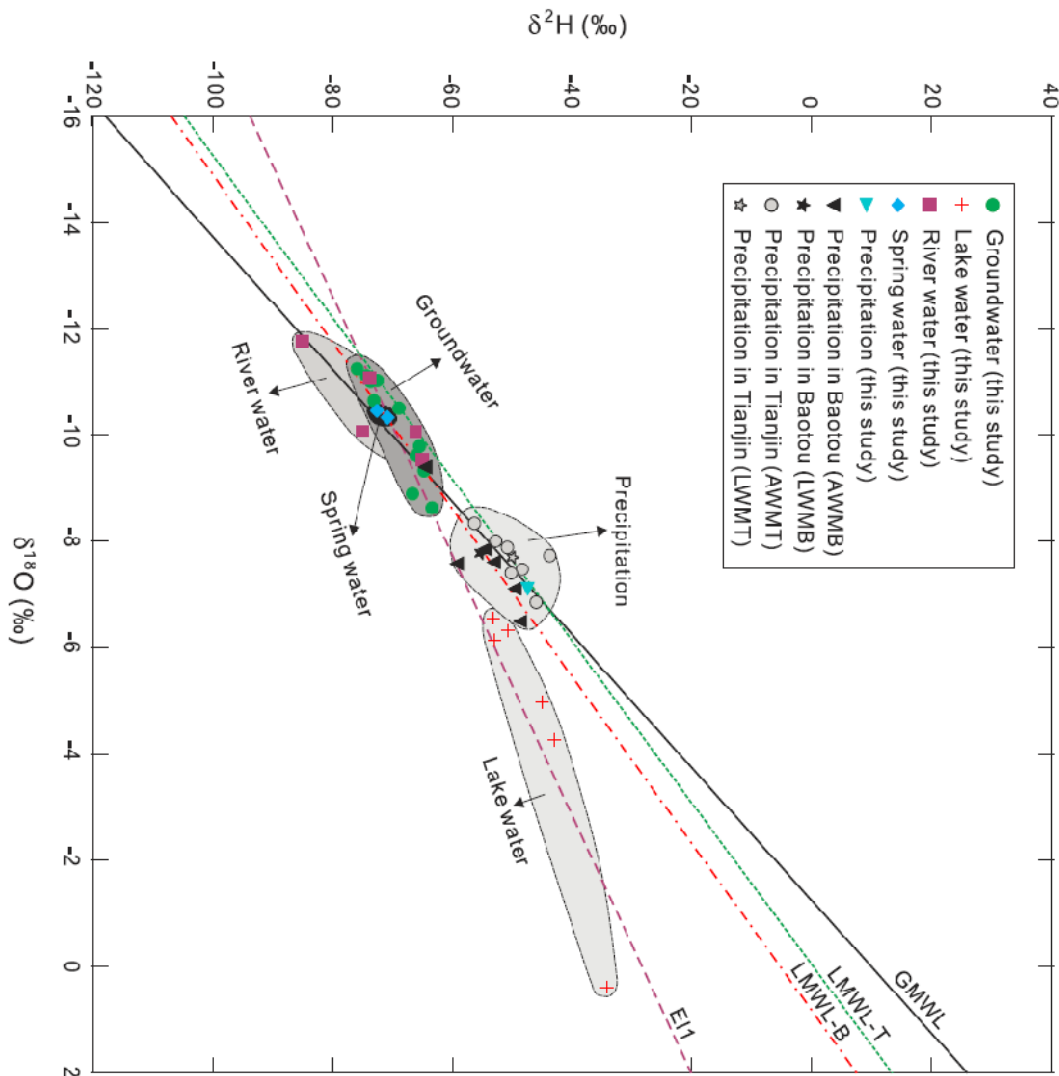
**Fig. 6.** The Piper diagram showing the relative abundances of major cations and anions in the studied water samples. Major water types are also shown in this diagram.



783  
784  
785  
786  
787  
788  
789  
790  
791  
792  
793  
794  
795  
796  
797  
798  
799  
800  
801  
802

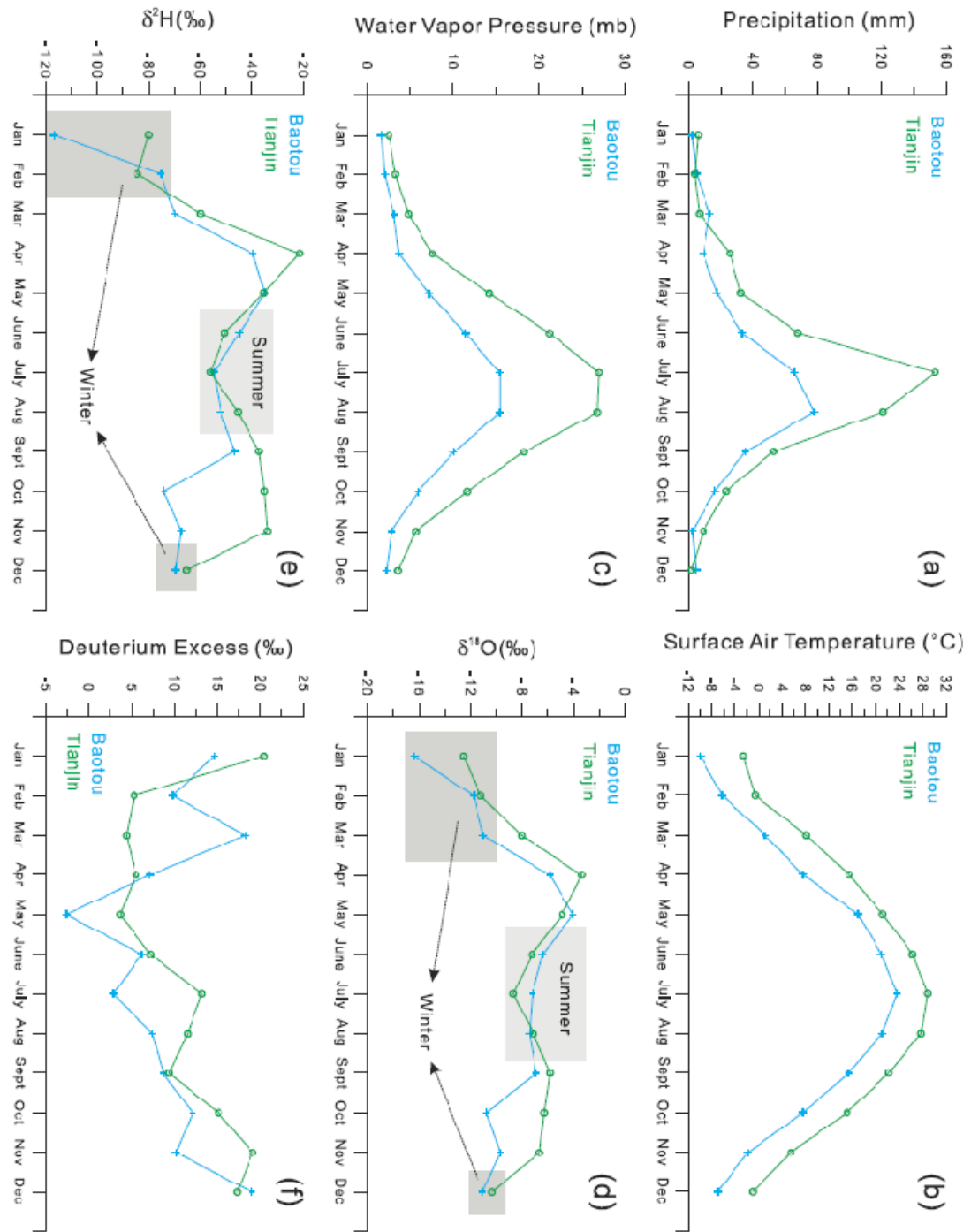
803  
 804  
 805  
 806  
 807  
 808  
 809  
 810  
 811

**Fig. 7.** The bivariate diagram of  $\delta D$  and  $\delta^{18}\text{O}$ , i.e. the Craig diagram, for the natural water samples in this study. Different relationships between the groundwaters, lake waters, river waters, spring waters and the precipitation waters are illustrated. AWMB, the annual weighted mean value at the Baotou station; AWMT, the annual weighted mean value at the Tianjin station; LWMB, the long-term weighted means at the Baotou station; LWMT, the long-term weighted means at the Tianjin station; GMWL, the Global Meteoric Water Line; LMWL-B, the local meteoric water line calculated based on the data from the Baotou station; LMWL-T, the local meteoric water line calculated based on the data from the Tianjin station; EL1, the evaporation line calculated based on the data of water samples collected in this study.



812  
 813  
 814  
 815  
 816  
 817  
 818  
 819  
 820  
 821  
 822  
 823  
 824  
 825  
 826

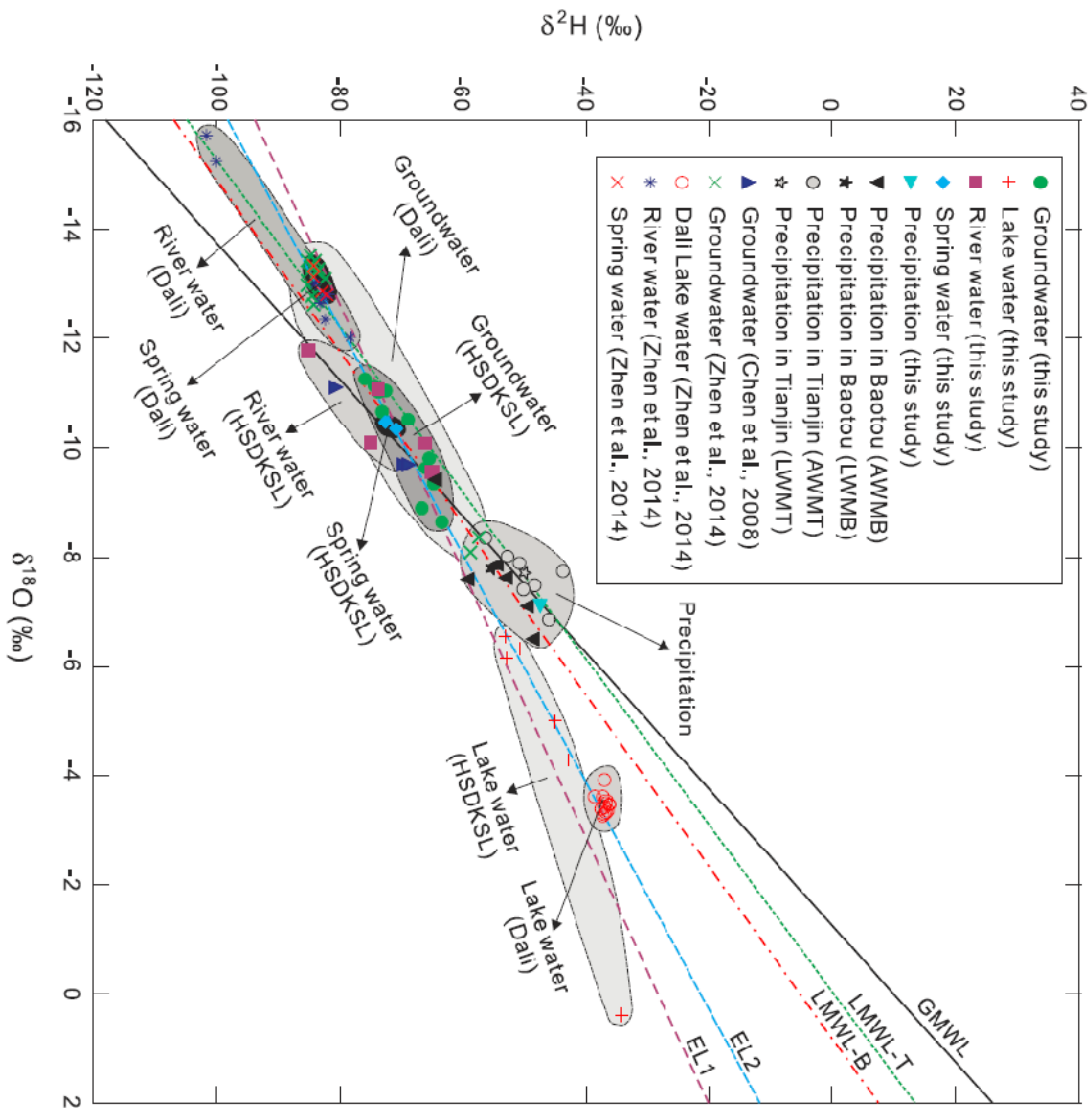
827  
 828  
 829  
 830  
 831  
**Fig. 8.** The seasonal mean distributions of (a) precipitation, (b) surface air temperature and (c) water  
 vapor pressure from the Baotou and Tianjin weather stations (station sites seen in **Fig. 1a**) in the  
 surrounding areas of the Otindag for the period 1981-2010. The seasonal mean distributions of (d)  $\delta^{18}\text{O}$   
 and (e)  $\delta\text{D}$  values in precipitation from the Baotou and Tianjin weather stations in the surrounding  
 areas of the Otindag for the period 1986-2001.



832  
 833  
 834  
 835  
 836  
 837  
 838  
 839  
 840  
 841

842  
843  
844  
845  
846  
847  
848

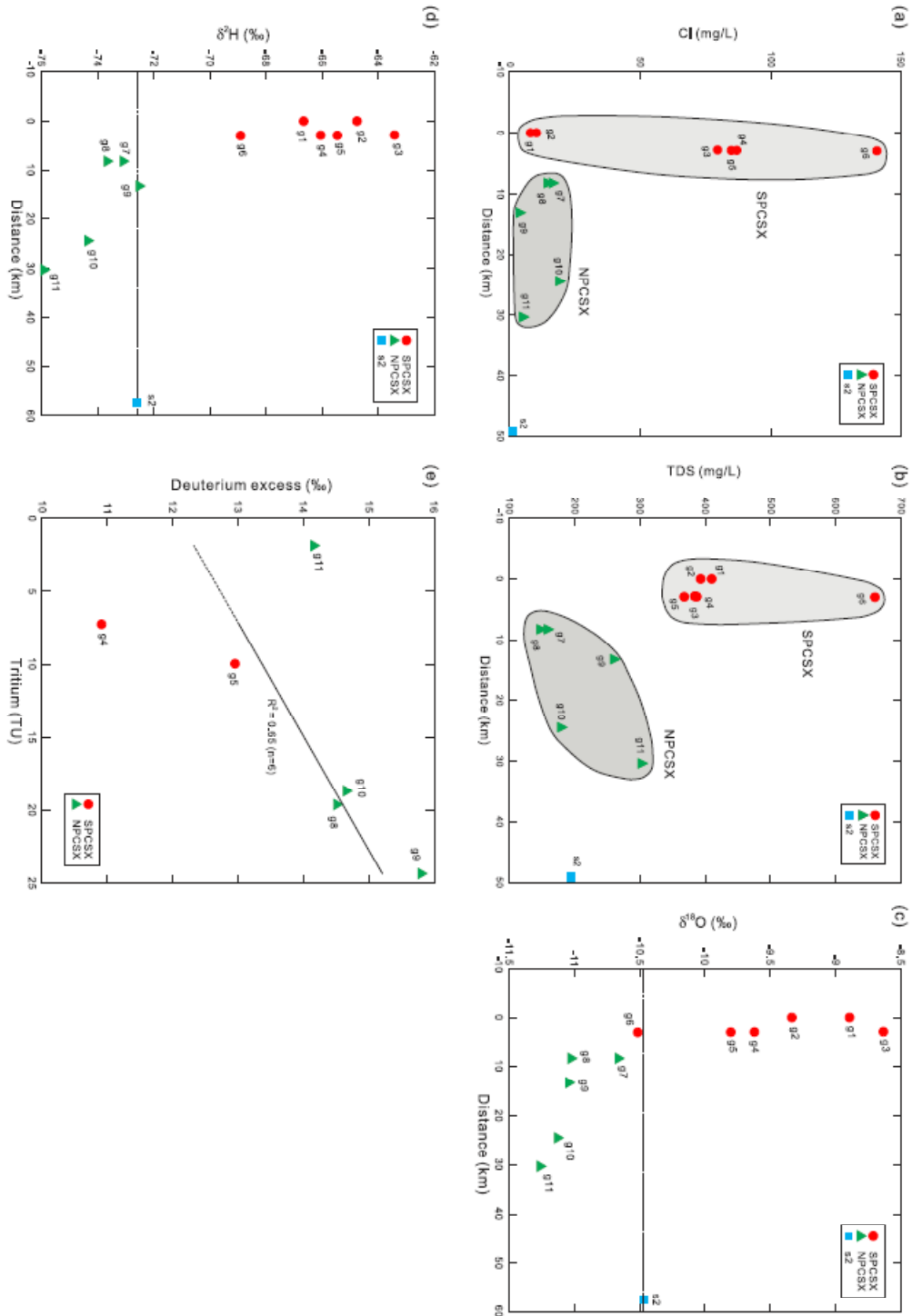
**Fig. 9.** The bivariate diagram of  $\delta D$  and  $\delta^{18}O$ , i.e. the Craig diagram, for the natural water samples collected in the Otindag (this study) and the Dali Basin. Different relationships between the groundwaters, lake waters, river waters, spring waters and the precipitation waters are clearly illustrated. AWMB, AWMT, LWMB, LWMT, GMWL, LMWL-B, LMWL-T, and EL1 are the same as in Fig. 7. EL2, the evaporation line calculated based on the data from the groundwater, lake water, river water and spring water samples collected from the Otindag and Dali Basin. The data for the Dali were taken from Chen et al. (2008) and Zhen et al. (2014).



849  
850  
851  
852  
853  
854  
855  
856  
857  
858  
859  
860  
861  
862  
863  
864  
865

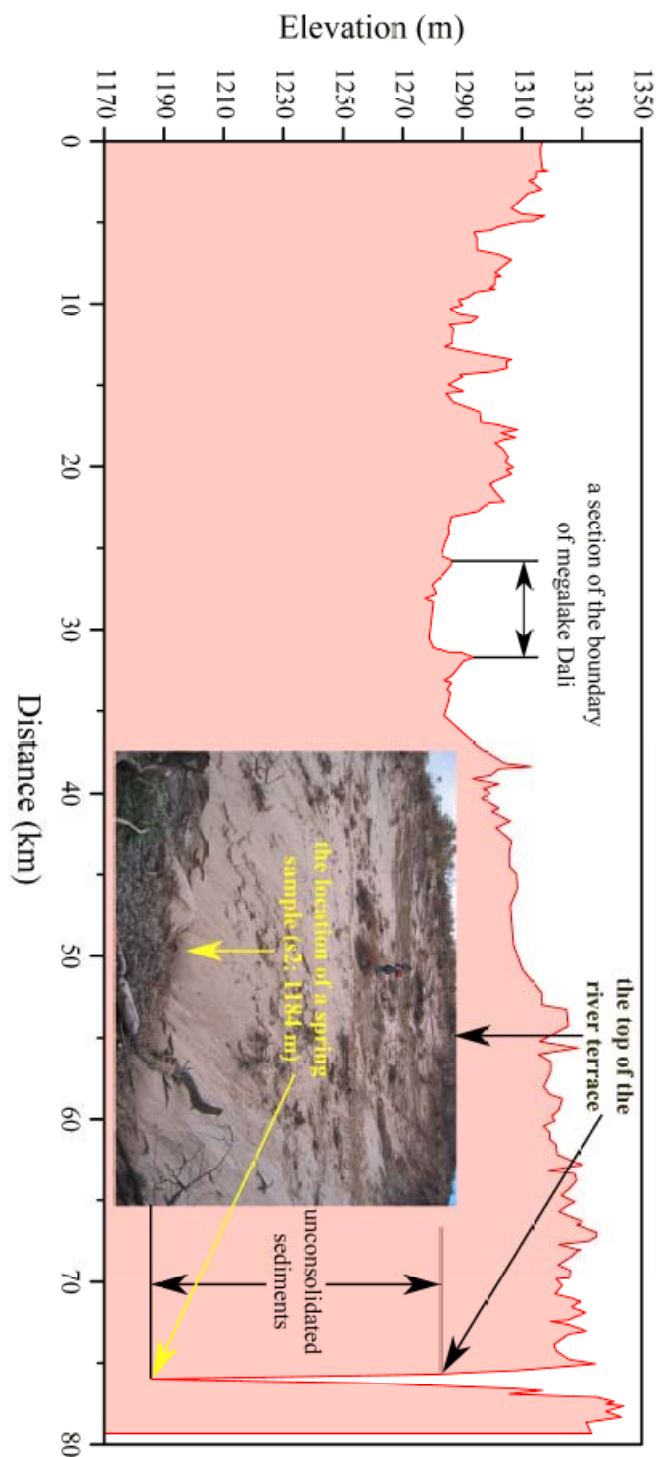
866  
 867  
 868  
 869  
 870  
 871  
 872

**Fig. 10.** (a) Sketch map showing the relationship between the groundwaters in the NPCSX and SPCSX areas, based on variations of (a) the chloride concentrations, (b) the TDS concentrations, (c) the  $\delta^{18}\text{O}$  values and (d) the  $\delta\text{D}$  values of these water samples versus their distances away from the water sample g1 along the palaeo river channel (PCSX) from south to north. The dashed line in (c) and (d) represents the corresponding values of the spring water sample s2, and divides samples into the NPCSX and SPCSX parts. (e) Variations of tritium contents vs. deuterium excess for the groundwater samples in the study area. The sample g6 was omitted due to its potential contamination.



873  
 874  
 875  
 876  
 877  
 878

879  
880  
881 **Fig. 11.** Variation of the topographical elevation along the section S1 (see Fig. 1b) from the upstream of  
the Dali Lake to the location site of the spring water sample (s2) in the riverhead of the Xilamulun  
River. Note that no river water samples are shown in this figure.



882  
883

884

**Table Captions:**

885

**Table 1.**The physical parameters measured for the natural water samples in the study area.

Sample ID	Water type	Latitude (N, degree)	Longitude (E, degree)	Elevation (m a.s.l)	Depth (m)	Temperature (°C)	pH	Eh (mV)	EC (µS/cm)	TDS (mg/L)	Salinity (%)	Alkalinity (meq/L)	Hardness (°dH)
g1	Groundwater	42.736306	116.747333	1396	12	5.8	6.72	3	769	410	0.6	5.47	9.42
g2	Groundwater	42.736306	116.747333	1396	26	6.0	6.91	-10	736	393	0.5	4.07	11.96
g3	Groundwater	42.760194	116.760139	1355	32	7.7	6.88	-6	725	384	0.5	2.39	11.94
g4	Groundwater	42.759694	116.760417	1360	7	10.0	6.74	1	725	387	0.5	2.20	12.28
g5	Groundwater	42.759556	116.760556	1362	27	7.6	6.46	16	691	368	0.5	2.23	15.57
g6	Groundwater	42.760111	116.760250	1365	7	10.3	6.26	22	1240	660	0.8	3.25	24.45
g7	Groundwater	42.806361	116.747806	1352	20	6.8	6.71	2	297	158	0.2	0.63	4.70
g8	Groundwater	42.806361	116.747806	1352	16	6.5	6.92	-8	276	147	0.2	0.58	5.00
g9	Groundwater	42.850333	116.735722	1347	30	7.2	6.74	-1	487	260	0.4	3.73	12.68
g10	Groundwater	42.949861	116.759194	1321	37	9.9	6.75	-2	337	179	0.2	1.66	7.23
g11	Groundwater	42.967111	116.827528	1317	60	8.6	6.99	-14	571	302	0.4	2.40	12.94
l1	Lake water	42.424611	116.769194	1368	/	16.9	9.44	-151	126	67	0.1	0.95	1.79
l2	Lake water	42.424611	116.769194	1368	/	19.6	9.18	-137	132	70	0.1	0.92	1.82
l3	Lake water	42.424611	116.757806	1365	/	20.2	7.38	-36	196	105	0.1	1.53	3.36
l4	Lake water	42.427083	116.757639	1366	/	20.5	7.87	-64	448	238	0.2	3.42	6.61
l5	Lake water	42.421806	116.756917	1360	/	20.1	8.23	-83	173	92	0.1	1.43	2.73
l6	Lake water	42.736389	116.747222	1374	/	10.7	8.35	-89	194	103	0.1	1.53	3.30
r1	River water	42.530917	116.641250	1355	/	20.6	7.31	-33	180	96	0.1	0.88	2.23
r2	River water	42.310883	116.494817	1231	/	14.9	7.67	-52	178	95	0.1	1.21	2.50
r3	River water	42.385778	116.886194	1362	/	9.5	7.62	-48	177	94	0.1	1.45	2.62
r4	River water	42.931417	117.585306	1217	/	10.5	7.97	-69	474	252	0.3	3.22	8.73
r5	River water	43.079083	117.457389	1006	/	12.9	7.87	-62	191	101	0.1	1.37	2.88
s1	Spring water	42.530917	116.641250	1359	/	20.9	6.63	5	165	88	0.1	0.40	1.81
s2	Spring water	42.965417	116.975361	1184	/	19.0	7.47	-46	371	195	0.2	1.07	6.40
p1	Precipitation	42.330750	116.551694	1260	/	20.2	4.61	109	78	42	0.0	/	0.61

886

887

**Table 2.** The concentrations of major cations and anions measured for the water samples in the study area.

Sample	F <sup>-</sup> (mg/L)	Cl <sup>-</sup> (mg/L)	NO <sub>2</sub> <sup>-</sup> (mg/L)	NO <sub>3</sub> <sup>-</sup> (mg/L)	SO <sub>4</sub> <sup>2-</sup> (mg/L)	CO <sub>3</sub> <sup>2-</sup> (mg/L)	HCO <sub>3</sub> <sup>-</sup> (mg/L)	Li <sup>+</sup> (mg/L)	Na <sup>+</sup> (mg/L)	NH <sub>4</sub> <sup>+</sup> (mg/L)	K <sup>+</sup> (mg/L)	Mg <sup>2+</sup> (mg/L)	Ca <sup>2+</sup> (mg/L)
g1	0.13	7.90	2.32	0.48	16.10	0.00	334.60	0.02	13.79	10.54	4.59	15.52	41.81
g2	0.21	10.21	0.00	6.15	70.61	0.10	247.70	0.02	13.36	6.56	3.45	17.91	56.04
g3	0.11	79.56	0.00	0.00	140.76	0.00	145.40	0.01	17.92	2.28	1.76	17.06	57.29
g4	0.10	86.90	0.00	5.73	164.80	0.00	133.70	0.02	18.02	0.00	2.02	18.50	57.32
g5	0.07	84.82	0.00	0.76	169.30	0.00	136.20	0.00	39.68	1.02	2.72	20.94	76.86
g6	0.07	140.54	0.00	110.77	228.80	0.00	198.20	0.00	79.80	0.00	29.47	29.25	126.68
g7	0.37	16.31	0.00	306.31	32.01	0.00	38.70	0.06	7.83	0.00	3.09	6.21	23.37
g8	0.29	14.28	0.00	35.49	29.89	0.00	35.50	0.02	16.21	0.11	3.38	6.44	25.14
g9	0.10	3.66	0.15	1.19	71.56	0.00	227.40	0.06	12.92	0.55	4.50	14.06	67.52
g10	0.24	18.80	0.00	49.49	9.97	0.00	101.10	0.00	18.54	0.00	2.09	7.92	38.68
g11	0.28	4.94	0.00	0.00	181.53	0.00	146.20	0.05	20.40	2.59	2.06	13.30	70.59
l1	0.16	3.15	0.00	0.07	4.32	0.00	57.90	0.01	5.42	0.00	0.86	3.24	7.49
l2	0.16	3.30	0.00	1.66	4.57	0.00	55.80	0.00	5.33	0.00	0.84	3.29	7.61
l3	0.11	3.27	0.00	0.61	2.33	0.00	93.30	0.01	5.88	0.00	1.19	5.68	14.66
l4	0.17	22.12	0.00	0.39	3.04	0.10	207.60	0.00	9.21	0.70	24.21	14.02	24.18
l5	0.09	6.24	0.00	0.65	2.97	0.10	86.80	0.01	6.72	0.00	1.16	4.91	11.41
l6	0.18	4.29	0.00	0.80	9.34	0.10	93.00	0.01	8.41	0.00	1.36	6.47	12.95
r1	0.30	5.76	0.00	2.38	26.67	0.30	52.40	0.01	7.15	0.00	2.99	3.41	10.34
r2	0.19	4.82	0.00	0.65	16.40	0.10	73.10	0.01	6.82	0.00	1.92	3.96	11.36
r3	0.64	5.46	0.00	0.43	5.57	0.00	88.10	0.01	7.11	0.00	1.13	4.04	12.06
r4	1.08	20.39	0.00	19.27	37.25	0.50	195.00	0.01	13.02	0.00	1.96	11.90	42.81
r5	0.19	4.10	0.00	1.08	15.57	0.00	82.60	0.01	6.71	0.00	2.08	4.38	13.40
s1	0.16	6.44	0.00	1.95	34.25	0.00	24.30	0.02	6.56	0.00	1.62	2.92	8.10
s2	0.05	0.98	0.00	0.45	17.15	0.00	64.90	0.02	9.87	0.00	3.32	9.10	30.79
p1	0.61	2.90	0.00	9.46	12.65	0.00	0.00	0.00	2.09	2.07	1.64	0.88	2.95

888

889

890

891

**Table 3.** The analytical data of stable and radioactive isotopes measured for the water samples in this study.

Sample ID	$\delta D$ (‰)	$\sigma_{\delta D}$ (‰)	$\delta^{18}O$ (‰)	$\sigma_{\delta^{18}O}$ (‰)	deuterium excess (d)	Tritium ( $^3H$ ) (TU)
g1	-66.664	0.199	-8.895	0.026	4.496	/
g2	-64.758	0.291	-9.336	0.039	9.930	/
g3	-63.424	0.269	-8.635	0.008	5.656	/
g4	-66.055	0.149	-9.621	0.062	10.913	7.250
g5	-65.462	0.111	-9.802	0.027	12.954	9.975
g6	-68.913	0.287	-10.514	0.039	15.199	22.908
g7	-73.105	0.298	-10.662	0.041	12.191	/
g8	-73.676	0.220	-11.023	0.037	14.508	19.611
g9	-72.530	0.181	-11.041	0.015	15.798	24.345
g10	-74.362	0.201	-11.127	0.026	14.654	18.681
g11	-75.924	0.340	-11.260	0.015	14.156	1.860
l1	-53.128	0.229	-6.553	0.002	-0.704	/
l2	-50.721	0.304	-6.320	0.026	-0.161	/
l3	-42.877	0.239	-4.292	0.034	-8.545	/
l4	-34.155	0.243	0.381	0.040	-37.203	/
l5	-45.057	0.206	-4.987	0.009	-5.161	/
l6	-52.866	0.187	-6.150	0.049	-3.666	/
r1	-66.157	0.118	-10.069	0.015	14.395	/
r2	-64.996	0.148	-9.549	0.012	11.396	/
r3	-73.790	0.315	-11.083	0.021	14.874	/
r4	-85.155	0.244	-11.781	0.005	9.093	/
r5	-74.978	0.195	-10.084	0.003	5.694	/
s1	-70.832	0.074	-10.340	0.007	11.888	/
s2	-72.601	0.281	-10.468	0.046	11.143	/
p1	-47.435	0.374	-7.141	0.017	9.693	/

892

893

894

895

**Table 4.**The statistical frequency of rainfall events being >20 mm per year during the recent 30 years from 1985 to 2014. The data come from the China Meteorological Data

896 Sharing Service System.

Station	One time/year	Two times/year	Three times/year	Four times/year	Five times/year	Six times/year	Seven times/year	Mean times/year
Duolun	2	8	8	4	4	3	1	3.4
Xilinhaote	8	5	2	6	3	2	0	2.5

897  
898 **Table 5.** The measured contents of tritium in the groundwater samples studied and the calculated ages of these samples.

Sample-ID	Tritium content (T.U.)	Possible ages (years)
g1	not measured	not clear
g2	not measured	not clear
g3	not measured	not clear
g4	7.25	20-40
g5	9.97	13-33
g6	22.91	0-20
g7	not measured	not clear
g8	19.61	0-20
g9	24.34	0-17
g10	18.68	0-22
g11	1.86	40-65

899

# 1 Direct or indirect recharge on groundwater in the 2 middle-latitude desert of Otindag, China?

3 Bing-Qi Zhu<sup>1\*</sup>, Xiao-Zong Ren<sup>2</sup>, Patrick Rioual<sup>3</sup>

带格式的：行距：1.5 倍行距

4 <sup>1</sup>KLWCRESP, IGSNRR, CAS, Beijing, China

5 <sup>2</sup>SGS, TYNU, Jinzhong, China

6 <sup>3</sup>KLCGE, IGGCAS, Beijing, China

带格式的：上标

7 Correspondence to: Bing-Qi Zhu (zhubingqi@sina.com)

带格式的：上标

域代码已更改

带格式的：字体颜色：自动设置

带格式的：无下划线，字体颜色：自动设置

8 **Abstract.** Although rainfall is scarce in most desert lands of the world, the Otindag Desert in the  
9 middle-latitude desert zone of northern China in Northern Hemisphere (NH) has abundant of water  
10 resources, mainly groundwater. To gain an insight into the origin of groundwater origin in this desert,  
11 stable and radioactive isotopes and major ion hydrochemistry of groundwater, as well as other natural  
12 waters including river water, spring water, lake water and precipitation water, were investigated in the  
13 eastern part of the Otindag. The results showed that the groundwaters in the Otindag were freshwater  
14 (TDS < 700 mg/L) and were depleted in  $\delta^{2}H$  and  $\delta^{18}O$ , when compared with the modern precipitation.  
15 The major water types are the  $Ca-HCO_3$  and  $Ca/Mg-SO_4$  types waters. No  $Cl$  type and  $Na$  type  
16 waters occurred in the study area. The ionic and depleted stable isotopic signals in groundwater, as well  
17 as the high values contents in of tritium contents (5.25 TU), indicated that  
18 these groundwaters studied were young but not of meteoric origin, i.e., out of control by the modern  
19 and paleo direct recharge. Clear differences in the isotopic signals were observed between the  
20 groundwaters in the north (NPCSX) and south (SPCSX) parts of the study area, but the signals were  
21 similar in between the groundwaters between in the NPCSX and its neighbouring catchment, the Dali  
22 Basin. The topographical elevation is decreasing from the SPCSX (1396 m a.s.l.) to the NPCSX  
23 (1317 m a.s.l.) and the Dali (1226 m a.s.l.). Groundwaters in the NPCSX were characterized by  
24 lower elevations, the lower chloride and TDS concentrations, higher tritium contents, higher deuterium  
25 excess, and more depleted values of  $\delta^{2}H$  and  $\delta^{18}O$  than those in the SPCSX. The spatial distribution  
26 pattern of these environmental parameters This indicates a discrepancy between in the one  
27 hand the hydraulic gradient of groundwater and in the other hand the isotopic and  
28 hydrochemical gradients of groundwater in the desert eastern Otindag. It also suggests that the  
29 groundwaters have different water recharge sources between the two areas parts in the study area.  
30 However, the groundwaters in the two areas shared a common evaporation line (EL2) in the Craig  
31 diagram of  $\delta^{2}H$  and  $\delta^{18}O$ , indicating a genetic relationship in their recharge sources. Combined analysis  
32 was further performed using the isotopic and physico-chemical data of natural waters collected from the  
33 Dali Basin and the surrounding mountains. It indicated that the major recharge sources of the  
34 groundwaters in the NPCSX, as well as the river waters and groundwaters in the Dali Basin, were mainly  
35 derived from the Daxin'Anling Mountains, by leaking of the Xilamulan River water through a thick  
36 aquifer in the eastern margins of the Otindag. By contrast, While the groundwaters in the

37 SPCSX were mainly recharged from two sources. One was the flash floods derived from the Yinshan  
38 Mountains and the river waters other was the Xilamulun River waters derived from the Daxin'Anlin  
39 Mountains. It indicates that the modern indirect recharge mechanism, instead of the direct recharge and  
40 the palaeo-water recharge, is the most significant for groundwater recharge in the eastern Otindag. This  
41 suggests that the tectonic settings at a regional scale, but not the climate, is at the origin of what  
42 was responsible for the groundwater origin in the Otindag. This study provides a new perspective into  
43 the origin and evolution of groundwater resources in the middle latitude desert zone of NH. The Otindag  
44 Desert is essential to the livestock-economy and ecoenvironment of northern China. Although surface  
45 water is the traditional source for China's socio-economy in arid areas, the groundwater resources  
46 underlying the desert are increasingly burdened by groundwater pumping, which increases interest in  
47 the status of the groundwater resources. Widespread fresh groundwater deep to 60 m was found at the  
48 eastern part of the Otindag Desert. The occurrence of this massive fresh groundwater raises doubts on  
49 the often-made assumption in the literature that regional atmospheric precipitation or palaeowater,  
50 namely the direct recharge, is the source of water in the middle-latitude desert aquifers of northern  
51 China and makes further investigation necessary. Knowledge on the origin and recharge of this fresh  
52 groundwater is key in assessing the possibility of groundwater exploitation and utilization. In this study  
53 we conducted hydrogeochemical and isotopical analyses to assess possible origin and recharge of these  
54 groundwaters. It is concluded that the fresh groundwater can neither originate from regional  
55 atmospheric precipitation derived from the Asian Summer Monsoon system, nor from palaeowater that  
56 formed during the last glacial period. Our results indicate that with groundwater dating it is possible to  
57 originate from remote mountain areas via the faults of the Solonker Suture zone, including the  
58 Daxing'Anlin and Yinshan Mountains. Furthermore, it is deduced that the hydrological connection  
59 between desert aquifers and mountain systems through the suture zone is crucial to the hydrogeological  
60 functioning of the Otindag aquifer. This suggests that the modern indirect recharge mechanism, instead  
61 of the direct recharge and the palaeo-water recharge, is the most significant for groundwater recharge in  
62 the Otindag Desert. This study provides a new perspective into the origin and evolution of groundwater  
63 resources in the middle-latitude desert zone of Asian continent.

带格式的: 无下划线, 字体颜色: 自动设置, 图案: 清除

带格式的: 无下划线, 字体颜色: 自动设置

带格式的: 无下划线, 字体颜色: 自动设置, 图案: 清除

带格式的: 无下划线, 字体颜色: 自动设置

64  
65 **Keywords:** fresh groundwater recharge origin atmospheric precipitation; direct recharge; indirect  
66 recharge; palaeowater recharge; fault hydrology; middle-latitude desert; direct and indirect recharge;  
67 stable and radioactive isotope; ion hydrochemistry; climate control; tectonic control Otindag Desert.

带格式的: 无下划线, 字体颜色: 自动设置

## 68 1. Introduction

69 Water Resources. In a semi-arid to arid region where rainfall is insufficient to supply the needs of  
70 a growing population and a higher standard of living, the deficit is normally made up by extracting  
71 groundwater. [Alsharhan, 2001, Hydrogeology of an Arid Region The Arabian Gulf and Adjoining  
72 Areas.] As rainfall events are infrequent in arid and semi-arid regions of the world, surface runoff  
73 and related water resources are globally scarce and ephemeral. These areas thus rely heavily on  
74 groundwater as the primary water resource to support local ecosystems (Herezeg and Leaney, 2011;  
75 Seanlon et al., 2006). It has been widely proved that the origin, quality and quantity of groundwater in

带格式的: 无下划线, 字体颜色: 自动设置

77 arid lands can be deeply influenced by environmental factors/processes, which controlling the  
78 groundwater recharge and evolution, such as in the arid lands of northwestern China and Central Asia  
79 (Zhu et al., 2015, 2016, 2017). For this reason these factors/processes become an essential component in  
80 the understanding of regional hydrological systems and the management of water resources  
81 (Dogramaci et al., 2012). For example, groundwater recharged by modern precipitation can refill  
82 quickly but is vulnerable to contamination by the surface wastes; inversely, groundwater containing  
83 mostly ancient water may not recharge to a useful extent over human timescales and cannot be affected  
84 by surface waters (Bethke and Johnson, 2008). Therefore, different strategies on groundwater  
85 resources management should be adopted when the different recharge mechanisms of groundwater  
86 occurring.

带格式的: 无下划线, 字体颜色: 自动设置

87 In general, groundwater recharge can be broadly classified into two ways, the direct  
88 recharge, namely diffuse recharge by native water resources, and the indirect recharge, namely focus  
89 recharge by external water resources. The direct recharge is replenished by precipitation infiltration  
90 through the unsaturated zone and the indirect recharge is defined as recharge from mappable features  
91 such as rivers, canals, and lakes originated from remote areas (Healy, 2010). It is well known that  
92 groundwater recharge can be influenced by environmental factors, including climate change,  
93 underlying soil and geology, land cover and population growth, over withdrawal and economic  
94 development (Zhu et al., 2015, 2017), thus the amount of groundwater in arid and semi-arid regions  
95 decrease rapidly while human demands on the limited water resources increase rather than decrease  
96 (Ma et al., 2013). Between environment and groundwater recharge, climate and land cover largely  
97 determine precipitation and evapotranspiration, whereas the underlying soil and geology dictate  
98 whether a water surplus (precipitation minus evapotranspiration) can be transmitted and stored in the  
99 subsurface (Giordano, 2009; Doll, 2009). Modelled estimates of diffuse recharge globally (Doll and  
100 Fedler, 2008; Wada et al., 2010) range from 13,000 to 15,000 km<sup>3</sup>/yr, equivalent to ~30% of the  
101 world's renewable freshwater resources (Doll, 2009) or a mean per capita groundwater recharge of  
102 2100 to 2500 m<sup>3</sup>/yr. These estimates represent potential recharge fluxes as they are based on a water  
103 surplus rather than measured contributions to aquifers. Furthermore, these modelled global recharge  
104 fluxes do not include focused recharge, which, in semi-arid and arid environments, can be substantial  
105 (Scanlon et al., 2006; Favreau et al., 2009). For keeping sustainable management of water resources, it  
106 requires urgently to understand both diffuse and focused recharge and meet both human and ecosystem  
107 needs in arid areas of the world, particularly in Central Asia and Northern China.

带格式的: 无下划线, 字体颜色: 自动设置

108 Many areas in the middle-latitude desert zone of northern China such as, many areas of these  
109 lands the Badanjilin Desert, the Mu Us sandy Land and the Hobq Desert (Chen et al., 2012a; Chen et  
110 al., 2012b), are unexpectedly rich in incommensurate with large groundwater resources, such as the  
111 Badanjilin Desert, the Mu Us Sandy Land and the Hobq Desert (Chen et al., 2012a; Chen et al., 2012b),  
112 although they have been under arid or hyper-arid climate for a long time (Sun et al., 2010). How these  
113 groundwater are originated and how they are recharged in these deserts are thus fundamental  
114 scientific becoming a keyquestions. Until now, however, no consensus has been achieved it has long  
115 been altered in the academic circles.

带格式的: 无下划线, 字体颜色: 自动设置

116 For some of the earth scientists, the direct recharge is thought to be very important for

117 groundwaters in the wide desertlands of northwestern China due to lack of surface runoff (Yang et al.,  
118 2010; Yang and Williams, 2003; Zhao et al., 2017). They argued that although the amount of  
119 atmospheric precipitation is small, the vast catchment area in the desert region could concentrate the  
120 rainfall into large inland basins, creating an aquifer with large storage capacity and great  
121 thickness. However, some hydrologists suggested that the estimate of direct recharge used by the  
122 chloride mass balance method was 1.4 mm/year, approximately only 1.7% of the mean annual  
123 precipitation in a cold large desert (Badanjilin) in northern China (Gates et al., 2008). A similar  
124 estimation was only 1 mm/year for Gobi deserts from the Hexi Corridor to the Inner Mongolia Plateau  
125 in northwestern China (Ma et al., 2008). Consequently, they thought that heavy potential evaporation  
126 and little precipitation make it difficult for direct recharge to meet the supply of groundwater in these  
127 desert areas. Thus, the indirect recharge is considered to be an important mechanism for groundwater  
128 recharge in these desert areas. For example, based on isotopic compositions of natural waters, Zhao et al.  
129 (2012) suggested that little precipitation had recharged into groundwaters in the Badain Jaran  
130 Desert. Chen et al. (2004) argued that the groundwaters in the Badanjilin Desert were recharged by  
131 paleo glacial melt water through faults and deep carbonate layers far away from the local desert. Many  
132 studies also suggested that paleowaters stored in aquifer during wetter climate periods could recharge  
133 to groundwater under certain conditions in arid lands (Edmunds et al., 2006; Ma and Edmunds,  
134 2006). Other kinds of indirect recharge, such as mountain front recharge from adjacent mountain  
135 blocks, are also proposed to offer an important inflow to aquifers within arid to semiarid  
136 catchments (Blasch and Bryson, 2007).

137 The Otindag Desert is one of the largest sandy desert lands located at the monsoon margin of  
138 northern China and is the geographical centre of the northeastern Asian Continent (Fig. 1), which can  
139 be regarded as a significant repository of information relating to the groundwater recharge in the arid  
140 Inner Asia. At present, the eastern Otindag is also a typical case for its unexpected incommensurate  
141 groundwater resources, because there is abundant groundwater in this desert land and even rivers  
142 originate there due to the spillover of spring water, such as the tributaries of Xilamulun River in its  
143 north and the Shandian River in its south (Fig. 1). Climatically, the monsoon margin of northern China  
144 refers to a strip along the present East Asian Summer Monsoon (EASM) limits and is considered to be  
145 sensitive to climate change (Wang and Feng, 2013). Geologically, the Otindag Desert lies in a tectonic  
146 depression of the central Solonker suture zone with a few faults stretching east and west (Fig. 2), with  
147 its northern margin along a fault marked by a series of lake basins. Thus, the large-scale  
148 hydrogeological conditions of the Otindag Desert belong to a fault zone under the influence of the  
149 EASM climate.

150  
151 Until now, however, whether the climate or other factors the tectonic faults affected the origin of  
152 groundwater recharge and the fluid flow patterns in groundwater aquifers in the Otindag are still not  
153 known. Because at present, until now, however, little data and documents about the groundwater  
154 and its origin is available in the literature in Otindag, and knowledge and reliable data on various  
155 hydrogeological characteristics of the desert such as the catchment extent, input/output, the hysteretic  
156 hydraulic functions, the transient hydraulic conditions, in-homogeneities, and on transfer functions to

带格式的: 无下划线, 字体颜色: 自动设置

域代码已更改

带格式的: 无下划线, 字体颜色: 自动设置

带格式的: 无下划线, 字体颜色: 自动设置

域代码已更改

带格式的: 无下划线, 字体颜色: 自动设置

带格式的: 行距: 1.5 倍行距

带格式的: 无下划线, 字体颜色: 自动设置

带格式的: 无下划线, 字体颜色: 自动设置, 检查拼写和语法, 图案: 清除

带格式的: 无下划线, 字体颜色: 自动设置

带格式的: 无下划线, 字体颜色: 自动设置, 图案: 清除

带格式的: 无下划线, 字体颜色: 自动设置

带格式的: 无下划线, 字体颜色: 自动设置

157 overcome scale problems are also missing. Under such conditions, conventional methods such as water  
158 balance and hydraulic methods sometimes fail in determining groundwater recharge, particularly in  
159 extreme environments (arid, semi-arid, or cold) (Drever, 1997). ~~Because~~ ~~because~~ pristine aquatic  
160 conditions may significantly differ from managed conditions in arid environment, and thus  
161 groundwater recharge is not a fixed number, but may vary with the boundary conditions of the recharge  
162 system (Seiler and Gat, 2007).

163 ~~can be obtained in literature. Whether the direct or indirect recharge is the major mechanism for~~  
164 ~~groundwater recharge in Otindag~~ ~~In general,~~ ~~Groundwater recharge can be broadly classified into two~~  
165 ~~categories: the direct recharge by native water resources and the indirect recharge by external water~~  
166 ~~resources (Herczeg and Leaney, 2011).~~ ~~Water infiltration of atmospheric precipitation through the~~  
167 ~~unsaturated zone to the groundwater is hydrologically defined as the direct recharge, and t~~ ~~The~~ ~~indirect~~  
168 ~~recharge is defined as recharge from mappable features such as rivers, canals, lakes and originates from~~  
169 ~~remote areas (Scanlon et al., 2006; Healy, 2010)~~ ~~(Healy, 2010)~~. It is well known that groundwater  
170 ~~recharge can be influenced by environmental factors, including climate change, underlying soil and~~  
171 ~~geology, land cover and the growth in human population that affects withdrawal and economic~~  
172 ~~development (Zhu et al., 2015, 2017).~~ Among these environmental factors, climate and land cover  
173 ~~largely determine precipitation and evapotranspiration, whereas the underlying soil and geology dictate~~  
174 ~~whether a water surplus (precipitation minus evapotranspiration) can be transmitted and stored in the~~  
175 ~~subsurface (Giordano, 2009; Doll, 2008, 2009; Giordano, 2009).~~

176 ~~For some earth scientists, the direct recharge is thought to be very important for groundwaters in~~  
177 ~~the wide desert lands of north China due to the lack of surface runoffs (Yang et al., 2010; Yang and~~  
178 ~~Williams, 2003; Zhao et al., 2017)~~ ~~(Yang et al., 2010; Yang and Williams, 2003; Zhao et al., 2017)~~. They argued that although the amount of atmospheric precipitation is small, the vast catchment area in  
179 ~~the desert region could concentrate the rainfall into large inland basins, creating an aquifer with large~~  
180 ~~storage capacity and great thickness. However, some hydrologists estimated by the chloride mass~~  
181 ~~balance method that the direct recharge was 1.4 mm/year, which represents approximately only 1.7% of~~  
182 ~~the mean annual precipitation in a cold large desert (Badanjilin) in northern China (Gates et al.,~~  
183 ~~2008)~~ ~~(Gates et al., 2008)~~. A similar estimation of 1 mm/year was given for Gobi deserts from the Hexi  
184 ~~Corridor to the Inner Mongolia Plateau in northwestern China (Ma et al., 2008)~~ ~~(Ma et al., 2008)~~. Consequently, they thought that heavy potential evaporation and little precipitation make it difficult for  
185 ~~direct recharge to meet the supply of groundwater in these desert areas. Thus, the indirect recharge is~~  
186 ~~considered to be an important mechanism for groundwater recharge in these desert areas. For example,~~  
187 ~~based on isotopic compositions of natural waters~~ ~~Zhao et al. (2012) suggested that little precipitation~~  
188 ~~had recharged into groundwaters in the Badain Jaran Desert. Chen et al. (2004) argued that the~~  
189 ~~groundwaters in the Badanjilin Desert were recharged by palaeo-glacial melt water through faults and~~  
190 ~~deep carbonate layers far away from the local desert. Many studies also suggested that palaeowaters~~  
191 ~~stored in an aquifer during wetter climate periods could recharge to groundwater under certain~~  
192 ~~conditions in arid lands (Edmunds et al., 2006; Ma and Edmunds, 2006).~~ Other kinds of indirect  
193 ~~recharge, such as mountain front recharge from adjacent mountain blocks, are also proposed to offer an~~  
194 ~~important inflow to aquifers within arid to semiarid catchments (Blasch and Bryson, 2007)~~ ~~(Blasch and~~  
195 ~~2007)~~

带格式的: 无下划线, 字体颜色: 自动设置

带格式的: 无下划线, 字体颜色: 自动设置, 图案: 15% (自动设置)  
带格式的: 无下划线, 字体颜色: 自动设置

197 Bryson, 2007:

198 In this paper, we focus to answer the a question that whether groundwater recharge in Otindag is  
199 mainly direct or indirect, using hydrochemical and isotopic indicators as tracers to offer a valuable  
200 support for identifying the contributions of precipitation recharge on groundwater, since these  
201 indicators reflect the composition of water molecules and are sensitive to physical processes such as  
202 mixing and evaporation (Lawrence et al., 1976; Coplen, 1993; Sultan et al., 2000; Guendouz et al., 2003;  
203 Petrides et al., 2006; Scanlon et al., 2006; Zhu et al., 2007, 2008; Jobbágy et al., 2011; Zhai et al., 2013;  
204 Eissa et al., 2014). T, as the abovementioned hot question for other deserts in China, is also unknown.

205 It should be kept in mind that virgin aquatic conditions may significantly differ from managed  
206 conditions in arid environment, because groundwater recharge is not a fixed number, but may vary with  
207 the boundary conditions of the recharge system (Seiler and Gat, 2007). Conventional methods such as  
208 water balance and hydraulic methods sometimes fail in determining groundwater recharge in extreme  
209 environments (arid, semi-arid, or cold) (Drever, 1997), because of missing knowledge and the lack of  
210 reliable data on various characteristics such as the catchment extent, input/output, the hysteretic  
211 hydraulic functions, the transient hydraulic conditions, in homogeneities, and on transfer functions to  
212 overcome scale problems (Seiler and Gat, 2007). Under such conditions, tracer methods offer a  
213 valuable support for natural water studies.

214 Geochemical elements and environmental isotopes have been widely used as effective tracers to  
215 determine the sources of groundwater recharge, which could be attributed to infiltration by rainfall,  
216 surface waters or both of them (Zhu et al., 2007, 2008; Zhu et al., 2017). For example, by comparing the  
217 composition of stable isotopes of hydrogen and oxygen in local meteoric waters with these in  
218 groundwaters, many studies successfully applied in identifying whether the rainfall play a vital role in  
219 recharging groundwater or not (Zhu et al., 2007; Petrides et al., 2006; Jobbágy et al., 2011; Zhai et al.,  
220 2013). Also, investigating the spatial distribution of groundwater age represented by the concentration  
221 of tritium or radioactive carbon ( $^{14}\text{C}$ ) can provide a way to understand the recharge relationship  
222 between the modern rainfall and the groundwater (Sultan et al., 2000; Zhu et al., 2008). For the indirect  
223 recharge, the groundwater flow regimes or its movement pathway deduced from hydrochemical and  
224 isotopical tracers can indicate its origin and recharge processes. For example, the groundwater  
225 mineralisation will increase as a result of dissolution of evaporite minerals along flow lines that begin  
226 with the recharge area (Guendouz et al., 2003). While, the geochemical and isotopic composition of  
227 groundwaters will be much complex at interface zones between groundwaters with different  
228 hydrochemistry or ages, they will show distinct physiochemical characteristics indicating how they  
229 mixed (Lawrence et al., 1976; Eissa et al., 2014).

230 The detailed The objectives of this study are: (1) to examine the distribution patterns of  
231 environmental signals in the stable and radioactive isotopes and the major ionic hydrochemistry of  
232 groundwater in the eastern Otindag drainage system, and (2) to recognize the major sources of  
233 groundwater in the area, and (3) to identify the key mechanism of groundwater recharge in the desert  
234 land, particularly to discriminate whether the direct recharge or the indirect recharge being the major  
235 control on groundwater recharge in the desert land.

236

带格式的: 无下划线, 字体颜色:  
自动设置, 图案: 清除

带格式的: 无下划线, 字体颜色:  
自动设置

带格式的: 无下划线, 字体颜色:  
自动设置, 图案: 清除

带格式的: 无下划线, 字体颜色:  
自动设置, 图案: 清除

带格式的: 无下划线, 字体颜色:  
自动设置

237 **2. Regional settings**

238 **Geographic setting.** The Otindag Desert lies between latitudes 42° and 44°N and longitudes 112°  
239 and 118° E (Fig. 1). It forms a part of the great middle-latitude desert belt in northern China which  
240 stretches from the Taklamakan Desert of northwestern China to the Kelqin Desert of northeastern  
241 China, near the west coast of the Pacific Ocean. The desert has an area of approximately The Otindag  
242 Desert (~21,400 square kilometers km<sup>2</sup>) is, a middle latitude sandy land desert located in the eastern  
243 of the Inner Mongolia Plateau and at situated at the monsoon margin of northern China as the  
244 geographical centre of the northeastern Asian Continent (Fig. 1). It is the fourth largest sandy lands in  
245 China (Yang et al., 2012) (Yang et al., 2012) and is bordered by a flat steppe terrain of Dali Basin to the  
246 north, the Yinshan Mountains Range and mountainous loess landscape to the south, and the the Greater  
247 Khingan (Daxing'Anling) Mountains Range to the east (Fig. 1). The Otindag Desert is essential to  
248 livestock-economy and ecoenvironment of northern China. Settlements in this desert are restricted to  
249 areas to permanent springs, shallow groundwater and oases to areas where irrigation is possible. Some  
250 nomads continue to eke out a precarious existence grazing livestock in the desert.

251 **Topography and geomorphology.** The Otindag Desert has a varied relief combining extensive  
252 dune fields with rugged mountains along the eastern, southern and southeastern rims. In the east, the  
253 Daxing'Anling Mountains stretch from the Heilong River Valley into the upper reach valleys of the  
254 Xilumulun River from northeast to southwest, gradually increasing in height northwards from about  
255 180 m near Huma to Huanggangliang, where the highest peaks reach 2,029 m with an average  
256 elevation range from 1,100 to 1,400 m. In the south and southeast, the Yinshan Mountains decline  
257 gradually near Duolun and Zhenglanqi, and in some areas leave wide alluvial plains. The terrain of the  
258 Otindag Desert is less rough and elevations decrease from ca. 1300 m in the southeast to ca. 1000 m in  
259 the northwest. Over the greater part of this desert the ground cover consists of fixed and semi-fixed  
260 sandy dunes, with a few mobile dunes in area of little vegetation. The dominated dune types are  
261 represented from parabolic to barchans, linear and grid-formed types, ranging from a few meters to  
262 over 40 m in height (Zhu et al., 1980; Yang et al., 2008).

263 **Climate, vegetation and soil.**

264 **The climate of the Otindag Desert was not uniform in geological period, with much sand**  
265 **movement, occasional rainy years, and several wetter intervals during the Holocene (Yang et al., 2015;**  
266 **Tian et al., 2017). At present, the Sandy Land is in a tectonic depression with a few faults stretching**  
267 **east and west, with its northern margin along a fault marked by a series of lake basins. Tertiary and**  
268 **Quaternary sandstones and mudstones are the common basement rocks under the dunes, and extensive**  
269 **volcanic basalts forming flat terrains are to the north (Zhu et al., 1980; Li et al., 1995). (Yang et al.,**  
270 **2007, Catena)**

271 **The Otindag's elevation is variable, ranging from ca. 1300 m in the southeast to ca. 1000 m in the**  
272 **northwest. The whole desert belongs to the temperate arid and semi-arid temperate zone of northern**  
273 **China, with a meanannual temperature of 2 °C in the north and 4°C in the south (Liu and Yang,**  
274 **2013) (Liu and Yang, 2013). At the regional scale, the climate of the desert climate is typically**  
275 **controlled by the East-Asian Monsoon system, characterized by a warm summer, with precipitation**  
276 **transported by the EASM, and by a cold and dry winter under the influence of the East Asian Winter**

带格式的: 无下划线, 字体颜色:  
自动设置

带格式的: 无下划线, 字体颜色:  
自动设置

带格式的: 行距: 1.5 倍行距

带格式的: 无下划线, 字体颜色:  
自动设置

带格式的: 无下划线, 字体颜色:  
自动设置

带格式的: 无下划线, 字体颜色:  
自动设置

带格式的: 无下划线, 字体颜色:  
自动设置

带格式的: 无下划线, 字体颜色:  
自动设置, 图案: 清除

带格式的: 无下划线, 字体颜色:  
自动设置

带格式的: 无下划线, 字体颜色:  
自动设置, 图案: 清除

带格式的: 无下划线, 字体颜色:  
自动设置

带格式的: 无下划线, 字体颜色:  
自动设置

带格式的: 无下划线, 字体颜色:  
自动设置, 图案: 清除

带格式的: 无下划线, 字体颜色:  
自动设置

带格式的: 无下划线, 字体颜色:  
自动设置

带格式的: 无下划线, 字体颜色:  
自动设置

带格式的: 字体: (默认) Times  
New Roman, 10 磅, 无下划线, 字  
体颜色: 自动设置

带格式的: 无下划线, 字体颜色:  
自动设置

带格式的: 无下划线, 字体颜色:  
自动设置

带格式的: 无下划线, 字体颜色:  
自动设置

277 Monsoon (EAWM). The rainfall in the desert exhibits a wide variation in space and time. Influence of the EASM is changes from southeast to northwest in the desert, and varies with latitude  
278 and distance from the Pacific Ocean, leading to the mean annual rainfall decreasing from ~450 mm in  
279 the southeast to ~150 mm in the northwest (Yang et al., 2013) (Yang et al., 2013). This uneven  
280 distribution of precipitation has a major influence on the availability of near-surface moisture,  
281 consequently on the distribution of vegetation, soil and the animal husbandry potential of local  
282 communities. The basic soil cover consists of grey desert soil in the west and changes to sierozems and  
283 chernozem or chestnut soil in the east. Through the desert, vegetation is sparse in the west and  
284 relatively abundant in the east. The natural vegetation is characteristic of desert or semi-deserts, with  
285 scrub woodland in the east and steppe in the west. Due to the scarcity of surface water, the growing  
286 season is affected by temperature, rainfall and elevation, and hence cultivation is restricted mainly to  
287 flood plains. Fixed and semi-fixed sandy dunes are dominate the landscaped in the desert land, with a  
288 few mobile dunes in area of little vegetation. Several dune types are represented various from  
289 parabolic to barchans, linear and grid formed types, ranging from a few meters to over 40 m in height  
290 (Yang et al., 2008; Zhu et al., 1980).

291 **Geology.** The Otindag Desert is located in a tectonic depression of the Solonker Suture Zone (Jian et al., 2010) bounded by the Northern Early to Mid-Paleozoic Orogen Zone and the Hatug Uul Block to the north, the Southern Early to Mid-Paleozoic Orogen Zone and the North China Craton system to the south (Fig. 2). A few faults such as the Xar Moron Fault and Chifeng-Bayan Obo Fault stretch east and west, with its northern margin along the Solonker Suture Zone marked by a series of lake basins (Figs. 1 and 2). The tectonostratigraphic units and overall structural trends are mainly oriented NE-SW (Fig. 2), which may be interpreted as resulting from overall compressive stresses oriented principally in the NW-SE quadrants during orogenesis (Jian et al., 2010; Zhang et al., 2015). Diverse rock types from unlithified and lithified clastic sediments through to carbonate, crystalline, and volcanic rocks are distributed in and around the Otindag Desert (Zhang et al., 2015) (Figs. 2 and 3XX).

302 (Bense et al., 2013, ESR-1)

303 **Tertiary and Quaternary sandstones and mudstones are the common basement rocks under the**  
304 **dunes of the Otindag, and extensive volcanic basalts forming flat terrains are to the north (Zhu et al.,**  
305 **1980; Li et al., 1995).**

306 **Hydrology and hydrogeology**

307 **The Otindag Desert originated during the Late Quaternary (Yang et al., 2015) and various**  
308 **alluvial fans formed at the margins of this desert during the early to middle Holocene. These are**  
309 **composed of conglomerate and sand deposits, where major periodic steams or wadis debouched into**  
310 **the Otindag. At present two rivers run through the eastern margin of the Otindag Desert, i.e. the**  
311 **Xilamulun River in the north and the Shandian River and its two tributaries, the Shepi River and**  
312 **Tuligen River in the south. Both stem from the eastern and southeastern parts of the Otindag (Fig. 1).**  
313 **The Xilamulun River, 380 km in length and  $32.54 \times 10^3 \text{ km}^2$  in area, is a neighboring river both to the**  
314 **northeastern Otindag and the southeastern Dali Basin, the northern catchment of the Otindag Desert.**  
315 **The Xilamulun River flows to the east and finally goes into the Xiliao River, with an annual mean**  
316 **runoff of  $6.58 \times 10^8 \text{ m}^3$  (Wu et al., 2014). The Shandian River is the upper reach of the Luan River.**

带格式的: 无下划线, 字体颜色: 自动设置

带格式的: 无下划线, 字体颜色: 自动设置

带格式的: 无下划线, 字体颜色: 自动设置

带格式的: 无下划线, 字体颜色: 自动设置

带格式的: 行距: 1.5 倍行距

带格式的: 无下划线, 字体颜色: 自动设置, 图案: 清除

带格式的: 无下划线, 字体颜色: 自动设置, 图案: 清除

带格式的: 无下划线, 字体颜色: 自动设置

带格式的: 无下划线, 字体颜色: 自动设置

带格式的: 无下划线, 字体颜色: 自动设置, 图案: 清除

带格式的: 无下划线, 字体颜色: 自动设置

带格式的: 无下划线, 字体颜色: 自动设置

带格式的: 无下划线, 字体颜色: 自动设置

带格式的: 无下划线, 字体颜色: 自动设置

带格式的: 缩进: 首行缩进: 2.5 字符, 行距: 1.5 倍行距

带格式的: 无下划线, 字体颜色: 自动设置

带格式的: 无下划线, 字体颜色: 自动设置

317 with a length of 254 km and a catchment area of  $4.11 \times 10^3 \text{ km}^2$  (Yao et al., 2013). Along the low, flat  
318 and sandy shorelines of some lakes in the Otindag, salt flats or sabkhas have formed in shallow  
319 depressions. Due to the high rate of evaporation, salt crusts develop which have been locally exploited  
320 where the salt is relatively free from sand. During rainy season, some rain and floodwaters (generally  
321 coming from the Yinshan piedmonts) are retained in low-lying areas, which may temporarily recharge  
322 shallow aquifers. Under storm conditions, occasional heavy, short rainstorms cause floods in soil-rich  
323 wadi channels. Under other conditions, sand dunes and sand sheets bury the ground and sabkhas.

324 The Otindag Desert can depend on several water-bearing formations and units (aquifers) for their  
325 groundwater resources (Fig. 3). Coarse- to fFault zone hydrogeology, [【Bense et al., 2013, ESR】](#)

326 Outerop observations indicate that fault zones commonly have a permeability structure suggesting  
327 they should act as complex conduit barrier systems in which along fault flow is encouraged and  
328 across fault flow is impeded. [【Bense et al., 2013, ESR】](#)

329 Hydrogeological observations of fault zones reported in the literature show a broad qualitative  
330 agreement with outerop-based conceptual models of fault zone hydrogeology. [【Bense et al., 2013, ESR】](#)

331 Nevertheless, the specific impact of a particular fault permeability structure on fault zone  
332 hydrogeology can only be assessed when the hydrogeological context of the fault zone is considered  
333 and not from outerop observations alone. [【Bense et al., 2013, ESR】](#)

334 Diverse rock types from unlithified and lithified clastic sediments through to carbonate, crystalline,  
335 and volcanic rocks are distributed in and around the Otindag Desert (Fig. XX). [【Bense et al., 2013, ESR】](#)

336 Fine-grained sedimentary rocks, magmatic rocks and aeolian sediments metamorphic rocks of the  
337 Inner Mongolia-Daxing'Anling Orogenic Belt (Zhang et al., 2015) XXXX geological province, form the  
338 major regional aquifer unit (Fig. 3). They are composed mainly of alluvial sediments (mid-Permian  
339 Zhesi Formation), melange (Solonker suture zone), A-type granite (early Permian), bimodal volcanic  
340 rocks with sedimentary intercalations (early Permian Dashizhai Formation), diorite-quartz  
341 diorite-granodiorite rocks (Carboniferous-Permian) and metamorphic complex (predominantly gneiss,  
342 early Paleozoic) (Fig. 2). The aquifer is generally unconfined in dune fields of the Otindag Desert,  
343 unconfined to semi-confined in the YinshanXXX Mountains' piedmont, and semi-confined to confined  
344 in the Daxing'AnlingXXX uplands (Fig. 3). Water-level measurement in June 2010 indicated that the  
345 general depth of unconfined groundwater level ranges between 10 to 70 m in the Otindag Desert (Fig.  
346 3). Local granular aquifers in the central desert are composed of coarseee coarse fluvial, lacustrine and  
347 aeolian sediments, but their extent and thickness vary throughout the watershed (Zhu et al., 1980; Li et  
348 al., 1995). [【Benoit et al., 2014, CWRJ】](#) The generally coarse-grained texture of the unconsolidated  
349 rock formations provides primary porosity in terms of groundwater flow in the desert.

350 Most of the tectonic fabric of the Appalachians was generated by compression or low angle  
351 thrusting; in those areas where major faults are strike-slip in nature, deformation is largely limited to  
352 rocks adjacent to the faults. The tectonostratigraphic units and overall structural trends are mainly  
353 oriented NE-SW, which may be interpreted as resulting from overall compressive stresses oriented  
354 principally in the NW-SE quadrants during orogenesis (Faure et al., 2004, 2006). The generally  
355 fine-grained texture of the rock formations provides negligible primary porosity in terms of

带格式的: 无下划线, 字体颜色: 自动设置

带格式的: 无下划线, 字体颜色: 自动设置

带格式的: 行距: 1.5 倍行距

带格式的: 无下划线, 字体颜色: 自动设置, 图案: 清除

带格式的: 无下划线, 字体颜色: 自动设置

带格式的: 无下划线, 字体颜色: 自动设置, 图案: 清除

带格式的: 无下划线, 字体颜色: 自动设置

带格式的: 无下划线, 字体颜色: 自动设置, 图案: 清除

带格式的: 无下划线, 字体颜色: 自动设置

带格式的: 无下划线, 字体颜色: 自动设置, 图案: 清除

带格式的: 无下划线, 字体颜色: 自动设置

带格式的: 无下划线, 字体颜色: 自动设置, 图案: 清除

带格式的: 无下划线, 字体颜色: 自动设置

带格式的: 无下划线, 字体颜色: 自动设置, 图案: 清除

带格式的: 无下划线, 字体颜色: 自动设置

带格式的: 无下划线, 字体颜色: 自动设置, 图案: 15% (自动设置前景, 白色 背景)

带格式的: 无下划线, 字体颜色: 自动设置

带格式的: 无下划线, 字体颜色: 自动设置

带格式的: 无下划线, 字体颜色: 自动设置

带格式的: 字体颜色: 自动设置

带格式的: 无下划线, 字体颜色: 自动设置

groundwater flow (Benoit et al. 2008). [Benoit et al., 2014, CWRJ].

Deformation along faults in the shallow crust (<1 km) introduces permeability heterogeneity anisotropy, which has an important impact on processes such as regional groundwater flow. Fault zones have the capacity to be hydraulic conduits connecting shallow and deep geological environments, but simultaneously the fault cores of many faults often form effective barriers to flow. The direct evaluation of the impact of faults to fluid flow patterns remains a challenge and requires a multidisciplinary research effort of structural geologists and hydrogeologists. [Bense et al., 2013, ESP]

The Uyundag Desert depend on several water bearing formations and units (aquifers) for their groundwater resources. They are composed mainly of sandstone and limestone. **[Alsharhan, 2001]**

Hydrogeology of an Arid Region The Arabian Gulf and Adjoining Areas

During rainy season, some rain and flood waters are retained behind dune dams and recharge shallow aquifers.

Two rivers inrun through the Otindag, i.e. the Xilamulun River in the north and the Shandian River and its with two tributaries of the Shepi River and the Tuligen River in the south. Both stem from the eastern and southeastern parts of the Otindag (Fig. 1). The Xilamulun River flows to the east and finally goes into the Xiliao River, with a catchment area of  $32.54 \times 10^3 \text{ km}^2$  and an annual mean runoff of  $6.58 \times 10^8 \text{ m}^3$  (Wu et al., 2014). The Shandian River is the upper reach of the Luan River, with a length of 254 km and a catchment area of  $4.11 \times 10^3 \text{ km}^2$  (Yao et al., 2013).

### 3. Methods

The hydrochemistry of natural water in the Otindag Desert, as related to the prevailing EASM climate, as well as, the dominant topographical, geological (tectonic) and hydrogeological conditions, are discussed here and interpreted, using chemical and isotope analyses of water samples from rain, springs, shallow aquifers and deep aquifers, rivers and lakes, and are represented on relevant graphs and diagrams. Fieldworks took place during the summer season of 2011 and the spring season of 2012. The water samples selected in this study were all collected from natural water, including the groundwater, river water, lake water, spring water and precipitation water in types A. Total of twenty five water samples were analyzed collected for ion chemical, stable and radioactive isotopic analysis for in this study. Water Groundwater samples is the major type among these waters, which were mainly retrieved taken from shallow and deep wells widely located over a wide area in dune fields of the study regions area. The detailed locations of the sampling sites are shown in Fig. 4.

Two groups of parameters are measured to characterize the chemistry of any water analysis: field-measured parameters and lab-measured parameters. The filed-measured parameters include temperature (°C), hydrogen-ion concentration (pH), electrical conductivity (EC in micro-Siemens per centimeter or  $\mu\text{S}/\text{cm}$ ) and total dissolved solid (TDS, mg/L). The values of these parameters change when they are not directly measured in the field. The number lab-measured parameters depend on the purpose of study. However, the measurement of major cations ( $\text{F}^-$ ,  $\text{Cl}^-$ ,  $\text{NO}_2^-$ ,  $\text{NO}_3^-$ ,  $\text{SO}_4^{2-}$ ,  $\text{HCO}_3^-$ ,  $\text{CO}_3^{2-}$  and  $\text{H}_2\text{PO}_4^-$ ) and anions ( $\text{Li}^+$ ,  $\text{Na}^+$ ,  $\text{NH}_4^+$ ,  $\text{K}^+$ ,  $\text{Mg}^{2+}$  and  $\text{Ca}^{2+}$ ) are determined in most chemical analyses. Analysis for stable ( $^2\text{H}$  and  $^{18}\text{O}$ ) and radioactive isotopes ( $^3\text{H}$ ) in rain and groundwater are

带格式的：字体颜色：自动设置

**带格式的:** 无下划线, 字体颜色:  
自动设置

**带格式的:** 无下划线, 字体颜色:  
自动设置

**带格式的:** 无下划线, 字体颜色:  
自动设置, 图案: 清除

**带格式的:** 无下划线, 字体颜色:  
自动设置

**带格式的:** 无下划线, 字体颜色:  
自动设置, 图案: 清除

**带格式的:** 无下划线, 字体颜色:  
自动设置

带格式的：行距：1.5 倍行距

带格式的：无划线，字体颜色：  
自动设置，下标

自动设置, 下标

带格式的：无下划线，字体颜色：

带格式的：无下划线，字体颜色：  
自动设置 上标

**带格式的:** 无下划线, 字体颜色:  
自动设置, 上标

**带格式的:** 无下划线, 字体颜色:  
自动设置, 上标

带格式的：无下划线，字体颜色：  
自动设置

396 also included. The analytical data of the physiochemical parameters and the stable and radioactive  
397 isotopes of the water samples collected in this study are listed in Tables 1, 2 and 3, respectively.

398 The surface waters were mainly sampled from rivers and lakes in the Otindag, and the spring  
399 waters were collected from the riverhead of the Xilamulun River, the Shepi River and the Tuligen River.  
400 One rainfall sample of the local atmospheric precipitation (p1) was also collected at the southeastern  
401 margin of the Otindag in the 2011 summer season. Water samples were filtered using 0.45  $\mu$ m  
402 membrane filters for cation and anion analysis, and were acidified with 1% HNO<sub>3</sub> for cation  
403 analysis. Water samples for stable and radioactive isotope analysis were collected in the field with a  
404 polyethylene bottles of 0.5 L in volume, respectively. Variables Some kinds of analysis were measured  
405 on site with a portable instrument (Eijkelkamp). These determinations included temperature, pH,  
406 oxidation reduction potential (Eh), electrical conductivity (EC), and total dissolved solid (TDS). The  
407 measurement errors bars were  $\pm 0.1$  °C for temperature,  $\pm 1\%$  for pH,  $\pm 5\%$  for Eh,  $\pm 5\%$  for EC, and  
408  $\pm 0.5\%$  for TDS, respectively.

409 The concentrations of major anions (F<sup>-</sup>, Cl<sup>-</sup>, NO<sub>3</sub><sup>-</sup>, NO<sub>2</sub><sup>-</sup>, SO<sub>4</sub><sup>2-</sup> and H<sub>2</sub>PO<sub>4</sub><sup>-</sup>) and cations (Li<sup>+</sup>, Na<sup>+</sup>,  
410 NH<sub>4</sub><sup>+</sup>, K<sup>+</sup>, Mg<sup>2+</sup> and Ca<sup>2+</sup>) were determined by electrochemical detectors of an ion chromatography  
411 (Dionex 600) in the Institute of Geology and Geophysics, Chinese Academy of Sciences, with  
412 measurement errors bars  $\pm 3\%$  for anions and  $\pm 2\%$  for cations. The concentrations of carbonate  
413 (alkaline) ions of HCO<sub>3</sub><sup>-</sup> and CO<sub>3</sub><sup>2-</sup> were measured by titration with HCl (0.1 M) following the Gran  
414 Method (Gran, 1952), with an error bar  $\pm 5\%$ . The hardness (HD, German standards) of these water  
415 samples was calculated based on the equation HD = ([Mg<sup>2+</sup>]  $\times$  100/24.305 + [Ca<sup>2+</sup>]  $\times$  100/40.08)/17.847,  
416 [Mg<sup>2+</sup>] and [Ca<sup>2+</sup>] referring to the concentration of Mg<sup>2+</sup> and Ca<sup>2+</sup> with unit of mg/L.

417 Two stable isotopes of <sup>2</sup>H and <sup>18</sup>O, as being expressed in  $\delta$  notation ( $\delta^{2H} = ^2H/H - ^2H/H_{VSMOW}$ ,  $\delta^{18O} = ^{18}O/^6O - ^{18}O/^6O_{VSMOW}$ )  
418 relative to the Vienna standard mean water (VSMOW), were measured for all of the water samples  
419 collected in this study using MAT 252 in the Laboratory for Stable Isotope Geochemistry, Institute of  
420 Geology and Geophysics, Chinese Academy of Sciences, with  $\pm 0.374\%$  for  $\delta^{2H}$  and  $\pm 0.062\%$  for  
421  $\delta^{18O}$  and  $\delta^{18O}$ , respectively.

422 Several groundwater samples (500 ml each), collected from wells (6–60 m deep) in the study area,  
423 were prepared for the analysis of radioactive isotope (tritium) analysis. 300 ml of water sample, added  
424 with addition of 1 g KMnO<sub>4</sub>, were distilled to remove any impurities. In order to increase the tritium  
425 concentration to an easily measurable level, electrolytic enrichment was applied (Kaufman, 1954;  
426 Baeza et al., 1999). A volume of 250 ml of previously distilled sample with 2.5 g NaOH was then put  
427 to the electrolysis apparatus containing electrolytic cells with co-axial stainless steel electrodes.  
428 Electrolysis was carried out until the volume of electrolyte was reduced to 8 ml and all runs were  
429 performed at a temperature of 2–5 °C to prevent the loss of tritiated water molecules by evaporation.  
430 After electrolysis CO<sub>2</sub> was bubbled through the cell to neutralize the water because the medium in  
431 which the electrolysis took place earlier is alkaline. The water sample was separated from the  
432 electrolyte by distilling. The pretreated samples were measured by a low level background liquid  
433 scintillation counter (Quantulus 1220-003) according to the manufacturer's guidelines. The error bar of  
434 the measurement errors are should be  $\pm 3\%$ . The tritium data of several groundwater samples collected  
435 in this study had been partially mentioned by Yang et al. (2015) as one of the supplementary materials.

带格式的: 无下划线, 字体颜色: 自动设置

带格式的: 无下划线, 字体颜色: 自动设置, 下标

带格式的: 无下划线, 字体颜色: 自动设置

带格式的: 无下划线, 字体颜色: 自动设置

带格式的: 无下划线, 字体颜色: 自动设置

436 It was systematically discussed in this study.

437

#### 438 **4. Results and Discussions**

439

440 The analytical data of the physicochemical parameters and the stable and radioactive isotopes of  
441 the water samples collected in this study were listed in Tables 1, 2 and 3, respectively. The study area  
442 and the sampling sites location for each sample analyzed were showed in Figs. 1 and 2, respectively.

443

##### 444 **4.1. Hydrochemical characteristics of natural the ground and surface waters in the Otindag**

445 The pH values of the water samples studied varied from 6.26 to 9.44 (except sample p1,  
446 precipitation, 4.61) (Table 1) with a median value of 7.27, indicating that the waters are generally  
447 neutral to slightly alkaline. The TDS ranged between 67 mg/L and 660 mg/L (average 211 mg/L) (Table  
448 1), all belonging to fresh water (TDS < 1000 mg/L) in the salination classification of natural water  
449 (Meybeck, 2004). The natural water samples collected in this study are generally neutral to slightly  
450 alkaline, with the pH values varying between 6.26 and 9.44 (except the precipitation sample p1, 4.61)  
451 (Table 1) and a median value of 7.27. The TDS values range between 67 and 660 mg/L (average 211  
452 mg/L) (Table 1), all belonging to fresh water (TDS < 1000 mg/L) in the salination classification of  
453 natural water (Meybeck, 2004).

454 The variations in ion concentrations of the major cations and anions in the studied water samples  
455 were displayed in a Schoeller diagram (Schoeller, 1955), a fingerprint diagram with a semi-logarithm  
456 offy-axis (Fig. 3). The rain water sample is the most depleted in ions among these samples. The general  
457 The the groundwater samples have had the highest concentrations of cations and anions while the  
458 precipitation sample (p1) had the lowest concentrations, and the lake, river and spring waters had  
459 intermediate the medium values. The calcium concentration is was the highest among cations in  
460 almost all of the water samples, and the  $\text{HCO}_3 + \text{CO}_3$  concentration (bicarbonate + carbonate, alkalinity)  
461 is was the highest among anions in most of the water samples. For except for several groundwater  
462 samples (g3, g4, g5, g6 and g11), and one of the spring sample (s1) and the precipitation sample (p1),  
463 they have which had the higher  $\text{SO}_4$  concentrations than the alkalinity (Fig. 5).

464 Two chemically distinct water types are recognized for the studied waters via a Piper diagram  
465 (Fig. 6) (Piper, 1944), calcium bicarbonate and calcium sulphate (Fig. 4). The relative differences in  
466 abundance of ion concentrations between different water can be detectable revealed in a Piper  
467 diagram (Piper, 1944). The water samples studied can be classified into two water types in the Piper  
468 diagram (Fig. 4). Type I, the  $\text{Ca}-\text{HCO}_3$  water, which generally represents the typical bicarbonate  
469 water experienced affected by near surface mineral weathering, and type II, the  $\text{Ca}/\text{Mg}-\text{SO}_4$  water, which  
470 indicates saline water dominated by alkaline earth metals (Zhu et al., 2011, 2012; Clark, 2015). For  
471 water type I, the weak acids exceeded the strong acids; the carbonate hardness (secondary alkalinity)  
472 exceeded 50% and was dominated by the alkaline earths. While for water Type II, the strong acids  
473 exceeded the weak acids and no carbonate hardness exceeded 50%. The alkaline earths ( $\text{Ca}+\text{Mg}$ )  
474 exceeded the alkalis ( $\text{Na}+\text{K}$ ) in all the water samples studied. There were no any Chloride-type and  
475 sodium Na-type waters occurring in the study area (Fig. 6). Based on more than 10,000 chemical

带格式的: 无下划线, 字体颜色: 自动设置

带格式的: 无下划线, 字体颜色: 自动设置, 图案: 15% (自动设置 前景, 白色 背景)

带格式的: 无下划线, 字体颜色: 自动设置



516  $\delta D = 6.36 \delta^{18}\text{O} + 5.21 (R^2 = 0.93, n = XX)$  for precipitation water in the Baotou Station.

517

518

519  $\delta D = 6.86 \delta^{18}\text{O} - 2.22 (R^2 = 0.91, n = XX)$  for precipitation water in spring in the Tianjin Station.

520

521  $\delta D = 6.68 \delta^{18}\text{O} - 0.98 (R^2 = 0.92, n = XX)$  for precipitation water in summer in the Tianjin Station.

522

523  $\delta D = 5.51 \delta^{18}\text{O} - 4.12 (R^2 = 0.55, n = XX)$  for precipitation water in autumn in the Tianjin Station.

524

525  $\delta D = 7.44 \delta^{18}\text{O} + 13.57 (R^2 = 0.94, n = XX)$  for precipitation water in winter in the Tianjin Station.

526

527

528  $\delta D = 6.66 \delta^{18}\text{O} + 0.30 (R^2 = 0.93, n = XX)$  for precipitation water in spring in the Baotou Station.

529

530

531 The stable isotopes of  $\delta^2\text{H}$  and  $\delta^{18}\text{O}$  were analyzed for all the water samples collected in this study, as shown in Table 3 and Fig. 6. The radioactive isotope of tritium ( $^3\text{H}$ ) was analyzed for a part of the groundwater samples.

532 The  $\delta D^2\text{H}$  values of the groundwater samples collected in this study varied from -63.42‰ to -75.92‰ (Table 3), with an average -69.53‰. The  $\delta^{18}\text{O}$  values ranged between -8.64‰ and -11.26‰ (Table 3), with an average -10.17‰.

533 The spring water samples, which directly drain into rivers, were relatively concentrated in  $\delta^2\text{H}$  and  $\delta^{18}\text{O}$  and were greatly similar to those of the groundwater samples (Fig. 76). The  $\delta^2\text{H}$  and  $\delta^{18}\text{O}$  values in the spring samples varied from -70.83‰ to -72.60‰ (mean value -71.72‰) and from -10.34‰ to -10.47‰ (mean value -10.40‰), respectively (Table 3).

534 The  $\delta D^2\text{H}$  and  $\delta^{18}\text{O}$  values in the river water samples were slightly more variable and were also similar to those of the groundwater (Fig. 76), with a range of between -65.00‰ and -85.16‰ (mean value -73.02‰) in  $\delta D^2\text{H}$  values and a range of between -9.55‰ and -11.78‰ (mean value -10.51‰) in  $\delta^{18}\text{O}$  (Table 3).

535 The lake water samples in this study were enriched in  $\delta^2\text{H}$  and  $\delta^{18}\text{O}$  by comparison to the groundwater samples (Fig. 6), with a variable range of between -34.16‰ and -53.13‰ (mean value -46.47‰) in  $\delta^2\text{H}$  values and a range of between 0.38‰ and -6.55‰ (mean value -4.65‰) in  $\delta^{18}\text{O}$  (Table 3).

536 The precipitation sample p1 was also enriched in  $\delta D$  and  $\delta^{18}\text{O}$  by comparison to the groundwater samples (Fig. 76), showed the  $\delta^2\text{H}$  value of -47.4‰ and the  $\delta^{18}\text{O}$  value of -7.14‰, respectively (Table 3). The content of radioactive isotope of tritium ( $^3\text{H}$ ) measured in seven well groundwater samples with 6-60 m depth ranged from 1.86 to 24.35 TU (Table 3), with an average 14.95 TU, higher than the mean tritium concentration (9.8 TU) of groundwater in the Vienna Basin, Austria (Stolp et al., 2010), the seat of the International Atomic Energy Agency (IAEA).

537 If we plot the relationships between oxygen and hydrogen isotopes of groundwater, spring, river water and lake water samples, we observed that the regression line that fits all data points can be

带格式的: 无下划线, 字体颜色: 自动设置

带格式的: 行距: 1.5 倍行距

带格式的: 无下划线, 字体颜色: 自动设置

带格式的: [1]

带格式的: [2]

带格式的: [3]

带格式的: [4]

described by the equation:  $\delta D = 4.09\delta^{18}\text{O} - 28.31$  ( $R^2=0.93$ ,  $n=24$ ) between two straight lines with a gradient of 4.4, but with different y intercepts (EL1 in Fig. 76 XX), as shown in. This local groundwater line (LGWL) is different from the Global Meteoric Water Line (GMWL,  $\delta D = 88\delta^{18}\text{O} + 10$ ) and the Mediterranean Meteoric Water Line (MMWL,  $\delta D = 88\delta^{18}\text{O} + 20$ ) estimated by Craig (1961), but it is similar to the local groundwater lines established for other deserts in northern China and central Asia with a same slope but different Y-intercepts, such as  $\delta D = 4.17\delta^{18}\text{O} - 31.3$  for the Badanjilin Desert (Jin et al., 2018),  $\delta D = 4.8\delta^{18}\text{O} - 15.2$  for the Ejina Desert in China (Wang et al., 2013), and  $\delta D = 4.26\delta^{18}\text{O} + 9.23$  for the Rub Al Khal Desert in the United Arab Emirates (Rizk and El-Etr, 1997). The scatter of stable isotope data points for the lake water samples (Fig. 76) in the Otindag suggests that the lake waters are affected by evaporation, but the other waters in the desert are not so, the following equations:

$$\delta D = 4.38\delta^{18}\text{O} - 24.97$$
 ( $R^2=0.87$ ,  $n=11$ ) for groundwater samples.

$$\delta D = 4.44\delta^{18}\text{O} - 24.56$$
 ( $R^2=0.86$ ,  $n=13$ ) for groundwater and spring water samples.

$\delta D = 4.09\delta^{18}\text{O} - 28.31$  ( $R^2=0.93$ ,  $n=24$ ) for groundwater, springer water, river water and lake water samples.

$$\delta D = 7.95\delta^{18}\text{O} + 10.52$$
 ( $R^2=0.77$ ,  $n=5$ ) for river water samples.

$$\delta D = 2.69\delta^{18}\text{O} - 33.94$$
 ( $R^2=0.92$ ,  $n=6$ ) for lake water samples.

$$\delta D = 6.57\delta^{18}\text{O} + 0.31$$
 ( $R^2=0.88$ ,  $n=XX$ ) for precipitation water in the Tianjin Station.

$$\delta D = 6.36\delta^{18}\text{O} - 5.21$$
 ( $R^2=0.93$ ,  $n=XX$ ) for precipitation water in the Baotou Station.

$$\delta D = 6.86\delta^{18}\text{O} - 2.23$$
 ( $R^2=0.91$ ,  $n=XX$ ) for precipitation water in spring in the Tianjin Station.

$$\delta D = 6.68\delta^{18}\text{O} - 0.98$$
 ( $R^2=0.93$ ,  $n=XX$ ) for precipitation water in summer in the Tianjin Station.

$$\delta D = 5.51\delta^{18}\text{O} - 4.13$$
 ( $R^2=0.55$ ,  $n=XX$ ) for precipitation water in autumn in the Tianjin Station.

$$\delta D = 7.44\delta^{18}\text{O} + 13.57$$
 ( $R^2=0.94$ ,  $n=XX$ ) for precipitation water in winter the Tianjin Station.

$$\delta D = 6.66\delta^{18}\text{O} + 0.30$$
 ( $R^2=0.93$ ,  $n=XX$ ) for precipitation water in spring in the Baotou Station.

$$\delta D = 5.07\delta^{18}\text{O} - 15.1$$
 ( $R^2=0.80$ ,  $n=XX$ ) for precipitation water in summer in the Baotou Station.

$$\delta D = 6.98\delta^{18}\text{O} + 0.85$$
 ( $R^2=0.95$ ,  $n=XX$ ) for precipitation water in autumn in the Baotou Station.

$$\delta D = 6.86\delta^{18}\text{O} - 0.72$$
 ( $R^2=0.98$ ,  $n=XX$ ) for precipitation water in winter in the Baotou Station.

The isotopic regression equation of the Otindag evaporation line (EL1) (Fig. 6), which was calculated based on the  $\delta^2\text{H}$  and  $\delta^{18}\text{O}$  data of the groundwater, lake, river and spring water samples in this study, was  $\delta^2\text{H} = 4.09\delta^{18}\text{O} - 28.31$  ( $R^2=0.93$ ,  $n=24$ ).

The content of radioactive isotope of tritium ( ${}^3\text{H}$ ) was measured in seven well groundwater samples with 6-60 m depth in this study. The tritium concentrations ranged from 1.86 to 24.35 TU (Table 3), with an average 14.95 TU, higher than the mean tritium concentration (9.8 TU) of groundwater in the Vienna Basin, Austria (Stolp et al., 2010), the seat of the International Atomic Energy Agency (IAEA).

域格式的: 无下划线, 字体颜色: 自动设置

域代码已更改

带格式的: 无下划线, 字体颜色: 自动设置

596 **5 Discussion**

597

598 **4.5.2.1 Evaluation of Local precipitation recharge on as a recharge source of groundwater in the**

599 **Otindag**

600 **Comparison of the isotopic signals between the modern regional precipitation and natural waters**

601 **in the Otindag**

602 To incorporate the isotopic analysis of precipitation with similar areas in the studied area, local  
603 data (p1) was plotted with those of Baotou (Fig. 76). The isotopic composition of rainfall in Baotou,  
604 the nearest long-term station to the Otindag Desert, was monitored for the period 1986-2001 within the  
605 scope of the International Atomic Energy Agency/World Meteorological Organization (IAEA/WMO)  
606 global survey. The stable isotope data available from this station was used to provide basic  
607 characteristics of the stable isotopic composition of the present-day meteoric water, especially in the  
608 westward inland areas of the Otindag Desert (Fig. 1). Stable isotope data of the Tianjin station was also  
609 used to characterize precipitation of the eastern coastal areas of the Otindag Desert (Fig. 1).

610 At present, the extensive record of stable isotope measurements from atmospheric precipitation  
611 areas still lacking from absent in the Otindag. Thus in this study, we used the decadal isotope data of  
612 atmospheric precipitation around the Otindag were collected in this study to determine the isotopic  
613 relationship between the local groundwater and the regional precipitation that are available from. A  
614 global database, the IAEA Global Network of Isotopes in Precipitation (GNIP) database, is available to  
615 use in this study. Taking into account the boundary between the northern hemispheric westerly and the  
616 Asian summer monsoon (Chen et al., 2010), which are the two major climate systems controlling the  
617 Otindag (Yang et al., 2013), we chose two GNIP meteorological stations as the representations of the  
618 atmospheric precipitation derived from the northern hemispheric westerly and the Asian summer  
619 monsoon, respectively. One is the Baotou station, located to the southwest of the Otindag as  
620 representative of (the westerly system), and another is the Tianjin station, located to the southeast of the  
621 Otindag, as representative of (the Asian summer monsoon system) (Fig. 1a). The historical isotopic data  
622 ( $\delta^2\text{H}$ ,  $\delta^3\text{H}$  and  $\delta^{18}\text{O}$ , ‰ VSMOW) over the last four decades from the two stations, as well as other data  
623 including the daily precipitation amount (mm) and air temperature (°C) in the same period, were taken  
624 as the references of the stable isotopic signals in precipitation in the Otindag.

625 The annual weighted mean values of  $\delta^2\text{H}$  and  $\delta^{18}\text{O}$  at the Baotou station varied were variable from  
626 -64.32‰ to -48.44‰ and from -9.40‰ to -6.50‰ during the period of 1986 to 1992, respectively. The  
627 annual weighted mean values of  $\delta^2\text{H}$  and  $\delta^{18}\text{O}$  at the Tianjin station varied from -56.30‰ to -43.72‰  
628 and from -8.35‰ to -6.86‰ during the period of 1988 to 1992 and of 2000 to 2001, respectively. The  
629 long term weighted mean values of  $\delta^2\text{H}$  and  $\delta^{18}\text{O}$  at the Baotou station (LWMB) were -55.27‰ and  
630 -7.78‰, respectively, and were -49.97‰ and -7.70‰ at the Tianjin station (LWMT), respectively. The  
631 radioactive isotope of  ${}^3\text{H}$  (TU) in precipitation was not stable at the GNIP Baotou station. The annual  
632 weighted mean values were higher than 30 TU in this station and tended to be decreased from 1986 to  
633 1991 (72.06, 57.81, 59.97, 52.79, 55.89, 34.35 TU, respectively). The annual weighted mean values of  
634  ${}^3\text{H}$  at the GNIP Tianjin station were lower than those of the Baotou station. The mean values were  
635 21.99, 21.65, 18.55, 25.72, 18.80 TU from 1988 to 1992, and 7.01 and 15.48 TU from 2000 to 2001.

带格式的: 无下划线, 字体颜色: 自动设置

带格式的: 无下划线, 字体颜色: 自动设置

带格式的: 无下划线, 字体颜色: 自动设置, 图案: 15% (自动设置 前景, 白色 背景)

带格式的: 图案: 15% (自动设置 前景, 白色 背景)

带格式的: 无下划线, 字体颜色: 自动设置

636 As the sample p1, the only one precipitation sample collected in this study (during the 2011  
637 summer rainfall event) of the Otindag, the sample p1 fell onto the Global Meteoric Water Line (GMWL,  
638  $\delta^2\text{H} = 8\delta^{18}\text{O} + 10$ ) estimated by Craig (1961). It showed similar  $\delta^2\text{H}$  and  $\delta^{18}\text{O}$  values to those of the  
639 precipitation collected in the GNIP stations of Baotou and Tianjin (Fig. 6).

640 Compared to the precipitation data from the GNIP Baotou and Tianjin stations and from the local  
641 precipitation (p1) in the Otindag, the groundwater samples were evidently depleted in heavy stable  
642 isotopes in the Otindag HSKDSL (Fig. 6).

643 In contrast to the precipitation data, the water samples from springs and rivers in the study area  
644 also showed a depletion characteristics in the stable isotopes of  $\delta^2\text{H}$  and  $\delta^{18}\text{O}$  (Fig. 6).

645 Based on the isotopic data from the Baotou station, the local regional meteoric water lines, i.e.,  
646 the regional Craig lines, can be statistically described as the isotopic regression equation of  
647  $\delta^2\text{H} = 6.36\delta^{18}\text{O} - 5.21$  (line-LMWL-B). It can also, based on the isotopic data from the Baotou  
648 station, and can be described as  $\delta^2\text{H} = 6.57\delta^{18}\text{O} + 0.31$  (line-LWML-T), based on the data  
649 from the Tianjin station (Fig. 7). The precipitation sample p1 collected in this study fell onto the  
650 GMWL (Fig. 7). It also showed similar  $\delta\text{D}$  and  $\delta^{18}\text{O}$  values to those of the precipitation collected in the  
651 GNIP stations of Baotou and Tianjin (Fig. 7).

652 Compared to the precipitation data from the GNIP stations and from the local precipitation (p1),  
653 the groundwater, spring, and river water samples were evidently depleted in heavy stable isotopes in  
654 the Otindag (Fig. 7). Except for the lake water samples, most of the groundwater, river water and  
655 spring water samples in the Otindag fell on or lay between the LMWL-B and the LMWL-T lines,  
656 and were located at the lower left area of the precipitation points (Fig. 7). This indicates indicated  
657 that no strong deep evaporation process was experienced by these ground and surface waters (except for  
658 lake waters) compared with than the precipitation.

659 For the Otindag evaporation line (EL1), its equation slope and intercept were significantly lower  
660 than that of the GMWL, LMWL B and LMWL T (Fig. 6). The points of intersection between the EL1  
661 and LMWL B were atwas 69.93% for  $\delta^2\text{H}$  and 10.18% for  $\delta^2\text{H}$  and for  $\delta^{18}\text{O}$ , respectively, while the  
662 intersection points between the EL1 and LMWL T werewas 75.51% for  $\delta^2\text{H}$  and 11.54% for  $\delta^2\text{H}$   
663 and  $\delta^{18}\text{O}$ , respectively.

## 664 5.2. The direct recharge of groundwater in the eastern Otindag

665 Water infiltration of atmospheric precipitation through the unsaturated zone to groundwater is  
666 hydrologically defined as the direct recharge. The deuterium and oxygen isotopes are the composition  
667 of water molecules and are sensitive to physical processes such as mixing and evaporation, hence they  
668 are ideal tracers of the origin of groundwater (Coplen, 1993; Seanlon et al., 2006). We used them to  
669 identify the contribution of precipitation recharge on groundwater in this study.

670 Because the annual mean precipitation amount in the semi-arid regions of northern China is  
671 between 200–400 mm, it seems that the direct recharge on groundwater cannot be neglected in the  
672 eastern Otindag under a semi-arid climate. However, when we checked the stable isotopic data from the  
673 GNIP stations both at the Baotou and Tianjin, we observed that almost all the annual weighted mean  
674 values of the stable isotope contents in precipitation were enriched in  $\delta^2\text{H}$  and  $\delta^{18}\text{O}$  compared with than

带格式的: 无下划线, 字体颜色: 自动设置

带格式的: 字体: (默认) +西文正文, 五号, 无下划线, 字体颜色: 自动设置

带格式的: 无下划线, 字体颜色: 自动设置

带格式的: 无下划线, 字体颜色: 自动设置

带格式的: 无下划线, 字体颜色: 自动设置

带格式的: 行距: 1.5 倍行距

带格式的: 无下划线, 字体颜色: 自动设置

带格式的: 无下划线, 字体颜色: 自动设置, 图案: 15% (自动设置前景, 白色 背景)

带格式的: 无下划线, 字体颜色: 自动设置

带格式的: 无下划线, 字体颜色: 自动设置

带格式的: 无下划线, 字体颜色: 自动设置

带格式的: 无下划线, 字体颜色: 自动设置

676 those values measured for the groundwater, spring water and river watersamples in this study (Fig.  
677 6). Because the isotopic evolution of  $\delta D^2H$  and  $\delta^{18}O$  in water illustrated in the Craig line represents a  
678 one-way and irreversible process, thus the water bodies distributed at the upper right area of the Craig  
679 line can not be recharge sources for the water bodies distributed at the lower left area of the line. Such  
680 results indicated that the groundwater, river water and spring water in the Otindag are not  
681 recharged by the regional precipitation, namely no significant modern direct recharge has taken place  
682 for groundwater in the Otindag.

683 Dogramaci et al. (2012) documented that only the intense and remarkable rainfall events of >20 mm could remarkably recharge groundwater in the semi-arid Hamersley Basin of northwest Australia,  
684 while the rainfall events <20 mm had limited influences on groundwater recharge. Chen et al. (2014) described that rainfall events  $\leq 5$  mm in the arid and semi-arid region of northern China would be evaporated into the atmosphere rapidly before it is infiltrated into the groundwater system. Based on the analysis on the data records from two meteorological stations around the Otindag, i.e., the Duolun station and the Xilinhaote stations (see Fig. 1a), we observed that the average times of rainfall events being >20 mm on average in amount were only occur 2.5-3.4 times per year (Table 4). In some years (e.g. from 2005 to 2007 at the Xilinhaote Station), no Even none of the rainfall events of >20 mm even occurred during the year from 2005 to 2007 at the Xilinhaote Station. It further indicated confirmed that the small amounts of intensive rainfall events had limited the contribution of regional precipitation on groundwater recharge in the Otindag.

695 In addition to groundwater, the river water and spring water samples from the the Otindag  
696 had the similar isotopic signals with those of groundwaters, and were also deviated from the local  
697 modern regional precipitation in the Craig diagram (Fig. 76). These water samples came from the Xilamulun, Shepi and Tuligen rivers. They shared the same evaporation line (EL1) with the groundwater and lake water samples (Fig. 76). Generally speaking, natural waters that have a same recharge source are can be distributed on a same line of evaporation in the  $\delta^2$  and  $\delta^{18}O$  diagram (Chen et al., 2012b) (Chen et al., 2012b). This indicates that the recharge sources of groundwater, river water, spring water and lake water in the Otindag are were genetically associated each other and were differ from ential to the local regional precipitation. During the field investigation, we observed that the elevation of spring outflow was lower than that of the groundwater table in some areas. This implies yes that the spring water can be originateds from the local phreatic water (groundwater). The same isotopic signals between the two kinds of water confirmed their close relationship in origin.

#### 707 45.3.3. Winter precipitation and palaeowater recharge on groundwater in the Otindag

708 Potential sources of groundwater other than summer precipitation in the Otindag: three  
709 hypotheses

710 Since the groundwater samples in the Otindag are were depleted in their  $\delta D^2H$  and  $\delta^{18}O$  values even more than those of the modern local rainfall (Fig. 76), they must be sourced from other waters characterized by similar with same or more depleted signals in their stable isotopes compositions. Due to the temperature effect (such as evaporation) on isotopic fractionation, only the waters issued from colder environments can be more depleted in their  $\delta D$  and  $\delta^{18}O$  values even more than those of the

带格式的: 字体: (默认) +西文正文, 五号, 无下划线, 字体颜色: 自动设置, 检查拼写和语法

带格式的: 缩进: 首行缩进: 2 字符

带格式的: 无下划线, 字体颜色: 自动设置

带格式的: 字体: (默认) +西文正文, 五号, 无下划线, 字体颜色: 自动设置, 检查拼写和语法

带格式的: 无下划线, 字体颜色: 自动设置

716 local rainfall.

717 Because the Otindag Desert is under the control of the EASM climate (Fig. 1), the local rainfall\*  
718 in the desert is mainly sourced from summer precipitation. This can also be illustrated by the seasonal  
719 distributions in annual mean precipitation (Fig. 87a), in annual mean air temperature (Fig. 87b) and in  
720 annual mean water vapor pressure (Fig. 87c) over the last forty years at the two surrounding GNIP  
721 weather stations in Baotou and Tianjin.

722 ~~Climatically (Because the Otindag Desert is under the control of the East Asian Summer Monsoon~~  
723 ~~climate (Yang et al., 2013), thus the local modern rainfall in the desert is mainly sourced from the~~  
724 ~~summer season's precipitation, with rain and heat over the same period. These climatic characteristics~~  
725 ~~were illustrated by the seasonal distributions of the annual mean precipitation amount (Fig. 7a), the annual~~  
726 ~~mean air temperature (Fig. 7b) and the annual mean water vapor pressure (Fig. 7c) over the last forty~~  
727 ~~years at the two surrounding GNIP weather stations in the Baotou and Tianjin. The seasonal~~  
728 ~~distributions of stable isotopes in the two stations (Fig. 8d-e) show that the se records indicates that the~~  
729 ~~summer rainfall is warmer and evidently relatively positive in its the signals of  $\delta D^2H$  and  $\delta^{18}O$  by~~  
730 ~~comparison with those of the winter rainfall, further suggesting that the waters issued from cold~~  
731 ~~environments can be more depleted in their  $\delta D$  and  $\delta^{18}O$  values than those of the summer rainfall, the~~  
732 ~~waters originated in a colder environment, due to the evaporation effect on isotopic fractionation. It~~  
733 ~~Thus we can be speculated that the potential water sources of groundwater in the Otindag can be~~  
734 ~~potentially must be derived from waters originated in a colder environment, such as (1) the modern~~  
735 ~~precipitation in winter, (2) the palaeowater formed in the past glacial period, or (3) remote/the~~  
736 ~~mountains waters that emanate in with colder and wetter conditions.~~

737 Given the hypothesis (1) “the modern winter precipitation”, we can get clues from the isotopic  
738 records of winter precipitation in the Baotou and Tianjin stations. It is shown that the annual mean  
739 values of  $\delta D^2H$  and  $\delta^{18}O$  over the last forty years are more depleted in the winter precipitation  
740 than in the summer precipitation at the Baotou and Tianjin stations (Fig. 8d-ea-b). This isotopic signal  
741 qualifies the suggested that the regional winter precipitation to be was qualified to be a potential source of  
742 groundwaters in the Otindag. However, the limited water amount of the winter precipitation in these  
743 regions seemed to be a question towards its importance as an efficient source of  
744 groundwater because the precipitation amounts and the water vapor pressures (effective moisture) in the  
745 winter months are much lower than those in the summer months at both the Baotou and Tianjin  
746 stations (Fig. 87a and 87c). It indicates that the winter seasons in these regions are relatively  
747 colder and drier but not colder and wetter. A colder-wetter pattern of winter season precipitation is a  
748 necessary condition for winter precipitation to be as a water source for the formation of groundwater  
749 under a summer monsoon climate. This is, because the bigger amounts of summer precipitation will  
750 easily remove or weaken the depleted isotopic signals of winter precipitation in groundwater. In this  
751 regard, view of this consideration, the modern winter precipitation is unlikely to might not be an  
752 important source of groundwater in the Otindag. The hypothesis (1) can be neglected.

753 As to the hypothesis (2) “the palaeowaters<sup>2</sup> formed in colder and wetter periods such as the last  
754 glacial<sup>2</sup>, it has been proposed to be a potential water source for groundwaters in the wide arid lands of  
755 the world. In fact, The depleted signals of stable isotopes ( $\delta D^2H$  and  $\delta^{18}O$ ) in groundwater have been

带格式的: 无下划线, 字体颜色: 自动设置

带格式的: 无下划线, 字体颜色: 自动设置

带格式的: 无下划线, 字体颜色: 自动设置, 图案: 清除

带格式的: 无下划线, 字体颜色: 自动设置

带格式的: 无下划线, 字体颜色: 自动设置, 图案: 清除

带格式的: 无下划线, 字体颜色: 自动设置

带格式的: 无下划线, 字体颜色: 自动设置, 图案: 清除

带格式的: 无下划线, 字体颜色: 自动设置

带格式的: 无下划线, 字体颜色: 自动设置, 图案: 清除

带格式的: 无下划线, 字体颜色: 自动设置

带格式的: 无下划线, 字体颜色: 自动设置, 图案: 清除

带格式的: 无下划线, 字体颜色: 自动设置

带格式的: 无下划线, 字体颜色: 自动设置, 图案: 15% (自动设置前景, 白色 背景)

带格式的: 无下划线, 字体颜色: 自动设置

带格式的: 无下划线, 字体颜色: 自动设置, 图案: 15% (自动设置前景, 白色 背景)

带格式的: 无下划线, 字体颜色: 自动设置

带格式的: 无下划线, 字体颜色: 自动设置, 图案: 15% (自动设置前景, 白色 背景)

带格式的: 无下划线, 字体颜色: 自动设置

带格式的: 无下划线, 字体颜色: 自动设置

756 recognized in global arid and semi-arid regions, such as the Sinai Desert in Egypt (Gat and Issar, 1974)  
757 (Gat and Issar, 1974), Israel (Gat, 1983) (Gat, 1983), South Australia (Love et al., 1994, 2000) (Love et  
758 al., 1994, 2000), northern China (Ma et al., 2010) (Ma et al., 2010), Saudi Arabia (Bazuhair and  
759 Wood, 1996) and North Africa (Moser et al., 1983; Guendouz et al., 2003). These signals are very often  
760 explained as palaeo-groundwater that recharged by precipitation during past wetter and colder periods  
761 (Love et al., 1994, 2000; Herczeg and Leaney, 2011) (Love et al., 1994, 2000; Herczeg and Leaney,  
762 2011). Gat and Issar (1974) reported that palaeowaters played a central role in the deep aquifers of the  
763 Sinai Desert, with the evidence that groundwater stable isotope compositions ( $\delta^{18}\text{O}$  and  $\delta\text{D}$ ) were  
764 more negative than those of weighted mean contemporary rainfall. Ma et al. (2010) presented data from  
765 groundwater in the aquifer of Jinchang city and the adjacent Gobi desert areas in northern China, which  
766 showed that palaeowaters were depleted in  $^{18}\text{O}$  and  $^2\text{H}$  relative to modern precipitation in the same  
767 region.

768 In order to identify the role of palaeowater recharge on groundwater in the Otindag, Here we use  
769 the tritium data as a environmental tracer to estimate the groundwater age in the Otindag. The half-life  
770 of tritium is 12.43yr. Based on this decay time and the tritium concentrations in groundwater, the  
771 exponential decay equation can be used to provide a qualitative age indication to interpretate the  
772 regional groundwater flow system (Ma et al., 2010). Due to the lack of tritium data of local  
773 precipitation in the Otindag, we still used the tritium data at the GNIP stations of the Baotou and  
774 Tianjin are also referenced as the background values in precipitation of recent years.

775 A “piston model (flow)” was used to evaluate the residence time of groundwater in aquifer and  
776 the residual tritium of a water body can be calculated by  $N = N_0 e^{-\lambda t}$  (Yang and Williams, 2003). Where  
777  $N$  = content of residual tritium in water sample,  $\lambda = 0.0565$ , the radioactive decay constant,  $N_0$  =  
778 content of tritium at the time of rainfall and  $t$  = years after precipitation. Based on this equation, the  
779 residual tritium was theoretically calculated and the standard for tritium dating was established for this  
780 study, the content of tritium was measured for seven groundwater samples in the Otindag Desert  
781 (Table 3). As a result, all of which were taken from the wells in the Otindag dune field. To the extent  
782 that the input function and piston model are reasonable approximations, ages of 0-60 years were  
783 obtained for these groundwater samples (Table 5). This which indicates that recent recharge took  
784 place several decades after the peak in global nuclear tests had been several decade years underway.  
785 Based on the relatively high tritium contents and the calculated datings of the groundwater samples in  
786 this study (Table 5), We thus concluded that groundwater is generally not older than 70 years in the  
787 study area. It means The hypothesis (2) that the groundwater in the Otindag are not were palaeowater  
788 recharged during glacial period in the Otindag is not valid.

789 Both the modern summer and winter precipitation recharge and the palaeowater recharge can be  
790 the hypotheses (1) and (2)-refuted, were proved to be valid, indicating ing that the direct recharge is not  
791 a major mechanism controlling the groundwater recharge in the Otindag.

792  
793 45. 44. Remote waters recharge on groundwater in the Otindag: Dali Basin

794 The indirect recharge of groundwater in the eastern Otindag?

795 Through the above analysis, it seemed that the modern winter meteoric water was not a

带格式的: 无下划线, 字体颜色: 自动设置, 图案: 15% (自动设置 前景, 白色 背景)

带格式的: 无下划线, 字体颜色: 自动设置

带格式的: 无下划线, 字体颜色: 自动设置

带格式的: 无下划线, 字体颜色: 自动设置

带格式的: 字体: (默认) +西文正文, 五号, 无下划线, 字体颜色: 自动设置, 检查拼写和语法, 图案: 15% (自动设置 前景, 白色 背景)

带格式的: 图案: 15% (自动设置 前景, 白色 背景)

带格式的: 无下划线, 字体颜色: 自动设置, 图案: 15% (自动设置 前景, 白色 背景)

带格式的: 无下划线, 字体颜色: 自动设置

带格式的: 无下划线, 字体颜色: 自动设置, 图案: 15% (自动设置 前景, 白色 背景)

带格式的: 无下划线, 字体颜色: 自动设置

带格式的: 无下划线, 字体颜色: 自动设置, 图案: 15% (自动设置 前景, 白色 背景)

带格式的: 无下划线, 字体颜色: 自动设置

带格式的: 无下划线, 字体颜色: 自动设置, 图案: 15% (自动设置 前景, 白色 背景)

带格式的: 无下划线, 字体颜色: 自动设置

带格式的: 无下划线, 字体颜色: 自动设置, 图案: 15% (自动设置 前景, 白色 背景)

带格式的: 无下划线, 字体颜色: 自动设置

带格式的: 无下划线, 字体颜色: 自动设置, 图案: 15% (自动设置 前景, 白色 背景)

带格式的: 无下划线, 字体颜色: 自动设置

带格式的: 无下划线, 字体颜色: 自动设置, 图案: 15% (自动设置 前景, 白色 背景)

带格式的: 无下划线, 字体颜色: 自动设置

带格式的: 无下划线, 字体颜色: 自动设置, 图案: 15% (自动设置 前景, 白色 背景)

带格式的: 无下划线, 字体颜色: 自动设置

796 volumetrically important source of groundwater in the Otindag, and the groundwater was not recharged  
797 by palaeowaters. Thus, The third hypothesis that “remote/the mountains waters emanate under with  
798 colder and wetter conditions” is further should be considered here as a key souce of groundwater in the  
799 Otindag. In essence, it is an indirect recharge mechanism, as the indirect recharge is defined as as  
800 water originates~~ed~~ from remote areas (Healy, 2010; Herczeg and Leaney, 2011) (Healy, 2010) and it  
801 generally occurs through rivers, canals, lakes and flash floodings (Herczeg and Leaney, 2011).

802 It ~~iswas~~ worth noting that the values of deuterium and oxygen-18 ~~in the groundwater samples of~~  
803 ~~the eastern Otindag are were variable. These values~~ for groundwater in the north part of the study area  
804 ~~arewere~~ more depleted in  $\delta D^2H$  and  $\delta^{18}O$  than those in the south part (Table 3). It suggests that the  
805 Otindag groundwater ~~in the study area~~ might be potentially recharged by water resources coming from  
806 the northern neighboring catchment ~~of the eastern Otindag~~, such as the Dali Basin.

807 In order to estimate the potential linkage between the eastern Otindag and the Dali Basin,  
808 Recently published data of  $\delta D$  and  $\delta^{18}O$ -deuterium and oxygen-18 in groundwaters, lake waters, river  
809 waters and spring water ~~ssampled~~ from the Dali Basin (e.g., Chen et al., 2008; Zhen et al., 2014) were  
810 compiled ~~collected~~ in this study and were co-analyzed with the data from the Otindag.

811 In total, There were totally ~~a~~ About 70 natural water samples from the Dali and Otindag with  $\delta D^2H$   
812 and  $\delta^{18}O$  values ~~arebeing~~ shown in a Craig diagram (Fig. 9). As a result, All of these samples fell on  
813 or lied near the evaporation line EL2 in the Craig diagram (Fig. 9), with a regression equation of  $\delta D$   
814  $^2H = 4.81\delta^{18}O - 21.55$  and a high ~~er~~ correlation coefficient ( $R^2=0.98$ ,  $n=70$ ) ~~than that of EL1 ( $R^2=0.93$ ,~~  
815 ~~n=24~~) for the Otindag samples.

816 Compared to the groundwater samples in the Otindag, water samples from the groundwaters,  
817 rivers and springs ~~fromin~~ the Dali Basin ~~arewere~~ more depleted in  $\delta^{18}O$  and  $\delta D^2H$  (Fig. 9). Such results  
818 further indicate ~~that~~, in terms of ~~itsthe~~ isotopic ~~signatureperspective~~, the groundwater in the ~~eastern~~  
819 Otindag has a close relationship with the natural waters in the Dali Basin, ~~except for the lake water in~~  
820 ~~Dali. It seems that the Dali water is a potential source for groundwater in the Otindag, or both of them~~  
821 ~~are recharged by a common souce derived from surrounding mountains.~~

#### 822 5.4.1. Linkage of the river water in the Dali and the groundwater in the Otindag

823 The similar signals of  $\delta D$  and  $\delta^{18}O$ -deuterium and oxygen-18 between the groundwater in the  
824 Otindag and the river water in the Dali (Fig. 9) point towards the~~gave us a possible~~ idea that the  
825 groundwater~~in~~ in the Otindag might be sourced from the river water in the Dali Basin, since the Dali has  
826 more depleted isotopic signals in water than the Otindag (Fig. 9).

827 Considering ~~Regarding to~~ the topographical gradient of the elevations between the two regions,  
828 however, river water in the Dali Basin ~~cannot~~ flow into the eastern Otindag, because the terrain  
829 elevation of the Dali Basin is lower than that of the Otindag (Fig. 1). This is also the reason why the  
830 huge Dali Lake ~~is formed that lies~~ in the Dali Basin ~~has no equivalent but not~~ in the Otindag (Fig. 1).  
831 If there is a hydraulic linkage between the two regions, water should flow from the Otindag into the the  
832 Dali, but not conversely.

833 A hypothesis that water flows from the Otindag into the Dali Lake has also been proposed by  
834 Yang et al. (2015). They argued that a mega palaeolake in Dali, who was almost twice the size of the

带格式的: 无下划线, 字体颜色:  
自动设置, 图案: 清除

带格式的: 无下划线, 字体颜色:  
自动设置

带格式的: 无下划线, 字体颜色:  
自动设置, 图案: 15% (自动设置  
前景, 白色 背景)

带格式的: 无下划线, 字体颜色:  
自动设置

带格式的: 无下划线, 字体颜色:  
自动设置

带格式的: 无下划线, 字体颜色:  
自动设置, 图案: 15% (自动设置  
前景, 白色 背景)

带格式的: 无下划线, 字体颜色:  
自动设置

带格式的: 无下划线, 字体颜色:  
自动设置

带格式的: 无下划线, 字体颜色:  
自动设置, 图案: 15% (自动设置  
前景, 白色 背景)

带格式的: 无下划线, 字体颜色:  
自动设置

带格式的: 无下划线, 字体颜色:  
自动设置, 图案: 15% (自动设置  
前景, 白色 背景)

带格式的: 无下划线, 字体颜色:  
自动设置

带格式的: 无下划线, 字体颜色:  
自动设置, 图案: 15% (自动设置  
前景, 白色 背景)

带格式的: 无下划线, 字体颜色:  
图案: 15% (自动设置  
前景, 白色 背景)

带格式的: 无下划线, 字体颜色:  
自动设置

带格式的: 无下划线, 字体颜色:  
自动设置

带格式的: 无下划线, 字体颜色:  
自动设置

带格式的: 无下划线, 字体颜色:  
自动设置, 图案: 清除

836 present Dali Lake in area, was recharged by river systems to its south in the Otindag ca. 4,200 years  
837 ago. After that, due to the catastrophic decrease in precipitation that occurred in monsoonal regions  
838 being experienced catastrophic precipitation decreasing and the groundwater in Otindag being  
839 sapping and captured of the Otindag groundwater by the Xilamulun River flowing eastward, the  
840 Otindag's water was no longer recharging the megalake Dali and left a palaeo channel between the two  
841 regions (Fig. 2). Since then the connection between surface waters in the two regions has been  
842 halted was broken.

843 In view of the hydraulic gradient, river water in the Dali Basin could not be a recharge source for  
844 groundwater in the Otindag. However, in view of the isotopic gradients, groundwater in the Otindag  
845 could not conversely be the source of river water in the Dali. at present, due to the more depleted  
846 values of deuterium and oxygen-18 in Dali than in Otindag (Fig. 9). Thus, the similar isotopic signals  
847 between the river water in Dali and the groundwater in Otindag indicated that these waters might be  
848 recharged from a common source.

#### 849 5.4.2 Linkage of groundwaters between the Otindag and the Dali

850 Similar isotopic signals also occurred in the groundwaters between the Otindag and the Dali Basin  
851 (Fig. 9). The linkage of groundwaters between the two regions is still unknown at present. In order to  
852 understand the linkage of groundwaters between the two regions, answer this question, we need to  
853 know the potential movement of groundwater in the transition zone of the two regions need to be  
854 known.

855 Due to the inherent difficulties to directly observe groundwater movement along its hydraulic  
856 gradient under ground, inert isotopic and hydrochemical tracers are often used to identify groundwater  
857 movement (Nakaya et al., 2007), such as chloride, TDS and H-O isotopes, which were used as  
858 environmental fingerprints to indicate groundwater movement in arid lands (Yang and Williams, 2003).  
859 In a theoretical line of groundwater evolution, the chloride in water is readily removed from matrix  
860 materials rather than being precipitated due to its high solubility, thus chloride concentrations tend to  
861 be increased with the increasing of the flow path's length and residence time of groundwater (Lloyd  
862 and Heathcote, 1985). The TDS has a similar trend with chloride in groundwater evolution, but its  
863 tendency might be disturbed due to potential precipitation of certain ions when reaching their saturation  
864 conditions. According to the salination classification of water, all the groundwater samples collected in  
865 this study were fresh water in type (TDS < 1000 mg/L). Thus evident precipitation of major ions can  
866 be considered as could be weak in the Otindag groundwaters.

867 In this study, a groundwater-sampling project was designed in the field along a N-S section of a  
868 palaeo-channel located at the transition zone between the Dali and Otindag (Figs. 1, 2). The channel is  
869 located near the south distal reach of the Xilamulun River and was named "PCSX" in this study, with its  
870 The north part of the channel, named "as-NPCSX" and, is located at the riverhead of the Xilamulun  
871 River and the south part named "as-SPCSX", is close to the eastern margin of the Yinshan Mountains  
872 (Figs. 1, 2).

873 Regarding to the topographical gradient in the Otindag, the GPS elevation of the northernmost  
874 sampling site in the NPCSX (g11, about 1317 m a.s.l.) was much lower than that of the southernmost

带格式的: 无下划线, 字体颜色: 自动设置

带格式的: 无下划线, 字体颜色: 自动设置, 图案: 15% (自动设置 前景, 白色 背景)

带格式的: 无下划线, 字体颜色: 自动设置

带格式的: 无下划线, 字体颜色: 自动设置

带格式的: 无下划线, 字体颜色: 自动设置

带格式的: 无下划线, 字体颜色: 自动设置, 图案: 15% (自动设置 前景, 白色 背景)

带格式的: 无下划线, 字体颜色: 自动设置

带格式的: 无下划线, 字体颜色: 自动设置

带格式的: 无下划线, 字体颜色: 自动设置

带格式的: 无下划线, 字体颜色: 自动设置

876 site in the SPCSX (g1, 1396 m.a.s.l.) (Fig. 2 and Table 1). Regarding to the topographical gradient in  
877 the channel, there is a drop of 11 m is about 80 m meter drop between the NPCSX and the SPCSX.  
878 Under such slope, the underground hydraulic gradient for groundwater flow can be roughly parallel  
879 with that of the surface water flow, namely that the groundwaterflow should move downwards from the  
880 SPCSX area into the NPCSX area. Thus we can speculate that groundwater in the NPCSX would have  
881 higher salinity concentration values of chloride and TDS in concentration than those in the SPCSX  
882 under such flowing direction, if the groundwater was flowing from the SPCSX to the NPCSX.

883 In order to verify check up this speculation, the actual variations of water thesalinity  
884 environmental tracers(chloride and TDS) were detected along the PCSX section. The sampling site g1  
885 was defined as the initial point and the distances between g1 and other sampling sites along the PCSX  
886 section were calculated, based on their GPS geographical coordinates records measured in the field.  
887 The results are shown in Fig. 10a-b. It is was very clear that the variations of chloride and TDS  
888 concentrations in groundwater did not increase along the palaeo-channel from south to north (Fig.  
889 10a-b). On the contrary, both the values of chloride and TDS are lower in the NPCSX area than  
890 those in the SPCSX area. Such kind of spatial variations in the chloride and TDS values was contradict  
891 to the speculated patterns abovementioned, suggesting that the hydraulic gradient of groundwater  
892 flowing path in this region is not controlled by the topographical gradient between the NPCSX and  
893 SPCSX areas.

894 a complicated movement of groundwater in the study area. It also indicatesd that the hydraulic  
895 linkage wasweak in the groundwaters between the NPCSX and SPCSX areas.

896 SThe stable and radioactive isotopic data were also used here as tracers to differentiate the  
897 groundwaters between the two regions. Before we use the stable isotopic signals, however, it is  
898 necessary to think about the effect of evaporation process on the fractionation of stable isotopes.  
899 During the evaporation process, dissolved chloride, the conservative ion, will be enriched along with  
900 the heavy isotopes, which is manifested as a correlation between the chloride concentration and the  
901 deuterium content in groundwater (Sklash and Mwangi, 1991; Taylor and Howard, 1996). Based on this  
902 consideration, a bivariate diagram can be was built using the chloride and deuterium data of the  
903 groundwater samples in this study, as shown in Fig. 11. The Groundwater samples from the PCSX  
904 section showed a very weak correlation between the chloride and deuterium (Fig. 11). This indicates  
905 that the groundwaters studied are werenot strongly affected by evaporation process in a deep degree.

906 Compared between the NPCSX and SPCSX regions, the stable isotopic values ( $\delta^{18}\text{O}$  and  $\delta\text{D}^2\text{H}$ ) of  
907 groundwaters in the SPCSX region varied greatly with a large amplitude, while those in the NPCSX  
908 are relatively constant (Fig. 10c-d12). This indicates that the recharge sources of groundwater in  
909 the SPCSX are more diverse were diversity than those in the NPCSX. The constant variations indicated  
910 that the recharge source of groundwater in the NPCSX is relatively unitary. The isotopic values in the  
911 SPCSX are much lighter than those in the NPCSX along the distance section from south to north  
912 (Fig. 10c-d12). The heaviest values occurred in the sample g11 collected from the NPCSX (Fig.  
913 10c-d12), indicating a water being earlier firsthand recharged. The spring water sample s2, a  
914 representation of discharge water, iswas characterized by medium values of  $\delta\text{D}^2\text{H}$  and  $\delta^{18}\text{O}$ . Similarly,  
the deuterium excess values of these groundwaters also showed such spatial patterns in the two regions

带格式的: 无下划线, 字体颜色: 自动设置

带格式的: 无下划线, 字体颜色: 自动设置, 图案: 15% (自动设置前景, 白色 背景)

带格式的: 图案: 15% (自动设置前景, 白色 背景)

带格式的: 无下划线, 字体颜色: 自动设置, 图案: 15% (自动设置前景, 白色 背景)

带格式的: 图案: 15% (自动设置前景, 白色 背景)

带格式的: 无下划线, 字体颜色: 自动设置

带格式的: 无下划线, 字体颜色: 自动设置, 图案: 15% (自动设置前景, 白色 背景)

带格式的: 无下划线, 字体颜色: 自动设置

带格式的: 无下划线, 字体颜色: 自动设置, 图案: 15% (自动设置前景, 白色 背景)

916 ~~(Fig. 10e f13)~~ These results indicate~~d~~ that the groundwaters in the SPCSX area, with relatively  
917 enriched isotopic signals in  $\delta^{2}H$  and  $\delta^{18}O$  by comparison with ~~than~~ those in the NPCsX area, are  
918 were composed of ~~a~~ mixture of the groundwaters in the NPCsX with ~~and~~ other waters. In consequence, thus  
919 resulting in the spring water sample s2 in the discharge zone ~~is being characterized by an intermediate~~  
920 ~~isotopic signal (Figs. 12, 13)~~. A similar case was also observed by Abdalla (2009), who reported ~~a~~  
921 ~~that progressive decrease of the isotopic compositions had decreased progressively along a~~  
922 ~~regional scale flow path of groundwater in the semi arid central Sudan, because of the mixture of~~  
923 ~~groundwaters with between the heavier/lighter isotope recharged and the lighter isotope recharged.~~

924 ~~In addition to stable isotopes, The tritium contents were broadly and positively related to the~~  
925 ~~values of deuterium excess in the groundwater samples in the PCSX section (Fig. 10e 14a). The~~  
926 ~~deuterium excess or d excess, computed from the equation  $d = \delta^2H - 8\delta^{18}O$  (Dansgaard, 1964), is~~  
927 ~~controlled primarily by the mean relative humidity of the air masses formed above the water surface~~  
928 ~~(Merlivat and Jouzel, 1979) and generally reflects the rate of evaporation process experienced during~~  
929 ~~the flowing paths (Dansgaard, 1964)~~. For a water that experiences ~~dan~~ evaporation process, the d-excess  
930 value will increase in the evaporated water vapor, but will decrease in the residual water body  
931 (Dansgaard, 1964; Merlivat and Jouzel, 1979). In this study, except for sample g11 (a sample very  
932 close to the riverhead area), the positive relationship between the tritium and the deuterium excess  
933 generally shows ~~ed~~ that the d-excess values are  
~~were~~ higher in the groundwaters collected from the  
934 NPCsX, ~~but are~~ were lower in those from the SPCSX (Fig. 10e 14a). This edistribution pattern  
935 indicates~~d~~ that the groundwaters in the NPCsX are  
~~were~~ relatively younger and ~~had~~ experienced a  
936 lower less degree of evaporation than those in the SPCSX. The d-excess gradient, increasing from ~~the~~  
937 south to north in the PCSX, further suggests~~confirmed~~ that groundwater does  
~~did~~ not flow from the  
938 SPCSX area to the NPCsX area, namely out of the topographical control.

939 ~~In Fig. 14b, the tritium contents of groundwater increased while the TDS decreased from the~~  
940 ~~south to north in the PCSX (Fig. 14b)~~. This distribution pattern of the two environmental tracers further  
941 proved that the groundwaters in the NPCsX are  
~~were~~ younger and fresher than those in the SPCSX. The  
942 reason why the older groundwater has a higher TDS value can be attributed to the fact that most  
943 minerals dissolve slowly in an aquifer and the older groundwater ~~stay~~ have more in contact with the  
944 surrounding rocks for a longer time allowing more time to act between water solution and soluble  
945 minerals to pass in solution into the water, leading to a higher TDS (Fitts, 2002). Many studies (e.g.,  
946 Boronina et al., 2005; Kazemi et al., 2006) have demonstrated that groundwater ~~will~~ flows in the  
947 direction in which it gets older. In view of this point, groundwaters in the PCSX region should  
948 theoretically flow from the NPCsX area to the SPCSX area, in opposition to evidently being paradoxical  
949 with the S-N topographical gradient between the Otindag and Dali in the PCSX regions. Thus  
950 groundwater in the Dali are not the source of groundwater in the Otindag. The similar isotopic signals  
951 between groundwaters in the two regions indicate that these waters might be recharged from a common  
952 source in other place.

953  
954 Overall, it implies~~d~~ that the hydraulic gradient of groundwater derived from their topography is  
955 not consistent with the isotopic and hydrogeochemical gradients of groundwater that is observed in the

带格式的: 无下划线, 字体颜色: 自动设置

带格式的: 无下划线, 字体颜色: 自动设置, 图案: 15% (自动设置前景, 白色 背景)

带格式的: 无下划线, 字体颜色: 自动设置, 图案: 15% (自动设置前景, 白色 背景)

带格式的: 无下划线, 字体颜色: 自动设置

带格式的: 无下划线, 字体颜色: 自动设置, 图案: 15% (自动设置前景, 白色 背景)

带格式的: 无下划线, 字体颜色: 自动设置

带格式的: 无下划线, 字体颜色: 自动设置

带格式的: 无下划线, 字体颜色: 自动设置

带格式的: 无下划线, 字体颜色: 自动设置

带格式的: 无下划线, 字体颜色: 自动设置, 图案: 清除

带格式的: 无下划线, 字体颜色: 自动设置

带格式的: 无下划线, 字体颜色: 自动设置, 图案: 15% (自动设置前景, 白色 背景)

956 eastern Otindag. This further indicates that the origin of groundwater in the Otindag Desert is not  
957 geomorphologically or topographically controlled.

带格式的: 图案: 15% (自动设置  
前景, 白色 背景)

#### 45. 55. Remote water recharge on groundwater in the Otindag: mountains waters

##### Potential sources of groundwater from recharge in the Otindag: the Daxinganling and Yinshan Mountains: tectonic control:

The discussions above revealed indicated that groundwater in the eastern Otindag has a close relationship with river water in the Dali Basin in terms of their isotopic signature perspective, and that both the river water and groundwaters in the Otindag and Dali two regions Basin might be recharged from a common source derived from another place. Considering the third hypothesis abovementioned that "remote/mountains waters emanate under colder and wetter conditions", we propose that this "common source" of the two regions are from mountains areas surrounding the Otindag and Dali Basin. Meanwhile, the isotopic and hydrochemical characteristics of groundwaters both in the NPCSX and SPCSX areas indicated that the groundwaters between the Dali (together with the northeast Otindag) and the southeast Otindag were different and the groundwater systems in the two regions were not integrated.

For the Dali catchment, the Dali Lake and its surrounding rivers are the most important water bodies in the Dali Basin. There are two large permanent rivers and lots of small intermittent streams entering the Dali Basin Lake (Xiao et al., 2008), including the Xilamulun River to the south and the Gongger River to the north, both of which are stemming from the Greater Khingan Mountains (Daxing'anling Mountains in Chinese pinyin, 1,100-1,400 m above seal level) (Fig. 1). The Xilamulun River, 380 km in length and  $32.54 \times 10^3 \text{ km}^2$  in area, is a neighboring river both to the southeastern Dali and to the northeastern Otindag (Figs. 1 and 2). The Xilamulun River carries a large amount of water (about  $6.58 \times 10^8 \text{ m}^3/\text{y}$ ) from the Daxing'anling Mountains flowing through the east margins of the Dali and Otindag (Wu et al., 2014). This is an important clue linking natural waters between groundwaters in the northeastern Otindag and the river waters and groundwaters in the Dali Basin.

Variation in elevation from the Dali Lake to the riverhead of the Xilamulun River can be clearly found along a land surface topographical section (Fig. 115). The channel of the Xilamulun River is located in a fault called the Xilamulun River Fault or the Xar Moron River Fault (Fig. 1), which is a part of the Selonker Suture Zone (Eizenhöfer et al., 2014) or the Xilamulun-Changchun-Yanji plate suture zone (Sun et al., 2004) or the Selonker Suture Zone (Eizenhöfer et al., 2014) in the regional tectonical settings (Figs. 1 and 2-31 and 2). Outcrop observations indicate that fault zones commonly have a permeability structure suggesting they should act as complex conduit-barrier systems in which along-fault flow is encouraged and across-fault flow is impeded (Bense et al., 2013). Thus the hydraulic gradient of groundwater flow in the Eastern margins of the Otindag and Dali Basin must be controlled by the fault zone hydrogeology. This may be the reason why the hydraulic gradient of groundwater represented by the isotopic and hydrogeochemical gradients of groundwater samples in this study is not consistent with the local topographical gradient in the Otindag Desert. On the other hand, the regional aquifer is generally unconfined in dune fields of the Otindag Desert but

带格式的: 无下划线, 字体颜色:  
自动设置

带格式的: 无下划线, 字体颜色:  
自动设置, 图案: 15% (自动设置  
前景, 白色 背景)

带格式的: 图案: 15% (自动设置  
前景, 白色 背景)

带格式的: 无下划线, 字体颜色:  
自动设置

带格式的: 无下划线, 字体颜色:  
自动设置, 图案: 清除

带格式的: 无下划线, 字体颜色:  
自动设置

带格式的: 无下划线, 字体颜色:  
自动设置, 图案: 15% (自动设置  
前景, 白色 背景)

带格式的: 无下划线, 字体颜色:  
自动设置

带格式的: 无下划线, 字体颜色:  
自动设置

带格式的: 无下划线, 字体颜色:  
自动设置, 图案: 15% (自动设置  
前景, 白色 背景)

带格式的: 无下划线, 字体颜色:  
自动设置

带格式的: 无下划线, 字体颜色:  
自动设置

带格式的: 无下划线, 字体颜色:  
自动设置

带格式的: 无下划线, 字体颜色:  
自动设置

带格式的: 无下划线, 字体颜色:  
自动设置, 不检查拼写或语法, 图  
案: 清除

带格式的: 无下划线, 字体颜色:  
自动设置

带格式的: 无下划线, 字体颜色:  
自动设置, 不检查拼写或语法, 图  
案: 清除

带格式的: 无下划线, 字体颜色:  
自动设置

带格式的: 无下划线, 字体颜色:  
自动设置, 不检查拼写或语法, 图  
案: 清除

带格式的: 无下划线, 字体颜色:  
自动设置

996 semi-confined to confined in the Daxing'Anling uplands (Fig. 3), thus the thick unconsolidated  
997 aquifers in the study area (Figs. 32 and 115) will be favourable conditions for groundwater storage and  
998 transportation along the Solonker Suture Zone. When rivers stem from the Daxing'Anling  
999 Mountains and flow downward to the marginal areas of the Dali and Otindag, leakage water from these  
1000 rivers can recharge the desert land through thick unconsolidated aquifers (Fig. 15). A strong isotopic  
1001 evidence is that the lake and river waters in the Dali Basin share the same evaporation line (EL2) with  
1002 the groundwaters in the PCSX area.

1003 Although groundwaters in the SPCSX area are different from those in the NPCSX area, their  
1004 isotopic data points still fell onto the EL2 (Fig. 9XX), which further indicates that the groundwaters in  
1005 the SPCSX are a mixture of waters from the Daxing'Anling Mountain and other sources. Another

1006 Another source for groundwater recharge in the SPCSX could be represented by  
1007 remote water such as flash floods derived from the north Yinshan Mountains (Fig. 1),  
1008 because it can be clearly observed from digital maps that many transient rivers or streams originated  
1009 from the Yinshan Mountains flow into the south and southeastern Otindag (Fig. 1). Supportive  
1010 evidence for this idea can be derived. A key clue for this view can also be obtained from the isotopic  
1011 signals of local precipitation and groundwater samples collected from the areas near to the Yinshan  
1012 Mountains in this study. Supportive evidence for this idea can also be observed in the summer rainy  
1013 season. During rainy days or under storm conditions, occasional heavy, short rainstorms cause floods in  
1014 soil-rich wadi channels and low-lying depressions in the unconfined to semi-confined areas of the  
1015 Yinshan Mountains' piedmont. These waters may temporarily recharge shallow aquifers in the SPCSX  
1016 area.

1017 It has been reported that temperature and altitude can deeply affect the  $\delta D$  and  $\delta^{18}O$  compositions  
1018 of precipitation. The isotope depleted signals of  $\delta^2H$  and  $\delta^{18}O$  in waters from mountain areas can be  
1019 passed into the groundwater in plain areas (Harrington et al., 2002; Vanderzalm et al., 2011; Liu and  
1020 Yamanaka, 2012; Rattray, 2015; Khalid and Hamid, 2017). Rattray (2015) attributed this isotopic  
1021 signature to the altitude effect on precipitation, because temperature and altitude can deeply affect the  
1022 deuterium and oxygen-18 compositions in precipitation. The values of  $\delta^2H$  and  $\delta^{18}O$  in precipitation  
1023 from the mountain areas will be depleted when compared with those in precipitation from the piedmont  
1024 areas (Rattray, 2015). Rattray (2015) attributed this isotopic signature to the altitude effect on  
1025 precipitation. For the Yinshan Mountain Range, there is lack of the data of stable isotopes in  
1026 precipitation. The GPS elevation of the sample location of p1 is about 1260 m a.s.l. and that of the top of the  
1027 Yinshan mountain range is around 1700–1800 m a.s.l., thus the elevation drop is approximately 500 m  
1028 between the two sites. Based on this difference in elevation drop and the potential effect of elevation  
1029 change on temperature (that elevation arises will lead to a decrease of temperature by  $0.65^{\circ}C$  per 100  
1030 m), the temperature difference between the two sites is about  $3.25^{\circ}C$ . According to an empirical  
1031 estimation for precipitation in NW China that the  $\delta^{18}O$  temperature gradient is  $0.37^{\circ}C$  and the  
1032  
1033  
1034  
1035

带格式的: 无下划线, 字体颜色: 自动设置

带格式的: 无下划线, 字体颜色: 自动设置

带格式的: 无下划线, 字体颜色: 自动设置

带格式的: 字体: (默认) +西文正文, 五号, 无下划线, 字体颜色: 自动设置, 检查拼写和语法

带格式的: 无下划线, 字体颜色: 自动设置

带格式的: 字体: (默认) +西文正文, 五号, 无下划线, 字体颜色: 自动设置, 检查拼写和语法

带格式的: 无下划线, 字体颜色: 自动设置

1036  $\delta^{18}\text{O}$  elevation gradient is  $-0.13\text{‰}/100\text{ m}$  (Liu et al., 2014), the  $\delta^{18}\text{O}$  value in precipitation at the  
1037 Yinshan Mountains shall be  $1.85\text{ ‰}$  lower than that in the sample p1, namely  $-8.99\text{‰}$  in  $\delta^{18}\text{O}$  for the  
1038 Yinshan mountain precipitation. This value is very similar to that of the groundwater ( $-9\text{‰}$ ) in the  
1039 SPCSX area. It indicates that the Yinshan Mountains area is area potential source area for the  
1040 groundwater recharge in the SPCSX area.

1041 In general, the above analyses revealed that the highland water resources from the Daxing'anling  
1042 and Yinshan Mountains were isotopically and geochemically traced to be a major source for the  
1043 groundwater in the Otindag. It suggests means that the modern indirect recharge mechanism, instead of  
1044 the direct recharge and the paleowater recharge, is responsible for groundwater recharge in this  
1045 the desert land in northern China. It also This implies that the tectonic settings (such as the Solonker suture  
1046 zone), but not the climatic and topographical control, iswassignificant for the groundwater origin in  
1047 the Otindag.

1048

## 5.6. Conclusions

1049 Water resources in arid lands of the world are generally scarce and highly uncertain. In the  
1050 middle-latitude desert zone of northern China, however, many deserts such as the Otindag and  
1051 Badanjilin Deserts, are unexpectedly rich in incommensurate groundwater resources, such as the  
1052 Otindag and the Badanjilin Deserts, although they have no surface runoff and have been under an arid  
1053 or hyper-arid climate for a long geological period of time. How the groundwaters are originated and  
1054 recharged in thesea desert's environment are thus becaming a key questions that are –longtime ago, but  
1055 it is still under an endless-debate at present in the academic circle. For some of the earth scientists, the  
1056 direct recharge is thought to be very important for groundwaters in the wide desert lands of northern  
1057 China, due to the lack of surface runoffs. However, the groundwater availability is very much as  
1058 function of the local- and regional-scale geological and climatic settingselements. To achieve an i  
1059 Integrated understanding of the groundwater recharge and its their controlling mechanisms is of great  
1060 significance. In this study, an effort to explore the groundwater recharge was explored carried out using  
1061 multiple environmental tracers in the eastern Otindag Desert of northern China, a region that where is  
1062 under the influence control of the East Asian Summer Monsoon (EASM) climate. The results showed  
1063 that (1), the natural waters in the study area were fresh water ( $\text{TDS} < 1000\text{ mg/L}$ ) with and were  
1064 neutral to slightly alkaline pH. The major water types were the  $\text{Ca-HCO}_3$  and  $\text{Ca/Mg-SO}_4$  types.  
1065 There were no  $\text{Cl}$  type and  $\text{Na}$  type waters occurring in the study area, indicating a primary stage of  
1066 water evolution in terms of the hydrogeochemicalperspective terms. (2) Compared to the modern  
1067 summer precipitation, the groundwaters, river waters and spring waters are were depleted in  $\delta\text{D-H}$  and  
1068  $\delta^{18}\text{O}$ , while the lake waters were enriched in  $\delta^2\text{H}$  and  $\delta^{18}\text{O}$ . All these waters, however, shared a same  
1069 line of evaporation in the Craig linediagram, indicating a genetic relationship on their recharge sources.  
1070 The more depleted stable isotopic signals of the groundwaters is more depleted than those of the  
1071 modern summer precipitation and this suggestse that the groundwaters studied here could only be  
1072 sourced from a colder water different from ether than the EASM precipitation. In general, the analyses  
1073 revealed that the highland remote water resources from the Daxing'anling and Yinshan Mountains  
1074 were isotopically and geochemically traced to be a major source for the groundwater in the Otindag.

带格式的: 无下划线, 字体颜色: 自动设置

带格式的: 无下划线, 字体颜色: 自动设置

带格式的: 无下划线, 字体颜色: 自动设置

带格式的: 无下划线, 字体颜色: 自动设置, 图案: 15% (自动设置前景, 白色 背景)

带格式的: 无下划线, 字体颜色: 自动设置

带格式的: 无下划线, 字体颜色: 自动设置, 图案: 15% (自动设置前景, 白色 背景)

带格式的: 无下划线, 字体颜色: 自动设置

1076 The contribution from local winter precipitation was very small due to its weak rainfall effect. The  
1077 high contents (5–25 TU) of tritium in these groundwaters indicated that they were young and were  
1078 could not be recharged by palaeowaters formed during the past glacial periods. (3) There are clear  
1079 difference in the isotopic signals occurred between the groundwaters in the north (NPCSX) and south  
1080 (SPCSX) parts of the study area, but the signals of were similar between the groundwaters in the  
1081 NPCSX and its neighbouring catchment, the Dali Basin. (4) Combined analysis  
1082 was further performed using the isotopic and physiochemical data of natural waters collected from the  
1083 Dali Basin and the surrounding mountains. The results indicated that the major sources of the  
1084 groundwaters in the NPCSX, as well as the river waters and groundwaters in the Dali Basin, were  
1085 mainly derived from the Daxin'Anling Mountains, by leaking the Xilamulan River water through a  
1086 thick aquifer in the eastern margins of the Otindag. By contrast, While the groundwaters in the SPCSX  
1087 were mainly recharged from two sources, the flash floods from the Yinshan Mountains and the river  
1088 waters from the Daxin'Anling Mountains. (5) It suggests that the modern indirect recharge mechanism,  
1089 instead of the direct recharge and the palaeo-water recharge, was the most significant for  
1090 groundwater recharge in the eastern Otindag. It indicates that the tectonic settings at a regional scale  
1091 but not the climate and topography, was at the origin of responsible for the groundwater origin in the  
1092 Otindag. This study provides a new perspective sight into the origin and evolution of groundwater  
1093 resources in the middle-latitude desert zone of northern China.

1094

1095

#### 1096 Acknowledgements

1097 This study was financially supported by the National Natural Science Foundation of China  
1098 (41602196, 41771014 and 41602196) and the National Key Research and Development Program of  
1099 China (2016YFA0601900). We thank the China Meteorological Data Sharing Service system for  
1100 providing the weather data. Sincere thanks are also extended to Profs. Xiaoping Yang, Xunming Wang,  
1101 Jule Xiao and other workmates, e.g., QiuHong Li, Ziting Liu, Hongwei Li, and Deguo Zhang for their  
1102 generous help in the research work.

1103

#### 1104 References:

- 1105 Abdalla, O.A.: Groundwater recharge/discharge in semi-arid regions interpreted from isotope and  
1106 chloride concentrations in north White Nile Rift, Sudan. *Hydrogeology Journal*, 17, 679–692, 2009.
- 1107 Al Bassam, A.M., Awad, H.S., and Al Alawi, J.A.: DurovPlot: a computer program for processing and  
1108 plotting hydrochemical data. *Ground Water*, 35, 362–367, 1997.
- 1109 Al Bassam, A.M., and Khalil, A.R.: DurovPwin: a new version to plot the expanded Durov diagram for  
1110 hydrochemical data analysis. *Computers & Geosciences*, 42, 1–6, 2012.
- 1111 Baeza, A., Garcia, E., and Miro, C.: A procedure for the determination of very low activity levels of  
1112 tritium in water samples. *Journal of Radioanalytical and Nuclear Chemistry*, 241, 93–100,  
1113 1999.
- 1114 Bazuhair, A.S., and Wood, W.W.: Chloride mass-balance method for estimating ground  
1115 water recharge in arid areas: examples from western Saudi Arabia. *Journal of Hydrology*, 186,  
153–159, 1996.

带格式的: 无下划线, 字体颜色:  
自动设置, 图案: 15% (自动设置  
前景, 白色 背景)

带格式的: 无下划线, 字体颜色:  
自动设置

带格式的: 无下划线, 字体颜色:  
自动设置, 图案: 15% (自动设置  
前景, 白色 背景)

带格式的: 无下划线, 字体颜色:  
自动设置

- 1116 Bense, V.F., Gleeson, T., Loveless, S.E., Bour, O., and Scibek, J.: Fault zone hydrogeology. 带格式的: 无下划线, 字体颜色: 自动设置
- 1117 Earth-Science Reviews, 127, 171-192, 2013.
- 1118 Bethke, C.M., and Johnson, T.M.: Groundwater Age and Groundwater Age Dating. Annual Review of Earth and Planetary Sciences, 36, 121-152, 2008. 带格式的: 无下划线, 字体颜色: 自动设置
- 1119 Blasch, K.W., and Bryson, J.R.: Distinguishing sources of ground water recharge by using  $\delta^2\text{H}$  and  $\delta^{18}\text{O}$ . Ground Water, 45, 294-308, 2007. 带格式的: 无下划线, 字体颜色: 自动设置
- 1120 Boronina, A., Renard, P., Balderer, W., and Stichler, W.: Application of tritium in precipitation and in groundwater of the Kouris catchment (Cyprus) for description of the regional groundwater flow. Applied Geochemistry, 20, 1292-1308, 2005. 带格式的: 无下划线, 字体颜色: 自动设置
- 1121 Chadha, D.K.: A proposed new diagram for geochemical classification of natural waters and interpretation of chemical data. Hydrogeology Journal, 7, 431-439, 1999. Chebotarev, I.I.: Metamorphism of natural waters in the crust of weathering. Geochimica et & Cosmochimica Acta, 8, 22-32, 1955. 带格式的: 无下划线, 字体颜色: 自动设置
- 1122 Chen, F., Chen, J., Holmes, J., Boomer, I., Austin, P., Gates, J.B., Wang, N., Brooks, S.J., and Zhang, J.: Moisture changes over the last millennium in arid central Asia: a review, synthesis and comparison with monsoon region. Quaternary Science Reviews, 29, 1055-1068, 2010. 带格式的: 无下划线, 字体颜色: 自动设置
- 1123 Chen, J., Chen, X., and Wang, T.: Isotopes tracer research of wet sand layer water sources in Alxa Desert. Advances in Water Science, 25, 196-206, 2014 (in Chinese). 带格式的: 无下划线, 字体颜色: 自动设置
- 1124 Chen, J., Li, L., Wang, J., Barry, D.A., Sheng, X., Gu, W., Zhao, X., and Chen, L.: Water resources: groundwater maintains dune landscape. Nature, 432, 459-460, 2004. 带格式的: 无下划线, 字体颜色: 自动设置
- 1125 Chen, J., Liu, X., Wang, C., Rao, W., Tan, H., Dong, H., Sun, X., Wang, Y., and Su, Z.: Isotopic constraints on the origin of groundwater in the Ordos Basin of northern China. Environmental Earth Sciences, 66, 505-517, 2012a. 带格式的: 无下划线, 字体颜色: 自动设置
- 1126 Chen, J., Sun, X., Gu, W., Tan, H., Rao, W., Dong, H., Liu, X., and Su, Z.: Isotopic and hydrochemical data to restrict the origin of the groundwater in the Badain Jaran Desert, Northern China. Geochemistry International 50, 455-465, 2012b. 带格式的: 无下划线, 字体颜色: 自动设置
- 1127 Chen, J., Yang, Q., and Hao, G.: Using hydrochemical and environmental isotopical data to analyse groundwater recharge in the Hunshandake Sandy Land. Inner Mongolia Science Technology & Economy, 17, 9-12, 2008 (in Chinese). 带格式的: 无下划线, 字体颜色: 自动设置
- 1128 Clark, I.D.: Groundwater Geochemistry and Isotopes. CRC Press, Boca Raton, 2015. 带格式的: 无下划线, 字体颜色: 自动设置
- 1129 Copley, T.: Uses of Environmental Isotopes, in: Alley, W.M. (Ed.): Regional Ground Water Quality. Van Nostrand Reinhold, New York, 1993. 带格式的: 无下划线, 字体颜色: 自动设置
- 1130 Craig, H.: Isotopic Variations in Meteoric Waters. Science, 133, 1702-1703, 1961. 带格式的: 无下划线, 字体颜色: 自动设置
- 1131 Dansgaard, W.: Stable isotopes in precipitation. Tellus, 16, 436-468, 1964. 带格式的: 无下划线, 字体颜色: 自动设置
- 1132 Dogramaci, S., Skrzypek, G., Dodson, W., and Grierson, P.F.: Stable isotope and hydrochemical evolution of groundwater in the semi-arid Hamersley Basin of subtropical northwest Australia. Journal of hydrology, 475, 281-293, 2012. 带格式的: 无下划线, 字体颜色: 自动设置
- 1133 Doll, P., and Fiedler, K.: Global-scale modeling of groundwater recharge. Hydrology and Earth System Sciences, 12, 863-885, 2008. 带格式的: 无下划线, 字体颜色: 自动设置
- 1134 Doll, P.: Vulnerability to the impact of climate change on renewable groundwater resources: a 带格式的: 无下划线, 字体颜色: 自动设置

- 1156 global-scale assessment. Environmental Research Letters, 4, 035006,  
1157 doi:10.1088/1748-9326/4/3/035006, 2009.
- 1158 Drever, J.I.: Catchment mass balance. In: Saether, O.M., and de Caritat, P. (Eds.), *Geochemical*  
1159 *Processes, Weathering and Groundwater Recharge in Catchments*. A.A. Balkema, Rotterdam, pp.  
1160 241-261, 1997.
- 1161 Durov, S.A.: *Natural waters and graphic representation of their composition Doklady Akademii Nauk*  
1162 *SSSR*, 59, 87-90, 1948.
- 1163 Edmunds, W.M., Ma, J., Aeschbach-Hertig, W., Kipfer, R., and Darbyshire, D.P.F.: Groundwater  
1164 recharge history and hydrogeochemical evolution in the Minqin Basin, North West China. *Applied*  
1165 *Geochemistry*, 21, 2148-2170, 2006.
- 1166 Eissa, M.A., Thomas, J.M., Hershey, R.L., Dawoud, M.I., Pohll, G., Dahab, K.A., Gomaa, M.A., and  
1167 Shabana, A.R.: *Geochemical and isotopic evolution of groundwater in the Wadi Watir watershed,*  
1168 *Sinai Peninsula, Egypt. Environmental Earth Sciences*, 71, 1855-1869, 2014.
- 1169 Eizenhöfer, P.R., Zhao, G., Zhang, J., and Sun, M.: Final closure of the Paleo-Asian Ocean along the  
1170 Solonker Suture Zone: Constraints from geochronological and geochemical data of Permian  
1171 volcanic and sedimentary rocks. *Tectonics*, 33, 441-463, 2014.
- 1172 Favreau, G., Cappaere, B., Massuel, S., Leblanc, M., Boucher, M., Boulain, N., and Leduc, C.: *Land*  
1173 *clearing, climate variability, and water resources increase in semiarid southwest Niger: a review.*  
1174 *Water Resources Research*, 45, W00A16, doi.org/10.1029/2007WR006785, 2009.
- 1175 Fitts, C.R.: *Groundwater science*. Academic Press, Amsterdam, 2002. Freeze, R.A., and Cherry, J.A.:  
1176 *Groundwater*. Prentice-Hall, Inc, New Jersey, 1979.
- 1177 Gat, J.R.: Precipitation, groundwater and surface waters: control of climate parameters on their isotopic  
1178 composition and their utilization as palaeoclimatological tools. In: *Palaeoclimates and*  
1179 *palaeowaters: a collection of environmental isotope studies. Proc. Adv. Gp. Meeting, Vienna,*  
1180 *25-28 Nov 1980*, pp 3-12, IAEA, Vienna, 1983.
- 1181 Gat, J.R., and Issar, A.: Desert isotope hydrology: water sources of the Sinai Desert. *Geochimica et &*  
1182 *Cosmochimica Acta*, 38, 1117-1131, 1974.
- 1183 Gates, J., Edmunds, W.M., Ma, J., and Scanlon, B.: Estimating groundwater recharge in a cold desert  
1184 environment in northern China using chloride. *Hydrogeology Journal*, 16, 893-910, 2008.
- 1185 Giordano, M.: Global groundwater? Issues and solutions. *Annual Review of Environment and*  
1186 *Resources*, 34, 153-178, 2009.
- 1187 Gran, G.: *Determination of the equivalence point in potentiometric titrations. Part II. Analyst*, 77,  
1188 661-671, 1952.
- 1189 Guendouz, A., Moulla, A.S., Edmunds, W.M., Zouari, K., Shand, P., and Mamou, A.:  
1190 Hydrogeochemical and isotopic evolution of water in the Complexe Terminal aquifer in the  
1191 Algerian Sahara. *Hydrogeology Journal*, 11, 483-495, 2003.
- 1192 Harrington, G.A., Cook, P.G., and Herczeg, A.L.: *Spatial and temporal variability of ground water*  
1193 *recharge in central Australia: a tracer approach. Ground Water*, 40, 518-527, 2002.
- 1194 Healy, R.W.: *Estimating groundwater recharge*. Cambridge University Press, New York, 2010.
- 1195 Herczeg, A.L., and Leaney, F.: Review: environmental tracers in arid-zone hydrology. *Hydrogeology*

带格式的: 无下划线, 字体颜色: 自动设置

- 1196 Journal, 19, 17-29, 2011.
- 1197 Jahn, B.M.: The Central Asian Orogenic Belt and growth of the continental crust in the Phanerozoic.  
Geological Society London Special Publications, 226, 73-100, 2004.
- 1198 带格式的: 无下划线, 字体颜色: 自动设置
- 1199 Jian, P., Liu, D., Kröner, A., Windley, B.F., Shi, Y., Zhang, W., Zhang, F., Miao, L., Zhang, L., and  
Tomurhui, D.: Evolution of a Permian intraoceanic arc-trench system in the Solonker suture zone,  
Central Asian Orogenic Belt, China and Mongolia. Lithos, 118, 169-190, 2010.
- 1200 带格式的: 无下划线, 字体颜色: 自动设置
- 1201 Jin, K., Rao, W., Tan, H., Song, Y., Yong, B., Zheng, Y., Chen, T., and Han, L.: H-O isotopic and  
chemical characteristics of a precipitation-lake water-groundwater system in a desert area. Journal  
of Hydrology, 559, 848-860, 2018.
- 1202 带格式的: 无下划线, 字体颜色: 自动设置
- 1203 Jobbágy, E., Noy, M., Villagra, P., and Jackson, R.: Water subsidies from mountains to deserts: their  
role in sustaining groundwater-fed oases in a sandy landscape. Ecological Applications, 21,  
678-694, 2011.
- 1204 带格式的: 缩进: 左侧: 0 厘米,  
首行缩进: 0 字符
- 1205 带格式的: 无下划线, 字体颜色: 自动设置
- 1206 Kaufman, S.L.W.F.: The natural distribution of tritium. Physical Review, 93, 1337-1344, 1954.
- 1207 带格式的: 无下划线, 字体颜色: 自动设置
- 1208 Kazemi, G.A., Lehr, J.H., and Perrochet, P.: Groundwater age. John Wiley & Sons, Hoboken, 2006.
- 1209 带格式的: 无下划线, 字体颜色: 自动设置
- 1210 Khalid, B., and Hamid, C.: Using major ion and stable isotopes to characterize groundwater Recharge  
and hydrochemical processes in a mountain plain area: a case study in High Atlas of Marrakech,  
Morocco. Journal of Environment and Earth Science, 7, 100-114, 2017.
- 1211 带格式的: 无下划线, 字体颜色: 自动设置
- 1212 带格式的: 无下划线, 字体颜色: 自动设置
- 1213 Lawrence, A.R., Lloyd, J.W., and Marsh, J.M.: Hydrochemistry and Groundws, Hoboken, in Part of  
the Lincolnshire Limestone Aquifer, England. Ground Water, 14, 320-327, 1976.Li, J.: Permian  
geodynamic settings of Northeast China and adjacent regions: closure of the Paleo-Asian Ocean  
and subduction of the Paleo-Pacific Plate. Journal of Asian Earth Sciences, 26, 207-224.
- 1214 带格式的: 无下划线, 字体颜色: 自动设置
- 1215 Li, S., Sun, W., Li, X., and Zhang, B.: Sedimentary characteristics and environmental evolution of  
Otindag sandy land in Holocene. Journal of Desert Research, 15, 323-331, 1995 (in Chinese).
- 1216 带格式的: 无下划线, 字体颜色: 自动设置
- 1217 Liu, J., Song, X., Yuan, G., and Sun, X.: Stable isotopic compositions of precipitation in China. Tellus  
B, 66, 1-17, 2014.
- 1218 带格式的: 无下划线, 字体颜色: 自动设置
- 1219 Liu, Y., and Yamanaka, T.: Tracing groundwater recharge sources in a mountain-plain transitional area  
using stable isotopes and hydrochemistry. Journal of Hydrology, 464-465, 116-126, 2012.
- 1220 带格式的: 无下划线, 字体颜色: 自动设置
- 1221 Liu, Z., and Yang, X.: Geochemical-geomorphological evidence for the provenance of aeolian  
sands and sedimentary environments in the Hunshandake Sandy Land, Eastern Inner  
Mongolia, China. Acta Geologica Sinica (English Edition), 87, 871-884, 2013.
- 1222 带格式的: 无下划线, 字体颜色: 自动设置
- 1223 Lloyd, J.W., and Heathcote, J.A.: Natural inorganic hydrochemistry in relation to groundwater: An  
introduction. Clarendon Press, Oxford, 1985.
- 1224 带格式的: 无下划线, 字体颜色: 自动设置
- 1225 Love, A.J., Herczeg, A.L., Leaney, F.W., Stadter, M.H., Dighton, J.C., and Armstrong, D.: Groundwater  
residence time and palaeohydrology in the Otway Basin, South Australia. Journal of Hydrology,  
153, 157-187, 1994.
- 1226 带格式的: 无下划线, 字体颜色: 自动设置
- 1227 Love, A.J., Herczeg, A.L., Sampson, L., Cresswell, R.G., and Fifield, L.K.: Sources of chloride and  
implications for  $^{36}\text{Cl}$  dating of old groundwater, south-western Great Artesian basin, Australia.  
Water Resources Research, 36(6), 1561-1574, 2000.
- 1228 带格式的: 无下划线, 字体颜色: 自动设置
- 1229 Ma, J., Ding, Z., Gates, J.B., and Su, Y.: Chloride and the environmental isotopes as the indicators of
- 1230 带格式的: 无下划线, 字体颜色: 自动设置
- 1231 带格式的: 无下划线, 字体颜色: 自动设置
- 1232 带格式的: 无下划线, 字体颜色: 自动设置
- 1233 带格式的: 无下划线, 字体颜色: 自动设置
- 1234 带格式的: 无下划线, 字体颜色: 自动设置
- 1235 带格式的: 无下划线, 字体颜色: 自动设置

- 1236 the groundwater recharge in the Gobi Desert, northwest China. *Environmental Geology*, 55,  
1237 1407-1419, 2008.
- 1238 Ma, J., and Edmunds, W.M.: Groundwater and lake evolution in the BadainJaran Desert ecosystem,  
1239 Inner Mongolia. *Hydrogeology Journal*, 14, 1231-1243, 2006.
- 1240 Ma, J., He, J., Qi, S., Zhu, G., Zhao, W., Edmunds, W. M., and Zhao, Y.: *Groundwater recharge and*  
1241 *evolution in the Dunhuang Basin, northwestern China*. *Applied Geochemistry*, 28, 19-31, 2013.
- 1242 Ma, J., Pan, F., Chen, L., Edmunds, W.M., Ding, Z., He, J., Zhou, K., and Huang, T.: Isotopic and  
1243 geochemical evidence of recharge sources and water quality in the Quaternary aquifer beneath  
1244 Jinchang city, NW China. *Applied Geochemistry*, 25, 996-1007, 2010.
- 1245 Merlivat, L., and Jouzel, J.: Global climatic interpretation of the deuterium-oxygen 18 relationship for  
1246 precipitation. *Journal of Geophysical Research*, 84, 5029-5033, 1979.
- 1247 Meybeck, M.: Global occurrence of major elements in rivers. In: Drever, J.I. (Ed.), *Surface and Ground*  
1248 *Water, Weathering, and Soils*. Holland, H.D., and Turekian, K.K. (Exec.Eds), *Treatise on*  
1249 *Geochemistry*, vol. 5. Elsevier-Pergamon, Oxford, pp. 207-223, 2004.
- 1250 Nakaya, S., Uesugi, K., Motodate, Y., Ohmiya, I., Komiya, H., Masuda, H., and Kusakabe, M.: *Spatial*  
1251 *separation of groundwater flow paths from a multi flow system by a simple mixing model using*  
1252 *stable isotopes of oxygen and hydrogen as natural tracers*. *Water Resources Research*, 43, 1-15,  
1253 2007.
- 1254 Petrides, B., Cartwright, I., and Weaver, T.R.: The evolution of groundwater in the Tyrrell catchment,  
1255 south-central Murray Basin, Victoria, Australia. *Hydrogeology Journal*, 14, 1522-1543, 2006.
- 1256 Piper, A.M.: *A graphic procedure in the geochemical interpretation of water analyses*. *Transactions*  
1257 *American Geophysical Union*, 25, 914-928, 1944.
- 1258 Rattray, G.: *Geochemical evolution of groundwater in the Mud Lake area, Eastern Idaho, USA*.  
1259 *Environmental Earth Sciences*, 73, 8251-8269, 2015.
- 1260 Rizk, Z.S., and El-Etr, H.A.: *Hydrogeology and hydrogeochemistry of some springs in the United Arab Emirates*. *Arabian Journal for Science*  
1261 *and Engineering*, 22, 95-111, 1997.
- 1262 Scanlon, B.R., Keese, K.E., Flint, A.L., Flint, L.E., Gaye, C.B., Edmunds, W.M., and Simmers, I.:  
1263 Global synthesis of groundwater recharge in semiarid and arid regions. *Hydrological Processes*, 20,  
1264 3335-3370, 2006.
- 1265 Schoeller, H.: *Géochimie des eaux souterraines: application aux eaux des gisements de pétrole*. *Société*  
1266 *des éditions Technip, Paris*, 1955.
- 1267 Seiler, K.P., and Gat, J.R.: *Groundwater Recharge From Run-Off, Infiltration and Percolation*. Springer,  
1268 The Netherlands, 2007.
- 1269 Sklath, M.G., and Mwangi, M.P.: *An isotopic study of groundwater supplies in the Eastern Province of*  
1270 *Kenya*. *Journal of Hydrology*, 128, 257-275, 1991.
- 1271 Stolp, B.J., Solomon, D.K., Suckow, A., Vitvar, T., Rank, D., Aggarwal, P.K., and Han, L.F.: Age dating  
1272 base flow at springs and gaining streams using helium - 3 and tritium: Fischa - Dagnitz system,  
1273 southern Vienna Basin, Austria. *Water Resources Research*, 46, W07503,  
1274 doi:10.1029/2009WR008006, 2010.
- 1275 Sultan, M., Sturchio, N., Gheith, H., Hady, Y.A., and Anbeawy, M.: *Chemical and Isotopic Constraints*

带格式的: 无下划线, 字体颜色: 自动设置

- 1276 on the Origin of Wadi EliTarma Ground Water, Eastern Desert, Egypt. *Ground Water*, 38, 743-751,  
1277 2000.
- 1278 ~~Sun, D., Wu, F., Zhang, Y., and Gao, S.: The final closing time of the west Lamulun~~  
1279 ~~River-Changchun-Yanji plate suture zone-Evidence from the Dayushan granitic pluton, Jilin~~  
1280 ~~Province. *Journal of Jilin University (Earth Science Edition)*, 34, 174-181, 2004 (in Chinese).~~
- 1281 ~~Sun, J., Ye, J., Wu, W., Ni, X., Bi, S., Zhang, Z., Liu, W., and Meng, J.: Late Oligocene-Miocene~~  
1282 ~~mid-latitude aridification and wind patterns in the Asian interior. *Geology*, 38, 515-518, 2010.~~
- 1283 ~~Taylor, R.G., and Howard, K.W.: Groundwater recharge in the Victoria Nile basin of east Africa: support for the soil moisture balance approach using stable isotope tracers and flow modelling. *Journal of Hydrology*, 180, 31-53, 1996.~~  
1284 ~~Tian, F., Wang, Y., Liu, J., Tang, W., and Jiang, N.: Late Holocene climate change inferred from a lacustrine sedimentary sequence in southern Inner Mongolia, China. *Quaternary International*, 452, 22-32, 2017.~~
- 1285 ~~Vanderzalm, J.L., Jeuken, B.M., Wischusen, J.D.H., Pavelle, P., Salle, C.L.G.L., Knapton, A., and Dillon, P.J.: Recharge sources and hydrogeochemical evolution of groundwater in alluvial basins in arid central Australia. *Journal of Hydrology*, 397, 71-82, 2011.~~
- 1286 ~~Wada, Y., van Beek, L.P.H.V., van Kempen, C.M., Reehman, J.W.T.M., Vasak, S., and Bierkens, M.F.P.: Global depletion of groundwater resources. *Geophysical Research Letters*, 37, L20402, doi.org/10.1029/2010GL044571, 2010.~~  
1287 ~~Wang, P., Yu, J., Zhang, Y., and Liu, C.: Groundwater recharge and hydrogeochemical evolution in the Ejina Basin, northwest China. *Journal of Hydrology*, 476, 72-86, 2013.~~
- 1288 ~~Wang, Q., and Liu, X.Y.: Paleoplate tectonics between Cathaysia and Angaraland in Inner Mongolia of China. *Tectonics*, 5, 1073-1088, 1986.~~
- 1289 ~~Wang, W., and Feng, Z.D.: 2013. Holocene moisture evolution across the Mongolian Plateau and its surrounding areas: a synthesis of climatic records. *Earth-Science Reviews* 122, 38-57, 2013.~~
- 1290
- 1291 ~~Wu, J., An, N., Ji, Y., and Wei, X.: Analysis on Characteristics of Precipitation and Runoff in Silas MuLun River Basin. *Meteorology Journal of Inner Mongolia*, 23-25, 2014 (in Chinese).~~
- 1292
- 1293 ~~Xiao, J., Si, B., Zhai, D., Itoh, S., and Lomtatidze, Z.: Hydrology of Dali Lake in central-eastern Inner Mongolia and Holocene East Asian monsoon variability. *Journal of Paleolimnology*, 40, 519-528, 2008.~~
- 1294
- 1295 ~~Yang, X., Li, H., and Conacher, A.: Large-scale controls on the development of sand seas in northern China. *Quaternary International*, 250, 74-83, 2012.~~
- 1296
- 1297 ~~Yang, X., Ma, N., Dong, J., Zhu, B., Xu, B., Ma, Z., and Liu, J.: Recharge to the inter-dune lakes and Holocene climatic changes in the BadainJaran Desert, western China. *Quaternary Research*, 73, 10-19, 2010.~~
- 1298
- 1299 ~~Yang, X., Scuderi, L.A., Wang, X., Scuderi, L.J., Zhang, D., Li, H., Forman, S., Xu, Q., Wang, R., Huang, W., and Yang, S.: Groundwater sapping as the cause of irreversible desertification of Hunshandake Sandy Lands, Inner Mongolia, northern China. *PNAS*, 112, 702-706, 2015.~~
- 1300
- 1301 ~~Yang, X., Wang, X., Liu, Z., Li, H., Ren, X., Zhang, D., Ma, Z., Rioual, P., Jin, X., and Scuderi, L.: Initiation and variation of the dune fields in semi-arid China – with a special reference to the~~

带格式的: 无下划线, 字体颜色: 自动设置

带格式的: 字体: (默认) Times New Roman, 10 磅, 无下划线, 字体颜色: 自动设置

带格式的: 缩进: 左侧: 0 厘米, 悬挂缩进: 2 字符, 行距: 1.5 倍行距

带格式的: 无下划线, 字体颜色: 自动设置

带格式的: 字体: (默认) Times New Roman, 10 磅, 无下划线, 字体颜色: 自动设置

带格式的: 无下划线, 字体颜色: 自动设置

带格式的: 字体: (默认) Times New Roman, 10 磅, 无下划线, 字体颜色: 自动设置

带格式的: 无下划线, 字体颜色: 自动设置

- 1316 Hunshandake Sandy Land, Inner Mongolia. *Quaternary Science Reviews*, 78, 369-380, 2013.
- 1317 Yang, X., and Williams, M.A.J.: The ion chemistry of lakes and late Holocene desiccation in the  
1318 BadainJaran Desert, Inner Mongolia, China. *Catena*, 51, 45-60, 2003. 带格式的: 无下划线, 字体颜色:  
自动设置
- 1319 Yang, X., Zhu, B., Wang, X., Li, C., Zhou, Z., Chen, J., Yin, J., and Lu, Y.: Late Quaternary  
1320 environmental changes and organic carbon density in the Hunshandake Sandy Land, eastern Inner  
1321 Mongolia, China. *Global and Planetary Change*, 61, 70-78, 2008.
- 1322 Yao, S., Zhu, Z., Zhang, S., Zhang, S., and Li, Y.: Using SWAT model to simulate the discharge of the  
1323 river Shandianhe in Inner Mongolia. *Journal of Arid Land Resources and Environment*, 27,  
1324 175-180, 2013 (in Chinese). 带格式的: 无下划线, 字体颜色:  
自动设置
- 1325 Zhai, Y., Wang, J., Teng, Y., and Zuo, R.: *Hydrogeochemical and isotopic evidence of groundwater  
1326 evolution and recharge in aquifers in Beijing Plain, China*. *Environmental Earth Sciences*, 69,  
1327 2167-2177, 2013. Zhang, Z., Li, K., Li, J., Tang, W., Chen, Y., and Luo, Z.: *Geochronology and  
1328 geochemistry of the Eastern Erenhot ophiolitic complex: implications for the tectonic evolution of  
1329 the Inner Mongolia-Daxinganling Orogenic Belt*. *Journal of Asian Earth Sciences*, 97, 279-293,  
1330 2015.
- 1331 Zhao, J., Ma, Y., Luo, X., Yue, D., Shao, T., and Dong, Z.: The discovery of surface runoff in the  
1332 megadunes of BadainJaran Desert, China, and its significance. *Science China Earth Sciences*, 60,  
1333 707-719, 2017. 带格式的: 无下划线, 字体颜色:  
自动设置
- 1334 Zhao, L., Xiao, H., Dong, Z., Xiao, S., Zhou, M., Cheng, G., Yin, L., and Yin, Z.: Origins of  
1335 groundwater inferred from isotopic patterns of the Badain Jaran Desert, Northwestern China.  
1336 *Ground Water*, 50, 715-725, 2012. 带格式的: 无下划线, 字体颜色:  
自动设置
- 1337 Zhen, Z., Li, C., Li, W., Hu, Q., Liu, X., Liu, Z., and Yu, R.: Characteristics of environmental isotopes  
1338 of surface water and groundwater and their recharge relationships in Lake Dali basin. *Journal of  
1339 Lake Sciences*, 26, 916-922, 2014 (in Chinese). 带格式的: 无下划线, 字体颜色:  
自动设置
- 1340 Zhu, B.Q., Yang, X.P., Rioual, P., Qin, X.G., Liu, Z.T., Xiong, H.G., and Yu, J.J.: *Hydrogeochemistry  
1341 of three watersheds (the Erlqis, Zhungarer and Yili) in northern Xinjiang, NW China*. *Applied  
1342 Geochemistry*, 26, 1535-1548, 2011. 带格式的: 无下划线, 字体颜色:  
自动设置
- 1343 Zhu, B.Q., Yu, J.J., Qin, X.G., Rioual, P., and Xiong, H.G.: *Climatic and geological factors contributing  
1344 to the natural water chemistry in an arid environment from watersheds in northern Xinjiang, China*.  
1345 *Geomorphology*, 153-154, 102-114, 2012. 带格式的: 无下划线, 字体颜色:  
自动设置
- 1346 Zhu, B.Q., Yu, J.J., Rioual, P., Gao, Y., Zhang, Y.C., and Xiong, H.G.: Climate effects on recharge and  
1347 evolution of natural water resources in middle-latitude watersheds under arid climate. In: Ramkumar, M. U., Kumaraswamy, K., and Mohanraj, R. (Eds.), *Environmental Management of River Basin Ecosystems*. Springer Earth System Sciences, Springer-Verlag, Heidelberg, pp. 91-109, 2015. 带格式的: 无下划线, 字体颜色:  
自动设置
- 1348 Zhu, B.Q., and Wang, Y.L.: *Statistical study to identify the key factors governing ground water  
1349 recharge in the watersheds of the arid Central Asia*. *Environmental Monitoring and Assessment*,  
1350 188(1), 66, doi: 10.1007/s10661-015-5075-4, 2016. 带格式的: 无下划线, 字体颜色:  
自动设置
- 1351 Zhu, B.Q., Wang, X.M., and Rioual, P.: Multivariate indications between environment and ground  
1352 water recharge in a sedimentary drainage basin in northwestern China. *Journal of Hydrology*, 2017,  
1353 520, 100-111. 带格式的: 无下划线, 字体颜色:  
自动设置

- 1356 549, 92-113, 2017.
- 1357 Zhu, G.F., Li, Z.Z., Su, Y.H., Ma, J.Z., and Zhang, Y.Y.: Hydrogeochemical and isotope evidence of  
1358 groundwater evolution and recharge in Minqin Basin, Northwest China. *Journal of Hydrology*,  
1359 333, 239-251, 2007.
- 1360 Zhu, G.F., Su, Y.H., and Feng, Q.: The hydrochemical characteristics and evolution of groundwater and  
1361 surface water in the Heihe River Basin, northwest China. *Hydrogeology Journal*, 16, 167-182,  
1362 2008.
- 1363 Zhu, Z., Wu, Z., Liu, S., and Di, X.: *An Outline of Chinese Deserts*. Science Press, Beijing, 1980 (in  
1364 Chinese).
- 1365
- 1366 | 

带格式的: 无下划线, 字体颜色:  
自动设置

带格式的: 无下划线, 字体颜色:  
自动设置

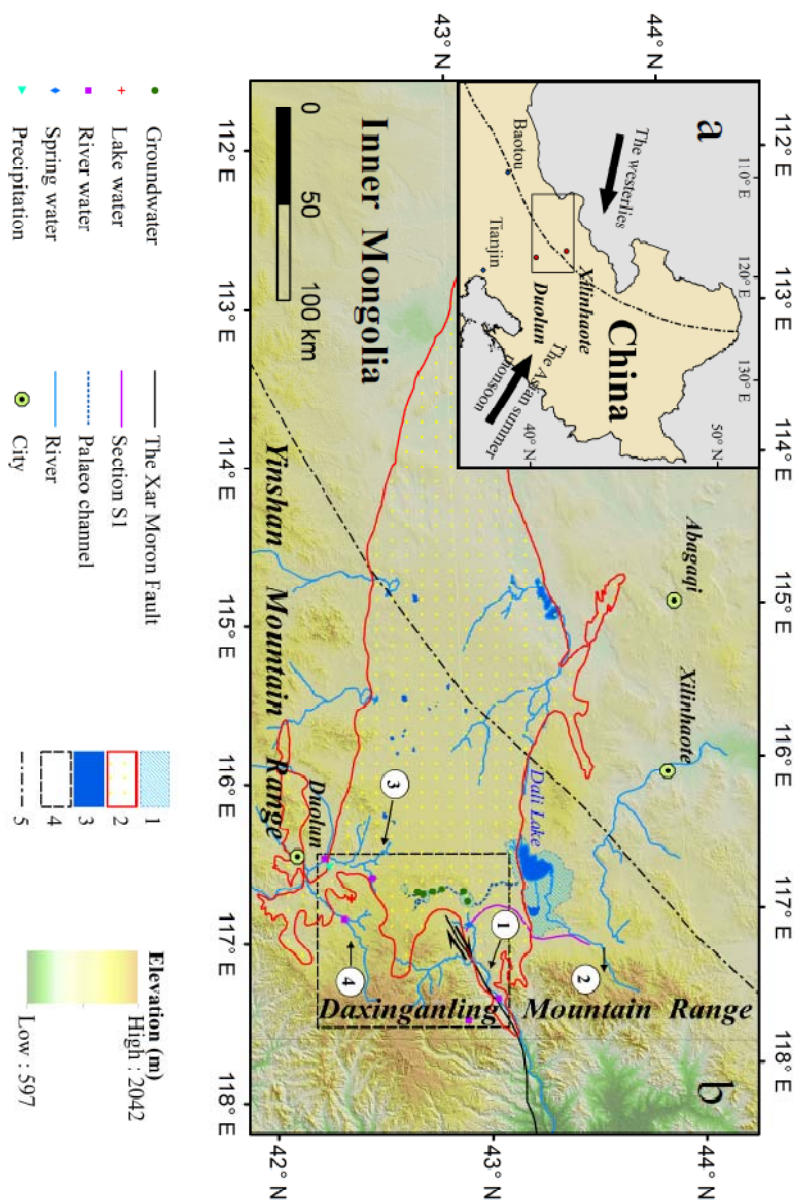
带格式的: 无下划线, 字体颜色:  
自动设置

带格式的: 无下划线, 字体颜色:  
自动设置

带格式的: 定义网格后不调整右  
缩进, 行距: 1.5 倍行距, 不对齐  
到网格

1367  
1368  
1369  
1370  
1371  
1372  
1373  
1374  
1375  
1376  
1377  
1378**Figure Captions:**

**Fig. 1.** The Geographical location of the Otindag Desert in northern China. (a) The study area shown at a large scale in a bigger scale, and (b) the study area shown at a smaller scale, with detailed information about the boundary and tectonic settings of the desert land. 1, the palaeo lake area of the megalake Dali; 2, the boundary of the Otindag; 3, the modern lake area; 4, the boundary of Fig. 2; 5, the boundary between the westerlies and the East Asian Summer Monsoon (EASM) climate systems. ①, the Xilamulun River. ②, the Gonggeer River. ③, the Shepi River. ④, the Tuligen River. The boundary between the westerlies and the EASMin (a) and (b) is modified from Chen et al. (2010). The palaeo lake area of the megalake Dali and the palaeo channel in (b) is modified from Yang et al. (2015). The location of the Xar Moron Fault is referenced from Eizenhöfer et al. (2014). Section S1 is an elevation section starting from the upstream of the Dali Lake and ending with at a spring sample (s2) in the riverhead of Xilamulun River.



1379

1380  
1381  
1382  
1383  
1384  
1385  
1386

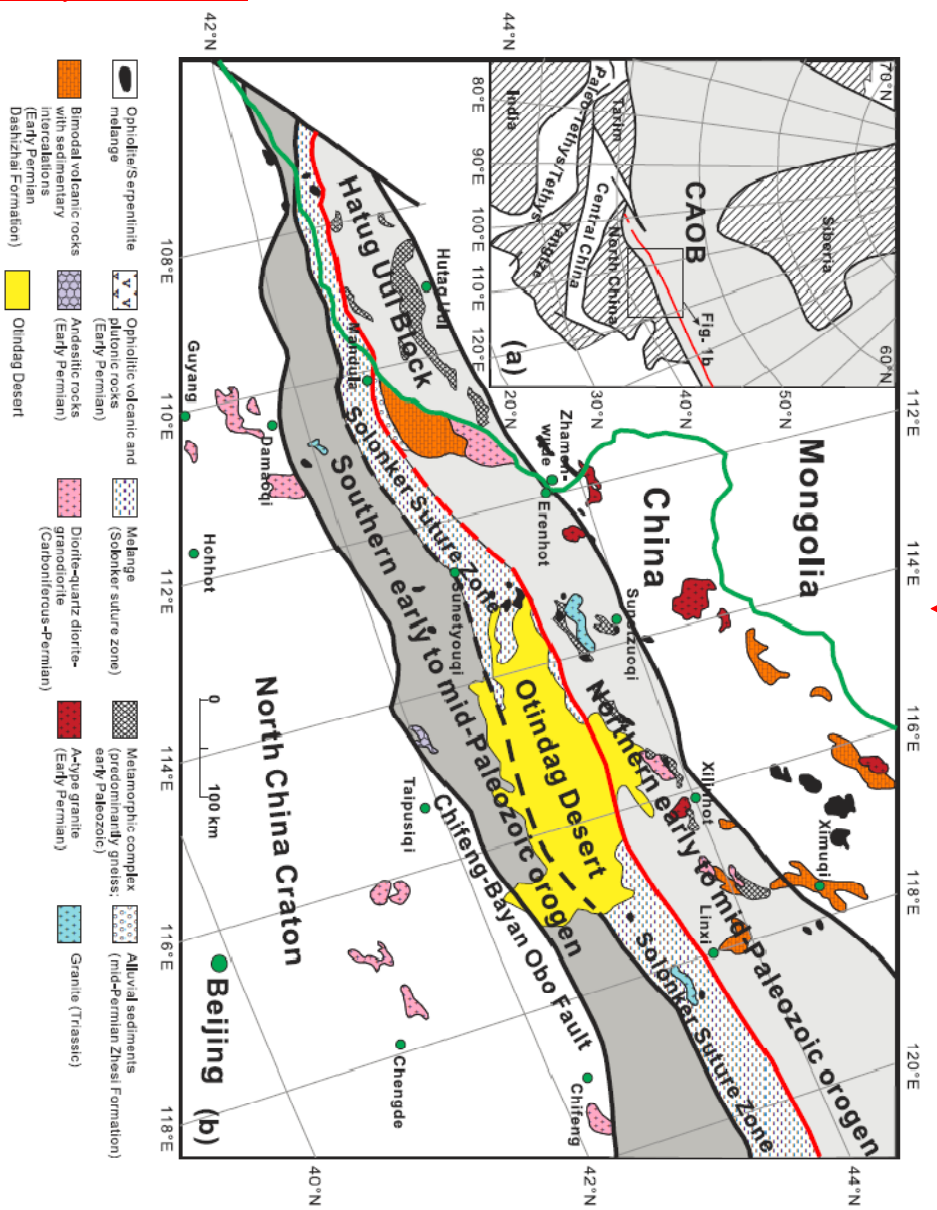
**Fig. 2.** (a) Tectonic framework of the north China-Mongolian segment of the Central Asian Orogenic Belt (modified after Jahn, 2004). (b) Geological sketch map of the northern China-Mongolia tract (modified after Jian et al., 2010). The Solonker suture zone represents the tectonic boundary between the northern (Hutug Uul Block-Northern orogen) and the southern (southern orogen-Northern margin of North China craton) continental blocks. Note that the red line marks the early Permian paleobiogeographical boundary (Wang and Liu, 1986; Li, 2006), which coincides with the northern boundary of the suture zone.

带格式的：字体：加粗，无下划线，字体颜色：自动设置

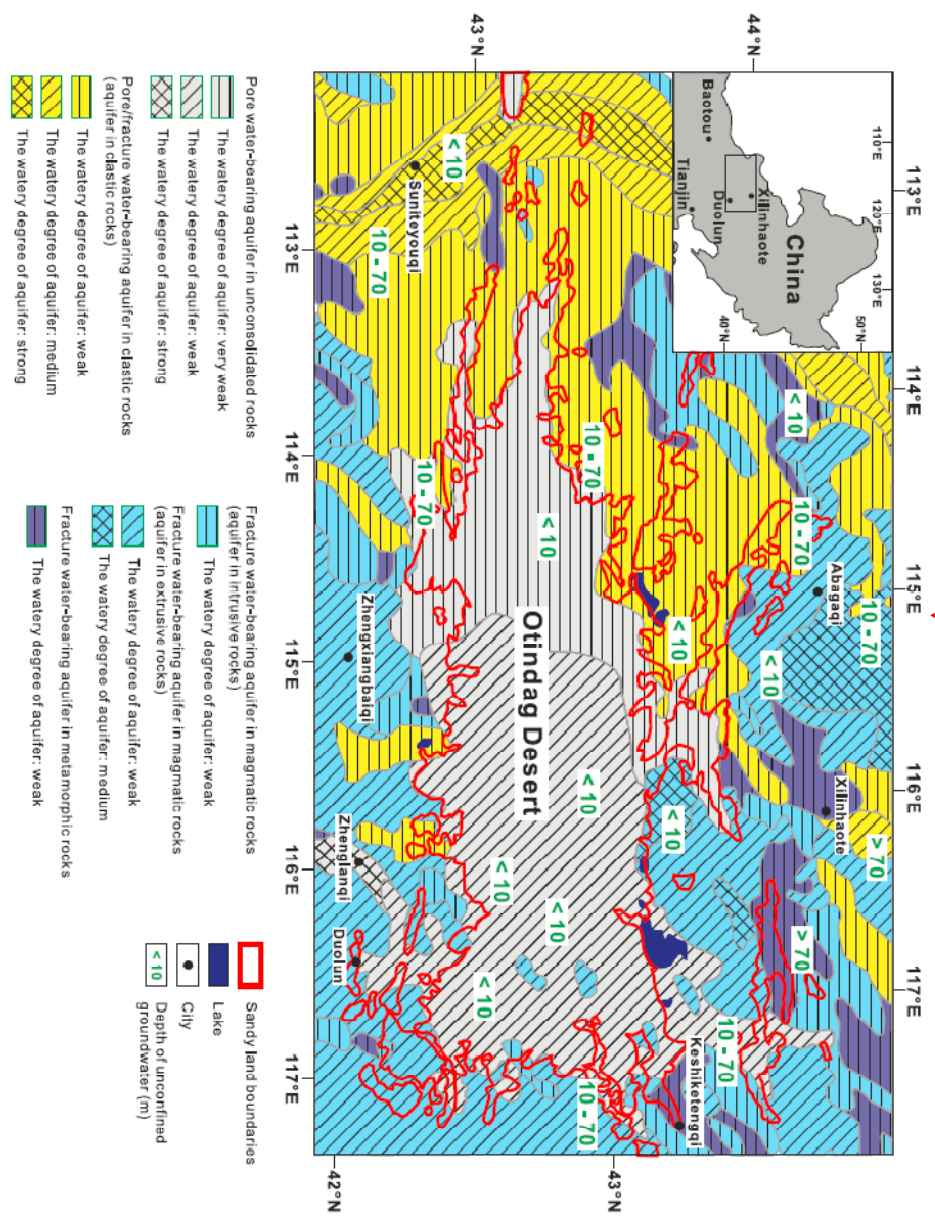
带格式的：无下划线，字体颜色：自动设置

带格式的：字体：(默认) Times New Roman, 10 磅，无下划线，字体颜色：自动设置

带格式的：居中



1387  
1388  
1389  
1390  
1391  
1392  
1393  
1394

**Fig. 3.** The hydrogeological division map of the Otindag Desert.

带格式的：字体：加粗，无下划线，字体颜色：自动设置

带格式的：无下划线，字体颜色：自动设置

带格式的：字体：(默认) Times New Roman, 10 磅，无下划线，字体颜色：自动设置

带格式的：居中

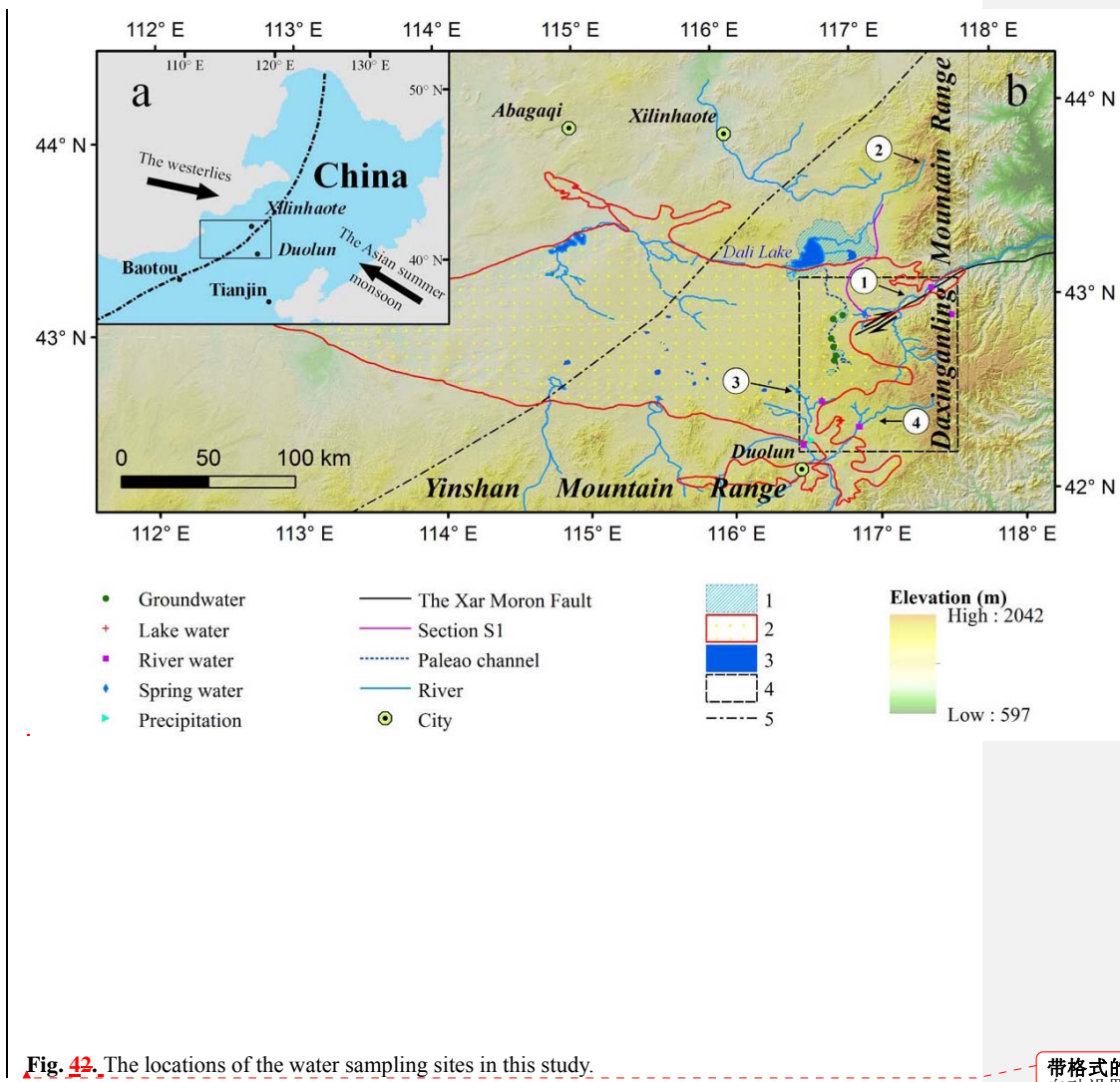
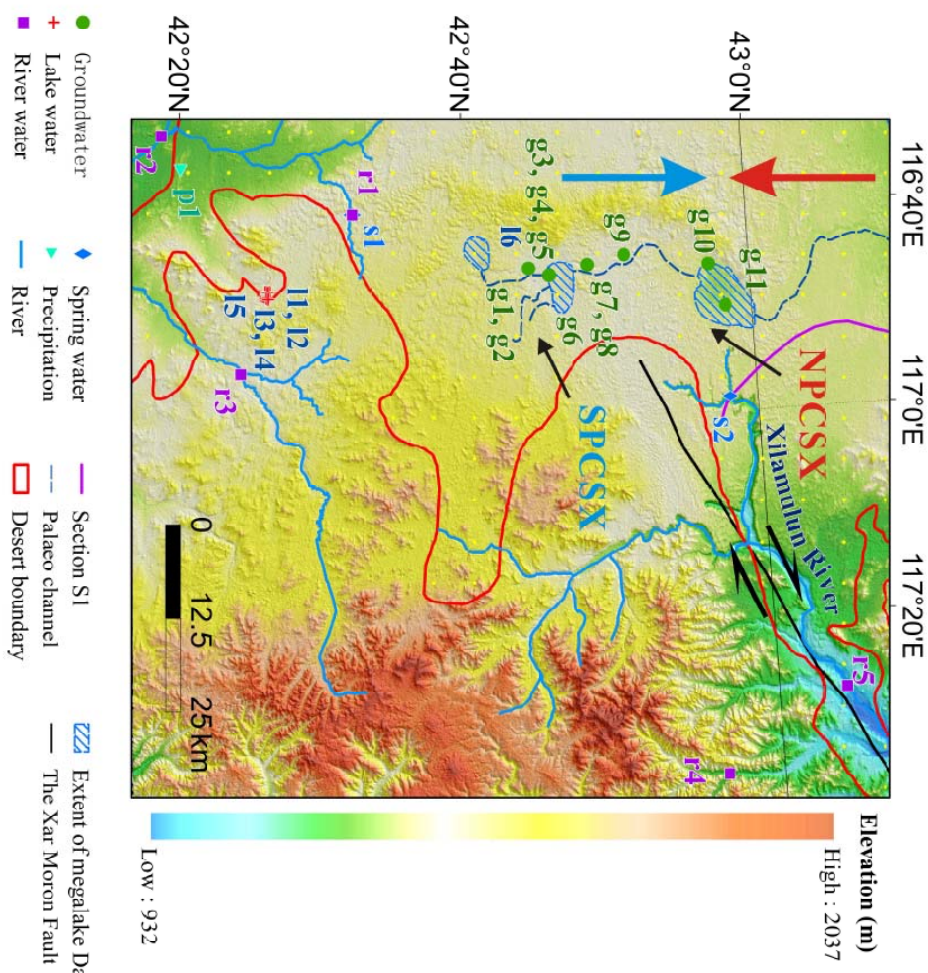


**Fig. 42.** The locations of the water sampling sites in this study.

带格式的: 无下划线, 字体颜色: 自动设置

带格式的：字体：(默认) Times New Roman, 10 磅, 无下划线, 字体颜色: 自动设置

带格式的：居中



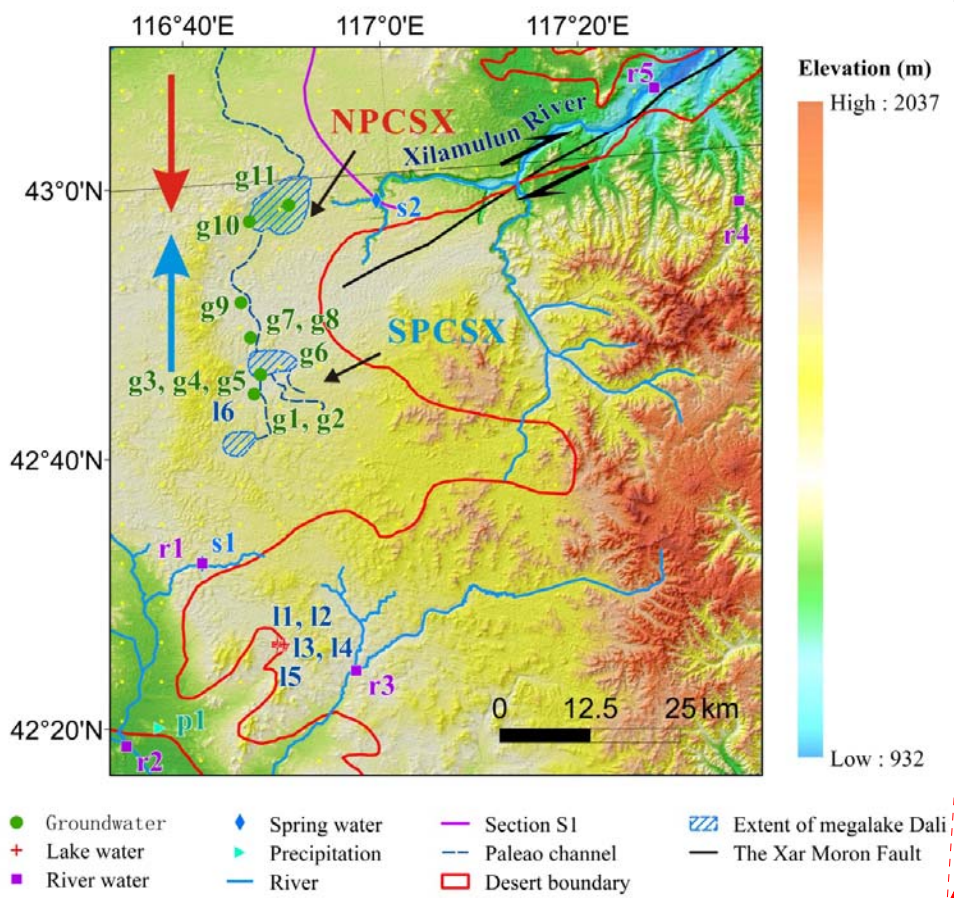
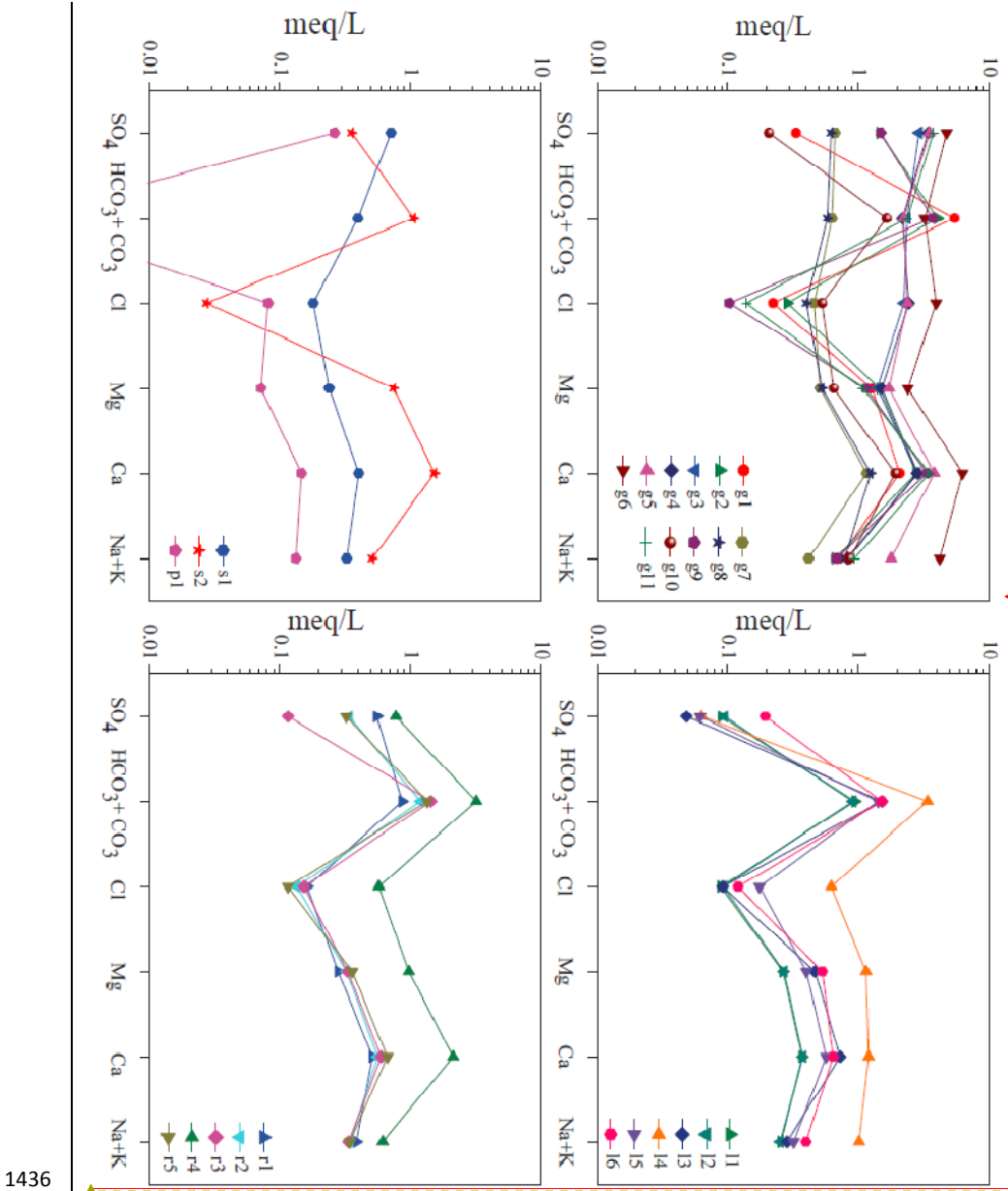
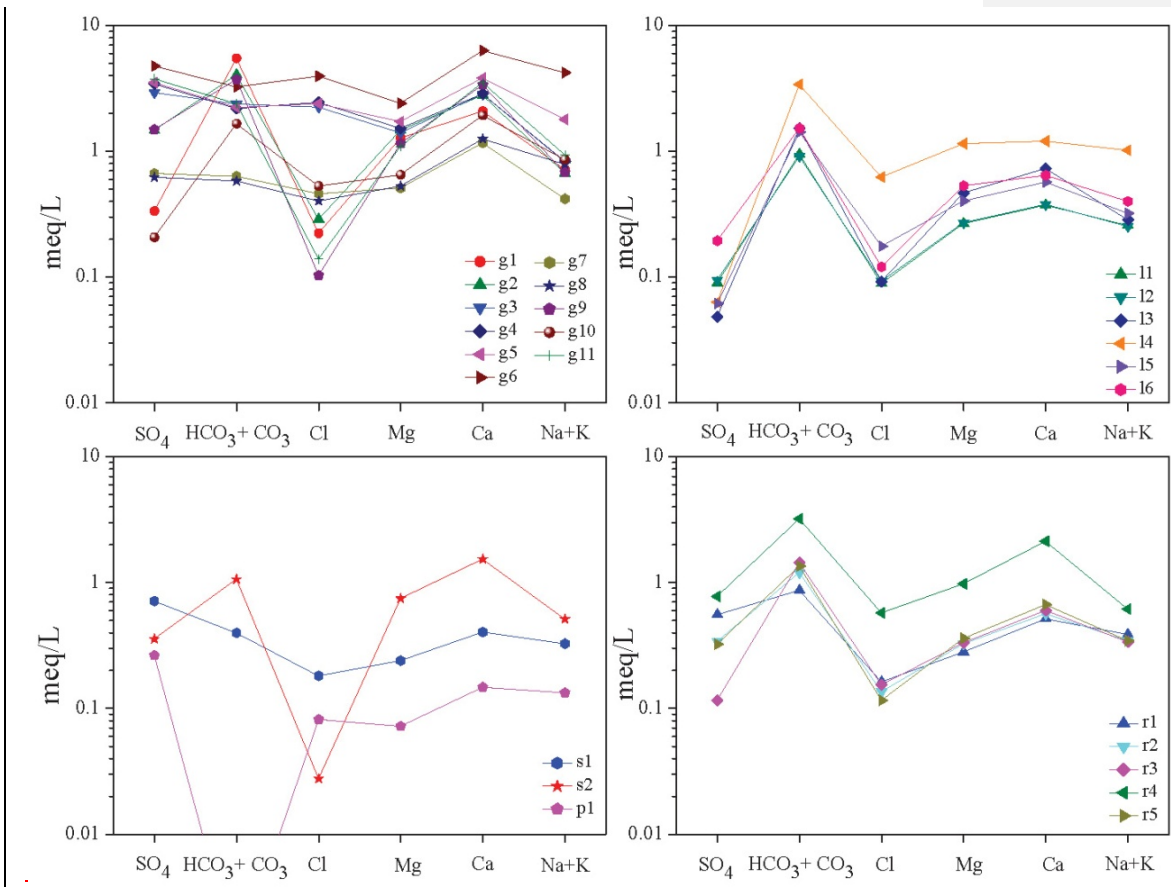


Fig. 53. The Schoeller diagram (Schoeller, 1955), a fingerprint diagram showing the variations of multiple ions' concentrations in the studied water samples in an equivalent unit. The  $\text{HCO}_3 + \text{CO}_3$  concentration in the sample p1 was not shown, due to its value being lower than the detection limit.

带格式的：字体：(默认) Times New Roman, 10 磅, 无下划线, 字体颜色: 自动设置

带格式的：居中





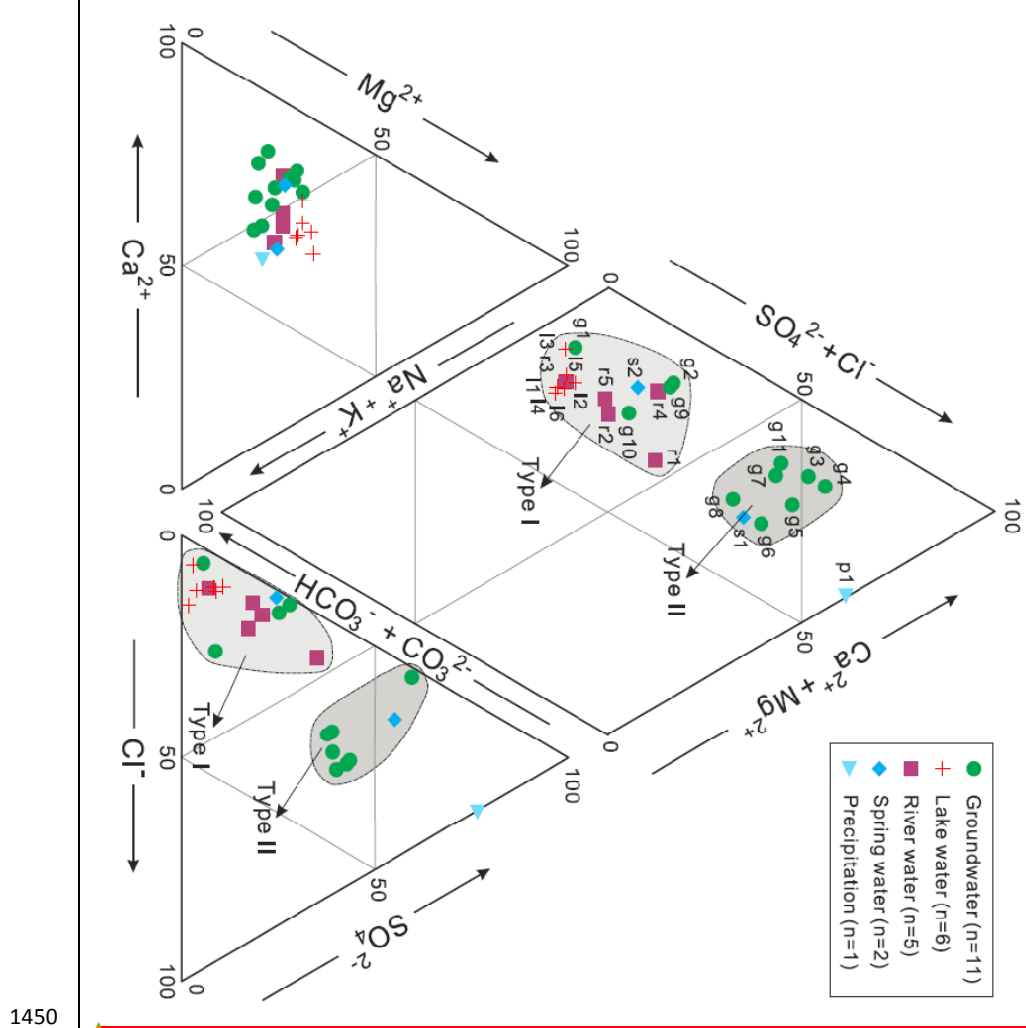
1437  
1438  
1439  
1440  
1441  
1442  
1443  
1444  
1445  
1446  
1447  
1448  
1449

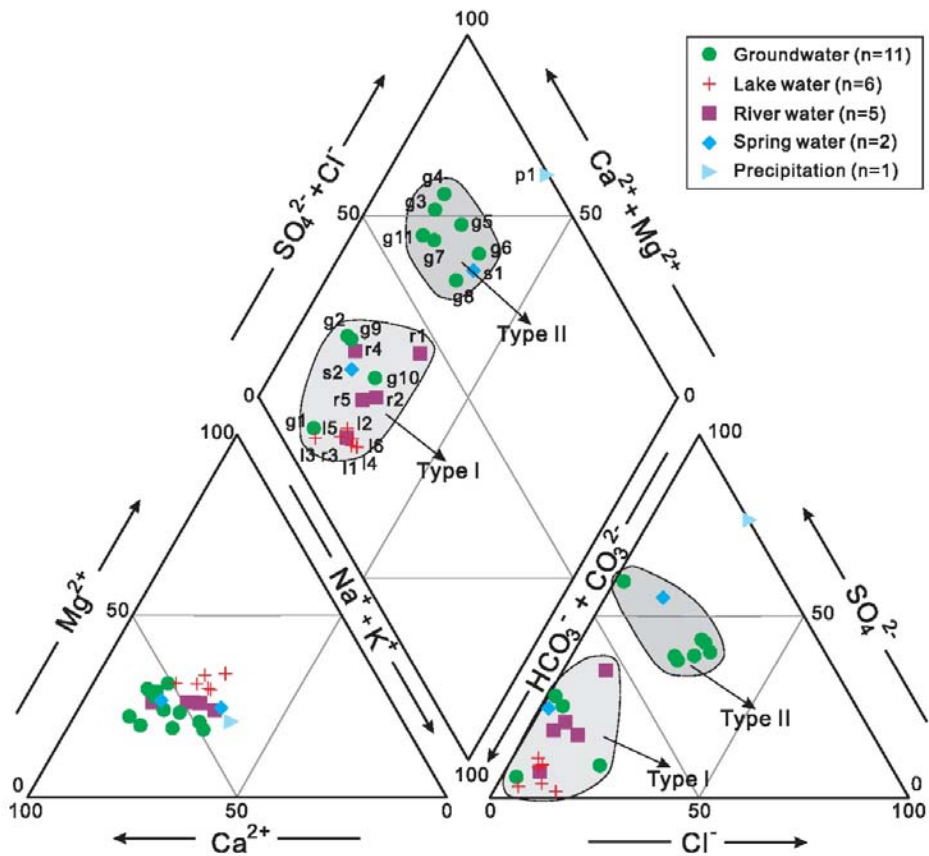
**Fig. 6-4.** The Piper diagram (Piper, 1944) showing the relative abundances of major cations and anions in the studied water samples. Major water types are also shown in this diagram.

带格式的: 无下划线, 字体颜色: 自动设置  
带格式的: 无下划线, 字体颜色: 自动设置  
带格式的: 无下划线, 字体颜色: 自动设置

带格式的：字体：(默认) Times New Roman, 10 磅, 无下划线, 字体颜色: 自动设置

带格式的：居中





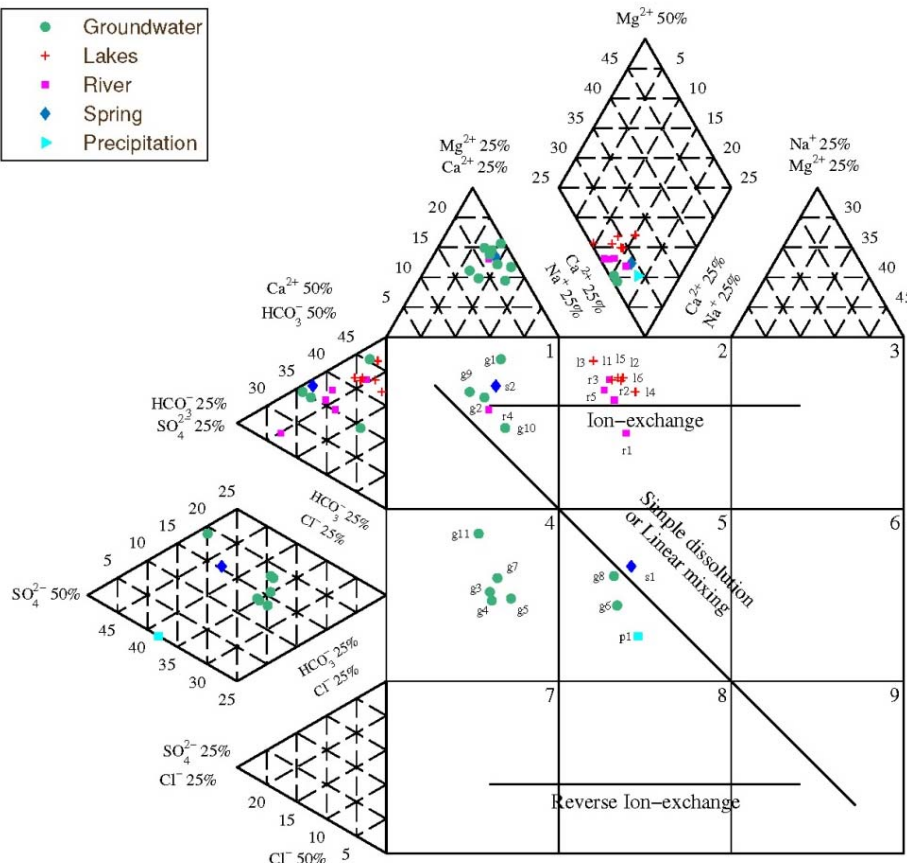
1451  
1452  
1453  
1454  
1455  
1456  
1457  
1458  
1459  
1460  
1461  
1462  
1463  
1464  
1465  
1466  
1467  
1468  
1469  
1470  
1471 **Fig. 5. An Expanded Durov diagram (Durov, 1948; Lloyd and Heathcote, 1985; Al-Bassam et al.,**  
1472 **1997; Chadha, 1999; Al-Bassam and Khalil, 2012) showing the linear dissolution or mixing**  
1473 **process for groundwater and the ion exchange process occurred in the groundwater and other**  
1474 **waters in the study area.**

带格式的: 无下划线, 字体颜色:  
自动设置

带格式的: 字体: 加粗, 无下划线,  
字体颜色: 自动设置

带格式的: 字体: 加粗

- Groundwater
- Lakes
- River
- Spring
- Precipitation



带格式的：字体：(默认) Times New Roman, 10 磅, 加粗, 无下划线, 字体颜色: 自动设置

带格式的：字体：加粗

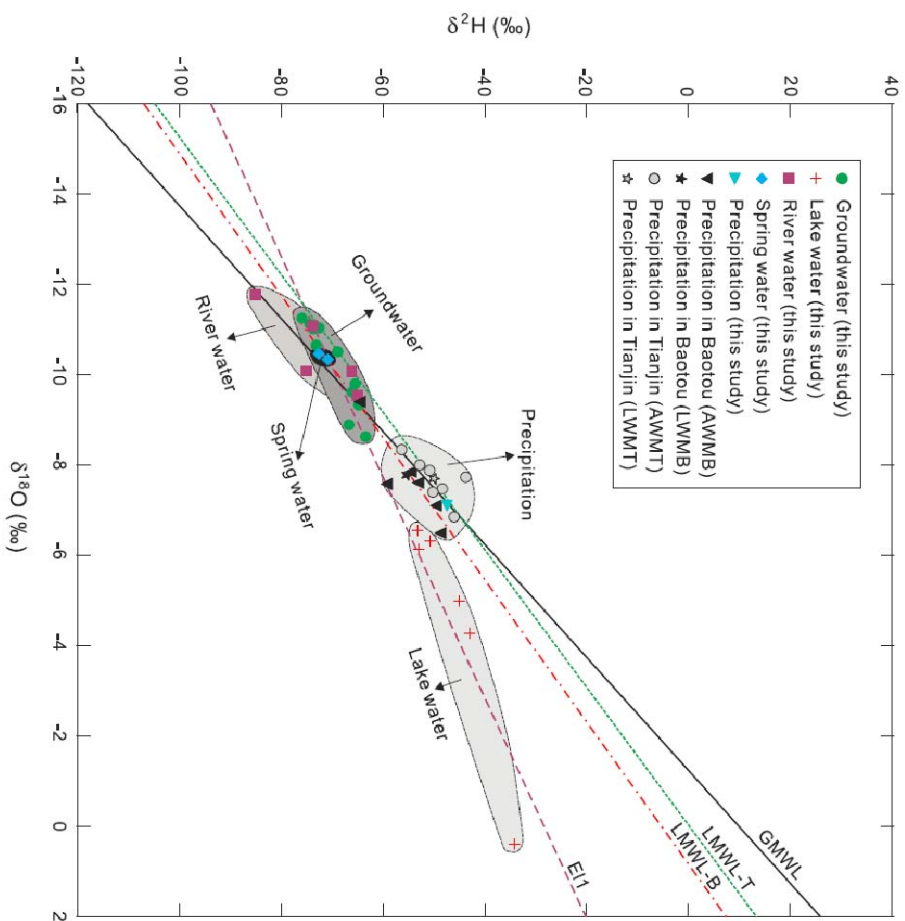
带格式的：无下划线, 字体颜色: 自动设置

1475  
1476  
1477  
1478  
1479  
1480  
1481  
1482  
1483  
1484

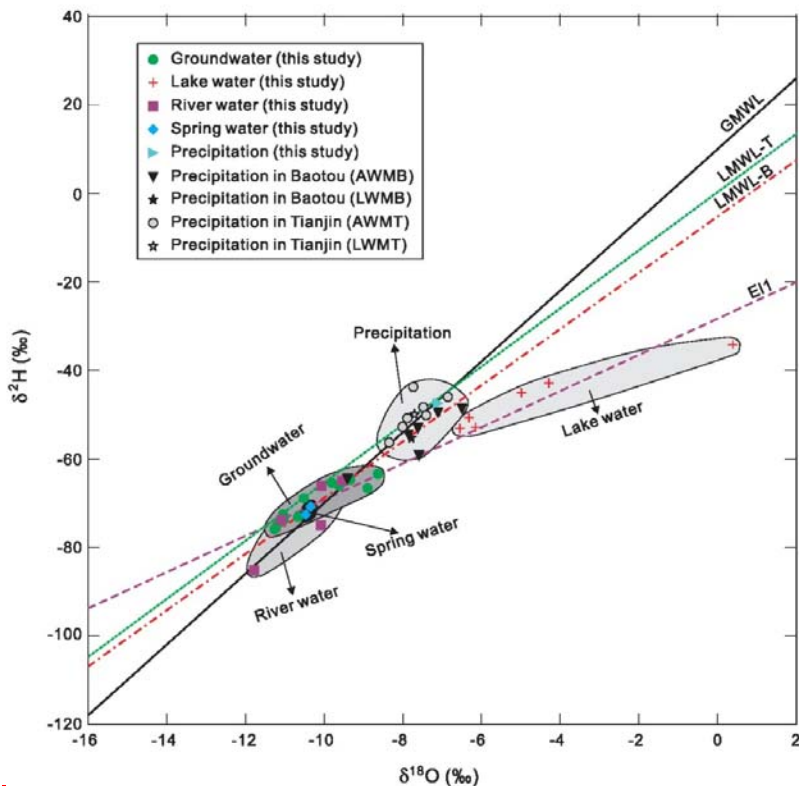
**Fig. 76.** The bivariate diagram of  $\delta\text{D}^{\text{H}}$  and  $\delta^{18}\text{O}$ , i.e. the Craig diagram, for the natural water samples in this study. Different relationships between the groundwaters, lake waters, river waters, spring waters and the precipitation waters are **emphasized** illustrated. AWMB, the annual weighted mean value at the Baotou station; AWMT, the annual weighted mean value at the Tianjin station; LWMB, the long-term weighted means at the Baotou station; LWMT, the long-term weighted means at the Tianjin station; GMWL, the Global Meteoric Water Line; LMWL-B, the local meteoric water line calculated based on the data from the Baotou station; LWML-T, the local meteoric water line calculated based on the data from the Tianjin station; EL1, the evaporation line calculated based on the data of water samples collected in [this study](#) [eastern](#) [Otindag](#).

带格式的：字体：(默认) Times  
New Roman, 10 磅, 无下划线, 字  
体颜色: 自动设置

带格式的：居中



1485



1486  
1487  
1488  
1489  
1490  
1491  
1492  
1493  
1494  
1495  
1496  
1497  
1498  
1499  
1500  
1501  
1502  
1503

**Fig. 87** The seasonal mean distributions of (a) precipitation (a), (b) surface air temperature (b) and (c) water vapor pressure (c) from the Baotou and Tianjin weather stations (station sites seen in Fig. 1a) in the surrounding areas of the Otindag for the period in recent thirty years (1981-2010).

带格式的: 无下划线, 字体颜色: 自动设置

带格式的: 字体: 加粗, 无下划线, 字体颜色: 自动设置

带格式的: 无下划线, 字体颜色: 自动设置

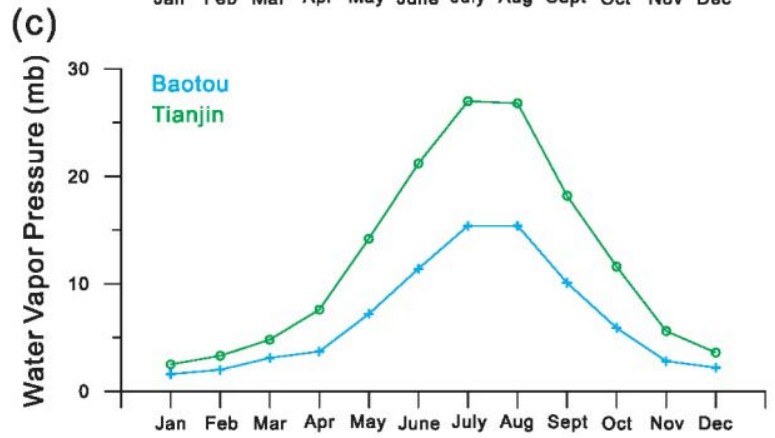
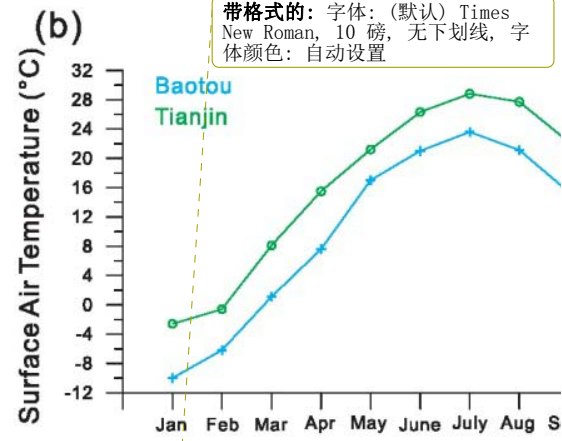
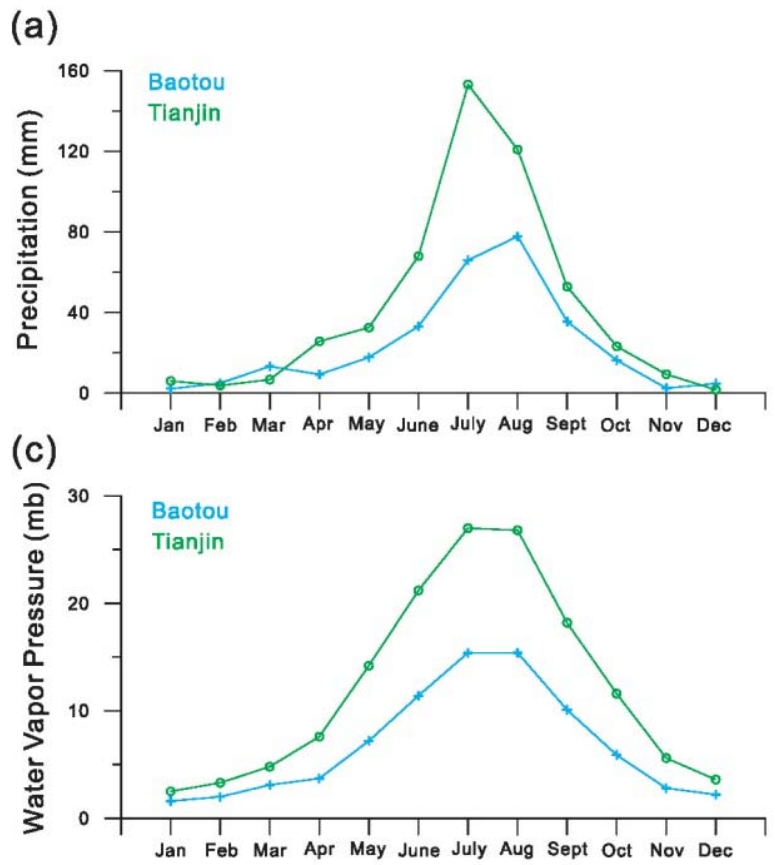
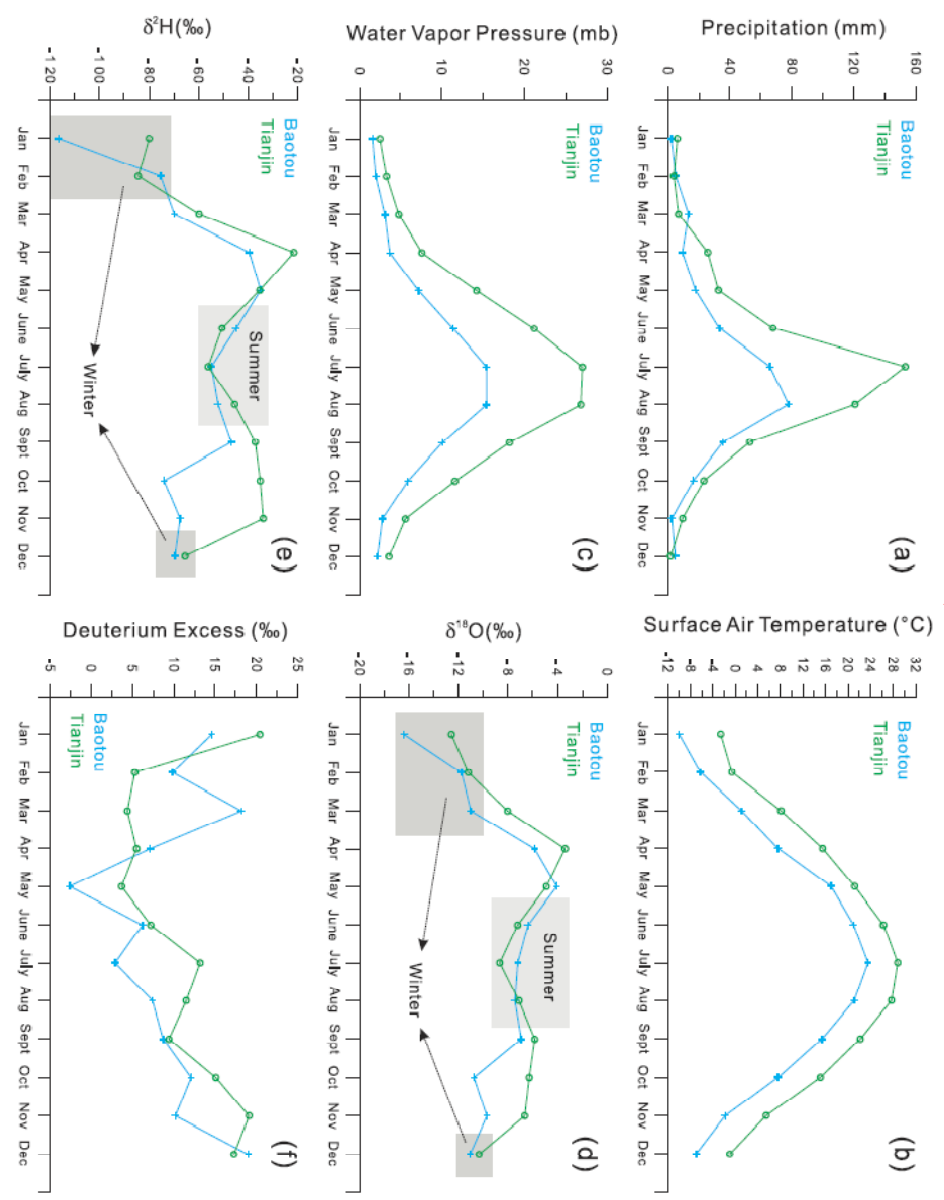


**Fig. 8.** The seasonal mean distributions of (d)  $\delta^{18}\text{O}$  (a) and (e)  $\delta\text{D}^2\text{H}$  (b) values in precipitation from the Baotou and Tianjin weather stations in the surrounding areas of the Otindag for the period in recent sixteen years (1986-2001).

带格式的: 字体: (默认) Times New Roman, 10 磅, 无下划线, 字体颜色: 自动设置

带格式的: 居中



1509  
1510  
1511  
1512  
1513  
1514  
1515  
1516  
1517  
1518  
1519  
1520  
1521  
1522  
1523  
1524  
1525  
1526

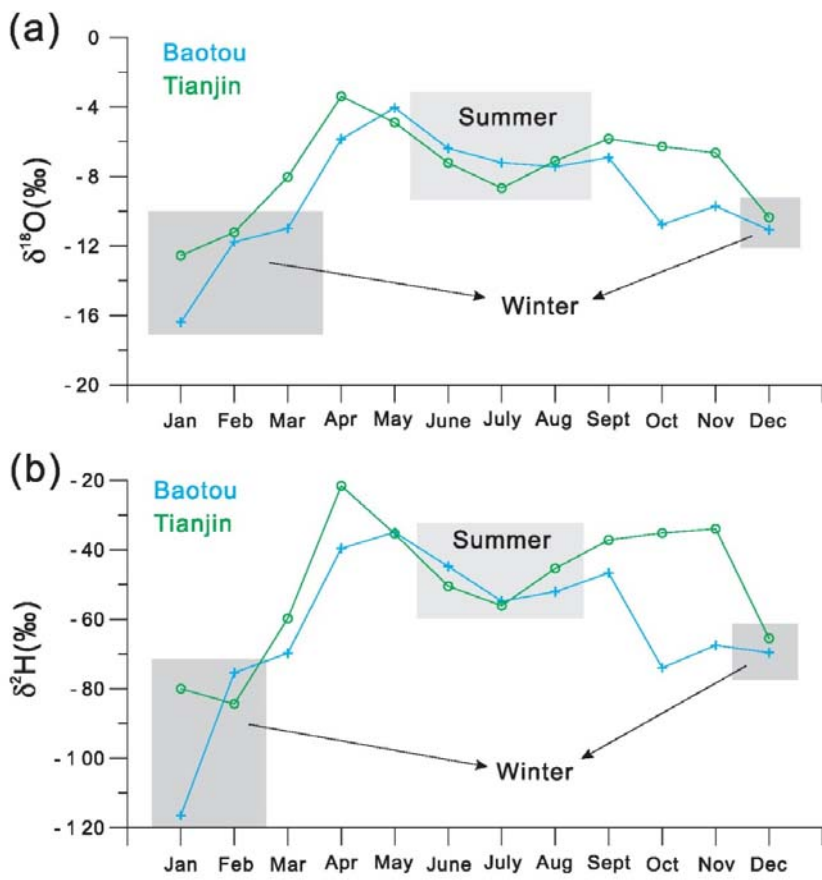


Fig. 9. The bivariate diagram of  $\delta\text{D}$  and  $\delta^{18}\text{O}$ , i.e. the Craig diagram, for the natural water samples collected in the Otindag (this study) and the Dali Basin's study. Different relationships between the groundwaters, lake waters, river waters, spring waters and the precipitation waters are emphasized clearly. AWMB, AWMT, LWMB, LWMT, GMWL, LMWL-B, LWML-T, and EL1 are the same as in to Fig. 7. EL2, the evaporation line calculated based on the data from the groundwater, lake water, river water and spring water samples collected from in the Otindag and in the Dali Basin. The data for of the Dali were taken from are cited from previous studies (Chen et al. (2008) and Zhen et al. (2014)).

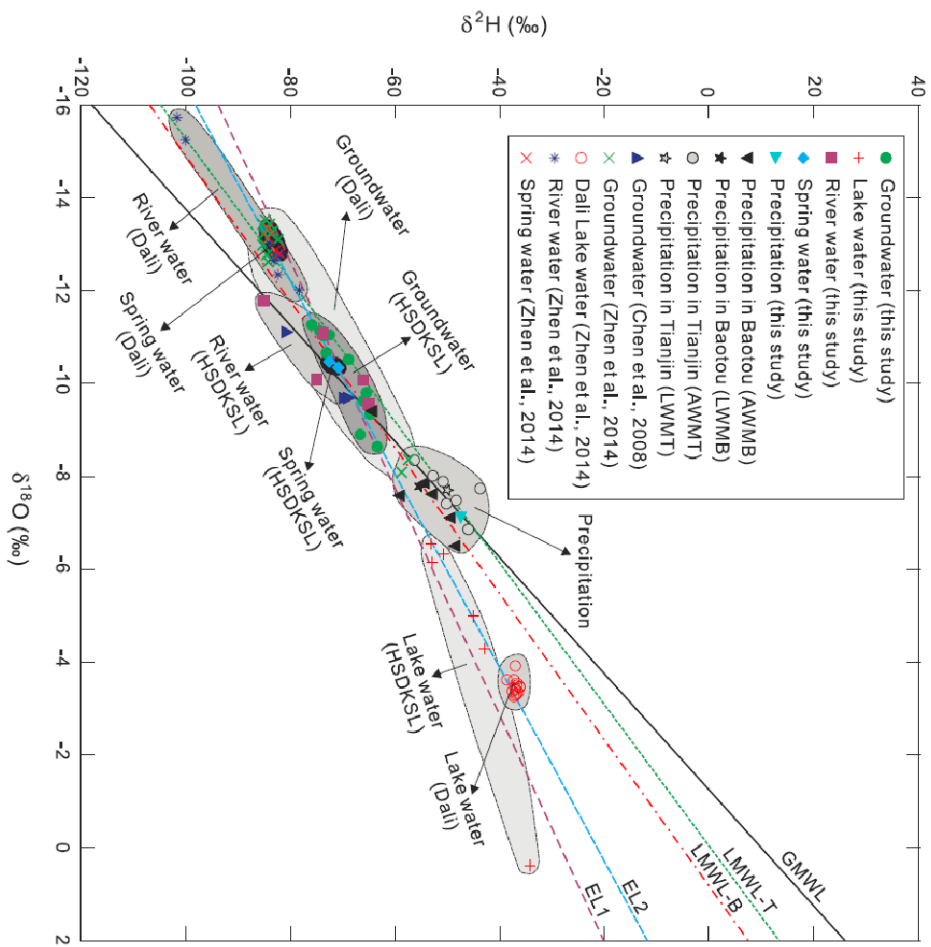
带格式的：无下划线，字体颜色：自动设置

带格式的：字体：非加粗，无下划线，字体颜色：自动设置

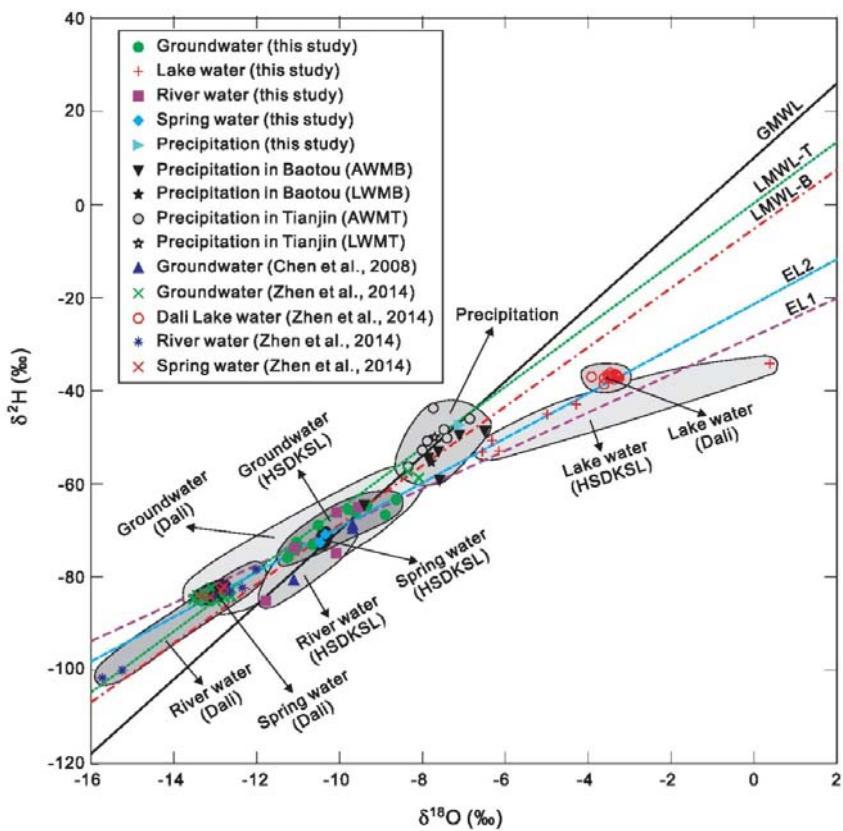
带格式的：无下划线，字体颜色：自动设置

带格式的：字体：(默认) Times  
New Roman, 10 磅, 无下划线, 字  
体颜色：自动设置

带格式的：居中



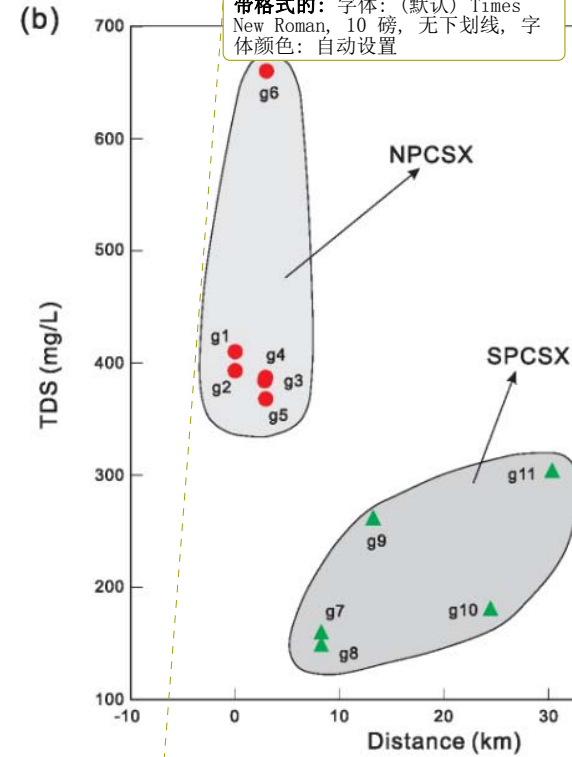
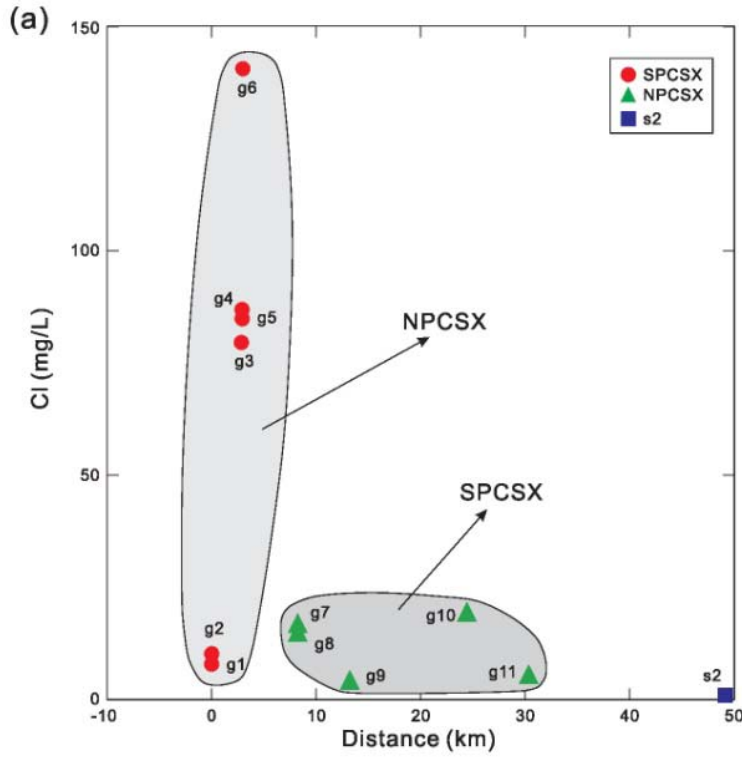
1527



1528  
1529  
1530  
1531  
1532  
1533  
1534  
1535  
1536  
1537  
1538  
1539  
1540  
1541  
1542  
1543  
1544  
1545  
1546  
1547  
1548

**Fig. 10.** (a) The sketch map showing the relationship between the groundwaters in the NPCSX and SPCSX areas, based on variations of (a) the chloride concentrations, (a) and (b) the TDS (b) concentrations, (c) the  $\delta^{18}\text{O}$  values and (d) the  $\delta\text{D}$  values of these water samples versus their distances away from the water sample g1 along the palaeo river channel (PCSX) from south to north.

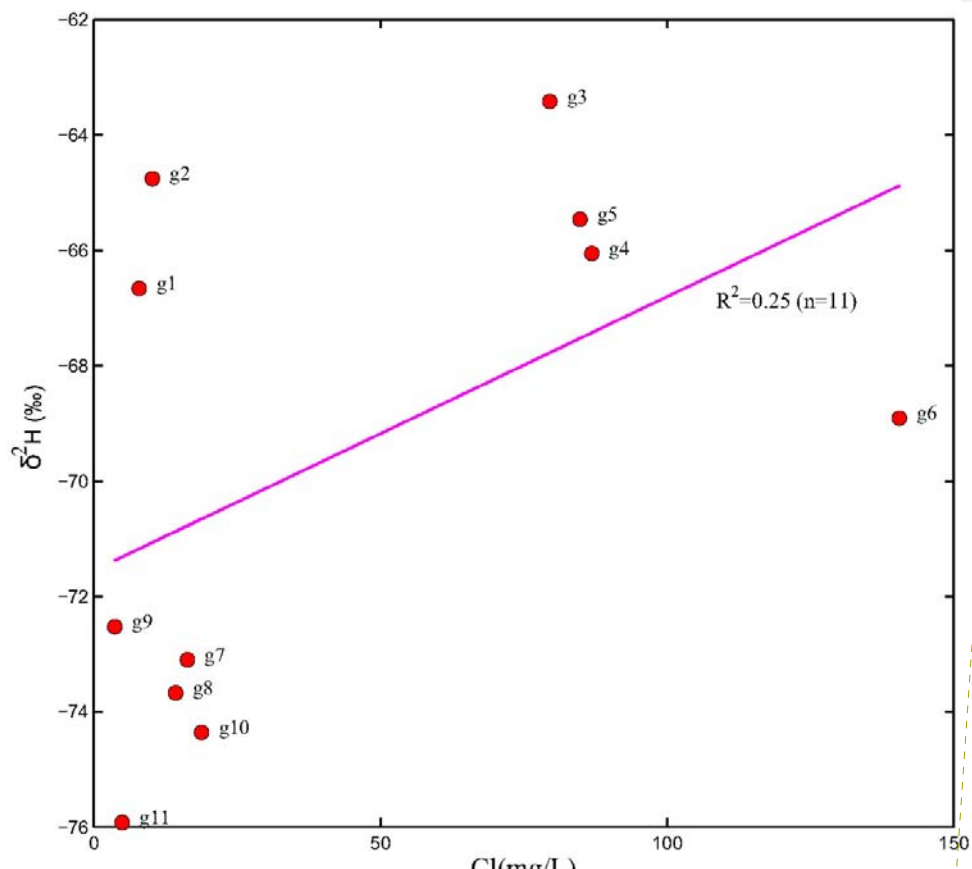
带格式的：无下划线，字体颜色：自动设置  
带格式的：无下划线，字体颜色：自动设置，图案：清除  
带格式的：无下划线，字体颜色：自动设置  
带格式的：无下划线，字体颜色：自动设置，图案：清除  
带格式的：无下划线，字体颜色：自动设置  
带格式的：无下划线，字体颜色：自动设置，图案：清除  
带格式的：无下划线，字体颜色：自动设置  
带格式的：无下划线，字体颜色：自动设置，图案：清除  
带格式的：无下划线，字体颜色：自动设置  
带格式的：无下划线，字体颜色：自动设置，图案：清除  
带格式的：无下划线，字体颜色：自动设置  
带格式的：无下划线，字体颜色：自动设置，图案：清除  
带格式的：无下划线，字体颜色：自动设置



1549  
1550  
1551  
1552  
1553  
1554  
1555

**Fig. 11.** The bivariate plot of Cl vs.  $\delta^{34}\text{H}$  in the groundwaters from the PCSX region, which showing that no significant evaporation process has been experienced by these groundwaters.

带格式的: 无下划线, 字体颜色: 自动设置



1556  
1557  
1558  
1559  
1560

**Fig. 12.** Variations of  $\delta^{18}\text{O}$  (a) and  $\delta^2\text{H}$  (b) in the groundwaters versus their distances away from the groundwater sample g1 along the palaeo river channel (PCSX) from south to north. The dashed line in (c) and (d) represents the corresponding values of the spring water sample s2, and which is just well divided the samples into the NPCsX and the SPCSX parts.

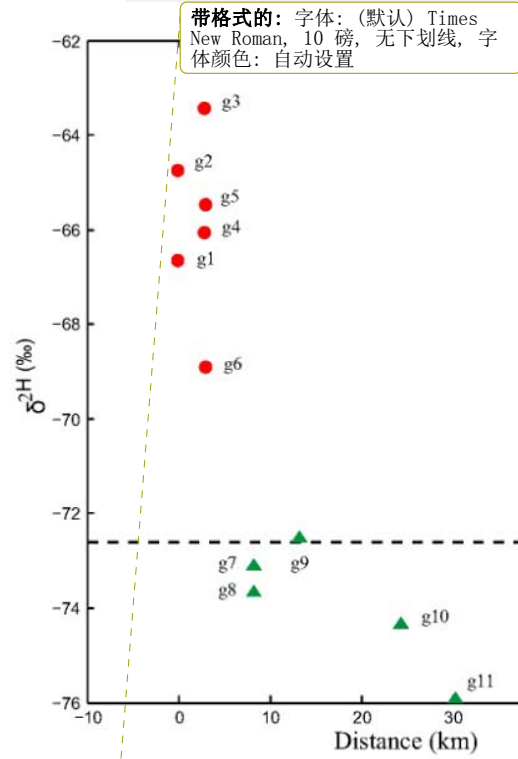
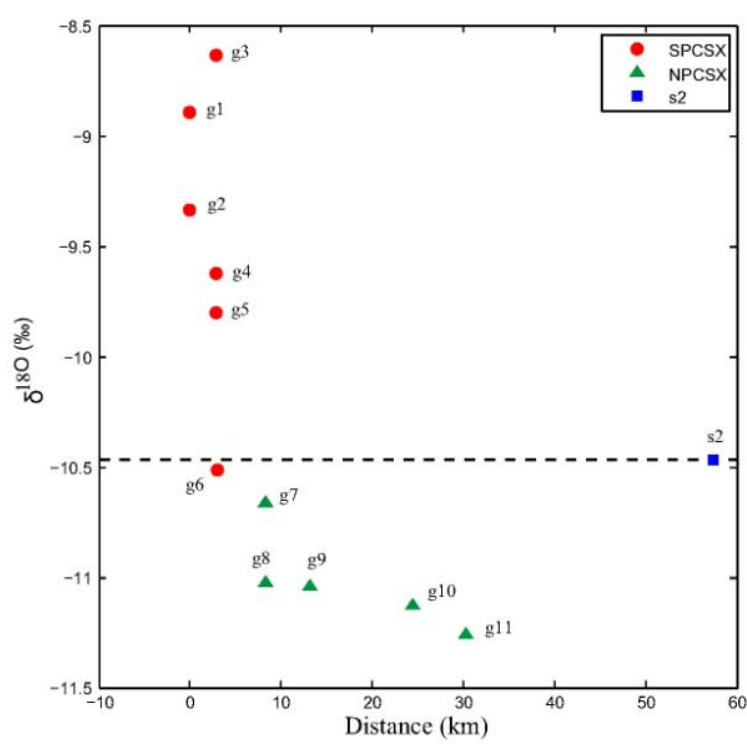
带格式的: 字体: (默认) Times New Roman, 10 磅, 无下划线, 字体颜色: 自动设置

带格式的: 无下划线, 字体颜色: 自动设置

带格式的: 无下划线, 字体颜色: 自动设置, 图案: 清除

带格式的: 无下划线, 字体颜色: 自动设置

带格式的: 无下划线, 字体颜色: 自动设置, 图案: 清除



1561  
1562  
1563  
1564  
1565  
1566

**Fig. 13.** The bivariate plots of  $\delta^2\text{H}$ (‰) and  $\delta^{18}\text{O}$ (‰) vs. deuterium excess for the groundwaters in the PCSX area. (e)

带格式的: 字体: (默认) Times New Roman, 10 像素, 无下划线, 字体颜色: 自动设置

带格式的: 无下划线, 字体颜色: 自动设置

带格式的: 无下划线, 字体颜色: 自动设置, 图案: 清除

带格式的: 字体颜色: 自动设置

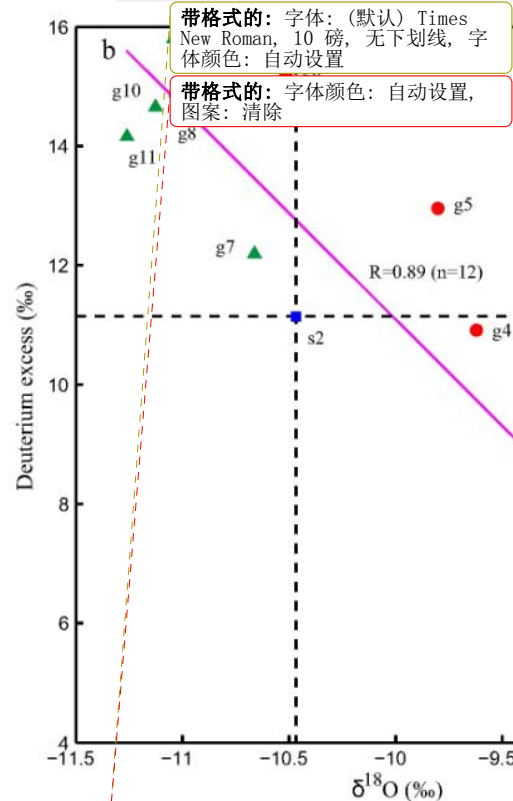
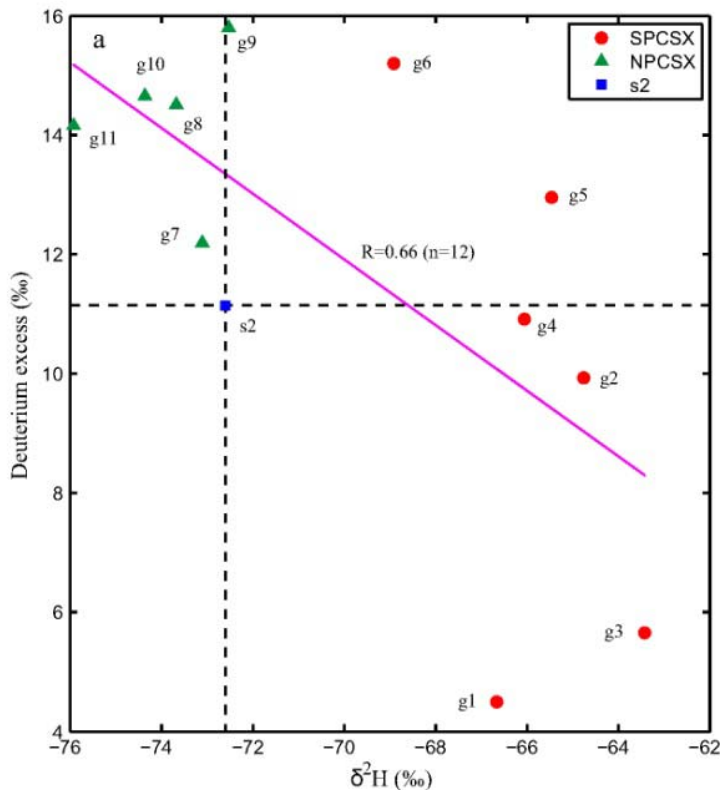
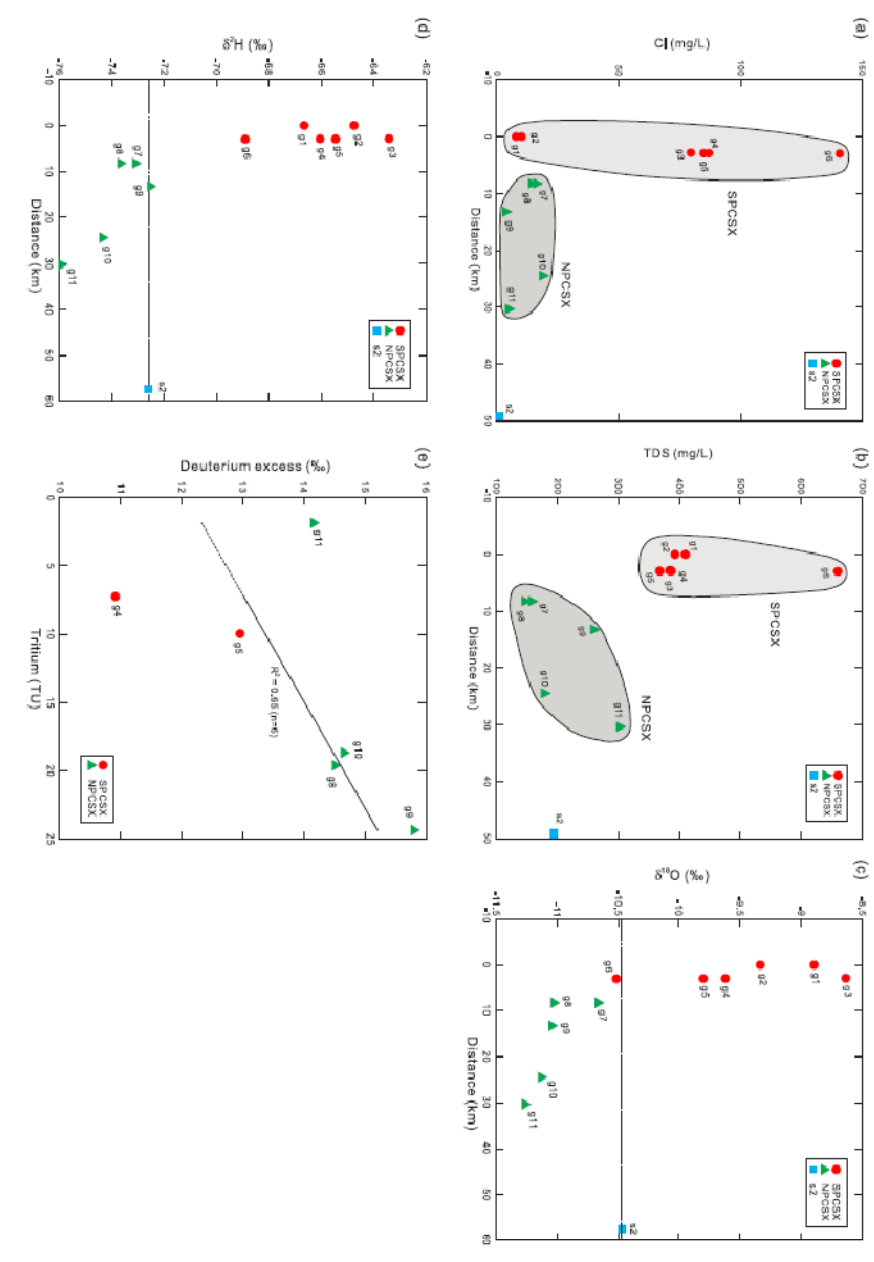


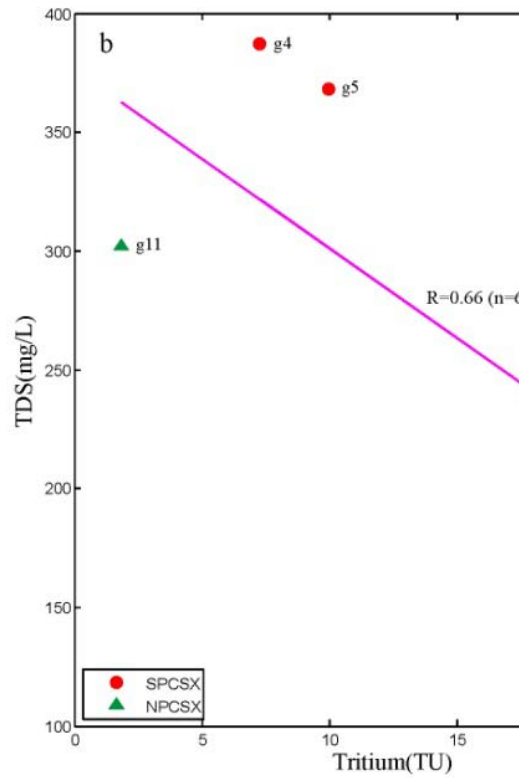
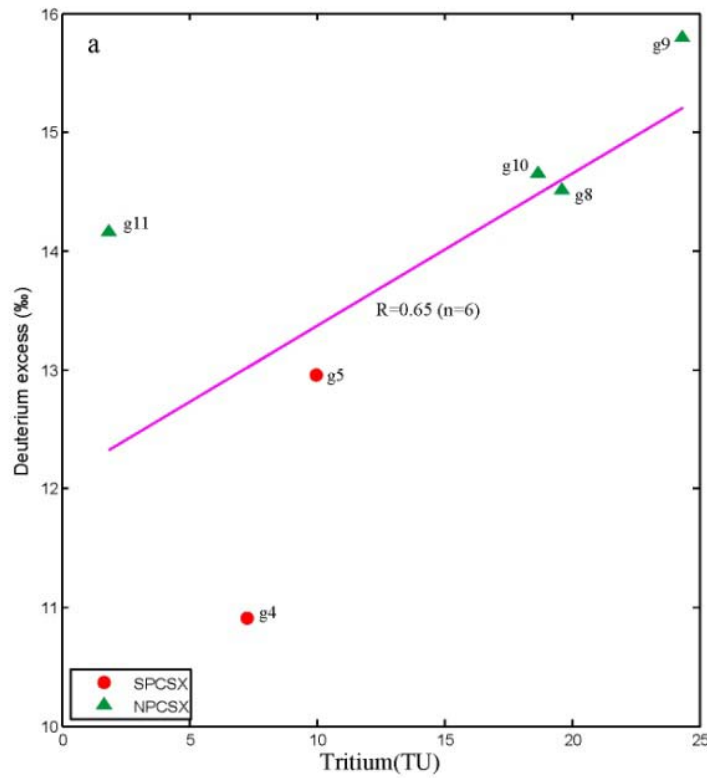
**Fig. 14.** Variations of tritium contents vs. deuterium excess (a) and TDS (b) for the groundwater samples in the study area. The sample g6 was omitted due to excluded because of its potential contamination.

1560  
1572  
1573  
1574  
1575  
1576  
1577

**带格式的:** 字体: (默认) Times New Roman, 10 磅, 加粗, 无下划线, 字体颜色: 自动设置

带格式的：居中





1579  
1580  
1581  
1582  
1583  
1584  
1585  
1586  
1587  
1588  
1589

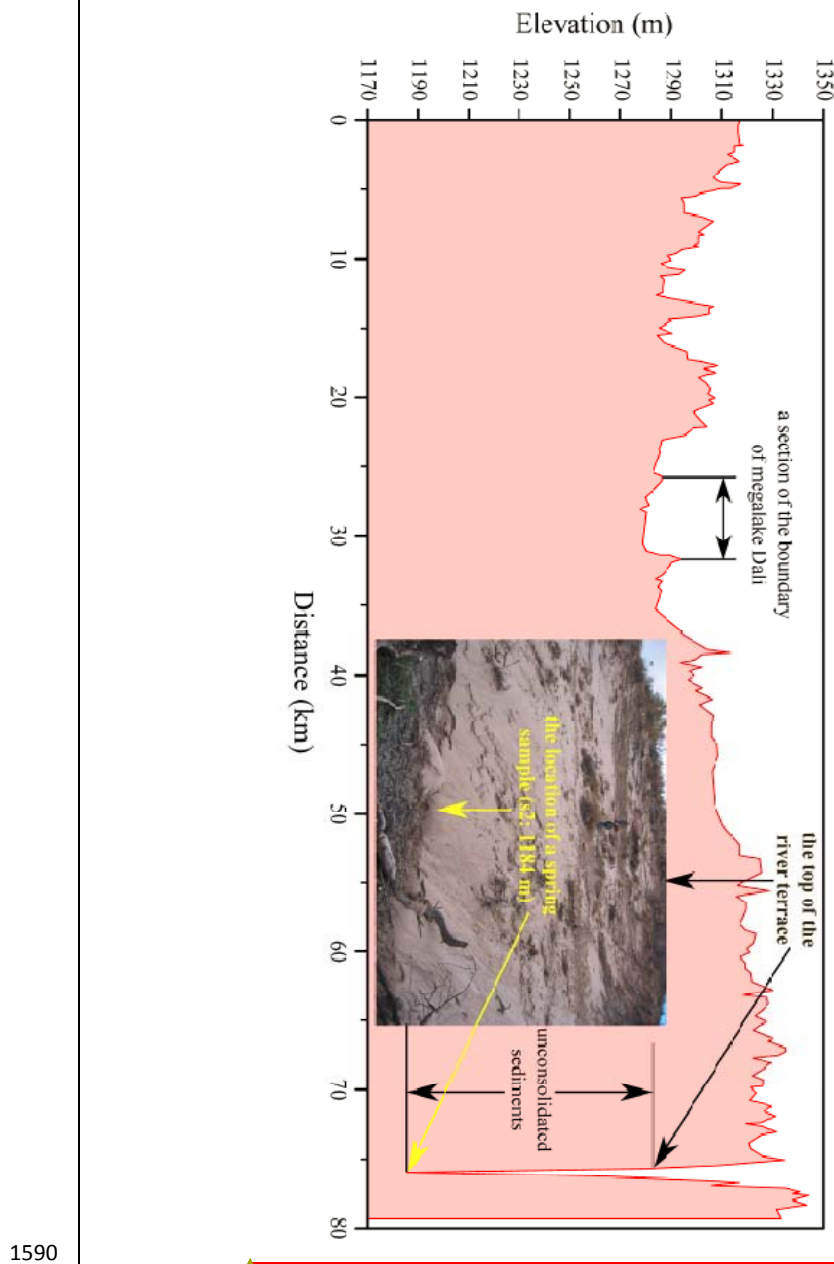
**Fig. 115.** Variation of the topographical elevation along the section S1 (see Fig. 1b) from the upstream of the Dali Lake to the location site of the spring water sample (s2) in the riverhead of the Xilamulun River. Note that no river water samples are shown in this figure.

带格式的：无下划线，字体颜色：自动设置

带格式的：字体颜色：自动设置

带格式的：字体：(默认) Times New Roman, 10 磅, 无下划线, 字体颜色: 自动设置

带格式的：居中, 行距: 单倍行距



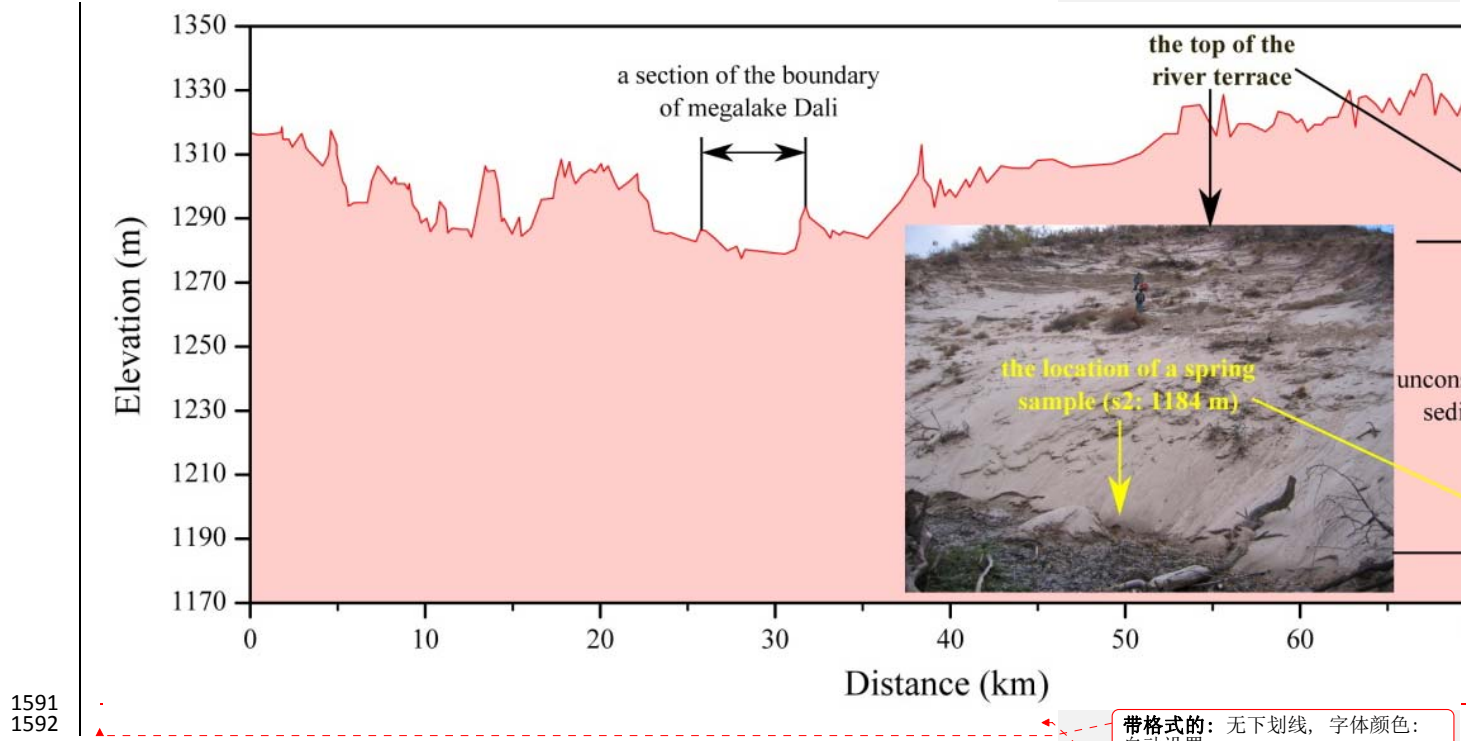


**Table Captions:****Table 1.**The physical parameters measured for the natural water samples in the study area.

Sample ID	Water type	Latitude (N, degree)	Longitude (E, degree)	Elevation (m a.s.l)	Depth (m)	Temperature (°C)	pH	Eh (mV)	EC (μS/cm)	TDS (mg/L)	Salinity (%)	Alkalinity (meq/L)	Hardness (°dH)
g1	Groundwater	42.736306	116.747333	1396	12	5.8	6.72	3	769	410	0.6	5.47	9.42
g2	Groundwater	42.736306	116.747333	1396	26	6.0	6.91	-10	736	393	0.5	4.07	11.96
g3	Groundwater	42.760194	116.760139	1355	32	7.7	6.88	-6	725	384	0.5	2.39	11.94
g4	Groundwater	42.759694	116.760417	1360	7	10.0	6.74	-1	725	387	0.5	2.20	12.28
g5	Groundwater	42.759556	116.760556	1362	27	7.6	6.46	-16	691	368	0.5	2.23	15.57
g6	Groundwater	42.760111	116.760250	1365	7	10.3	6.26	-22	1240	660	0.8	3.25	24.45
g7	Groundwater	42.806361	116.747806	1352	20	6.8	6.71	-2	297	158	0.2	0.63	4.70
g8	Groundwater	42.806361	116.747806	1352	16	6.5	6.92	-8	276	147	0.2	0.58	5.00
g9	Groundwater	42.850333	116.735722	1347	30	7.2	6.74	-1	487	260	0.4	3.73	12.68
g10	Groundwater	42.949861	116.759194	1321	37	9.9	6.75	-2	337	179	0.2	1.66	7.23
g11	Groundwater	42.967111	116.827528	1317	60	8.6	6.99	-14	571	302	0.4	2.40	12.94
l1	Lake water	42.424611	116.769194	1368	/	16.9	9.44	-151	126	67	0.1	0.95	1.79
l2	Lake water	42.424611	116.769194	1368	/	19.6	9.18	-137	132	70	0.1	0.92	1.82
l3	Lake water	42.424611	116.757806	1365	/	20.2	7.38	-36	196	105	0.1	1.53	3.36
l4	Lake water	42.427083	116.757639	1366	/	20.5	7.87	-64	448	238	0.2	3.42	6.61
l5	Lake water	42.421806	116.756917	1360	/	20.1	8.23	-83	173	92	0.1	1.43	2.73
l6	Lake water	42.736389	116.747222	1374	/	10.7	8.35	-89	194	103	0.1	1.53	3.30
r1	River water	42.530917	116.641250	1355	/	20.6	7.31	-33	180	96	0.1	0.88	2.23
r2	River water	42.310883	116.494817	1231	/	14.9	7.67	-52	178	95	0.1	1.21	2.50
r3	River water	42.385778	116.886194	1362	/	9.5	7.62	-48	177	94	0.1	1.45	2.62
r4	River water	42.931417	117.585306	1217	/	10.5	7.97	-69	474	252	0.3	3.22	8.73
r5	RiverLake water	43.079083	117.457389	1006	/	12.9	7.87	-62	191	101	0.1	1.37	2.88
s1	Spring water	42.530917	116.641250	1359	/	20.9	6.63	5	165	88	0.1	0.40	1.81
s2	Spring water	42.965417	116.975361	1184	/	19.0	7.47	-46	371	195	0.2	1.07	6.40
p1	Precipitation	42.330750	116.551694	1260	/	20.2	4.61	109	78	42	0.0	/	0.61

- 带格式的 [5]  
 带格式的: 行距: 单倍行距  
 带格式的 [6]  
 带格式的 [7]  
 带格式的 [8]  
 带格式的 [10]  
 带格式的 [11]  
 带格式的 [12]  
 带格式的 [14]  
 带格式的 [18]  
 带格式的 [19]  
 带格式的 [20]  
 带格式的 [21]  
 带格式的 [9]  
 带格式的 [13]  
 带格式的 [15]  
 带格式的 [16]  
 带格式的 [17]  
 带格式的 [22]  
 带格式的 [24]  
 带格式的 [23]  
 带格式的 [25]  
 带格式的 [26]  
 带格式的 [27]  
 带格式的 [28]  
 带格式的 [29]  
 带格式的 [30]  
 带格式的 [31]  
 带格式的 [32]  
 带格式的 [33]  
 带格式的 [34]  
 带格式的 [35]  
 带格式的 [36]  
 带格式的 [37]  
 带格式的 [38]  
 带格式的 [39]  
 带格式的 [40]  
 带格式的 [41]  
 带格式的 [42]  
 带格式的 [43]  
 带格式的 [44]  
 带格式的 [45]  
 带格式的 [46]  
 带格式的 [47]

**Table 2.** The concentrations of major cations and anions measured for the water samples in the study area.

Sample	F <sup>-</sup> (mg/L)	Cl <sup>-</sup> (mg/L)	NO <sub>2</sub> <sup>-</sup> (mg/L)	NO <sub>3</sub> <sup>-</sup> (mg/L)	SO <sub>4</sub> <sup>2-</sup> (mg/L)	CO <sub>3</sub> <sup>2-</sup> (mg/L)	HCO <sub>3</sub> <sup>-</sup> (mg/L)	Li <sup>+</sup> (mg/L)	Na <sup>+</sup> (mg/L)	NH <sub>4</sub> <sup>+</sup> (mg/L)	K <sup>+</sup> (mg/L)	Mg <sup>2+</sup> (mg/L)	Ca <sup>2+</sup> (mg/L)
g1	0.13	7.90	2.32	0.48	16.10	0.00	334.60	0.02	13.79	10.54	4.59	15.52	41.8
g2	0.21	10.21	0.00	6.15	70.61	0.10	247.70	0.02	13.36	6.56	3.45	17.91	56.0
g3	0.11	79.56	0.00	0.00	140.76	0.00	145.40	0.01	17.92	2.28	1.76	17.06	57.2
g4	0.10	86.90	0.00	5.73	164.80	0.00	133.70	0.02	18.02	0.00	2.02	18.50	57.3
g5	0.07	84.82	0.00	0.76	169.30	0.00	136.20	0.00	39.68	1.02	2.72	20.94	76.8
g6	0.07	140.54	0.00	110.77	228.80	0.00	198.20	0.00	79.80	0.00	29.47	29.25	126
g7	0.37	16.31	0.00	306.31	32.01	0.00	38.70	0.06	7.83	0.00	3.09	6.21	23.3
g8	0.29	14.28	0.00	35.49	29.89	0.00	35.50	0.02	16.21	0.11	3.38	6.44	25.1
g9	0.10	3.66	0.15	1.19	71.56	0.00	227.40	0.06	12.92	0.55	4.50	14.06	67.5
g10	0.24	18.80	0.00	49.49	9.97	0.00	101.10	0.00	18.54	0.00	2.09	7.92	38.6
g11	0.28	4.94	0.00	0.00	181.53	0.00	146.20	0.05	20.40	2.59	2.06	13.30	70.5
l1	0.16	3.15	0.00	0.07	4.32	0.00	57.90	0.01	5.42	0.00	0.86	3.24	7.49
l2	0.16	3.30	0.00	1.66	4.57	0.00	55.80	0.00	5.33	0.00	0.84	3.29	7.61
l3	0.11	3.27	0.00	0.61	2.33	0.00	93.30	0.01	5.88	0.00	1.19	5.68	14.6
l4	0.17	22.12	0.00	0.39	3.04	0.10	207.60	0.00	9.21	0.70	24.21	14.02	24.1
l5	0.09	6.24	0.00	0.65	2.97	0.10	86.80	0.01	6.72	0.00	1.16	4.91	11.4
l6	0.18	4.29	0.00	0.80	9.34	0.10	93.00	0.01	8.41	0.00	1.36	6.47	12.9
r1	0.30	5.76	0.00	2.38	26.67	0.30	52.40	0.01	7.15	0.00	2.99	3.41	10.3
r2	0.19	4.82	0.00	0.65	16.40	0.10	73.10	0.01	6.82	0.00	1.92	3.96	11.3
r3	0.64	5.46	0.00	0.43	5.57	0.00	88.10	0.01	7.11	0.00	1.13	4.04	12.0
r4	1.08	20.39	0.00	19.27	37.25	0.50	195.00	0.01	13.02	0.00	1.96	11.90	42.8
r5	0.19	4.10	0.00	1.08	15.57	0.00	82.60	0.01	6.71	0.00	2.08	4.38	13.4
s1	0.16	6.44	0.00	1.95	34.25	0.00	24.30	0.02	6.56	0.00	1.62	2.92	8.10
s2	0.05	0.98	0.00	0.45	17.15	0.00	64.90	0.02	9.87	0.00	3.32	9.10	30.7
p1	0.61	2.90	0.00	9.46	12.65	0.00	0.00	0.00	2.09	2.07	1.64	0.88	2.95

- 带格式的 ..... [397]
- 带格式的 ..... [400]
- 带格式的 ..... [402]
- 带格式的 ..... [404]
- 带格式的 ..... [406]
- 带格式的 ..... [408]
- 带格式的 ..... [410]
- 带格式的 ..... [412]
- 带格式的 ..... [414]
- 带格式的 ..... [416]
- 带格式的 ..... [418]
- 带格式的 ..... [420]
- 带格式的 ..... [422]
- 带格式的 ..... [424]
- 带格式的 ..... [398]
- 带格式的: 字体颜色: 自动设置
- 带格式的 ..... [399]
- 带格式的 ..... [401]
- 带格式的 ..... [403]
- 带格式的 ..... [405]
- 带格式的 ..... [407]
- 带格式的 ..... [409]
- 带格式的 ..... [411]
- 带格式的 ..... [413]
- 带格式的 ..... [415]
- 带格式的 ..... [417]
- 带格式的 ..... [419]
- 带格式的 ..... [421]
- 带格式的 ..... [423]
- 带格式的 ..... [425]
- 带格式的 ..... [426]
- 带格式的: 字体颜色: 自动设置
- 带格式的 ..... [428]
- 带格式的 ..... [429]
- 带格式的 ..... [430]
- 带格式的 ..... [431]
- 带格式的 ..... [432]
- 带格式的 ..... [433]
- 带格式的 ..... [434]
- 带格式的 ..... [435]
- 带格式的 ..... [436]
- 带格式的 ..... [437]
- 带格式的 ..... [438]
- 带格式的 ..... [439]

带格式的	... [801]
带格式的	... [802]
带格式的	... [810]
带格式的	... [803]
带格式的	... [804]
带格式的	... [807]
带格式的	... [811]
带格式的	... [806]
带格式的	... [809]
带格式的	... [805]
带格式的	... [808]
带格式的	... [812]
带格式的	... [816]
带格式的	... [813]
带格式的	... [814]
带格式的	... [815]
带格式的	... [817]
带格式的	... [818]
带格式的	... [819]
带格式的	... [820]
带格式的	... [822]
带格式的	... [821]
带格式的	... [823]
带格式的	... [824]
带格式的	... [825]
带格式的	... [826]
带格式的	... [827]
带格式的	... [828]
带格式的	... [829]
带格式的	... [830]
带格式的	... [831]
带格式的	... [832]
带格式的	... [833]
带格式的	... [834]
带格式的	... [835]
带格式的	... [836]
带格式的	... [837]
带格式的	... [838]
带格式的	... [839]
带格式的	... [840]
带格式的	... [841]
带格式的	... [842]
带格式的	... [843]
带格式的	... [844]

1600 | **Table 3.** The analytical data of stable and radioactive isotopes measured for the water samples in this study.

Sample ID	$\delta D^2H$ (‰)	$\delta^{18}O$ (‰)	deuterium excess (d)	Tritium ( $^3H$ ) (TU)	
g1	-66.664	0.199	-8.895	0.026	4.496 /
g2	-64.758	0.291	-9.336	0.039	9.930 /
g3	-63.424	0.269	-8.635	0.008	5.656 /
g4	-66.055	0.149	-9.621	0.062	10.913 7.250
g5	-65.462	0.111	-9.802	0.027	12.954 9.975
g6	-68.913	0.287	-10.514	0.039	15.199 22.908
g7	-73.105	0.298	-10.662	0.041	12.191 /
g8	-73.676	0.220	-11.023	0.037	14.508 19.611
g9	-72.530	0.181	-11.041	0.015	15.798 24.345
g10	-74.362	0.201	-11.127	0.026	14.654 18.681
g11	-75.924	0.340	-11.260	0.015	14.156 1.860
l1	-53.128	0.229	-6.553	0.002	-0.704 /
l2	-50.721	0.304	-6.320	0.026	-0.161 /
l3	-42.877	0.239	-4.292	0.034	-8.545 /
l4	-34.155	0.243	0.381	0.040	-37.203 /
l5	-45.057	0.206	-4.987	0.009	-5.161 /
l6	-52.866	0.187	-6.150	0.049	-3.666 /
r1	-66.157	0.118	-10.069	0.015	14.395 /
r2	-64.996	0.148	-9.549	0.012	11.396 /
r3	-73.790	0.315	-11.083	0.021	14.874 /
r4	-85.155	0.244	-11.781	0.005	9.093 /
r5	-74.978	0.195	-10.084	0.003	5.694 /
s1	-70.832	0.074	-10.340	0.007	11.888 /
s2	-72.601	0.281	-10.468	0.046	11.143 /
p1	-47.435	0.374	-7.141	0.017	9.693 /

1601

1602

1603

带格式的	... [1012]
带格式的	... [1015]
带格式的	... [1017]
带格式的	... [1019]
带格式的	... [1021]
带格式的	... [1023]
带格式的	... [1025]
带格式的	... [1027]
带格式的	... [1029]
带格式的	... [1013]
带格式的	... [1014]
带格式的: 字体颜色: 自动设置	
带格式的	... [1016]
带格式的	... [1018]
带格式的	... [1020]
带格式的	... [1022]
带格式的	... [1024]
带格式的	... [1026]
带格式的	... [1028]
带格式的	... [1030]
带格式的	... [1031]
带格式的	... [1032]
带格式的: 字体颜色: 自动设置	
带格式的	... [1033]
带格式的	... [1034]
带格式的	... [1035]
带格式的	... [1036]
带格式的	... [1037]
带格式的	... [1038]
带格式的	... [1039]
带格式的	... [1040]
带格式的	... [1041]
带格式的	... [1042]
带格式的: 字体颜色: 自动设置	
带格式的	... [1043]
带格式的	... [1044]
带格式的	... [1045]
带格式的	... [1046]
带格式的	... [1047]
带格式的	... [1048]
带格式的	... [1049]
带格式的	... [1050]
带格式的	... [1051]
带格式的	... [1052]

1604 | **Table 4.**The statistical frequency of rainfall events being  $\geq 20$  mm per year during the recent 30 years from 1985 to 2014. The data come from the China Meteorological Data  
1605 | Sharing Service System.

Station	One time/year	Two times/year	Three times/year	Four times/year	Five times/year	Six times/year	Seven times/year	Mean
Duolun	2	8	8	4	4	3	1	3.4
Xilinhaote	8	5	2	6	3	2	0	2.5

1606 |  
1607 | **Table 5.** The measured contents of tritium in the groundwater samples studied and the calculated ages of these samples.

Sample-ID	Tritium content (T.U.)	Possible ages (years)
g1	not measured	not clear
g2	not measured	not clear
g3	not measured	not clear
g4	7.25	20-40
g5	9.97	13-33
g6	22.91	0-20
g7	not measured	not clear
g8	19.61	0-20
g9	24.34	0-17
g10	18.68	0-22
g11	1.86	40-65

1608 |

页 14: [1] 带格式的 User 2018/6/30 17:02:00

无下划线, 字体颜色: 自动设置

页 14: [2] 带格式的 User 2018/6/30 17:02:00

无下划线, 字体颜色: 自动设置

页 14: [3] 带格式的 User 2018/6/30 17:02:00

无下划线, 字体颜色: 自动设置

页 14: [4] 带格式的 User 2018/6/30 17:02:00

无下划线, 字体颜色: 自动设置

页 62: [5] 带格式的 User 2018/6/30 17:02:00

无下划线, 字体颜色: 自动设置

页 62: [6] 带格式的 User 2018/6/30 17:02:00

无下划线, 字体颜色: 自动设置

页 62: [7] 带格式的 User 2018/6/30 17:02:00

无下划线, 字体颜色: 自动设置

页 62: [8] 带格式的 User 2018/6/30 17:15:00

定义网格后不调整右缩进, 不对齐到网格

页 62: [9] 带格式的 User 2018/6/30 17:02:00

无下划线, 字体颜色: 自动设置

页 62: [10] 带格式的 User 2018/6/30 17:02:00

无下划线, 字体颜色: 自动设置

页 62: [11] 带格式的 User 2018/6/30 17:02:00

无下划线, 字体颜色: 自动设置

页 62: [12] 带格式的 User 2018/6/30 17:02:00

无下划线, 字体颜色: 自动设置

页 62: [13] 带格式的 User 2018/6/30 17:02:00

无下划线, 字体颜色: 自动设置

页 62: [14] 带格式的 User 2018/6/30 17:02:00

无下划线, 字体颜色: 自动设置

页 62: [15] 带格式的 User 2018/6/30 17:02:00

无下划线, 字体颜色: 自动设置

页 62: [16] 带格式的 User 2018/6/30 17:02:00

无下划线, 字体颜色: 自动设置

页 62: [17] 带格式的 User 2018/6/30 17:02:00

无下划线, 字体颜色: 自动设置

页 62: [18] 带格式的 User 2018/6/30 17:02:00

无下划线, 字体颜色: 自动设置

页 62: [19] 带格式的 User 2018/6/30 17:02:00

无下划线, 字体颜色: 自动设置

页 62: [20] 带格式的 User 2018/6/30 17:02:00

无下划线, 字体颜色: 自动设置

页 62: [21] 带格式的 User 2018/6/30 17:02:00

无下划线, 字体颜色: 自动设置

页 62: [22] 带格式的 User 2018/6/30 17:02:00

无下划线, 字体颜色: 自动设置

页 62: [23] 带格式的 User 2018/6/30 17:15:00

定义网格后不调整右缩进, 不对齐到网格

页 62: [24] 带格式的 User 2018/6/30 17:02:00

无下划线, 字体颜色: 自动设置

页 62: [25] 带格式的 User 2018/6/30 17:02:00

无下划线, 字体颜色: 自动设置

页 62: [26] 带格式的 User 2018/6/30 17:02:00

无下划线, 字体颜色: 自动设置

页 62: [27] 带格式的 User 2018/6/30 17:02:00

无下划线, 字体颜色: 自动设置

页 62: [28] 带格式的 User 2018/6/30 17:02:00

无下划线, 字体颜色: 自动设置

页 62: [29] 带格式的 User 2018/6/30 17:02:00

无下划线, 字体颜色: 自动设置

页 62: [30] 带格式的 User 2018/6/30 17:02:00

无下划线, 字体颜色: 自动设置

页 62: [31] 带格式的 User 2018/6/30 17:02:00

无下划线, 字体颜色: 自动设置

页 62: [32] 带格式的 User 2018/6/30 17:02:00

无下划线, 字体颜色: 自动设置

页 62: [33] 带格式的 User 2018/6/30 17:02:00

无下划线, 字体颜色: 自动设置

页 62: [34] 带格式的 User 2018/6/30 17:02:00

无下划线, 字体颜色: 自动设置

页 62: [35] 带格式的 User 2018/6/30 17:02:00

无下划线, 字体颜色: 自动设置

页 62: [36] 带格式的 User 2018/6/30 17:02:00

无下划线, 字体颜色: 自动设置

页 62: [37] 带格式的 User 2018/6/30 17:02:00

无下划线, 字体颜色: 自动设置

页 62: [38] 带格式的 User 2018/6/30 17:15:00

定义网格后不调整右缩进, 不对齐到网格

页 62: [39] 带格式的 User 2018/6/30 17:02:00

无下划线, 字体颜色: 自动设置

页 62: [40] 带格式的 User 2018/6/30 17:02:00

无下划线, 字体颜色: 自动设置

页 62: [41] 带格式的 User 2018/6/30 17:02:00

无下划线, 字体颜色: 自动设置

页 62: [42] 带格式的 User 2018/6/30 17:02:00

无下划线, 字体颜色: 自动设置

页 62: [43] 带格式的 User 2018/6/30 17:02:00

无下划线, 字体颜色: 自动设置

页 62: [44] 带格式的 User 2018/6/30 17:02:00

无下划线, 字体颜色: 自动设置

页 62: [45] 带格式的 User 2018/6/30 17:02:00

无下划线, 字体颜色: 自动设置

页 62: [46] 带格式的 User 2018/6/30 17:02:00

无下划线, 字体颜色: 自动设置

页 62: [47] 带格式的 User 2018/6/30 17:02:00

无下划线, 字体颜色: 自动设置

页 62: [48] 带格式的 User 2018/6/30 17:02:00

无下划线, 字体颜色: 自动设置

页 62: [49] 带格式的 User 2018/6/30 17:02:00

无下划线, 字体颜色: 自动设置

页 62: [50] 带格式的 User 2018/6/30 17:02:00

无下划线, 字体颜色: 自动设置

页 62: [51] 带格式的 User 2018/6/30 17:02:00

无下划线, 字体颜色: 自动设置

页 62: [52] 带格式的 User 2018/6/30 17:02:00

无下划线, 字体颜色: 自动设置

页 62: [53] 带格式的 User 2018/6/30 17:15:00

定义网格后不调整右缩进, 不对齐到网格

页 62: [54] 带格式的 User 2018/6/30 17:02:00

无下划线, 字体颜色: 自动设置

页 62: [55] 带格式的 User 2018/6/30 17:02:00

无下划线, 字体颜色: 自动设置

页 62: [56] 带格式的 User 2018/6/30 17:02:00

无下划线, 字体颜色: 自动设置

页 62: [57] 带格式的 User 2018/6/30 17:02:00

无下划线, 字体颜色: 自动设置

页 62: [58] 带格式的 User 2018/6/30 17:02:00

无下划线, 字体颜色: 自动设置

页 62: [59] 带格式的 User 2018/6/30 17:02:00

无下划线, 字体颜色: 自动设置

页 62: [60] 带格式的 User 2018/6/30 17:02:00

无下划线, 字体颜色: 自动设置

页 62: [61] 带格式的 User 2018/6/30 17:02:00

无下划线, 字体颜色: 自动设置

页 62: [62] 带格式的 User 2018/6/30 17:02:00

无下划线, 字体颜色: 自动设置

页 62: [63] 带格式的 User 2018/6/30 17:02:00

无下划线, 字体颜色: 自动设置

页 62: [64] 带格式的 User 2018/6/30 17:02:00

无下划线, 字体颜色: 自动设置

页 62: [65] 带格式的 User 2018/6/30 17:02:00

无下划线, 字体颜色: 自动设置

页 62: [66] 带格式的 User 2018/6/30 17:02:00

无下划线, 字体颜色: 自动设置

页 62: [67] 带格式的 User 2018/6/30 17:02:00

无下划线, 字体颜色: 自动设置

页 62: [68] 带格式的 User 2018/6/30 17:15:00

定义网格后不调整右缩进, 不对齐到网格

页 62: [69] 带格式的 User 2018/6/30 17:02:00

无下划线, 字体颜色: 自动设置

页 62: [70] 带格式的 User 2018/6/30 17:02:00

无下划线, 字体颜色: 自动设置

页 62: [71] 带格式的 User 2018/6/30 17:02:00

无下划线, 字体颜色: 自动设置

页 62: [72] 带格式的 User 2018/6/30 17:02:00

无下划线, 字体颜色: 自动设置

页 62: [73] 带格式的 User 2018/6/30 17:02:00

无下划线, 字体颜色: 自动设置

页 62: [74] 带格式的 User 2018/6/30 17:02:00

无下划线, 字体颜色: 自动设置

页 62: [75] 带格式的 User 2018/6/30 17:02:00

无下划线, 字体颜色: 自动设置

页 62: [76] 带格式的 User 2018/6/30 17:02:00

无下划线, 字体颜色: 自动设置

页 62: [77] 带格式的 User 2018/6/30 17:02:00

无下划线, 字体颜色: 自动设置

页 62: [78] 带格式的 User 2018/6/30 17:02:00

无下划线, 字体颜色: 自动设置

页 62: [79] 带格式的 User 2018/6/30 17:02:00

无下划线, 字体颜色: 自动设置

页 62: [80] 带格式的 User 2018/6/30 17:02:00

无下划线, 字体颜色: 自动设置

页 62: [81] 带格式的 User 2018/6/30 17:02:00

无下划线, 字体颜色: 自动设置

页 62: [82] 带格式的 User 2018/6/30 17:02:00

无下划线, 字体颜色: 自动设置

页 62: [83] 带格式的 User 2018/6/30 17:15:00

定义网格后不调整右缩进, 不对齐到网格

页 62: [84] 带格式的 User 2018/6/30 17:02:00

无下划线, 字体颜色: 自动设置

页 62: [85] 带格式的 User 2018/6/30 17:02:00

无下划线, 字体颜色: 自动设置

页 62: [86] 带格式的 User 2018/6/30 17:02:00

无下划线, 字体颜色: 自动设置

页 62: [87] 带格式的 User 2018/6/30 17:02:00

无下划线, 字体颜色: 自动设置

页 62: [88] 带格式的 User 2018/6/30 17:02:00

无下划线, 字体颜色: 自动设置

页 62: [89] 带格式的 User 2018/6/30 17:02:00

无下划线, 字体颜色: 自动设置

页 62: [90] 带格式的 User 2018/6/30 17:02:00

无下划线, 字体颜色: 自动设置

页 62: [91] 带格式的 User 2018/6/30 17:02:00

无下划线, 字体颜色: 自动设置

页 62: [92] 带格式的 User 2018/6/30 17:02:00

无下划线, 字体颜色: 自动设置

页 62: [93] 带格式的 User 2018/6/30 17:02:00

无下划线, 字体颜色: 自动设置

页 62: [94] 带格式的 User 2018/6/30 17:02:00

无下划线, 字体颜色: 自动设置

页 62: [95] 带格式的 User 2018/6/30 17:02:00

无下划线, 字体颜色: 自动设置

页 62: [96] 带格式的 User 2018/6/30 17:02:00

无下划线, 字体颜色: 自动设置

页 62: [97] 带格式的 User 2018/6/30 17:02:00

无下划线, 字体颜色: 自动设置

页 62: [98] 带格式的 User 2018/6/30 17:15:00

定义网格后不调整右缩进, 不对齐到网格

页 62: [99] 带格式的 User 2018/6/30 17:02:00

无下划线, 字体颜色: 自动设置

页 62: [100] 带格式的 User 2018/6/30 17:02:00

无下划线, 字体颜色: 自动设置

页 62: [101] 带格式的 User 2018/6/30 17:02:00

无下划线, 字体颜色: 自动设置

页 62: [102] 带格式的 User 2018/6/30 17:02:00

无下划线, 字体颜色: 自动设置

页 62: [103] 带格式的 User 2018/6/30 17:02:00

无下划线, 字体颜色: 自动设置

页 62: [104] 带格式的 User 2018/6/30 17:02:00

无下划线, 字体颜色: 自动设置

页 62: [105] 带格式的 User 2018/6/30 17:02:00

无下划线, 字体颜色: 自动设置

页 62: [106] 带格式的 User 2018/6/30 17:02:00

无下划线, 字体颜色: 自动设置

页 62: [107] 带格式的 User 2018/6/30 17:02:00

无下划线, 字体颜色: 自动设置

页 62: [108] 带格式的 User 2018/6/30 17:02:00

无下划线, 字体颜色: 自动设置

页 62: [109] 带格式的 User 2018/6/30 17:02:00

无下划线, 字体颜色: 自动设置

页 62: [110] 带格式的 User 2018/6/30 17:02:00

无下划线, 字体颜色: 自动设置

页 62: [111] 带格式的 User 2018/6/30 17:02:00

无下划线, 字体颜色: 自动设置

页 62: [112] 带格式的 User 2018/6/30 17:02:00

无下划线, 字体颜色: 自动设置

页 62: [113] 带格式的 User 2018/6/30 17:15:00

定义网格后不调整右缩进, 不对齐到网格

页 62: [114] 带格式的 User 2018/6/30 17:02:00

无下划线, 字体颜色: 自动设置

页 62: [115] 带格式的 User 2018/6/30 17:02:00

无下划线, 字体颜色: 自动设置

页 62: [116] 带格式的 User 2018/6/30 17:02:00

无下划线, 字体颜色: 自动设置

页 62: [117] 带格式的 User 2018/6/30 17:02:00

无下划线, 字体颜色: 自动设置

页 62: [118] 带格式的 User 2018/6/30 17:02:00

无下划线, 字体颜色: 自动设置

页 62: [119] 带格式的 User 2018/6/30 17:02:00

无下划线, 字体颜色: 自动设置

页 62: [120] 带格式的 User 2018/6/30 17:02:00

无下划线, 字体颜色: 自动设置

页 62: [121] 带格式的 User 2018/6/30 17:02:00

无下划线, 字体颜色: 自动设置

页 62: [122] 带格式的 User 2018/6/30 17:02:00

无下划线, 字体颜色: 自动设置

页 62: [123] 带格式的 User 2018/6/30 17:02:00

无下划线, 字体颜色: 自动设置

页 62: [124] 带格式的 User 2018/6/30 17:02:00

无下划线, 字体颜色: 自动设置

页 62: [125] 带格式的 User 2018/6/30 17:02:00

无下划线, 字体颜色: 自动设置

页 62: [126] 带格式的 User 2018/6/30 17:02:00

无下划线, 字体颜色: 自动设置

页 62: [127] 带格式的 User 2018/6/30 17:02:00

无下划线, 字体颜色: 自动设置

页 62: [128] 带格式的 User 2018/6/30 17:15:00

定义网格后不调整右缩进, 不对齐到网格

页 62: [129] 带格式的 User 2018/6/30 17:02:00

无下划线, 字体颜色: 自动设置

页 62: [130] 带格式的 User 2018/6/30 17:02:00

无下划线, 字体颜色: 自动设置

页 62: [131] 带格式的 User 2018/6/30 17:02:00

无下划线, 字体颜色: 自动设置

页 62: [132] 带格式的 User 2018/6/30 17:02:00

无下划线, 字体颜色: 自动设置

页 62: [133] 带格式的 User 2018/6/30 17:02:00

无下划线, 字体颜色: 自动设置

页 62: [134] 带格式的 User 2018/6/30 17:02:00

无下划线, 字体颜色: 自动设置

页 62: [135] 带格式的 User 2018/6/30 17:02:00

无下划线, 字体颜色: 自动设置

页 62: [136] 带格式的 User 2018/6/30 17:02:00

无下划线, 字体颜色: 自动设置

页 62: [137] 带格式的 User 2018/6/30 17:02:00

无下划线, 字体颜色: 自动设置

页 62: [138] 带格式的 User 2018/6/30 17:02:00

无下划线, 字体颜色: 自动设置

页 62: [139] 带格式的 User 2018/6/30 17:02:00

无下划线, 字体颜色: 自动设置

页 62: [140] 带格式的 User 2018/6/30 17:02:00

无下划线, 字体颜色: 自动设置

页 62: [141] 带格式的 User 2018/6/30 17:02:00

无下划线, 字体颜色: 自动设置

页 62: [142] 带格式的 User 2018/6/30 17:02:00

无下划线, 字体颜色: 自动设置

页 62: [143] 带格式的 User 2018/6/30 17:15:00

定义网格后不调整右缩进, 不对齐到网格

页 62: [144] 带格式的 User 2018/6/30 17:02:00

无下划线, 字体颜色: 自动设置

页 62: [145] 带格式的 User 2018/6/30 17:02:00

无下划线, 字体颜色: 自动设置

页 62: [146] 带格式的 User 2018/6/30 17:02:00

无下划线, 字体颜色: 自动设置

页 62: [147] 带格式的 User 2018/6/30 17:02:00

无下划线, 字体颜色: 自动设置

页 62: [148] 带格式的 User 2018/6/30 17:02:00

无下划线, 字体颜色: 自动设置

页 62: [149] 带格式的 User 2018/6/30 17:02:00

无下划线, 字体颜色: 自动设置

页 62: [150] 带格式的 User 2018/6/30 17:02:00

无下划线, 字体颜色: 自动设置

页 62: [151] 带格式的 User 2018/6/30 17:02:00

无下划线, 字体颜色: 自动设置

页 62: [152] 带格式的 User 2018/6/30 17:02:00

无下划线, 字体颜色: 自动设置

页 62: [153] 带格式的 User 2018/6/30 17:02:00

无下划线, 字体颜色: 自动设置

页 62: [154] 带格式的 User 2018/6/30 17:02:00

无下划线, 字体颜色: 自动设置

页 62: [155] 带格式的 User 2018/6/30 17:02:00

无下划线, 字体颜色: 自动设置

页 62: [156] 带格式的 User 2018/6/30 17:02:00

无下划线, 字体颜色: 自动设置

页 62: [157] 带格式的 User 2018/6/30 17:02:00

无下划线, 字体颜色: 自动设置

页 62: [158] 带格式的 User 2018/6/30 17:15:00

定义网格后不调整右缩进, 不对齐到网格

页 62: [159] 带格式的 User 2018/6/30 17:02:00

无下划线, 字体颜色: 自动设置

页 62: [160] 带格式的 User 2018/6/30 17:02:00

无下划线, 字体颜色: 自动设置

页 62: [161] 带格式的 User 2018/6/30 17:02:00

无下划线, 字体颜色: 自动设置

页 62: [162] 带格式的 User 2018/6/30 17:02:00

无下划线, 字体颜色: 自动设置

页 62: [163] 带格式的 User 2018/6/30 17:02:00

无下划线, 字体颜色: 自动设置

页 62: [164] 带格式的 User 2018/6/30 17:02:00

无下划线, 字体颜色: 自动设置

页 62: [165] 带格式的 User 2018/6/30 17:02:00

无下划线, 字体颜色: 自动设置

页 62: [166] 带格式的 User 2018/6/30 17:02:00

无下划线, 字体颜色: 自动设置

页 62: [167] 带格式的 User 2018/6/30 17:02:00

无下划线, 字体颜色: 自动设置

页 62: [168] 带格式的 User 2018/6/30 17:02:00

无下划线, 字体颜色: 自动设置

页 62: [169] 带格式的 User 2018/6/30 17:02:00

无下划线, 字体颜色: 自动设置

页 62: [170] 带格式的 User 2018/6/30 17:02:00

无下划线, 字体颜色: 自动设置

页 62: [171] 带格式的 User 2018/6/30 17:02:00

无下划线, 字体颜色: 自动设置

页 62: [172] 带格式的 User 2018/6/30 17:02:00

无下划线, 字体颜色: 自动设置

页 62: [173] 带格式的 User 2018/6/30 17:15:00

定义网格后不调整右缩进, 不对齐到网格

页 62: [174] 带格式的 User 2018/6/30 17:02:00

无下划线, 字体颜色: 自动设置

页 62: [175] 带格式的 User 2018/6/30 17:02:00

无下划线, 字体颜色: 自动设置

页 62: [176] 带格式的 User 2018/6/30 17:02:00

无下划线, 字体颜色: 自动设置

页 62: [177] 带格式的 User 2018/6/30 17:02:00

无下划线, 字体颜色: 自动设置

页 62: [178] 带格式的 User 2018/6/30 17:02:00

无下划线, 字体颜色: 自动设置

页 62: [179] 带格式的 User 2018/6/30 17:02:00

无下划线, 字体颜色: 自动设置

页 62: [180] 带格式的 User 2018/6/30 17:02:00

无下划线, 字体颜色: 自动设置

页 62: [181] 带格式的 User 2018/6/30 17:02:00

无下划线, 字体颜色: 自动设置

页 62: [182] 带格式的 User 2018/6/30 17:02:00

无下划线, 字体颜色: 自动设置

页 62: [183] 带格式的 User 2018/6/30 17:02:00

无下划线, 字体颜色: 自动设置

页 62: [184] 带格式的 User 2018/6/30 17:02:00

无下划线, 字体颜色: 自动设置

页 62: [185] 带格式的 User 2018/6/30 17:02:00

无下划线, 字体颜色: 自动设置

页 62: [186] 带格式的 User 2018/6/30 17:02:00

无下划线, 字体颜色: 自动设置

页 62: [187] 带格式的 User 2018/6/30 17:02:00

无下划线, 字体颜色: 自动设置

页 62: [188] 带格式的 User 2018/6/30 17:15:00

定义网格后不调整右缩进, 不对齐到网格

页 62: [189] 带格式的 User 2018/6/30 17:02:00

无下划线, 字体颜色: 自动设置

页 62: [190] 带格式的 User 2018/6/30 17:02:00

无下划线, 字体颜色: 自动设置

页 62: [191] 带格式的 User 2018/6/30 17:02:00

无下划线, 字体颜色: 自动设置

页 62: [192] 带格式的 User 2018/6/30 17:02:00

无下划线, 字体颜色: 自动设置

页 62: [193] 带格式的 User 2018/6/30 17:02:00

无下划线, 字体颜色: 自动设置

页 62: [194] 带格式的 User 2018/6/30 17:02:00

无下划线, 字体颜色: 自动设置

页 62: [195] 带格式的 User 2018/6/30 17:02:00

无下划线, 字体颜色: 自动设置

页 62: [196] 带格式的 User 2018/6/30 17:02:00

无下划线, 字体颜色: 自动设置

页 62: [197] 带格式的 User 2018/6/30 17:02:00

无下划线, 字体颜色: 自动设置

页 62: [198] 带格式的 User 2018/6/30 17:02:00

无下划线, 字体颜色: 自动设置

页 62: [199] 带格式的 User 2018/6/30 17:02:00

无下划线, 字体颜色: 自动设置

页 62: [200] 带格式的 User 2018/6/30 17:02:00

无下划线, 字体颜色: 自动设置

页 62: [201] 带格式的 User 2018/6/30 17:02:00

无下划线, 字体颜色: 自动设置

页 62: [202] 带格式的 User 2018/6/30 17:02:00

无下划线, 字体颜色: 自动设置

页 62: [203] 带格式的 User 2018/6/30 17:15:00

定义网格后不调整右缩进, 不对齐到网格

页 62: [204] 带格式的 User 2018/6/30 17:02:00

无下划线, 字体颜色: 自动设置

页 62: [205] 带格式的 User 2018/6/30 17:02:00

无下划线, 字体颜色: 自动设置

页 62: [206] 带格式的 User 2018/6/30 17:02:00

无下划线, 字体颜色: 自动设置

页 62: [207] 带格式的 User 2018/6/30 17:02:00

无下划线, 字体颜色: 自动设置

页 62: [208] 带格式的 User 2018/6/30 17:02:00

无下划线, 字体颜色: 自动设置

页 62: [209] 带格式的 User 2018/6/30 17:02:00

无下划线, 字体颜色: 自动设置

页 62: [210] 带格式的 User 2018/6/30 17:02:00

无下划线, 字体颜色: 自动设置

页 62: [211] 带格式的 User 2018/6/30 17:02:00

无下划线, 字体颜色: 自动设置

页 62: [212] 带格式的 User 2018/6/30 17:02:00

无下划线, 字体颜色: 自动设置

页 62: [213] 带格式的 User 2018/6/30 17:02:00

无下划线, 字体颜色: 自动设置

页 62: [214] 带格式的 User 2018/6/30 17:02:00

无下划线, 字体颜色: 自动设置

页 62: [215] 带格式的 User 2018/6/30 17:02:00

无下划线, 字体颜色: 自动设置

页 62: [216] 带格式的 User 2018/6/30 17:02:00

无下划线, 字体颜色: 自动设置

页 62: [217] 带格式的 User 2018/6/30 17:02:00

无下划线, 字体颜色: 自动设置

页 62: [218] 带格式的 User 2018/6/30 17:15:00

定义网格后不调整右缩进, 不对齐到网格

页 62: [219] 带格式的 User 2018/6/30 17:02:00

无下划线, 字体颜色: 自动设置

页 62: [220] 带格式的 User 2018/6/30 17:02:00

无下划线, 字体颜色: 自动设置

页 62: [221] 带格式的 User 2018/6/30 17:02:00

无下划线, 字体颜色: 自动设置

页 62: [222] 带格式的 User 2018/6/30 17:02:00

无下划线, 字体颜色: 自动设置

页 62: [223] 带格式的 User 2018/6/30 17:02:00

无下划线, 字体颜色: 自动设置

页 62: [224] 带格式的 User 2018/6/30 17:02:00

无下划线, 字体颜色: 自动设置

页 62: [225] 带格式的 User 2018/6/30 17:02:00

无下划线, 字体颜色: 自动设置

页 62: [226] 带格式的 User 2018/6/30 17:02:00

无下划线, 字体颜色: 自动设置

页 62: [227] 带格式的 User 2018/6/30 17:02:00

无下划线, 字体颜色: 自动设置

页 62: [228] 带格式的 User 2018/6/30 17:02:00

无下划线, 字体颜色: 自动设置

页 62: [229] 带格式的 User 2018/6/30 17:02:00

无下划线, 字体颜色: 自动设置

页 62: [230] 带格式的 User 2018/6/30 17:02:00

无下划线, 字体颜色: 自动设置

页 62: [231] 带格式的 User 2018/6/30 17:02:00

无下划线, 字体颜色: 自动设置

页 62: [232] 带格式的 User 2018/6/30 17:02:00

无下划线, 字体颜色: 自动设置

页 62: [233] 带格式的 User 2018/6/30 17:15:00

定义网格后不调整右缩进, 不对齐到网格

页 62: [234] 带格式的 User 2018/6/30 17:02:00

无下划线, 字体颜色: 自动设置

页 62: [235] 带格式的 User 2018/6/30 17:02:00

无下划线, 字体颜色: 自动设置

页 62: [236] 带格式的 User 2018/6/30 17:02:00

无下划线, 字体颜色: 自动设置

页 62: [237] 带格式的 User 2018/6/30 17:02:00

无下划线, 字体颜色: 自动设置

页 62: [238] 带格式的 User 2018/6/30 17:02:00

无下划线, 字体颜色: 自动设置

页 62: [239] 带格式的 User 2018/6/30 17:02:00

无下划线, 字体颜色: 自动设置

页 62: [240] 带格式的 User 2018/6/30 17:02:00

无下划线, 字体颜色: 自动设置

页 62: [241] 带格式的 User 2018/6/30 17:02:00

无下划线, 字体颜色: 自动设置

页 62: [242] 带格式的 User 2018/6/30 17:02:00

无下划线, 字体颜色: 自动设置

页 62: [243] 带格式的 User 2018/6/30 17:02:00

无下划线, 字体颜色: 自动设置

页 62: [244] 带格式的 User 2018/6/30 17:02:00

无下划线, 字体颜色: 自动设置

页 62: [245] 带格式的 User 2018/6/30 17:02:00

无下划线, 字体颜色: 自动设置

页 62: [246] 带格式的 User 2018/6/30 17:02:00

无下划线, 字体颜色: 自动设置

页 62: [247] 带格式的 User 2018/6/30 17:02:00

无下划线, 字体颜色: 自动设置

页 62: [248] 带格式的 User 2018/6/30 17:15:00

定义网格后不调整右缩进, 不对齐到网格

页 62: [249] 带格式的 User 2018/6/30 17:02:00

无下划线, 字体颜色: 自动设置

页 62: [250] 带格式的 User 2018/6/30 17:02:00

无下划线, 字体颜色: 自动设置

页 62: [251] 带格式的 User 2018/6/30 17:02:00

无下划线, 字体颜色: 自动设置

页 62: [252] 带格式的 User 2018/6/30 17:02:00

无下划线, 字体颜色: 自动设置

页 62: [253] 带格式的 User 2018/6/30 17:02:00

无下划线, 字体颜色: 自动设置

页 62: [254] 带格式的 User 2018/6/30 17:02:00

无下划线, 字体颜色: 自动设置

页 62: [255] 带格式的 User 2018/6/30 17:02:00

无下划线, 字体颜色: 自动设置

页 62: [256] 带格式的 User 2018/6/30 17:02:00

无下划线, 字体颜色: 自动设置

页 62: [257] 带格式的 User 2018/6/30 17:02:00

无下划线, 字体颜色: 自动设置

页 62: [258] 带格式的 User 2018/6/30 17:02:00

无下划线, 字体颜色: 自动设置

页 62: [259] 带格式的 User 2018/6/30 17:02:00

无下划线, 字体颜色: 自动设置

页 62: [260] 带格式的 User 2018/6/30 17:02:00

无下划线, 字体颜色: 自动设置

页 62: [261] 带格式的 User 2018/6/30 17:02:00

无下划线, 字体颜色: 自动设置

页 62: [262] 带格式的 User 2018/6/30 17:02:00

无下划线, 字体颜色: 自动设置

页 62: [263] 带格式的 User 2018/6/30 17:15:00

定义网格后不调整右缩进, 不对齐到网格

页 62: [264] 带格式的 User 2018/6/30 17:02:00

无下划线, 字体颜色: 自动设置

页 62: [265] 带格式的 User 2018/6/30 17:02:00

无下划线, 字体颜色: 自动设置

页 62: [266] 带格式的 User 2018/6/30 17:02:00

无下划线, 字体颜色: 自动设置

页 62: [267] 带格式的 User 2018/6/30 17:02:00

无下划线, 字体颜色: 自动设置

页 62: [268] 带格式的 User 2018/6/30 17:02:00

无下划线, 字体颜色: 自动设置

页 62: [269] 带格式的 User 2018/6/30 17:02:00

无下划线, 字体颜色: 自动设置

页 62: [270] 带格式的 User 2018/6/30 17:02:00

无下划线, 字体颜色: 自动设置

页 62: [271] 带格式的 User 2018/6/30 17:02:00

无下划线, 字体颜色: 自动设置

页 62: [272] 带格式的 User 2018/6/30 17:02:00

无下划线, 字体颜色: 自动设置

页 62: [273] 带格式的 User 2018/6/30 17:02:00

无下划线, 字体颜色: 自动设置

页 62: [274] 带格式的 User 2018/6/30 17:02:00

无下划线, 字体颜色: 自动设置

页 62: [275] 带格式的 User 2018/6/30 17:02:00

无下划线, 字体颜色: 自动设置

页 62: [276] 带格式的 User 2018/6/30 17:02:00

无下划线, 字体颜色: 自动设置

页 62: [277] 带格式的 User 2018/6/30 17:02:00

无下划线, 字体颜色: 自动设置

页 62: [278] 带格式的 User 2018/6/30 17:15:00

定义网格后不调整右缩进, 不对齐到网格

页 62: [279] 带格式的 User 2018/6/30 17:02:00

无下划线, 字体颜色: 自动设置

页 62: [280] 带格式的 User 2018/6/30 17:02:00

无下划线, 字体颜色: 自动设置

页 62: [281] 带格式的 User 2018/6/30 17:02:00

无下划线, 字体颜色: 自动设置

页 62: [282] 带格式的 User 2018/6/30 17:02:00

无下划线, 字体颜色: 自动设置

页 62: [283] 带格式的 User 2018/6/30 17:02:00

无下划线, 字体颜色: 自动设置

页 62: [284] 带格式的 User 2018/6/30 17:02:00

无下划线, 字体颜色: 自动设置

页 62: [285] 带格式的 User 2018/6/30 17:02:00

无下划线, 字体颜色: 自动设置

页 62: [286] 带格式的 User 2018/6/30 17:02:00

无下划线, 字体颜色: 自动设置

页 62: [287] 带格式的 User 2018/6/30 17:02:00

无下划线, 字体颜色: 自动设置

页 62: [288] 带格式的 User 2018/6/30 17:02:00

无下划线, 字体颜色: 自动设置

页 62: [289] 带格式的 User 2018/6/30 17:02:00

无下划线, 字体颜色: 自动设置

页 62: [290] 带格式的 User 2018/6/30 17:02:00

无下划线, 字体颜色: 自动设置

页 62: [291] 带格式的 User 2018/6/30 17:02:00

无下划线, 字体颜色: 自动设置

页 62: [292] 带格式的 User 2018/6/30 17:02:00

无下划线, 字体颜色: 自动设置

页 62: [293] 带格式的 User 2018/6/30 17:15:00

定义网格后不调整右缩进, 不对齐到网格

页 62: [294] 带格式的 User 2018/6/30 17:02:00

无下划线, 字体颜色: 自动设置

页 62: [295] 带格式的 User 2018/6/30 17:02:00

无下划线, 字体颜色: 自动设置

页 62: [296] 带格式的 User 2018/6/30 17:02:00

无下划线, 字体颜色: 自动设置

页 62: [297] 带格式的 User 2018/6/30 17:02:00

无下划线, 字体颜色: 自动设置

页 62: [298] 带格式的 User 2018/6/30 17:02:00

无下划线, 字体颜色: 自动设置

页 62: [299] 带格式的 User 2018/6/30 17:02:00

无下划线, 字体颜色: 自动设置

页 62: [300] 带格式的 User 2018/6/30 17:02:00

无下划线, 字体颜色: 自动设置

页 62: [301] 带格式的 User 2018/6/30 17:02:00

无下划线, 字体颜色: 自动设置

页 62: [302] 带格式的 User 2018/6/30 17:02:00

无下划线, 字体颜色: 自动设置

页 62: [303] 带格式的 User 2018/6/30 17:02:00

无下划线, 字体颜色: 自动设置

页 62: [304] 带格式的 User 2018/6/30 17:02:00

无下划线, 字体颜色: 自动设置

页 62: [305] 带格式的 User 2018/6/30 17:02:00

无下划线, 字体颜色: 自动设置

页 62: [306] 带格式的 User 2018/6/30 17:02:00

无下划线, 字体颜色: 自动设置

页 62: [307] 带格式的 User 2018/6/30 17:02:00

无下划线, 字体颜色: 自动设置

页 62: [308] 带格式的 User 2018/6/30 17:15:00

定义网格后不调整右缩进, 不对齐到网格

页 62: [309] 带格式的 User 2018/6/30 17:02:00

无下划线, 字体颜色: 自动设置

页 62: [310] 带格式的 User 2018/6/30 17:02:00

无下划线, 字体颜色: 自动设置

页 62: [311] 带格式的 User 2018/6/30 17:02:00

无下划线, 字体颜色: 自动设置

页 62: [312] 带格式的 User 2018/6/30 17:02:00

无下划线, 字体颜色: 自动设置

页 62: [313] 带格式的 User 2018/6/30 17:02:00

无下划线, 字体颜色: 自动设置

页 62: [314] 带格式的 User 2018/6/30 17:02:00

无下划线, 字体颜色: 自动设置

页 62: [315] 带格式的 User 2018/6/30 17:02:00

无下划线, 字体颜色: 自动设置

页 62: [316] 带格式的 User 2018/6/30 17:02:00

无下划线, 字体颜色: 自动设置

页 62: [317] 带格式的 User 2018/6/30 17:02:00

无下划线, 字体颜色: 自动设置

页 62: [318] 带格式的 User 2018/6/30 17:02:00

无下划线, 字体颜色: 自动设置

页 62: [319] 带格式的 User 2018/6/30 17:02:00

无下划线, 字体颜色: 自动设置

页 62: [320] 带格式的 User 2018/6/30 17:02:00

无下划线, 字体颜色: 自动设置

页 62: [321] 带格式的 User 2018/6/30 17:02:00

无下划线, 字体颜色: 自动设置

页 62: [322] 带格式的 User 2018/6/30 17:02:00

无下划线, 字体颜色: 自动设置

页 62: [323] 带格式的 User 2018/6/30 17:15:00

定义网格后不调整右缩进, 不对齐到网格

页 62: [324] 带格式的 User 2018/6/30 17:02:00

无下划线, 字体颜色: 自动设置

页 62: [325] 带格式的 User 2018/6/30 17:02:00

无下划线, 字体颜色: 自动设置

页 62: [326] 带格式的 User 2018/6/30 17:02:00

无下划线, 字体颜色: 自动设置

页 62: [327] 带格式的 User 2018/6/30 17:02:00

无下划线, 字体颜色: 自动设置

页 62: [328] 带格式的 User 2018/6/30 17:02:00

无下划线, 字体颜色: 自动设置

页 62: [329] 带格式的 User 2018/6/30 17:02:00

无下划线, 字体颜色: 自动设置

页 62: [330] 带格式的 User 2018/6/30 17:02:00

无下划线, 字体颜色: 自动设置

页 62: [331] 带格式的 User 2018/6/30 17:02:00

无下划线, 字体颜色: 自动设置

页 62: [332] 带格式的 User 2018/6/30 17:02:00

无下划线, 字体颜色: 自动设置

页 62: [333] 带格式的 User 2018/6/30 17:02:00

无下划线, 字体颜色: 自动设置

页 62: [334] 带格式的 User 2018/6/30 17:02:00

无下划线, 字体颜色: 自动设置

页 62: [335] 带格式的 User 2018/6/30 17:02:00

无下划线, 字体颜色: 自动设置

页 62: [336] 带格式的 User 2018/6/30 17:02:00

无下划线, 字体颜色: 自动设置

页 62: [337] 带格式的 User 2018/6/30 17:02:00

无下划线, 字体颜色: 自动设置

页 62: [338] 带格式的 User 2018/6/30 17:15:00

定义网格后不调整右缩进, 不对齐到网格

页 62: [339] 带格式的 User 2018/6/30 17:02:00

无下划线, 字体颜色: 自动设置

页 62: [340] 带格式的 User 2018/6/30 17:02:00

无下划线, 字体颜色: 自动设置

页 62: [341] 带格式的 User 2018/6/30 17:02:00

无下划线, 字体颜色: 自动设置

页 62: [342] 带格式的 User 2018/6/30 17:02:00

无下划线, 字体颜色: 自动设置

页 62: [343] 带格式的 User 2018/6/30 17:02:00

无下划线, 字体颜色: 自动设置

页 62: [344] 带格式的 User 2018/6/30 17:02:00

无下划线, 字体颜色: 自动设置

页 62: [345] 带格式的 User 2018/6/30 17:02:00

无下划线, 字体颜色: 自动设置

页 62: [346] 带格式的 User 2018/6/30 17:02:00

无下划线, 字体颜色: 自动设置

页 62: [347] 带格式的 User 2018/6/30 17:02:00

无下划线, 字体颜色: 自动设置

页 62: [348] 带格式的 User 2018/6/30 17:02:00

无下划线, 字体颜色: 自动设置

页 62: [349] 带格式的 User 2018/6/30 17:02:00

无下划线, 字体颜色: 自动设置

页 62: [350] 带格式的 User 2018/6/30 17:02:00

无下划线, 字体颜色: 自动设置

页 62: [351] 带格式的 User 2018/6/30 17:02:00

无下划线, 字体颜色: 自动设置

页 62: [352] 带格式的 User 2018/6/30 17:02:00

无下划线, 字体颜色: 自动设置

页 62: [353] 带格式的 User 2018/6/30 17:15:00

定义网格后不调整右缩进, 不对齐到网格

页 62: [354] 带格式的 User 2018/6/30 17:02:00

无下划线, 字体颜色: 自动设置

页 62: [355] 带格式的 User 2018/6/30 17:02:00

无下划线, 字体颜色: 自动设置

页 62: [356] 带格式的 User 2018/6/30 17:02:00

无下划线, 字体颜色: 自动设置

页 62: [357] 带格式的 User 2018/6/30 17:02:00

无下划线, 字体颜色: 自动设置

页 62: [358] 带格式的 User 2018/6/30 17:02:00

无下划线, 字体颜色: 自动设置

页 62: [359] 带格式的 User 2018/6/30 17:02:00

无下划线, 字体颜色: 自动设置

页 62: [360] 带格式的 User 2018/6/30 17:02:00

无下划线, 字体颜色: 自动设置

页 62: [361] 带格式的 User 2018/6/30 17:02:00

无下划线, 字体颜色: 自动设置

页 62: [362] 带格式的 User 2018/6/30 17:02:00

无下划线, 字体颜色: 自动设置

页 62: [363] 带格式的 User 2018/6/30 17:02:00

无下划线, 字体颜色: 自动设置

页 62: [364] 带格式的 User 2018/6/30 17:02:00

无下划线, 字体颜色: 自动设置

页 62: [365] 带格式的 User 2018/6/30 17:02:00

无下划线, 字体颜色: 自动设置

页 62: [366] 带格式的 User 2018/6/30 17:02:00

无下划线, 字体颜色: 自动设置

页 62: [367] 带格式的 User 2018/6/30 17:02:00

无下划线, 字体颜色: 自动设置

页 62: [368] 带格式的 User 2018/6/30 17:15:00

定义网格后不调整右缩进, 不对齐到网格

页 62: [369] 带格式的 User 2018/6/30 17:02:00

无下划线, 字体颜色: 自动设置

页 62: [370] 带格式的 User 2018/6/30 17:02:00

无下划线, 字体颜色: 自动设置

页 62: [371] 带格式的 User 2018/6/30 17:02:00

无下划线, 字体颜色: 自动设置

页 62: [372] 带格式的 User 2018/6/30 17:02:00

无下划线, 字体颜色: 自动设置

页 62: [373] 带格式的 User 2018/6/30 17:02:00

无下划线, 字体颜色: 自动设置

页 62: [374] 带格式的 User 2018/6/30 17:02:00

无下划线, 字体颜色: 自动设置

页 62: [375] 带格式的 User 2018/6/30 17:02:00

无下划线, 字体颜色: 自动设置

页 62: [376] 带格式的 User 2018/6/30 17:02:00

无下划线, 字体颜色: 自动设置

页 62: [377] 带格式的 User 2018/6/30 17:02:00

无下划线, 字体颜色: 自动设置

页 62: [378] 带格式的 User 2018/6/30 17:02:00

无下划线, 字体颜色: 自动设置

页 62: [379] 带格式的 User 2018/6/30 17:02:00

无下划线, 字体颜色: 自动设置

页 62: [380] 带格式的 User 2018/6/30 17:02:00

无下划线, 字体颜色: 自动设置

页 62: [381] 带格式的 User 2018/6/30 17:02:00

无下划线, 字体颜色: 自动设置

页 62: [382] 带格式的 User 2018/6/30 17:02:00

无下划线, 字体颜色: 自动设置

页 62: [383] 带格式的 User 2018/6/30 17:15:00

定义网格后不调整右缩进, 不对齐到网格

页 62: [384] 带格式的 User 2018/6/30 17:02:00

无下划线, 字体颜色: 自动设置

页 62: [385] 带格式的 User 2018/6/30 17:02:00

无下划线, 字体颜色: 自动设置

页 62: [386] 带格式的 User 2018/6/30 17:02:00

无下划线, 字体颜色: 自动设置

页 62: [387] 带格式的 User 2018/6/30 17:02:00

无下划线, 字体颜色: 自动设置

页 62: [388] 带格式的 User 2018/6/30 17:02:00

无下划线, 字体颜色: 自动设置

页 62: [389] 带格式的 User 2018/6/30 17:02:00

无下划线, 字体颜色: 自动设置

页 62: [390] 带格式的 User 2018/6/30 17:02:00

无下划线, 字体颜色: 自动设置

页 62: [391] 带格式的 User 2018/6/30 17:02:00

无下划线, 字体颜色: 自动设置

页 62: [392] 带格式的 User 2018/6/30 17:02:00

无下划线, 字体颜色: 自动设置

页 62: [393] 带格式的 User 2018/6/30 17:02:00

无下划线, 字体颜色: 自动设置

页 62: [394] 带格式的 User 2018/6/30 17:02:00

无下划线, 字体颜色: 自动设置

页 62: [395] 带格式的 User 2018/6/30 17:02:00

无下划线, 字体颜色: 自动设置

页 62: [396] 带格式的 User 2018/6/30 17:02:00

无下划线, 字体颜色: 自动设置

页 63: [397] 带格式的 User 2018/6/30 17:02:00

无下划线, 字体颜色: 自动设置

页 63: [398] 带格式的 User 2018/6/30 17:02:00

无下划线, 字体颜色: 自动设置

页 63: [399] 带格式的 User 2018/6/30 17:15:00

定义网格后不调整右缩进, 不对齐到网格

页 63: [400] 带格式的 User 2018/6/30 17:02:00

无下划线, 字体颜色: 自动设置

页 63: [400] 带格式的 User 2018/6/30 17:02:00

无下划线, 字体颜色: 自动设置

页 63: [401] 带格式的 User 2018/6/30 17:02:00

无下划线, 字体颜色: 自动设置

页 63: [401] 带格式的 User 2018/6/30 17:02:00

无下划线, 字体颜色: 自动设置

页 63: [402] 带格式的 User 2018/6/30 17:02:00

无下划线, 字体颜色: 自动设置

页 63: [402] 带格式的 User 2018/6/30 17:02:00

无下划线, 字体颜色: 自动设置

页 63: [403] 带格式的 User 2018/6/30 17:02:00

无下划线, 字体颜色: 自动设置

页 63: [403] 带格式的 User 2018/6/30 17:02:00

无下划线, 字体颜色: 自动设置

页 63: [404] 带格式的 User 2018/6/30 17:02:00

无下划线, 字体颜色: 自动设置

页 63: [404] 带格式的 User 2018/6/30 17:02:00

无下划线, 字体颜色: 自动设置

页 63: [405] 带格式的 User 2018/6/30 17:02:00

无下划线, 字体颜色: 自动设置

页 63: [405] 带格式的 User 2018/6/30 17:02:00

无下划线, 字体颜色: 自动设置

页 63: [406] 带格式的 User 2018/6/30 17:02:00

无下划线, 字体颜色: 自动设置

页 63: [406] 带格式的 User 2018/6/30 17:02:00

无下划线, 字体颜色: 自动设置

页 63: [407] 带格式的 User 2018/6/30 17:02:00

无下划线, 字体颜色: 自动设置

页 63: [407] 带格式的 User 2018/6/30 17:02:00

无下划线, 字体颜色: 自动设置

页 63: [408] 带格式的 User 2018/6/30 17:02:00

无下划线, 字体颜色: 自动设置

页 63: [408] 带格式的 User 2018/6/30 17:02:00

无下划线, 字体颜色: 自动设置

页 63: [409] 带格式的 User 2018/6/30 17:02:00

无下划线, 字体颜色: 自动设置

页 63: [409] 带格式的 User 2018/6/30 17:02:00

无下划线, 字体颜色: 自动设置

页 63: [410] 带格式的 User 2018/6/30 17:02:00

无下划线, 字体颜色: 自动设置

页 63: [410] 带格式的 User 2018/6/30 17:02:00

无下划线, 字体颜色: 自动设置

页 63: [411] 带格式的 User 2018/6/30 17:02:00

无下划线, 字体颜色: 自动设置

页 63: [411] 带格式的 User 2018/6/30 17:02:00

无下划线, 字体颜色: 自动设置

页 63: [412] 带格式的 User 2018/6/30 17:02:00

无下划线, 字体颜色: 自动设置

页 63: [412] 带格式的 User 2018/6/30 17:02:00

无下划线, 字体颜色: 自动设置

页 63: [413] 带格式的 User 2018/6/30 17:02:00

无下划线, 字体颜色: 自动设置

页 63: [413] 带格式的 User 2018/6/30 17:02:00

无下划线, 字体颜色: 自动设置

页 63: [414] 带格式的 User 2018/6/30 17:02:00

无下划线, 字体颜色: 自动设置

页 63: [414] 带格式的 User 2018/6/30 17:02:00

无下划线, 字体颜色: 自动设置

页 63: [415] 带格式的 User 2018/6/30 17:02:00

无下划线, 字体颜色: 自动设置

页 63: [415] 带格式的 User 2018/6/30 17:02:00

无下划线, 字体颜色: 自动设置

页 63: [416] 带格式的 User 2018/6/30 17:02:00

无下划线, 字体颜色: 自动设置

页 63: [416] 带格式的 User 2018/6/30 17:02:00

无下划线, 字体颜色: 自动设置

页 63: [417] 带格式的 User 2018/6/30 17:02:00

无下划线, 字体颜色: 自动设置

页 63: [417] 带格式的 User 2018/6/30 17:02:00

无下划线, 字体颜色: 自动设置

页 63: [418] 带格式的 User 2018/6/30 17:02:00

无下划线, 字体颜色: 自动设置

页 63: [418] 带格式的 User 2018/6/30 17:02:00

无下划线, 字体颜色: 自动设置

页 63: [419] 带格式的 User 2018/6/30 17:02:00

无下划线, 字体颜色: 自动设置

页 63: [419] 带格式的 User 2018/6/30 17:02:00

无下划线, 字体颜色: 自动设置

页 63: [420] 带格式的 User 2018/6/30 17:02:00

无下划线, 字体颜色: 自动设置

页 63: [420] 带格式的 User 2018/6/30 17:02:00

无下划线, 字体颜色: 自动设置

页 63: [421] 带格式的 User 2018/6/30 17:02:00

无下划线, 字体颜色: 自动设置

页 63: [421] 带格式的 User 2018/6/30 17:02:00

无下划线, 字体颜色: 自动设置

页 63: [422] 带格式的 User 2018/6/30 17:02:00

无下划线, 字体颜色: 自动设置

页 63: [422] 带格式的 User 2018/6/30 17:02:00

无下划线, 字体颜色: 自动设置

页 63: [423] 带格式的 User 2018/6/30 17:02:00

无下划线, 字体颜色: 自动设置

页 63: [423] 带格式的 User 2018/6/30 17:02:00

无下划线, 字体颜色: 自动设置

页 63: [424] 带格式的 User 2018/6/30 17:02:00

无下划线, 字体颜色: 自动设置

页 63: [424] 带格式的 User 2018/6/30 17:02:00

无下划线, 字体颜色: 自动设置

页 63: [425] 带格式的 User 2018/6/30 17:02:00

无下划线, 字体颜色: 自动设置

页 63: [425] 带格式的 User 2018/6/30 17:02:00

无下划线, 字体颜色: 自动设置

页 63: [426] 带格式的 User 2018/6/30 17:02:00

无下划线, 字体颜色: 自动设置

页 63: [427] 带格式的 User 2018/6/30 17:15:00

定义网格后不调整右缩进, 不对齐到网格

页 63: [428] 带格式的 User 2018/6/30 17:02:00

无下划线, 字体颜色: 自动设置

页 63: [428] 带格式的 User 2018/6/30 17:02:00

无下划线, 字体颜色: 自动设置

页 63: [429] 带格式的 User 2018/6/30 17:02:00

无下划线, 字体颜色: 自动设置

页 63: [429] 带格式的 User 2018/6/30 17:02:00

无下划线, 字体颜色: 自动设置

页 63: [430] 带格式的 User 2018/6/30 17:02:00

无下划线, 字体颜色: 自动设置

页 63: [430] 带格式的 User 2018/6/30 17:02:00

无下划线, 字体颜色: 自动设置

页 63: [431] 带格式的 User 2018/6/30 17:02:00

无下划线, 字体颜色: 自动设置

页 63: [431] 带格式的 User 2018/6/30 17:02:00

无下划线, 字体颜色: 自动设置

页 63: [432] 带格式的 User 2018/6/30 17:02:00

无下划线, 字体颜色: 自动设置

页 63: [432] 带格式的 User 2018/6/30 17:02:00

无下划线, 字体颜色: 自动设置

页 63: [433] 带格式的 User 2018/6/30 17:02:00

无下划线, 字体颜色: 自动设置

页 63: [433] 带格式的 User 2018/6/30 17:02:00

无下划线, 字体颜色: 自动设置

页 63: [434] 带格式的 User 2018/6/30 17:02:00

无下划线, 字体颜色: 自动设置

页 63: [434] 带格式的 User 2018/6/30 17:02:00

无下划线, 字体颜色: 自动设置

页 63: [435] 带格式的 User 2018/6/30 17:02:00

无下划线, 字体颜色: 自动设置

页 63: [435] 带格式的 User 2018/6/30 17:02:00

无下划线, 字体颜色: 自动设置

页 63: [436] 带格式的 User 2018/6/30 17:02:00

无下划线, 字体颜色: 自动设置

页 63: [436] 带格式的 User 2018/6/30 17:02:00

无下划线, 字体颜色: 自动设置

页 63: [437] 带格式的 User 2018/6/30 17:02:00

无下划线, 字体颜色: 自动设置

页 63: [437] 带格式的 User 2018/6/30 17:02:00

无下划线, 字体颜色: 自动设置

页 63: [438] 带格式的 User 2018/6/30 17:02:00

无下划线, 字体颜色: 自动设置

页 63: [438] 带格式的 User 2018/6/30 17:02:00

无下划线, 字体颜色: 自动设置

页 63: [439] 带格式的 User 2018/6/30 17:02:00

无下划线, 字体颜色: 自动设置

页 63: [439] 带格式的 User 2018/6/30 17:02:00

无下划线, 字体颜色: 自动设置

页 63: [440] 带格式的 User 2018/6/30 17:02:00

无下划线, 字体颜色: 自动设置

页 63: [440] 带格式的 User 2018/6/30 17:02:00

无下划线, 字体颜色: 自动设置

页 63: [441] 带格式的 User 2018/6/30 17:02:00

无下划线, 字体颜色: 自动设置

页 63: [442] 带格式的 User 2018/6/30 17:15:00

定义网格后不调整右缩进, 不对齐到网格

页 63: [443] 带格式的 User 2018/6/30 17:02:00

无下划线, 字体颜色: 自动设置

页 63: [443] 带格式的 User 2018/6/30 17:02:00

无下划线, 字体颜色: 自动设置

页 63: [444] 带格式的 User 2018/6/30 17:02:00

无下划线, 字体颜色: 自动设置

页 63: [444] 带格式的 User 2018/6/30 17:02:00

无下划线, 字体颜色: 自动设置

页 63: [445] 带格式的 User 2018/6/30 17:02:00

无下划线, 字体颜色: 自动设置

页 63: [445] 带格式的 User 2018/6/30 17:02:00

无下划线, 字体颜色: 自动设置

页 63: [446] 带格式的 User 2018/6/30 17:02:00

无下划线, 字体颜色: 自动设置

页 63: [446] 带格式的 User 2018/6/30 17:02:00

无下划线, 字体颜色: 自动设置

页 63: [447] 带格式的 User 2018/6/30 17:02:00

无下划线, 字体颜色: 自动设置

页 63: [447] 带格式的 User 2018/6/30 17:02:00

无下划线, 字体颜色: 自动设置

页 63: [448] 带格式的 User 2018/6/30 17:02:00

无下划线, 字体颜色: 自动设置

页 63: [448] 带格式的 User 2018/6/30 17:02:00

无下划线, 字体颜色: 自动设置

页 63: [449] 带格式的 User 2018/6/30 17:02:00

无下划线, 字体颜色: 自动设置

页 63: [449] 带格式的 User 2018/6/30 17:02:00

无下划线, 字体颜色: 自动设置

页 63: [450] 带格式的 User 2018/6/30 17:02:00

无下划线, 字体颜色: 自动设置

页 63: [450] 带格式的 User 2018/6/30 17:02:00

无下划线, 字体颜色: 自动设置

页 63: [451] 带格式的 User 2018/6/30 17:02:00

无下划线, 字体颜色: 自动设置

页 63: [451] 带格式的 User 2018/6/30 17:02:00

无下划线, 字体颜色: 自动设置

页 63: [452] 带格式的 User 2018/6/30 17:02:00

无下划线, 字体颜色: 自动设置

页 63: [452] 带格式的 User 2018/6/30 17:02:00

无下划线, 字体颜色: 自动设置

页 63: [453] 带格式的 User 2018/6/30 17:02:00

无下划线, 字体颜色: 自动设置

页 63: [453] 带格式的 User 2018/6/30 17:02:00

无下划线, 字体颜色: 自动设置

页 63: [454] 带格式的 User 2018/6/30 17:02:00

无下划线, 字体颜色: 自动设置

页 63: [454] 带格式的 User 2018/6/30 17:02:00

无下划线, 字体颜色: 自动设置

页 63: [455] 带格式的 User 2018/6/30 17:02:00

无下划线, 字体颜色: 自动设置

页 63: [455] 带格式的 User 2018/6/30 17:02:00

无下划线, 字体颜色: 自动设置

页 63: [456] 带格式的 User 2018/6/30 17:02:00

无下划线, 字体颜色: 自动设置

页 63: [457] 带格式的 User 2018/6/30 17:15:00

定义网格后不调整右缩进, 不对齐到网格

页 63: [458] 带格式的 User 2018/6/30 17:02:00

无下划线, 字体颜色: 自动设置

页 63: [458] 带格式的 User 2018/6/30 17:02:00

无下划线, 字体颜色: 自动设置

页 63: [459] 带格式的 User 2018/6/30 17:02:00

无下划线, 字体颜色: 自动设置

页 63: [459] 带格式的 User 2018/6/30 17:02:00

无下划线, 字体颜色: 自动设置

页 63: [460] 带格式的 User 2018/6/30 17:02:00

无下划线, 字体颜色: 自动设置

页 63: [460] 带格式的 User 2018/6/30 17:02:00

无下划线, 字体颜色: 自动设置

页 63: [461] 带格式的 User 2018/6/30 17:02:00

无下划线, 字体颜色: 自动设置

页 63: [461] 带格式的 User 2018/6/30 17:02:00

无下划线, 字体颜色: 自动设置

页 63: [462] 带格式的 User 2018/6/30 17:02:00

无下划线, 字体颜色: 自动设置

页 63: [462] 带格式的 User 2018/6/30 17:02:00

无下划线, 字体颜色: 自动设置

页 63: [463] 带格式的 User 2018/6/30 17:02:00

无下划线, 字体颜色: 自动设置

页 63: [463] 带格式的 User 2018/6/30 17:02:00

无下划线, 字体颜色: 自动设置

页 63: [464] 带格式的 User 2018/6/30 17:02:00

无下划线, 字体颜色: 自动设置

页 63: [464] 带格式的 User 2018/6/30 17:02:00

无下划线, 字体颜色: 自动设置

页 63: [465] 带格式的 User 2018/6/30 17:02:00

无下划线, 字体颜色: 自动设置

页 63: [465] 带格式的 User 2018/6/30 17:02:00

无下划线, 字体颜色: 自动设置

页 63: [466] 带格式的 User 2018/6/30 17:02:00

无下划线, 字体颜色: 自动设置

页 63: [466] 带格式的 User 2018/6/30 17:02:00

无下划线, 字体颜色: 自动设置

页 63: [467] 带格式的 User 2018/6/30 17:02:00

无下划线, 字体颜色: 自动设置

页 63: [467] 带格式的 User 2018/6/30 17:02:00

无下划线, 字体颜色: 自动设置

页 63: [468] 带格式的 User 2018/6/30 17:02:00

无下划线, 字体颜色: 自动设置

页 63: [468] 带格式的 User 2018/6/30 17:02:00

无下划线, 字体颜色: 自动设置

页 63: [469] 带格式的 User 2018/6/30 17:02:00

无下划线, 字体颜色: 自动设置

页 63: [469] 带格式的 User 2018/6/30 17:02:00

无下划线, 字体颜色: 自动设置

页 63: [470] 带格式的 User 2018/6/30 17:02:00

无下划线, 字体颜色: 自动设置

页 63: [470] 带格式的 User 2018/6/30 17:02:00

无下划线, 字体颜色: 自动设置

页 63: [471] 带格式的 User 2018/6/30 17:02:00

无下划线, 字体颜色: 自动设置

页 63: [472] 带格式的 User 2018/6/30 17:15:00

定义网格后不调整右缩进, 不对齐到网格

页 63: [473] 带格式的 User 2018/6/30 17:02:00

无下划线, 字体颜色: 自动设置

页 63: [473] 带格式的 User 2018/6/30 17:02:00

无下划线, 字体颜色: 自动设置

页 63: [474] 带格式的 User 2018/6/30 17:02:00

无下划线, 字体颜色: 自动设置

页 63: [474] 带格式的 User 2018/6/30 17:02:00

无下划线, 字体颜色: 自动设置

页 63: [475] 带格式的 User 2018/6/30 17:02:00

无下划线, 字体颜色: 自动设置

页 63: [475] 带格式的 User 2018/6/30 17:02:00

无下划线, 字体颜色: 自动设置

页 63: [476] 带格式的 User 2018/6/30 17:02:00

无下划线, 字体颜色: 自动设置

页 63: [476] 带格式的 User 2018/6/30 17:02:00

无下划线, 字体颜色: 自动设置

页 63: [477] 带格式的 User 2018/6/30 17:02:00

无下划线, 字体颜色: 自动设置

页 63: [477] 带格式的 User 2018/6/30 17:02:00

无下划线, 字体颜色: 自动设置

页 63: [478] 带格式的 User 2018/6/30 17:02:00

无下划线, 字体颜色: 自动设置

页 63: [478] 带格式的 User 2018/6/30 17:02:00

无下划线, 字体颜色: 自动设置

页 63: [479] 带格式的 User 2018/6/30 17:02:00

无下划线, 字体颜色: 自动设置

页 63: [479] 带格式的 User 2018/6/30 17:02:00

无下划线, 字体颜色: 自动设置

页 63: [480] 带格式的 User 2018/6/30 17:02:00

无下划线, 字体颜色: 自动设置

页 63: [480] 带格式的 User 2018/6/30 17:02:00

无下划线, 字体颜色: 自动设置

页 63: [481] 带格式的 User 2018/6/30 17:02:00

无下划线, 字体颜色: 自动设置

页 63: [481] 带格式的 User 2018/6/30 17:02:00

无下划线, 字体颜色: 自动设置

页 63: [482] 带格式的 User 2018/6/30 17:02:00

无下划线, 字体颜色: 自动设置

页 63: [482] 带格式的 User 2018/6/30 17:02:00

无下划线, 字体颜色: 自动设置

页 63: [483] 带格式的 User 2018/6/30 17:02:00

无下划线, 字体颜色: 自动设置

页 63: [483] 带格式的 User 2018/6/30 17:02:00

无下划线, 字体颜色: 自动设置

页 63: [484] 带格式的 User 2018/6/30 17:02:00

无下划线, 字体颜色: 自动设置

页 63: [484] 带格式的 User 2018/6/30 17:02:00

无下划线, 字体颜色: 自动设置

页 63: [485] 带格式的 User 2018/6/30 17:02:00

无下划线, 字体颜色: 自动设置

页 63: [485] 带格式的 User 2018/6/30 17:02:00

无下划线, 字体颜色: 自动设置

页 63: [486] 带格式的 User 2018/6/30 17:02:00

无下划线, 字体颜色: 自动设置

页 63: [487] 带格式的 User 2018/6/30 17:15:00

定义网格后不调整右缩进, 不对齐到网格

页 63: [488] 带格式的 User 2018/6/30 17:02:00

无下划线, 字体颜色: 自动设置

页 63: [488] 带格式的 User 2018/6/30 17:02:00

无下划线, 字体颜色: 自动设置

页 63: [489] 带格式的 User 2018/6/30 17:02:00

无下划线, 字体颜色: 自动设置

页 63: [489] 带格式的 User 2018/6/30 17:02:00

无下划线, 字体颜色: 自动设置

页 63: [490] 带格式的 User 2018/6/30 17:02:00

无下划线, 字体颜色: 自动设置

页 63: [490] 带格式的 User 2018/6/30 17:02:00

无下划线, 字体颜色: 自动设置

页 63: [491] 带格式的 User 2018/6/30 17:02:00

无下划线, 字体颜色: 自动设置

页 63: [491] 带格式的 User 2018/6/30 17:02:00

无下划线, 字体颜色: 自动设置

页 63: [492] 带格式的 User 2018/6/30 17:02:00

无下划线, 字体颜色: 自动设置

页 63: [492] 带格式的 User 2018/6/30 17:02:00

无下划线, 字体颜色: 自动设置

页 63: [493] 带格式的 User 2018/6/30 17:02:00

无下划线, 字体颜色: 自动设置

页 63: [493] 带格式的 User 2018/6/30 17:02:00

无下划线, 字体颜色: 自动设置

页 63: [494] 带格式的 User 2018/6/30 17:02:00

无下划线, 字体颜色: 自动设置

页 63: [494] 带格式的 User 2018/6/30 17:02:00

无下划线, 字体颜色: 自动设置

页 63: [495] 带格式的 User 2018/6/30 17:02:00

无下划线, 字体颜色: 自动设置

页 63: [495] 带格式的 User 2018/6/30 17:02:00

无下划线, 字体颜色: 自动设置

页 63: [496] 带格式的 User 2018/6/30 17:02:00

无下划线, 字体颜色: 自动设置

页 63: [496] 带格式的 User 2018/6/30 17:02:00

无下划线, 字体颜色: 自动设置

页 63: [497] 带格式的 User 2018/6/30 17:02:00

无下划线, 字体颜色: 自动设置

页 63: [497] 带格式的 User 2018/6/30 17:02:00

无下划线, 字体颜色: 自动设置

页 63: [498] 带格式的 User 2018/6/30 17:02:00

无下划线, 字体颜色: 自动设置

页 63: [498] 带格式的 User 2018/6/30 17:02:00

无下划线, 字体颜色: 自动设置

页 63: [499] 带格式的 User 2018/6/30 17:02:00

无下划线, 字体颜色: 自动设置

页 63: [499] 带格式的 User 2018/6/30 17:02:00

无下划线, 字体颜色: 自动设置

页 63: [500] 带格式的 User 2018/6/30 17:02:00

无下划线, 字体颜色: 自动设置

页 63: [500] 带格式的 User 2018/6/30 17:02:00

无下划线, 字体颜色: 自动设置

页 63: [501] 带格式的 User 2018/6/30 17:02:00

无下划线, 字体颜色: 自动设置

页 63: [502] 带格式的 User 2018/6/30 17:15:00

定义网格后不调整右缩进, 不对齐到网格

页 63: [503] 带格式的 User 2018/6/30 17:02:00

无下划线, 字体颜色: 自动设置

页 63: [503] 带格式的 User 2018/6/30 17:02:00

无下划线, 字体颜色: 自动设置

页 63: [504] 带格式的 User 2018/6/30 17:02:00

无下划线, 字体颜色: 自动设置

页 63: [504] 带格式的 User 2018/6/30 17:02:00

无下划线, 字体颜色: 自动设置

页 63: [505] 带格式的 User 2018/6/30 17:02:00

无下划线, 字体颜色: 自动设置

页 63: [505] 带格式的 User 2018/6/30 17:02:00

无下划线, 字体颜色: 自动设置

页 63: [506] 带格式的 User 2018/6/30 17:02:00

无下划线, 字体颜色: 自动设置

页 63: [506] 带格式的 User 2018/6/30 17:02:00

无下划线, 字体颜色: 自动设置

页 63: [507] 带格式的 User 2018/6/30 17:02:00

无下划线, 字体颜色: 自动设置

页 63: [507] 带格式的 User 2018/6/30 17:02:00

无下划线, 字体颜色: 自动设置

页 63: [508] 带格式的 User 2018/6/30 17:02:00

无下划线, 字体颜色: 自动设置

页 63: [508] 带格式的 User 2018/6/30 17:02:00

无下划线, 字体颜色: 自动设置

页 63: [509] 带格式的 User 2018/6/30 17:02:00

无下划线, 字体颜色: 自动设置

页 63: [509] 带格式的 User 2018/6/30 17:02:00

无下划线, 字体颜色: 自动设置

页 63: [510] 带格式的 User 2018/6/30 17:02:00

无下划线, 字体颜色: 自动设置

页 63: [510] 带格式的 User 2018/6/30 17:02:00

无下划线, 字体颜色: 自动设置

页 63: [511] 带格式的 User 2018/6/30 17:02:00

无下划线, 字体颜色: 自动设置

页 63: [511] 带格式的 User 2018/6/30 17:02:00

无下划线, 字体颜色: 自动设置

页 63: [512] 带格式的 User 2018/6/30 17:02:00

无下划线, 字体颜色: 自动设置

页 63: [512] 带格式的 User 2018/6/30 17:02:00

无下划线, 字体颜色: 自动设置

页 63: [513] 带格式的 User 2018/6/30 17:02:00

无下划线, 字体颜色: 自动设置

页 63: [513] 带格式的 User 2018/6/30 17:02:00

无下划线, 字体颜色: 自动设置

页 63: [514] 带格式的 User 2018/6/30 17:02:00

无下划线, 字体颜色: 自动设置

页 63: [514] 带格式的 User 2018/6/30 17:02:00

无下划线, 字体颜色: 自动设置

页 63: [515] 带格式的 User 2018/6/30 17:02:00

无下划线, 字体颜色: 自动设置

页 63: [515] 带格式的 User 2018/6/30 17:02:00

无下划线, 字体颜色: 自动设置

页 63: [516] 带格式的 User 2018/6/30 17:02:00

无下划线, 字体颜色: 自动设置

页 63: [517] 带格式的 User 2018/6/30 17:15:00

定义网格后不调整右缩进, 不对齐到网格

页 63: [518] 带格式的 User 2018/6/30 17:02:00

无下划线, 字体颜色: 自动设置

页 63: [518] 带格式的 User 2018/6/30 17:02:00

无下划线, 字体颜色: 自动设置

页 63: [519] 带格式的 User 2018/6/30 17:02:00

无下划线, 字体颜色: 自动设置

页 63: [519] 带格式的 User 2018/6/30 17:02:00

无下划线, 字体颜色: 自动设置

页 63: [520] 带格式的 User 2018/6/30 17:02:00

无下划线, 字体颜色: 自动设置

页 63: [520] 带格式的 User 2018/6/30 17:02:00

无下划线, 字体颜色: 自动设置

页 63: [521] 带格式的 User 2018/6/30 17:02:00

无下划线, 字体颜色: 自动设置

页 63: [521] 带格式的 User 2018/6/30 17:02:00

无下划线, 字体颜色: 自动设置

页 63: [522] 带格式的 User 2018/6/30 17:02:00

无下划线, 字体颜色: 自动设置

页 63: [522] 带格式的 User 2018/6/30 17:02:00

无下划线, 字体颜色: 自动设置

页 63: [523] 带格式的 User 2018/6/30 17:02:00

无下划线, 字体颜色: 自动设置

页 63: [523] 带格式的 User 2018/6/30 17:02:00

无下划线, 字体颜色: 自动设置

页 63: [524] 带格式的 User 2018/6/30 17:02:00

无下划线, 字体颜色: 自动设置

页 63: [524] 带格式的 User 2018/6/30 17:02:00

无下划线, 字体颜色: 自动设置

页 63: [525] 带格式的 User 2018/6/30 17:02:00

无下划线, 字体颜色: 自动设置

页 63: [525] 带格式的 User 2018/6/30 17:02:00

无下划线, 字体颜色: 自动设置

页 63: [526] 带格式的 User 2018/6/30 17:02:00

无下划线, 字体颜色: 自动设置

页 63: [526] 带格式的 User 2018/6/30 17:02:00

无下划线, 字体颜色: 自动设置

页 63: [527] 带格式的 User 2018/6/30 17:02:00

无下划线, 字体颜色: 自动设置

页 63: [527] 带格式的 User 2018/6/30 17:02:00

无下划线, 字体颜色: 自动设置

页 63: [528] 带格式的 User 2018/6/30 17:02:00

无下划线, 字体颜色: 自动设置

页 63: [528] 带格式的 User 2018/6/30 17:02:00

无下划线, 字体颜色: 自动设置

页 63: [529] 带格式的 User 2018/6/30 17:02:00

无下划线, 字体颜色: 自动设置

页 63: [529] 带格式的 User 2018/6/30 17:02:00

无下划线, 字体颜色: 自动设置

页 63: [530] 带格式的 User 2018/6/30 17:02:00

无下划线, 字体颜色: 自动设置

页 63: [530] 带格式的 User 2018/6/30 17:02:00

无下划线, 字体颜色: 自动设置

页 63: [531] 带格式的 User 2018/6/30 17:02:00

无下划线, 字体颜色: 自动设置

页 63: [532] 带格式的 User 2018/6/30 17:15:00

定义网格后不调整右缩进, 不对齐到网格

页 63: [533] 带格式的 User 2018/6/30 17:02:00

无下划线, 字体颜色: 自动设置

页 63: [533] 带格式的 User 2018/6/30 17:02:00

无下划线, 字体颜色: 自动设置

页 63: [534] 带格式的 User 2018/6/30 17:02:00

无下划线, 字体颜色: 自动设置

页 63: [534] 带格式的 User 2018/6/30 17:02:00

无下划线, 字体颜色: 自动设置

页 63: [535] 带格式的 User 2018/6/30 17:02:00

无下划线, 字体颜色: 自动设置

页 63: [535] 带格式的 User 2018/6/30 17:02:00

无下划线, 字体颜色: 自动设置

页 63: [536] 带格式的 User 2018/6/30 17:02:00

无下划线, 字体颜色: 自动设置

页 63: [536] 带格式的 User 2018/6/30 17:02:00

无下划线, 字体颜色: 自动设置

页 63: [537] 带格式的 User 2018/6/30 17:02:00

无下划线, 字体颜色: 自动设置

页 63: [537] 带格式的 User 2018/6/30 17:02:00

无下划线, 字体颜色: 自动设置

页 63: [538] 带格式的 User 2018/6/30 17:02:00

无下划线, 字体颜色: 自动设置

页 63: [538] 带格式的 User 2018/6/30 17:02:00

无下划线, 字体颜色: 自动设置

页 63: [539] 带格式的 User 2018/6/30 17:02:00

无下划线, 字体颜色: 自动设置

页 63: [539] 带格式的 User 2018/6/30 17:02:00

无下划线, 字体颜色: 自动设置

页 63: [540] 带格式的 User 2018/6/30 17:02:00

无下划线, 字体颜色: 自动设置

页 63: [540] 带格式的 User 2018/6/30 17:02:00

无下划线, 字体颜色: 自动设置

页 63: [541] 带格式的 User 2018/6/30 17:02:00

无下划线, 字体颜色: 自动设置

页 63: [541] 带格式的 User 2018/6/30 17:02:00

无下划线, 字体颜色: 自动设置

页 63: [542] 带格式的 User 2018/6/30 17:02:00

无下划线, 字体颜色: 自动设置

页 63: [542] 带格式的 User 2018/6/30 17:02:00

无下划线, 字体颜色: 自动设置

页 63: [543] 带格式的 User 2018/6/30 17:02:00

无下划线, 字体颜色: 自动设置

页 63: [543] 带格式的 User 2018/6/30 17:02:00

无下划线, 字体颜色: 自动设置

页 63: [544] 带格式的 User 2018/6/30 17:02:00

无下划线, 字体颜色: 自动设置

页 63: [544] 带格式的 User 2018/6/30 17:02:00

无下划线, 字体颜色: 自动设置

页 63: [545] 带格式的 User 2018/6/30 17:02:00

无下划线, 字体颜色: 自动设置

页 63: [545] 带格式的 User 2018/6/30 17:02:00

无下划线, 字体颜色: 自动设置

页 63: [546] 带格式的 User 2018/6/30 17:02:00

无下划线, 字体颜色: 自动设置

页 63: [547] 带格式的 User 2018/6/30 17:15:00

定义网格后不调整右缩进, 不对齐到网格

页 63: [548] 带格式的 User 2018/6/30 17:02:00

无下划线, 字体颜色: 自动设置

页 63: [548] 带格式的 User 2018/6/30 17:02:00

无下划线, 字体颜色: 自动设置

页 63: [549] 带格式的 User 2018/6/30 17:02:00

无下划线, 字体颜色: 自动设置

页 63: [549] 带格式的 User 2018/6/30 17:02:00

无下划线, 字体颜色: 自动设置

页 63: [550] 带格式的 User 2018/6/30 17:02:00

无下划线, 字体颜色: 自动设置

页 63: [550] 带格式的 User 2018/6/30 17:02:00

无下划线, 字体颜色: 自动设置

页 63: [551] 带格式的 User 2018/6/30 17:02:00

无下划线, 字体颜色: 自动设置

页 63: [551] 带格式的 User 2018/6/30 17:02:00

无下划线, 字体颜色: 自动设置

页 63: [552] 带格式的 User 2018/6/30 17:02:00

无下划线, 字体颜色: 自动设置

页 63: [552] 带格式的 User 2018/6/30 17:02:00

无下划线, 字体颜色: 自动设置

页 63: [553] 带格式的 User 2018/6/30 17:02:00

无下划线, 字体颜色: 自动设置

页 63: [553] 带格式的 User 2018/6/30 17:02:00

无下划线, 字体颜色: 自动设置

页 63: [554] 带格式的 User 2018/6/30 17:02:00

无下划线, 字体颜色: 自动设置

页 63: [554] 带格式的 User 2018/6/30 17:02:00

无下划线, 字体颜色: 自动设置

页 63: [555] 带格式的 User 2018/6/30 17:02:00

无下划线, 字体颜色: 自动设置

页 63: [555] 带格式的 User 2018/6/30 17:02:00

无下划线, 字体颜色: 自动设置

页 63: [556] 带格式的 User 2018/6/30 17:02:00

无下划线, 字体颜色: 自动设置

页 63: [556] 带格式的 User 2018/6/30 17:02:00

无下划线, 字体颜色: 自动设置

页 63: [557] 带格式的 User 2018/6/30 17:02:00

无下划线, 字体颜色: 自动设置

页 63: [557] 带格式的 User 2018/6/30 17:02:00

无下划线, 字体颜色: 自动设置

页 63: [558] 带格式的 User 2018/6/30 17:02:00

无下划线, 字体颜色: 自动设置

页 63: [558] 带格式的 User 2018/6/30 17:02:00

无下划线, 字体颜色: 自动设置

页 63: [559] 带格式的 User 2018/6/30 17:02:00

无下划线, 字体颜色: 自动设置

页 63: [559] 带格式的 User 2018/6/30 17:02:00

无下划线, 字体颜色: 自动设置

页 63: [560] 带格式的 User 2018/6/30 17:02:00

无下划线, 字体颜色: 自动设置

页 63: [560] 带格式的 User 2018/6/30 17:02:00

无下划线, 字体颜色: 自动设置

页 63: [561] 带格式的 User 2018/6/30 17:02:00

无下划线, 字体颜色: 自动设置

页 63: [562] 带格式的 User 2018/6/30 17:15:00

定义网格后不调整右缩进, 不对齐到网格

页 63: [563] 带格式的 User 2018/6/30 17:02:00

无下划线, 字体颜色: 自动设置

页 63: [563] 带格式的 User 2018/6/30 17:02:00

无下划线, 字体颜色: 自动设置

页 63: [564] 带格式的 User 2018/6/30 17:02:00

无下划线, 字体颜色: 自动设置

页 63: [564] 带格式的 User 2018/6/30 17:02:00

无下划线, 字体颜色: 自动设置

页 63: [565] 带格式的 User 2018/6/30 17:02:00

无下划线, 字体颜色: 自动设置

页 63: [565] 带格式的 User 2018/6/30 17:02:00

无下划线, 字体颜色: 自动设置

页 63: [566] 带格式的 User 2018/6/30 17:02:00

无下划线, 字体颜色: 自动设置

页 63: [566] 带格式的 User 2018/6/30 17:02:00

无下划线, 字体颜色: 自动设置

页 63: [567] 带格式的 User 2018/6/30 17:02:00

无下划线, 字体颜色: 自动设置

页 63: [567] 带格式的 User 2018/6/30 17:02:00

无下划线, 字体颜色: 自动设置

页 63: [568] 带格式的 User 2018/6/30 17:02:00

无下划线, 字体颜色: 自动设置

页 63: [568] 带格式的 User 2018/6/30 17:02:00

无下划线, 字体颜色: 自动设置

页 63: [569] 带格式的 User 2018/6/30 17:02:00

无下划线, 字体颜色: 自动设置

页 63: [569] 带格式的 User 2018/6/30 17:02:00

无下划线, 字体颜色: 自动设置

页 63: [570] 带格式的 User 2018/6/30 17:02:00

无下划线, 字体颜色: 自动设置

页 63: [570] 带格式的 User 2018/6/30 17:02:00

无下划线, 字体颜色: 自动设置

页 63: [571] 带格式的 User 2018/6/30 17:02:00

无下划线, 字体颜色: 自动设置

页 63: [571] 带格式的 User 2018/6/30 17:02:00

无下划线, 字体颜色: 自动设置

页 63: [572] 带格式的 User 2018/6/30 17:02:00

无下划线, 字体颜色: 自动设置

页 63: [572] 带格式的 User 2018/6/30 17:02:00

无下划线, 字体颜色: 自动设置

页 63: [573] 带格式的 User 2018/6/30 17:02:00

无下划线, 字体颜色: 自动设置

页 63: [573] 带格式的 User 2018/6/30 17:02:00

无下划线, 字体颜色: 自动设置

页 63: [574] 带格式的 User 2018/6/30 17:02:00

无下划线, 字体颜色: 自动设置

页 63: [574] 带格式的 User 2018/6/30 17:02:00

无下划线, 字体颜色: 自动设置

页 63: [575] 带格式的 User 2018/6/30 17:02:00

无下划线, 字体颜色: 自动设置

页 63: [575] 带格式的 User 2018/6/30 17:02:00

无下划线, 字体颜色: 自动设置

页 63: [576] 带格式的 User 2018/6/30 17:02:00

无下划线, 字体颜色: 自动设置

页 63: [577] 带格式的 User 2018/6/30 17:15:00

定义网格后不调整右缩进, 不对齐到网格

页 63: [578] 带格式的 User 2018/6/30 17:02:00

无下划线, 字体颜色: 自动设置

页 63: [578] 带格式的 User 2018/6/30 17:02:00

无下划线, 字体颜色: 自动设置

页 63: [579] 带格式的 User 2018/6/30 17:02:00

无下划线, 字体颜色: 自动设置

页 63: [579] 带格式的 User 2018/6/30 17:02:00

无下划线, 字体颜色: 自动设置

页 63: [580] 带格式的 User 2018/6/30 17:02:00

无下划线, 字体颜色: 自动设置

页 63: [580] 带格式的 User 2018/6/30 17:02:00

无下划线, 字体颜色: 自动设置

页 63: [581] 带格式的 User 2018/6/30 17:02:00

无下划线, 字体颜色: 自动设置

页 63: [581] 带格式的 User 2018/6/30 17:02:00

无下划线, 字体颜色: 自动设置

页 63: [582] 带格式的 User 2018/6/30 17:02:00

无下划线, 字体颜色: 自动设置

页 63: [582] 带格式的 User 2018/6/30 17:02:00

无下划线, 字体颜色: 自动设置

页 63: [583] 带格式的 User 2018/6/30 17:02:00

无下划线, 字体颜色: 自动设置

页 63: [583] 带格式的 User 2018/6/30 17:02:00

无下划线, 字体颜色: 自动设置

页 63: [584] 带格式的 User 2018/6/30 17:02:00

无下划线, 字体颜色: 自动设置

页 63: [584] 带格式的 User 2018/6/30 17:02:00

无下划线, 字体颜色: 自动设置

页 63: [585] 带格式的 User 2018/6/30 17:02:00

无下划线, 字体颜色: 自动设置

页 63: [585] 带格式的 User 2018/6/30 17:02:00

无下划线, 字体颜色: 自动设置

页 63: [586] 带格式的 User 2018/6/30 17:02:00

无下划线, 字体颜色: 自动设置

页 63: [586] 带格式的 User 2018/6/30 17:02:00

无下划线, 字体颜色: 自动设置

页 63: [587] 带格式的 User 2018/6/30 17:02:00

无下划线, 字体颜色: 自动设置

页 63: [587] 带格式的 User 2018/6/30 17:02:00

无下划线, 字体颜色: 自动设置

页 63: [588] 带格式的 User 2018/6/30 17:02:00

无下划线, 字体颜色: 自动设置

页 63: [588] 带格式的 User 2018/6/30 17:02:00

无下划线, 字体颜色: 自动设置

页 63: [589] 带格式的 User 2018/6/30 17:02:00

无下划线, 字体颜色: 自动设置

页 63: [589] 带格式的 User 2018/6/30 17:02:00

无下划线, 字体颜色: 自动设置

页 63: [590] 带格式的 User 2018/6/30 17:02:00

无下划线, 字体颜色: 自动设置

页 63: [590] 带格式的 User 2018/6/30 17:02:00

无下划线, 字体颜色: 自动设置

页 63: [591] 带格式的 User 2018/6/30 17:02:00

无下划线, 字体颜色: 自动设置

页 63: [592] 带格式的 User 2018/6/30 17:15:00

定义网格后不调整右缩进, 不对齐到网格

页 63: [593] 带格式的 User 2018/6/30 17:02:00

无下划线, 字体颜色: 自动设置

页 63: [593] 带格式的 User 2018/6/30 17:02:00

无下划线, 字体颜色: 自动设置

页 63: [594] 带格式的 User 2018/6/30 17:02:00

无下划线, 字体颜色: 自动设置

页 63: [594] 带格式的 User 2018/6/30 17:02:00

无下划线, 字体颜色: 自动设置

页 63: [595] 带格式的 User 2018/6/30 17:02:00

无下划线, 字体颜色: 自动设置

页 63: [595] 带格式的 User 2018/6/30 17:02:00

无下划线, 字体颜色: 自动设置

页 63: [596] 带格式的 User 2018/6/30 17:02:00

无下划线, 字体颜色: 自动设置

页 63: [596] 带格式的 User 2018/6/30 17:02:00

无下划线, 字体颜色: 自动设置

页 63: [597] 带格式的 User 2018/6/30 17:02:00

无下划线, 字体颜色: 自动设置

页 63: [597] 带格式的 User 2018/6/30 17:02:00

无下划线, 字体颜色: 自动设置

页 63: [598] 带格式的 User 2018/6/30 17:02:00

无下划线, 字体颜色: 自动设置

页 63: [598] 带格式的 User 2018/6/30 17:02:00

无下划线, 字体颜色: 自动设置

页 63: [599] 带格式的 User 2018/6/30 17:02:00

无下划线, 字体颜色: 自动设置

页 63: [599] 带格式的 User 2018/6/30 17:02:00

无下划线, 字体颜色: 自动设置

页 63: [600] 带格式的 User 2018/6/30 17:02:00

无下划线, 字体颜色: 自动设置

页 63: [600] 带格式的 User 2018/6/30 17:02:00

无下划线, 字体颜色: 自动设置

页 63: [601] 带格式的 User 2018/6/30 17:02:00

无下划线, 字体颜色: 自动设置

页 63: [601] 带格式的 User 2018/6/30 17:02:00

无下划线, 字体颜色: 自动设置

页 63: [602] 带格式的 User 2018/6/30 17:02:00

无下划线, 字体颜色: 自动设置

页 63: [602] 带格式的 User 2018/6/30 17:02:00

无下划线, 字体颜色: 自动设置

页 63: [603] 带格式的 User 2018/6/30 17:02:00

无下划线, 字体颜色: 自动设置

页 63: [603] 带格式的 User 2018/6/30 17:02:00

无下划线, 字体颜色: 自动设置

页 63: [604] 带格式的 User 2018/6/30 17:02:00

无下划线, 字体颜色: 自动设置

页 63: [604] 带格式的 User 2018/6/30 17:02:00

无下划线, 字体颜色: 自动设置

页 63: [605] 带格式的 User 2018/6/30 17:02:00

无下划线, 字体颜色: 自动设置

页 63: [605] 带格式的 User 2018/6/30 17:02:00

无下划线, 字体颜色: 自动设置

页 63: [606] 带格式的 User 2018/6/30 17:02:00

无下划线, 字体颜色: 自动设置

页 63: [607] 带格式的 User 2018/6/30 17:15:00

定义网格后不调整右缩进, 不对齐到网格

页 63: [608] 带格式的 User 2018/6/30 17:02:00

无下划线, 字体颜色: 自动设置

页 63: [608] 带格式的 User 2018/6/30 17:02:00

无下划线, 字体颜色: 自动设置

页 63: [609] 带格式的 User 2018/6/30 17:02:00

无下划线, 字体颜色: 自动设置

页 63: [609] 带格式的 User 2018/6/30 17:02:00

无下划线, 字体颜色: 自动设置

页 63: [610] 带格式的 User 2018/6/30 17:02:00

无下划线, 字体颜色: 自动设置

页 63: [610] 带格式的 User 2018/6/30 17:02:00

无下划线, 字体颜色: 自动设置

页 63: [611] 带格式的 User 2018/6/30 17:02:00

无下划线, 字体颜色: 自动设置

页 63: [611] 带格式的 User 2018/6/30 17:02:00

无下划线, 字体颜色: 自动设置

页 63: [612] 带格式的 User 2018/6/30 17:02:00

无下划线, 字体颜色: 自动设置

页 63: [612] 带格式的 User 2018/6/30 17:02:00

无下划线, 字体颜色: 自动设置

页 63: [613] 带格式的 User 2018/6/30 17:02:00

无下划线, 字体颜色: 自动设置

页 63: [613] 带格式的 User 2018/6/30 17:02:00

无下划线, 字体颜色: 自动设置

页 63: [614] 带格式的 User 2018/6/30 17:02:00

无下划线, 字体颜色: 自动设置

页 63: [614] 带格式的 User 2018/6/30 17:02:00

无下划线, 字体颜色: 自动设置

页 63: [615] 带格式的 User 2018/6/30 17:02:00

无下划线, 字体颜色: 自动设置

页 63: [615] 带格式的 User 2018/6/30 17:02:00

无下划线, 字体颜色: 自动设置

页 63: [616] 带格式的 User 2018/6/30 17:02:00

无下划线, 字体颜色: 自动设置

页 63: [616] 带格式的 User 2018/6/30 17:02:00

无下划线, 字体颜色: 自动设置

页 63: [617] 带格式的 User 2018/6/30 17:02:00

无下划线, 字体颜色: 自动设置

页 63: [617] 带格式的 User 2018/6/30 17:02:00

无下划线, 字体颜色: 自动设置

页 63: [618] 带格式的 User 2018/6/30 17:02:00

无下划线, 字体颜色: 自动设置

页 63: [618] 带格式的 User 2018/6/30 17:02:00

无下划线, 字体颜色: 自动设置

页 63: [619] 带格式的 User 2018/6/30 17:02:00

无下划线, 字体颜色: 自动设置

页 63: [619] 带格式的 User 2018/6/30 17:02:00

无下划线, 字体颜色: 自动设置

页 63: [620] 带格式的 User 2018/6/30 17:02:00

无下划线, 字体颜色: 自动设置

页 63: [620] 带格式的 User 2018/6/30 17:02:00

无下划线, 字体颜色: 自动设置

页 63: [621] 带格式的 User 2018/6/30 17:02:00

无下划线, 字体颜色: 自动设置

页 63: [622] 带格式的 User 2018/6/30 17:15:00

定义网格后不调整右缩进, 不对齐到网格

页 63: [623] 带格式的 User 2018/6/30 17:02:00

无下划线, 字体颜色: 自动设置

页 63: [623] 带格式的 User 2018/6/30 17:02:00

无下划线, 字体颜色: 自动设置

页 63: [624] 带格式的 User 2018/6/30 17:02:00

无下划线, 字体颜色: 自动设置

页 63: [624] 带格式的 User 2018/6/30 17:02:00

无下划线, 字体颜色: 自动设置

页 63: [625] 带格式的 User 2018/6/30 17:02:00

无下划线, 字体颜色: 自动设置

页 63: [625] 带格式的 User 2018/6/30 17:02:00

无下划线, 字体颜色: 自动设置

页 63: [626] 带格式的 User 2018/6/30 17:02:00

无下划线, 字体颜色: 自动设置

页 63: [626] 带格式的 User 2018/6/30 17:02:00

无下划线, 字体颜色: 自动设置

页 63: [627] 带格式的 User 2018/6/30 17:02:00

无下划线, 字体颜色: 自动设置

页 63: [627] 带格式的 User 2018/6/30 17:02:00

无下划线, 字体颜色: 自动设置

页 63: [628] 带格式的 User 2018/6/30 17:02:00

无下划线, 字体颜色: 自动设置

页 63: [628] 带格式的 User 2018/6/30 17:02:00

无下划线, 字体颜色: 自动设置

页 63: [629] 带格式的 User 2018/6/30 17:02:00

无下划线, 字体颜色: 自动设置

页 63: [629] 带格式的 User 2018/6/30 17:02:00

无下划线, 字体颜色: 自动设置

页 63: [630] 带格式的 User 2018/6/30 17:02:00

无下划线, 字体颜色: 自动设置

页 63: [630] 带格式的 User 2018/6/30 17:02:00

无下划线, 字体颜色: 自动设置

页 63: [631] 带格式的 User 2018/6/30 17:02:00

无下划线, 字体颜色: 自动设置

页 63: [631] 带格式的 User 2018/6/30 17:02:00

无下划线, 字体颜色: 自动设置

页 63: [632] 带格式的 User 2018/6/30 17:02:00

无下划线, 字体颜色: 自动设置

页 63: [632] 带格式的 User 2018/6/30 17:02:00

无下划线, 字体颜色: 自动设置

页 63: [633] 带格式的 User 2018/6/30 17:02:00

无下划线, 字体颜色: 自动设置

页 63: [633] 带格式的 User 2018/6/30 17:02:00

无下划线, 字体颜色: 自动设置

页 63: [634] 带格式的 User 2018/6/30 17:02:00

无下划线, 字体颜色: 自动设置

页 63: [634] 带格式的 User 2018/6/30 17:02:00

无下划线, 字体颜色: 自动设置

页 63: [635] 带格式的 User 2018/6/30 17:02:00

无下划线, 字体颜色: 自动设置

页 63: [635] 带格式的 User 2018/6/30 17:02:00

无下划线, 字体颜色: 自动设置

页 63: [636] 带格式的 User 2018/6/30 17:02:00

无下划线, 字体颜色: 自动设置

页 63: [637] 带格式的 User 2018/6/30 17:15:00

定义网格后不调整右缩进, 不对齐到网格

页 63: [638] 带格式的 User 2018/6/30 17:02:00

无下划线, 字体颜色: 自动设置

页 63: [638] 带格式的 User 2018/6/30 17:02:00

无下划线, 字体颜色: 自动设置

页 63: [639] 带格式的 User 2018/6/30 17:02:00

无下划线, 字体颜色: 自动设置

页 63: [639] 带格式的 User 2018/6/30 17:02:00

无下划线, 字体颜色: 自动设置

页 63: [640] 带格式的 User 2018/6/30 17:02:00

无下划线, 字体颜色: 自动设置

页 63: [640] 带格式的 User 2018/6/30 17:02:00

无下划线, 字体颜色: 自动设置

页 63: [641] 带格式的 User 2018/6/30 17:02:00

无下划线, 字体颜色: 自动设置

页 63: [641] 带格式的 User 2018/6/30 17:02:00

无下划线, 字体颜色: 自动设置

页 63: [642] 带格式的 User 2018/6/30 17:02:00

无下划线, 字体颜色: 自动设置

页 63: [642] 带格式的 User 2018/6/30 17:02:00

无下划线, 字体颜色: 自动设置

页 63: [643] 带格式的 User 2018/6/30 17:02:00

无下划线, 字体颜色: 自动设置

页 63: [643] 带格式的 User 2018/6/30 17:02:00

无下划线, 字体颜色: 自动设置

页 63: [644] 带格式的 User 2018/6/30 17:02:00

无下划线, 字体颜色: 自动设置

页 63: [644] 带格式的 User 2018/6/30 17:02:00

无下划线, 字体颜色: 自动设置

页 63: [645] 带格式的 User 2018/6/30 17:02:00

无下划线, 字体颜色: 自动设置

页 63: [645] 带格式的 User 2018/6/30 17:02:00

无下划线, 字体颜色: 自动设置

页 63: [646] 带格式的 User 2018/6/30 17:02:00

无下划线, 字体颜色: 自动设置

页 63: [646] 带格式的 User 2018/6/30 17:02:00

无下划线, 字体颜色: 自动设置

页 63: [647] 带格式的 User 2018/6/30 17:02:00

无下划线, 字体颜色: 自动设置

页 63: [647] 带格式的 User 2018/6/30 17:02:00

无下划线, 字体颜色: 自动设置

页 63: [648] 带格式的 User 2018/6/30 17:02:00

无下划线, 字体颜色: 自动设置

页 63: [648] 带格式的 User 2018/6/30 17:02:00

无下划线, 字体颜色: 自动设置

页 63: [649] 带格式的 User 2018/6/30 17:02:00

无下划线, 字体颜色: 自动设置

页 63: [649] 带格式的 User 2018/6/30 17:02:00

无下划线, 字体颜色: 自动设置

页 63: [650] 带格式的 User 2018/6/30 17:02:00

无下划线, 字体颜色: 自动设置

页 63: [650] 带格式的 User 2018/6/30 17:02:00

无下划线, 字体颜色: 自动设置

页 63: [651] 带格式的 User 2018/6/30 17:02:00

无下划线, 字体颜色: 自动设置

页 63: [652] 带格式的 User 2018/6/30 17:15:00

定义网格后不调整右缩进, 不对齐到网格

页 63: [653] 带格式的 User 2018/6/30 17:02:00

无下划线, 字体颜色: 自动设置

页 63: [653] 带格式的 User 2018/6/30 17:02:00

无下划线, 字体颜色: 自动设置

页 63: [654] 带格式的 User 2018/6/30 17:02:00

无下划线, 字体颜色: 自动设置

页 63: [654] 带格式的 User 2018/6/30 17:02:00

无下划线, 字体颜色: 自动设置

页 63: [655] 带格式的 User 2018/6/30 17:02:00

无下划线, 字体颜色: 自动设置

页 63: [655] 带格式的 User 2018/6/30 17:02:00

无下划线, 字体颜色: 自动设置

页 63: [656] 带格式的 User 2018/6/30 17:02:00

无下划线, 字体颜色: 自动设置

页 63: [656] 带格式的 User 2018/6/30 17:02:00

无下划线, 字体颜色: 自动设置

页 63: [657] 带格式的 User 2018/6/30 17:02:00

无下划线, 字体颜色: 自动设置

页 63: [657] 带格式的 User 2018/6/30 17:02:00

无下划线, 字体颜色: 自动设置

页 63: [658] 带格式的 User 2018/6/30 17:02:00

无下划线, 字体颜色: 自动设置

页 63: [658] 带格式的 User 2018/6/30 17:02:00

无下划线, 字体颜色: 自动设置

页 63: [659] 带格式的 User 2018/6/30 17:02:00

无下划线, 字体颜色: 自动设置

页 63: [659] 带格式的 User 2018/6/30 17:02:00

无下划线, 字体颜色: 自动设置

页 63: [660] 带格式的 User 2018/6/30 17:02:00

无下划线, 字体颜色: 自动设置

页 63: [660] 带格式的 User 2018/6/30 17:02:00

无下划线, 字体颜色: 自动设置

页 63: [661] 带格式的 User 2018/6/30 17:02:00

无下划线, 字体颜色: 自动设置

页 63: [661] 带格式的 User 2018/6/30 17:02:00

无下划线, 字体颜色: 自动设置

页 63: [662] 带格式的 User 2018/6/30 17:02:00

无下划线, 字体颜色: 自动设置

页 63: [662] 带格式的 User 2018/6/30 17:02:00

无下划线, 字体颜色: 自动设置

页 63: [663] 带格式的 User 2018/6/30 17:02:00

无下划线, 字体颜色: 自动设置

页 63: [663] 带格式的 User 2018/6/30 17:02:00

无下划线, 字体颜色: 自动设置

页 63: [664] 带格式的 User 2018/6/30 17:02:00

无下划线, 字体颜色: 自动设置

页 63: [664] 带格式的 User 2018/6/30 17:02:00

无下划线, 字体颜色: 自动设置

页 63: [665] 带格式的 User 2018/6/30 17:02:00

无下划线, 字体颜色: 自动设置

页 63: [665] 带格式的 User 2018/6/30 17:02:00

无下划线, 字体颜色: 自动设置

页 63: [666] 带格式的 User 2018/6/30 17:02:00

无下划线, 字体颜色: 自动设置

页 63: [667] 带格式的 User 2018/6/30 17:15:00

定义网格后不调整右缩进, 不对齐到网格

页 63: [668] 带格式的 User 2018/6/30 17:02:00

无下划线, 字体颜色: 自动设置

页 63: [668] 带格式的 User 2018/6/30 17:02:00

无下划线, 字体颜色: 自动设置

页 63: [669] 带格式的 User 2018/6/30 17:02:00

无下划线, 字体颜色: 自动设置

页 63: [669] 带格式的 User 2018/6/30 17:02:00

无下划线, 字体颜色: 自动设置

页 63: [670] 带格式的 User 2018/6/30 17:02:00

无下划线, 字体颜色: 自动设置

页 63: [670] 带格式的 User 2018/6/30 17:02:00

无下划线, 字体颜色: 自动设置

页 63: [671] 带格式的 User 2018/6/30 17:02:00

无下划线, 字体颜色: 自动设置

页 63: [671] 带格式的 User 2018/6/30 17:02:00

无下划线, 字体颜色: 自动设置

页 63: [672] 带格式的 User 2018/6/30 17:02:00

无下划线, 字体颜色: 自动设置

页 63: [672] 带格式的 User 2018/6/30 17:02:00

无下划线, 字体颜色: 自动设置

页 63: [673] 带格式的 User 2018/6/30 17:02:00

无下划线, 字体颜色: 自动设置

页 63: [673] 带格式的 User 2018/6/30 17:02:00

无下划线, 字体颜色: 自动设置

页 63: [674] 带格式的 User 2018/6/30 17:02:00

无下划线, 字体颜色: 自动设置

页 63: [674] 带格式的 User 2018/6/30 17:02:00

无下划线, 字体颜色: 自动设置

页 63: [675] 带格式的 User 2018/6/30 17:02:00

无下划线, 字体颜色: 自动设置

页 63: [675] 带格式的 User 2018/6/30 17:02:00

无下划线, 字体颜色: 自动设置

页 63: [676] 带格式的 User 2018/6/30 17:02:00

无下划线, 字体颜色: 自动设置

页 63: [676] 带格式的 User 2018/6/30 17:02:00

无下划线, 字体颜色: 自动设置

页 63: [677] 带格式的 User 2018/6/30 17:02:00

无下划线, 字体颜色: 自动设置

页 63: [677] 带格式的 User 2018/6/30 17:02:00

无下划线, 字体颜色: 自动设置

页 63: [678] 带格式的 User 2018/6/30 17:02:00

无下划线, 字体颜色: 自动设置

页 63: [678] 带格式的 User 2018/6/30 17:02:00

无下划线, 字体颜色: 自动设置

页 63: [679] 带格式的 User 2018/6/30 17:02:00

无下划线, 字体颜色: 自动设置

页 63: [679] 带格式的 User 2018/6/30 17:02:00

无下划线, 字体颜色: 自动设置

页 63: [680] 带格式的 User 2018/6/30 17:02:00

无下划线, 字体颜色: 自动设置

页 63: [680] 带格式的 User 2018/6/30 17:02:00

无下划线, 字体颜色: 自动设置

页 63: [681] 带格式的 User 2018/6/30 17:02:00

无下划线, 字体颜色: 自动设置

页 63: [682] 带格式的 User 2018/6/30 17:15:00

定义网格后不调整右缩进, 不对齐到网格

页 63: [683] 带格式的 User 2018/6/30 17:02:00

无下划线, 字体颜色: 自动设置

页 63: [683] 带格式的 User 2018/6/30 17:02:00

无下划线, 字体颜色: 自动设置

页 63: [684] 带格式的 User 2018/6/30 17:02:00

无下划线, 字体颜色: 自动设置

页 63: [684] 带格式的 User 2018/6/30 17:02:00

无下划线, 字体颜色: 自动设置

页 63: [685] 带格式的 User 2018/6/30 17:02:00

无下划线, 字体颜色: 自动设置

页 63: [685] 带格式的 User 2018/6/30 17:02:00

无下划线, 字体颜色: 自动设置

页 63: [686] 带格式的 User 2018/6/30 17:02:00

无下划线, 字体颜色: 自动设置

页 63: [686] 带格式的 User 2018/6/30 17:02:00

无下划线, 字体颜色: 自动设置

页 63: [687] 带格式的 User 2018/6/30 17:02:00

无下划线, 字体颜色: 自动设置

页 63: [687] 带格式的 User 2018/6/30 17:02:00

无下划线, 字体颜色: 自动设置

页 63: [688] 带格式的 User 2018/6/30 17:02:00

无下划线, 字体颜色: 自动设置

页 63: [688] 带格式的 User 2018/6/30 17:02:00

无下划线, 字体颜色: 自动设置

页 63: [689] 带格式的 User 2018/6/30 17:02:00

无下划线, 字体颜色: 自动设置

页 63: [689] 带格式的 User 2018/6/30 17:02:00

无下划线, 字体颜色: 自动设置

页 63: [690] 带格式的 User 2018/6/30 17:02:00

无下划线, 字体颜色: 自动设置

页 63: [690] 带格式的 User 2018/6/30 17:02:00

无下划线, 字体颜色: 自动设置

页 63: [691] 带格式的 User 2018/6/30 17:02:00

无下划线, 字体颜色: 自动设置

页 63: [691] 带格式的 User 2018/6/30 17:02:00

无下划线, 字体颜色: 自动设置

页 63: [692] 带格式的 User 2018/6/30 17:02:00

无下划线, 字体颜色: 自动设置

页 63: [692] 带格式的 User 2018/6/30 17:02:00

无下划线, 字体颜色: 自动设置

页 63: [693] 带格式的 User 2018/6/30 17:02:00

无下划线, 字体颜色: 自动设置

页 63: [693] 带格式的 User 2018/6/30 17:02:00

无下划线, 字体颜色: 自动设置

页 63: [694] 带格式的 User 2018/6/30 17:02:00

无下划线, 字体颜色: 自动设置

页 63: [694] 带格式的 User 2018/6/30 17:02:00

无下划线, 字体颜色: 自动设置

页 63: [695] 带格式的 User 2018/6/30 17:02:00

无下划线, 字体颜色: 自动设置

页 63: [695] 带格式的 User 2018/6/30 17:02:00

无下划线, 字体颜色: 自动设置

页 63: [696] 带格式的 User 2018/6/30 17:02:00

无下划线, 字体颜色: 自动设置

页 63: [697] 带格式的 User 2018/6/30 17:15:00

定义网格后不调整右缩进, 不对齐到网格

页 63: [698] 带格式的 User 2018/6/30 17:02:00

无下划线, 字体颜色: 自动设置

页 63: [698] 带格式的 User 2018/6/30 17:02:00

无下划线, 字体颜色: 自动设置

页 63: [699] 带格式的 User 2018/6/30 17:02:00

无下划线, 字体颜色: 自动设置

页 63: [699] 带格式的 User 2018/6/30 17:02:00

无下划线, 字体颜色: 自动设置

页 63: [700] 带格式的 User 2018/6/30 17:02:00

无下划线, 字体颜色: 自动设置

页 63: [700] 带格式的 User 2018/6/30 17:02:00

无下划线, 字体颜色: 自动设置

页 63: [701] 带格式的 User 2018/6/30 17:02:00

无下划线, 字体颜色: 自动设置

页 63: [701] 带格式的 User 2018/6/30 17:02:00

无下划线, 字体颜色: 自动设置

页 63: [702] 带格式的 User 2018/6/30 17:02:00

无下划线, 字体颜色: 自动设置

页 63: [702] 带格式的 User 2018/6/30 17:02:00

无下划线, 字体颜色: 自动设置

页 63: [703] 带格式的 User 2018/6/30 17:02:00

无下划线, 字体颜色: 自动设置

页 63: [703] 带格式的 User 2018/6/30 17:02:00

无下划线, 字体颜色: 自动设置

页 63: [704] 带格式的 User 2018/6/30 17:02:00

无下划线, 字体颜色: 自动设置

页 63: [704] 带格式的 User 2018/6/30 17:02:00

无下划线, 字体颜色: 自动设置

页 63: [705] 带格式的 User 2018/6/30 17:02:00

无下划线, 字体颜色: 自动设置

页 63: [705] 带格式的 User 2018/6/30 17:02:00

无下划线, 字体颜色: 自动设置

页 63: [706] 带格式的 User 2018/6/30 17:02:00

无下划线, 字体颜色: 自动设置

页 63: [706] 带格式的 User 2018/6/30 17:02:00

无下划线, 字体颜色: 自动设置

页 63: [707] 带格式的 User 2018/6/30 17:02:00

无下划线, 字体颜色: 自动设置

页 63: [707] 带格式的 User 2018/6/30 17:02:00

无下划线, 字体颜色: 自动设置

页 63: [708] 带格式的 User 2018/6/30 17:02:00

无下划线, 字体颜色: 自动设置

页 63: [708] 带格式的 User 2018/6/30 17:02:00

无下划线, 字体颜色: 自动设置

页 63: [709] 带格式的 User 2018/6/30 17:02:00

无下划线, 字体颜色: 自动设置

页 63: [709] 带格式的 User 2018/6/30 17:02:00

无下划线, 字体颜色: 自动设置

页 63: [710] 带格式的 User 2018/6/30 17:02:00

无下划线, 字体颜色: 自动设置

页 63: [710] 带格式的 User 2018/6/30 17:02:00

无下划线, 字体颜色: 自动设置

页 63: [711] 带格式的 User 2018/6/30 17:02:00

无下划线, 字体颜色: 自动设置

页 63: [712] 带格式的 User 2018/6/30 17:15:00

定义网格后不调整右缩进, 不对齐到网格

页 63: [713] 带格式的 User 2018/6/30 17:02:00

无下划线, 字体颜色: 自动设置

页 63: [713] 带格式的 User 2018/6/30 17:02:00

无下划线, 字体颜色: 自动设置

页 63: [714] 带格式的 User 2018/6/30 17:02:00

无下划线, 字体颜色: 自动设置

页 63: [714] 带格式的 User 2018/6/30 17:02:00

无下划线, 字体颜色: 自动设置

页 63: [715] 带格式的 User 2018/6/30 17:02:00

无下划线, 字体颜色: 自动设置

页 63: [715] 带格式的 User 2018/6/30 17:02:00

无下划线, 字体颜色: 自动设置

页 63: [716] 带格式的 User 2018/6/30 17:02:00

无下划线, 字体颜色: 自动设置

页 63: [716] 带格式的 User 2018/6/30 17:02:00

无下划线, 字体颜色: 自动设置

页 63: [717] 带格式的 User 2018/6/30 17:02:00

无下划线, 字体颜色: 自动设置

页 63: [717] 带格式的 User 2018/6/30 17:02:00

无下划线, 字体颜色: 自动设置

页 63: [718] 带格式的 User 2018/6/30 17:02:00

无下划线, 字体颜色: 自动设置

页 63: [718] 带格式的 User 2018/6/30 17:02:00

无下划线, 字体颜色: 自动设置

页 63: [719] 带格式的 User 2018/6/30 17:02:00

无下划线, 字体颜色: 自动设置

页 63: [719] 带格式的 User 2018/6/30 17:02:00

无下划线, 字体颜色: 自动设置

页 63: [720] 带格式的 User 2018/6/30 17:02:00

无下划线, 字体颜色: 自动设置

页 63: [720] 带格式的 User 2018/6/30 17:02:00

无下划线, 字体颜色: 自动设置

页 63: [721] 带格式的 User 2018/6/30 17:02:00

无下划线, 字体颜色: 自动设置

页 63: [721] 带格式的 User 2018/6/30 17:02:00

无下划线, 字体颜色: 自动设置

页 63: [722] 带格式的 User 2018/6/30 17:02:00

无下划线, 字体颜色: 自动设置

页 63: [722] 带格式的 User 2018/6/30 17:02:00

无下划线, 字体颜色: 自动设置

页 63: [723] 带格式的 User 2018/6/30 17:02:00

无下划线, 字体颜色: 自动设置

页 63: [723] 带格式的 User 2018/6/30 17:02:00

无下划线, 字体颜色: 自动设置

页 63: [724] 带格式的 User 2018/6/30 17:02:00

无下划线, 字体颜色: 自动设置

页 63: [724] 带格式的 User 2018/6/30 17:02:00

无下划线, 字体颜色: 自动设置

页 63: [725] 带格式的 User 2018/6/30 17:02:00

无下划线, 字体颜色: 自动设置

页 63: [725] 带格式的 User 2018/6/30 17:02:00

无下划线, 字体颜色: 自动设置

页 63: [726] 带格式的 User 2018/6/30 17:02:00

无下划线, 字体颜色: 自动设置

页 63: [727] 带格式的 User 2018/6/30 17:15:00

定义网格后不调整右缩进, 不对齐到网格

页 63: [728] 带格式的 User 2018/6/30 17:02:00

无下划线, 字体颜色: 自动设置

页 63: [728] 带格式的 User 2018/6/30 17:02:00

无下划线, 字体颜色: 自动设置

页 63: [729] 带格式的 User 2018/6/30 17:02:00

无下划线, 字体颜色: 自动设置

页 63: [729] 带格式的 User 2018/6/30 17:02:00

无下划线, 字体颜色: 自动设置

页 63: [730] 带格式的 User 2018/6/30 17:02:00

无下划线, 字体颜色: 自动设置

页 63: [730] 带格式的 User 2018/6/30 17:02:00

无下划线, 字体颜色: 自动设置

页 63: [731] 带格式的 User 2018/6/30 17:02:00

无下划线, 字体颜色: 自动设置

页 63: [731] 带格式的 User 2018/6/30 17:02:00

无下划线, 字体颜色: 自动设置

页 63: [732] 带格式的 User 2018/6/30 17:02:00

无下划线, 字体颜色: 自动设置

页 63: [732] 带格式的 User 2018/6/30 17:02:00

无下划线, 字体颜色: 自动设置

页 63: [733] 带格式的 User 2018/6/30 17:02:00

无下划线, 字体颜色: 自动设置

页 63: [733] 带格式的 User 2018/6/30 17:02:00

无下划线, 字体颜色: 自动设置

页 63: [734] 带格式的 User 2018/6/30 17:02:00

无下划线, 字体颜色: 自动设置

页 63: [734] 带格式的 User 2018/6/30 17:02:00

无下划线, 字体颜色: 自动设置

页 63: [735] 带格式的 User 2018/6/30 17:02:00

无下划线, 字体颜色: 自动设置

页 63: [735] 带格式的 User 2018/6/30 17:02:00

无下划线, 字体颜色: 自动设置

页 63: [736] 带格式的 User 2018/6/30 17:02:00

无下划线, 字体颜色: 自动设置

页 63: [736] 带格式的 User 2018/6/30 17:02:00

无下划线, 字体颜色: 自动设置

页 63: [737] 带格式的 User 2018/6/30 17:02:00

无下划线, 字体颜色: 自动设置

页 63: [737] 带格式的 User 2018/6/30 17:02:00

无下划线, 字体颜色: 自动设置

页 63: [738] 带格式的 User 2018/6/30 17:02:00

无下划线, 字体颜色: 自动设置

页 63: [738] 带格式的 User 2018/6/30 17:02:00

无下划线, 字体颜色: 自动设置

页 63: [739] 带格式的 User 2018/6/30 17:02:00

无下划线, 字体颜色: 自动设置

页 63: [739] 带格式的 User 2018/6/30 17:02:00

无下划线, 字体颜色: 自动设置

页 63: [740] 带格式的 User 2018/6/30 17:02:00

无下划线, 字体颜色: 自动设置

页 63: [740] 带格式的 User 2018/6/30 17:02:00

无下划线, 字体颜色: 自动设置

页 63: [741] 带格式的 User 2018/6/30 17:02:00

无下划线, 字体颜色: 自动设置

页 63: [742] 带格式的 User 2018/6/30 17:15:00

定义网格后不调整右缩进, 不对齐到网格

页 63: [743] 带格式的 User 2018/6/30 17:02:00

无下划线, 字体颜色: 自动设置

页 63: [743] 带格式的 User 2018/6/30 17:02:00

无下划线, 字体颜色: 自动设置

页 63: [744] 带格式的 User 2018/6/30 17:02:00

无下划线, 字体颜色: 自动设置

页 63: [744] 带格式的 User 2018/6/30 17:02:00

无下划线, 字体颜色: 自动设置

页 63: [745] 带格式的 User 2018/6/30 17:02:00

无下划线, 字体颜色: 自动设置

页 63: [745] 带格式的 User 2018/6/30 17:02:00

无下划线, 字体颜色: 自动设置

页 63: [746] 带格式的 User 2018/6/30 17:02:00

无下划线, 字体颜色: 自动设置

页 63: [746] 带格式的 User 2018/6/30 17:02:00

无下划线, 字体颜色: 自动设置

页 63: [747] 带格式的 User 2018/6/30 17:02:00

无下划线, 字体颜色: 自动设置

页 63: [747] 带格式的 User 2018/6/30 17:02:00

无下划线, 字体颜色: 自动设置

页 63: [748] 带格式的 User 2018/6/30 17:02:00

无下划线, 字体颜色: 自动设置

页 63: [748] 带格式的 User 2018/6/30 17:02:00

无下划线, 字体颜色: 自动设置

页 63: [749] 带格式的 User 2018/6/30 17:02:00

无下划线, 字体颜色: 自动设置

页 63: [749] 带格式的 User 2018/6/30 17:02:00

无下划线, 字体颜色: 自动设置

页 63: [750] 带格式的 User 2018/6/30 17:02:00

无下划线, 字体颜色: 自动设置

页 63: [750] 带格式的 User 2018/6/30 17:02:00

无下划线, 字体颜色: 自动设置

页 63: [751] 带格式的 User 2018/6/30 17:02:00

无下划线, 字体颜色: 自动设置

页 63: [751] 带格式的 User 2018/6/30 17:02:00

无下划线, 字体颜色: 自动设置

页 63: [752] 带格式的 User 2018/6/30 17:02:00

无下划线, 字体颜色: 自动设置

页 63: [752] 带格式的 User 2018/6/30 17:02:00

无下划线, 字体颜色: 自动设置

页 63: [753] 带格式的 User 2018/6/30 17:02:00

无下划线, 字体颜色: 自动设置

页 63: [753] 带格式的 User 2018/6/30 17:02:00

无下划线, 字体颜色: 自动设置

页 63: [754] 带格式的 User 2018/6/30 17:02:00

无下划线, 字体颜色: 自动设置

页 63: [754] 带格式的 User 2018/6/30 17:02:00

无下划线, 字体颜色: 自动设置

页 63: [755] 带格式的 User 2018/6/30 17:02:00

无下划线, 字体颜色: 自动设置

页 63: [755] 带格式的 User 2018/6/30 17:02:00

无下划线, 字体颜色: 自动设置

页 63: [756] 带格式的 User 2018/6/30 17:02:00

无下划线, 字体颜色: 自动设置

页 63: [757] 带格式的 User 2018/6/30 17:15:00

定义网格后不调整右缩进, 不对齐到网格

页 63: [758] 带格式的 User 2018/6/30 17:02:00

无下划线, 字体颜色: 自动设置

页 63: [758] 带格式的 User 2018/6/30 17:02:00

无下划线, 字体颜色: 自动设置

页 63: [759] 带格式的 User 2018/6/30 17:02:00

无下划线, 字体颜色: 自动设置

页 63: [759] 带格式的 User 2018/6/30 17:02:00

无下划线, 字体颜色: 自动设置

页 63: [760] 带格式的 User 2018/6/30 17:02:00

无下划线, 字体颜色: 自动设置

页 63: [760] 带格式的 User 2018/6/30 17:02:00

无下划线, 字体颜色: 自动设置

页 63: [761] 带格式的 User 2018/6/30 17:02:00

无下划线, 字体颜色: 自动设置

页 63: [761] 带格式的 User 2018/6/30 17:02:00

无下划线, 字体颜色: 自动设置

页 63: [762] 带格式的 User 2018/6/30 17:02:00

无下划线, 字体颜色: 自动设置

页 63: [762] 带格式的 User 2018/6/30 17:02:00

无下划线, 字体颜色: 自动设置

页 63: [763] 带格式的 User 2018/6/30 17:02:00

无下划线, 字体颜色: 自动设置

页 63: [763] 带格式的 User 2018/6/30 17:02:00

无下划线, 字体颜色: 自动设置

页 63: [764] 带格式的 User 2018/6/30 17:02:00

无下划线, 字体颜色: 自动设置

页 63: [764] 带格式的 User 2018/6/30 17:02:00

无下划线, 字体颜色: 自动设置

页 63: [765] 带格式的 User 2018/6/30 17:02:00

无下划线, 字体颜色: 自动设置

页 63: [765] 带格式的 User 2018/6/30 17:02:00

无下划线, 字体颜色: 自动设置

页 63: [766] 带格式的 User 2018/6/30 17:02:00

无下划线, 字体颜色: 自动设置

页 63: [766] 带格式的 User 2018/6/30 17:02:00

无下划线, 字体颜色: 自动设置

页 63: [767] 带格式的 User 2018/6/30 17:02:00

无下划线, 字体颜色: 自动设置

页 63: [767] 带格式的 User 2018/6/30 17:02:00

无下划线, 字体颜色: 自动设置

页 63: [768] 带格式的 User 2018/6/30 17:02:00

无下划线, 字体颜色: 自动设置

页 63: [768] 带格式的 User 2018/6/30 17:02:00

无下划线, 字体颜色: 自动设置

页 63: [769] 带格式的 User 2018/6/30 17:02:00

无下划线, 字体颜色: 自动设置

页 63: [769] 带格式的 User 2018/6/30 17:02:00

无下划线, 字体颜色: 自动设置

页 63: [770] 带格式的 User 2018/6/30 17:02:00

无下划线, 字体颜色: 自动设置

页 63: [770] 带格式的 User 2018/6/30 17:02:00

无下划线, 字体颜色: 自动设置

页 63: [771] 带格式的 User 2018/6/30 17:02:00

无下划线, 字体颜色: 自动设置

页 63: [772] 带格式的 User 2018/6/30 17:15:00

定义网格后不调整右缩进, 不对齐到网格

页 63: [773] 带格式的 User 2018/6/30 17:02:00

无下划线, 字体颜色: 自动设置

页 63: [773] 带格式的 User 2018/6/30 17:02:00

无下划线, 字体颜色: 自动设置

页 63: [774] 带格式的 User 2018/6/30 17:02:00

无下划线, 字体颜色: 自动设置

页 63: [774] 带格式的 User 2018/6/30 17:02:00

无下划线, 字体颜色: 自动设置

页 63: [775] 带格式的 User 2018/6/30 17:02:00

无下划线, 字体颜色: 自动设置

页 63: [775] 带格式的 User 2018/6/30 17:02:00

无下划线, 字体颜色: 自动设置

页 63: [776] 带格式的 User 2018/6/30 17:02:00

无下划线, 字体颜色: 自动设置

页 63: [776] 带格式的 User 2018/6/30 17:02:00

无下划线, 字体颜色: 自动设置

页 63: [777] 带格式的 User 2018/6/30 17:02:00

无下划线, 字体颜色: 自动设置

页 63: [777] 带格式的 User 2018/6/30 17:02:00

无下划线, 字体颜色: 自动设置

页 63: [778] 带格式的 User 2018/6/30 17:02:00

无下划线, 字体颜色: 自动设置

页 63: [778] 带格式的 User 2018/6/30 17:02:00

无下划线, 字体颜色: 自动设置

页 63: [779] 带格式的 User 2018/6/30 17:02:00

无下划线, 字体颜色: 自动设置

页 63: [779] 带格式的 User 2018/6/30 17:02:00

无下划线, 字体颜色: 自动设置

页 63: [780] 带格式的 User 2018/6/30 17:02:00

无下划线, 字体颜色: 自动设置

页 63: [780] 带格式的 User 2018/6/30 17:02:00

无下划线, 字体颜色: 自动设置

页 63: [781] 带格式的 User 2018/6/30 17:02:00

无下划线, 字体颜色: 自动设置

页 63: [781] 带格式的 User 2018/6/30 17:02:00

无下划线, 字体颜色: 自动设置

页 63: [782] 带格式的 User 2018/6/30 17:02:00

无下划线, 字体颜色: 自动设置

页 63: [782] 带格式的 User 2018/6/30 17:02:00

无下划线, 字体颜色: 自动设置

页 63: [783] 带格式的 User 2018/6/30 17:02:00

无下划线, 字体颜色: 自动设置

页 63: [783] 带格式的 User 2018/6/30 17:02:00

无下划线, 字体颜色: 自动设置

页 63: [784] 带格式的 User 2018/6/30 17:02:00

无下划线, 字体颜色: 自动设置

页 63: [784] 带格式的 User 2018/6/30 17:02:00

无下划线, 字体颜色: 自动设置

页 63: [785] 带格式的 User 2018/6/30 17:02:00

无下划线, 字体颜色: 自动设置

页 63: [785] 带格式的 User 2018/6/30 17:02:00

无下划线, 字体颜色: 自动设置

页 63: [786] 带格式的 User 2018/6/30 17:02:00

无下划线, 字体颜色: 自动设置

页 63: [787] 带格式的 User 2018/6/30 17:15:00

定义网格后不调整右缩进, 不对齐到网格

页 63: [788] 带格式的 User 2018/6/30 17:02:00

无下划线, 字体颜色: 自动设置

页 63: [788] 带格式的 User 2018/6/30 17:02:00

无下划线, 字体颜色: 自动设置

页 63: [789] 带格式的 User 2018/6/30 17:02:00

无下划线, 字体颜色: 自动设置

页 63: [789] 带格式的 User 2018/6/30 17:02:00

无下划线, 字体颜色: 自动设置

页 63: [790] 带格式的 User 2018/6/30 17:02:00

无下划线, 字体颜色: 自动设置

页 63: [790] 带格式的 User 2018/6/30 17:02:00

无下划线, 字体颜色: 自动设置

页 63: [791] 带格式的 User 2018/6/30 17:02:00

无下划线, 字体颜色: 自动设置

页 63: [791] 带格式的 User 2018/6/30 17:02:00

无下划线, 字体颜色: 自动设置

页 63: [792] 带格式的 User 2018/6/30 17:02:00

无下划线, 字体颜色: 自动设置

页 63: [792] 带格式的 User 2018/6/30 17:02:00

无下划线, 字体颜色: 自动设置

页 63: [793] 带格式的 User 2018/6/30 17:02:00

无下划线, 字体颜色: 自动设置

页 63: [793] 带格式的 User 2018/6/30 17:02:00

无下划线, 字体颜色: 自动设置

页 63: [794] 带格式的 User 2018/6/30 17:02:00

无下划线, 字体颜色: 自动设置

页 63: [794] 带格式的 User 2018/6/30 17:02:00

无下划线, 字体颜色: 自动设置

页 63: [795] 带格式的 User 2018/6/30 17:02:00

无下划线, 字体颜色: 自动设置

页 63: [795] 带格式的 User 2018/6/30 17:02:00

无下划线, 字体颜色: 自动设置

页 63: [796] 带格式的 User 2018/6/30 17:02:00

无下划线, 字体颜色: 自动设置

页 63: [796] 带格式的 User 2018/6/30 17:02:00

无下划线, 字体颜色: 自动设置

页 63: [797] 带格式的 User 2018/6/30 17:02:00

无下划线, 字体颜色: 自动设置

页 63: [797] 带格式的 User 2018/6/30 17:02:00

无下划线, 字体颜色: 自动设置

页 63: [798] 带格式的 User 2018/6/30 17:02:00

无下划线, 字体颜色: 自动设置

页 63: [798] 带格式的 User 2018/6/30 17:02:00

无下划线, 字体颜色: 自动设置

页 63: [799] 带格式的 User 2018/6/30 17:02:00

无下划线, 字体颜色: 自动设置

页 63: [799] 带格式的 User 2018/6/30 17:02:00

无下划线, 字体颜色: 自动设置

页 63: [800] 带格式的 User 2018/6/30 17:02:00

无下划线, 字体颜色: 自动设置

页 63: [800] 带格式的 User 2018/6/30 17:02:00

无下划线, 字体颜色: 自动设置

页 64: [801] 带格式的 User 2018/6/30 17:02:00

无下划线, 字体颜色: 自动设置

页 64: [802] 带格式的 User 2018/6/30 17:02:00

无下划线, 字体颜色: 自动设置

页 64: [803] 带格式的 User 2018/6/30 17:15:00

定义网格后不调整右缩进, 不对齐到网格

页 64: [804] 带格式的 User 2018/6/30 17:02:00

无下划线, 字体颜色: 自动设置

页 64: [804] 带格式的 User 2018/6/30 17:02:00

无下划线, 字体颜色: 自动设置

页 64: [805] 带格式的 User 2018/6/30 17:02:00

无下划线, 字体颜色: 自动设置

页 64: [805] 带格式的 User 2018/6/30 17:02:00

无下划线, 字体颜色: 自动设置

页 64: [806] 带格式的 User 2018/6/30 17:02:00

无下划线, 字体颜色: 自动设置

页 64: [806] 带格式的 User 2018/6/30 17:02:00

无下划线, 字体颜色: 自动设置

页 64: [807] 带格式的 User 2018/6/30 17:02:00

无下划线, 字体颜色: 自动设置

页 64: [807] 带格式的 User 2018/6/30 17:02:00

无下划线, 字体颜色: 自动设置

页 64: [808] 带格式的 User 2018/6/30 17:02:00

无下划线, 字体颜色: 自动设置

页 64: [808] 带格式的 User 2018/6/30 17:02:00

无下划线, 字体颜色: 自动设置

页 64: [809] 带格式的 User 2018/6/30 17:02:00

无下划线, 字体颜色: 自动设置

页 64: [809] 带格式的 User 2018/6/30 17:02:00

无下划线, 字体颜色: 自动设置

页 64: [810] 带格式的 User 2018/6/30 17:02:00

无下划线, 字体颜色: 自动设置

页 64: [810] 带格式的 User 2018/6/30 17:02:00

无下划线, 字体颜色: 自动设置

页 64: [811] 带格式的 User 2018/6/30 17:02:00

无下划线, 字体颜色: 自动设置

页 64: [811] 带格式的 User 2018/6/30 17:02:00

无下划线, 字体颜色: 自动设置

页 64: [812] 带格式的 User 2018/6/30 17:02:00

无下划线, 字体颜色: 自动设置

页 64: [813] 带格式的 User 2018/6/30 17:15:00

定义网格后不调整右缩进, 不对齐到网格

页 64: [814] 带格式的 User 2018/6/30 17:02:00

无下划线, 字体颜色: 自动设置

页 64: [815] 带格式的 User 2018/6/30 17:02:00

无下划线, 字体颜色: 自动设置

页 64: [816] 带格式的 User 2018/6/30 17:02:00

无下划线, 字体颜色: 自动设置

页 64: [817] 带格式的 User 2018/6/30 17:02:00

无下划线, 字体颜色: 自动设置

页 64: [818] 带格式的 User 2018/6/30 17:02:00

无下划线, 字体颜色: 自动设置

页 64: [819] 带格式的 User 2018/6/30 17:02:00

无下划线, 字体颜色: 自动设置

页 64: [820] 带格式的 User 2018/6/30 17:02:00

无下划线, 字体颜色: 自动设置

页 64: [821] 带格式的 User 2018/6/30 17:15:00

定义网格后不调整右缩进, 不对齐到网格

页 64: [822] 带格式的 User 2018/6/30 17:02:00

无下划线, 字体颜色: 自动设置

页 64: [823] 带格式的 User 2018/6/30 17:02:00

无下划线, 字体颜色: 自动设置

页 64: [824] 带格式的 User 2018/6/30 17:02:00

无下划线, 字体颜色: 自动设置

页 64: [825] 带格式的 User 2018/6/30 17:02:00

无下划线, 字体颜色: 自动设置

页 64: [826] 带格式的 User 2018/6/30 17:02:00

无下划线, 字体颜色: 自动设置

页 64: [827] 带格式的 User 2018/6/30 17:02:00

无下划线, 字体颜色: 自动设置

页 64: [828] 带格式的 User 2018/6/30 17:02:00

无下划线, 字体颜色: 自动设置

页 64: [829] 带格式的 User 2018/6/30 17:15:00

定义网格后不调整右缩进, 不对齐到网格

页 64: [830] 带格式的 User 2018/6/30 17:02:00

无下划线, 字体颜色: 自动设置

页 64: [831] 带格式的 User 2018/6/30 17:02:00

无下划线, 字体颜色: 自动设置

页 64: [832] 带格式的 User 2018/6/30 17:02:00

无下划线, 字体颜色: 自动设置

页 64: [833] 带格式的 User 2018/6/30 17:02:00

无下划线, 字体颜色: 自动设置

页 64: [834] 带格式的 User 2018/6/30 17:02:00

无下划线, 字体颜色: 自动设置

页 64: [835] 带格式的 User 2018/6/30 17:02:00

无下划线, 字体颜色: 自动设置

页 64: [836] 带格式的 User 2018/6/30 17:02:00

无下划线, 字体颜色: 自动设置

页 64: [837] 带格式的 User 2018/6/30 17:15:00

定义网格后不调整右缩进, 不对齐到网格

页 64: [838] 带格式的 User 2018/6/30 17:02:00

无下划线, 字体颜色: 自动设置

页 64: [839] 带格式的 User 2018/6/30 17:02:00

无下划线, 字体颜色: 自动设置

页 64: [840] 带格式的 User 2018/6/30 17:02:00

无下划线, 字体颜色: 自动设置

页 64: [841] 带格式的 User 2018/6/30 17:02:00

无下划线, 字体颜色: 自动设置

页 64: [842] 带格式的 User 2018/6/30 17:02:00

无下划线, 字体颜色: 自动设置

页 64: [843] 带格式的 User 2018/6/30 17:02:00

无下划线, 字体颜色: 自动设置

页 64: [844] 带格式的 User 2018/6/30 17:02:00

无下划线, 字体颜色: 自动设置

页 64: [845] 带格式的 User 2018/6/30 17:15:00

定义网格后不调整右缩进, 不对齐到网格

页 64: [846] 带格式的 User 2018/6/30 17:02:00

无下划线, 字体颜色: 自动设置

页 64: [847] 带格式的 User 2018/6/30 17:02:00

无下划线, 字体颜色: 自动设置

页 64: [848] 带格式的 User 2018/6/30 17:02:00

无下划线, 字体颜色: 自动设置

页 64: [849] 带格式的 User 2018/6/30 17:02:00

无下划线, 字体颜色: 自动设置

页 64: [850] 带格式的 User 2018/6/30 17:02:00

无下划线, 字体颜色: 自动设置

页 64: [851] 带格式的 User 2018/6/30 17:02:00

无下划线, 字体颜色: 自动设置

页 64: [852] 带格式的 User 2018/6/30 17:02:00

无下划线, 字体颜色: 自动设置

页 64: [853] 带格式的 User 2018/6/30 17:15:00

定义网格后不调整右缩进, 不对齐到网格

页 64: [854] 带格式的 User 2018/6/30 17:02:00

无下划线, 字体颜色: 自动设置

页 64: [855] 带格式的 User 2018/6/30 17:02:00

无下划线, 字体颜色: 自动设置

页 64: [856] 带格式的 User 2018/6/30 17:02:00

无下划线, 字体颜色: 自动设置

页 64: [857] 带格式的 User 2018/6/30 17:02:00

无下划线, 字体颜色: 自动设置

页 64: [858] 带格式的 User 2018/6/30 17:02:00

无下划线, 字体颜色: 自动设置

页 64: [859] 带格式的 User 2018/6/30 17:02:00

无下划线, 字体颜色: 自动设置

页 64: [860] 带格式的 User 2018/6/30 17:02:00

无下划线, 字体颜色: 自动设置

页 64: [861] 带格式的 User 2018/6/30 17:15:00

定义网格后不调整右缩进, 不对齐到网格

页 64: [862] 带格式的 User 2018/6/30 17:02:00

无下划线, 字体颜色: 自动设置

页 64: [863] 带格式的 User 2018/6/30 17:02:00

无下划线, 字体颜色: 自动设置

页 64: [864] 带格式的 User 2018/6/30 17:02:00

无下划线, 字体颜色: 自动设置

页 64: [865] 带格式的 User 2018/6/30 17:02:00

无下划线, 字体颜色: 自动设置

页 64: [866] 带格式的 User 2018/6/30 17:02:00

无下划线, 字体颜色: 自动设置

页 64: [867] 带格式的 User 2018/6/30 17:02:00

无下划线, 字体颜色: 自动设置

页 64: [868] 带格式的 User 2018/6/30 17:02:00

无下划线, 字体颜色: 自动设置

页 64: [869] 带格式的 User 2018/6/30 17:15:00

定义网格后不调整右缩进, 不对齐到网格

页 64: [870] 带格式的 User 2018/6/30 17:02:00

无下划线, 字体颜色: 自动设置

页 64: [871] 带格式的 User 2018/6/30 17:02:00

无下划线, 字体颜色: 自动设置

页 64: [872] 带格式的 User 2018/6/30 17:02:00

无下划线, 字体颜色: 自动设置

页 64: [873] 带格式的 User 2018/6/30 17:02:00

无下划线, 字体颜色: 自动设置

页 64: [874] 带格式的 User 2018/6/30 17:02:00

无下划线, 字体颜色: 自动设置

页 64: [875] 带格式的 User 2018/6/30 17:02:00

无下划线, 字体颜色: 自动设置

页 64: [876] 带格式的 User 2018/6/30 17:02:00

无下划线, 字体颜色: 自动设置

页 64: [877] 带格式的 User 2018/6/30 17:15:00

定义网格后不调整右缩进, 不对齐到网格

页 64: [878] 带格式的 User 2018/6/30 17:02:00

无下划线, 字体颜色: 自动设置

页 64: [879] 带格式的 User 2018/6/30 17:02:00

无下划线, 字体颜色: 自动设置

页 64: [880] 带格式的 User 2018/6/30 17:02:00

无下划线, 字体颜色: 自动设置

页 64: [881] 带格式的 User 2018/6/30 17:02:00

无下划线, 字体颜色: 自动设置

页 64: [882] 带格式的 User 2018/6/30 17:02:00

无下划线, 字体颜色: 自动设置

页 64: [883] 带格式的 User 2018/6/30 17:02:00

无下划线, 字体颜色: 自动设置

页 64: [884] 带格式的 User 2018/6/30 17:02:00

无下划线, 字体颜色: 自动设置

页 64: [885] 带格式的 User 2018/6/30 17:15:00

定义网格后不调整右缩进, 不对齐到网格

页 64: [886] 带格式的 User 2018/6/30 17:02:00

无下划线, 字体颜色: 自动设置

页 64: [887] 带格式的 User 2018/6/30 17:02:00

无下划线, 字体颜色: 自动设置

页 64: [888] 带格式的 User 2018/6/30 17:02:00

无下划线, 字体颜色: 自动设置

页 64: [889] 带格式的 User 2018/6/30 17:02:00

无下划线, 字体颜色: 自动设置

页 64: [890] 带格式的 User 2018/6/30 17:02:00

无下划线, 字体颜色: 自动设置

页 64: [891] 带格式的 User 2018/6/30 17:02:00

无下划线, 字体颜色: 自动设置

页 64: [892] 带格式的 User 2018/6/30 17:02:00

无下划线, 字体颜色: 自动设置

页 64: [893] 带格式的 User 2018/6/30 17:15:00

定义网格后不调整右缩进, 不对齐到网格

页 64: [894] 带格式的 User 2018/6/30 17:02:00

无下划线, 字体颜色: 自动设置

页 64: [895] 带格式的 User 2018/6/30 17:02:00

无下划线, 字体颜色: 自动设置

页 64: [896] 带格式的 User 2018/6/30 17:02:00

无下划线, 字体颜色: 自动设置

页 64: [897] 带格式的 User 2018/6/30 17:02:00

无下划线, 字体颜色: 自动设置

页 64: [898] 带格式的 User 2018/6/30 17:02:00

无下划线, 字体颜色: 自动设置

页 64: [899] 带格式的 User 2018/6/30 17:02:00

无下划线, 字体颜色: 自动设置

页 64: [900] 带格式的 User 2018/6/30 17:02:00

无下划线, 字体颜色: 自动设置

页 64: [901] 带格式的 User 2018/6/30 17:15:00

定义网格后不调整右缩进, 不对齐到网格

页 64: [902] 带格式的 User 2018/6/30 17:02:00

无下划线, 字体颜色: 自动设置

页 64: [903] 带格式的 User 2018/6/30 17:02:00

无下划线, 字体颜色: 自动设置

页 64: [904] 带格式的 User 2018/6/30 17:02:00

无下划线, 字体颜色: 自动设置

页 64: [905] 带格式的 User 2018/6/30 17:02:00

无下划线, 字体颜色: 自动设置

页 64: [906] 带格式的 User 2018/6/30 17:02:00

无下划线, 字体颜色: 自动设置

页 64: [907] 带格式的 User 2018/6/30 17:02:00

无下划线, 字体颜色: 自动设置

页 64: [908] 带格式的 User 2018/6/30 17:02:00

无下划线, 字体颜色: 自动设置

页 64: [909] 带格式的 User 2018/6/30 17:15:00

定义网格后不调整右缩进, 不对齐到网格

页 64: [910] 带格式的 User 2018/6/30 17:02:00

无下划线, 字体颜色: 自动设置

页 64: [911] 带格式的 User 2018/6/30 17:02:00

无下划线, 字体颜色: 自动设置

页 64: [912] 带格式的 User 2018/6/30 17:02:00

无下划线, 字体颜色: 自动设置

页 64: [913] 带格式的 User 2018/6/30 17:02:00

无下划线, 字体颜色: 自动设置

页 64: [914] 带格式的 User 2018/6/30 17:02:00

无下划线, 字体颜色: 自动设置

页 64: [915] 带格式的 User 2018/6/30 17:02:00

无下划线, 字体颜色: 自动设置

页 64: [916] 带格式的 User 2018/6/30 17:02:00

无下划线, 字体颜色: 自动设置

页 64: [917] 带格式的 User 2018/6/30 17:15:00

定义网格后不调整右缩进, 不对齐到网格

页 64: [918] 带格式的 User 2018/6/30 17:02:00

无下划线, 字体颜色: 自动设置

页 64: [919] 带格式的 User 2018/6/30 17:02:00

无下划线, 字体颜色: 自动设置

页 64: [920] 带格式的 User 2018/6/30 17:02:00

无下划线, 字体颜色: 自动设置

页 64: [921] 带格式的 User 2018/6/30 17:02:00

无下划线, 字体颜色: 自动设置

页 64: [922] 带格式的 User 2018/6/30 17:02:00

无下划线, 字体颜色: 自动设置

页 64: [923] 带格式的 User 2018/6/30 17:02:00

无下划线, 字体颜色: 自动设置

页 64: [924] 带格式的 User 2018/6/30 17:02:00

无下划线, 字体颜色: 自动设置

页 64: [925] 带格式的 User 2018/6/30 17:15:00

定义网格后不调整右缩进, 不对齐到网格

页 64: [926] 带格式的 User 2018/6/30 17:02:00

无下划线, 字体颜色: 自动设置

页 64: [927] 带格式的 User 2018/6/30 17:02:00

无下划线, 字体颜色: 自动设置

页 64: [928] 带格式的 User 2018/6/30 17:02:00

无下划线, 字体颜色: 自动设置

页 64: [929] 带格式的 User 2018/6/30 17:02:00

无下划线, 字体颜色: 自动设置

页 64: [930] 带格式的 User 2018/6/30 17:02:00

无下划线, 字体颜色: 自动设置

页 64: [931] 带格式的 User 2018/6/30 17:02:00

无下划线, 字体颜色: 自动设置

页 64: [932] 带格式的 User 2018/6/30 17:02:00

无下划线, 字体颜色: 自动设置

页 64: [933] 带格式的 User 2018/6/30 17:15:00

定义网格后不调整右缩进, 不对齐到网格

页 64: [934] 带格式的 User 2018/6/30 17:02:00

无下划线, 字体颜色: 自动设置

页 64: [935] 带格式的 User 2018/6/30 17:02:00

无下划线, 字体颜色: 自动设置

页 64: [936] 带格式的 User 2018/6/30 17:02:00

无下划线, 字体颜色: 自动设置

页 64: [937] 带格式的 User 2018/6/30 17:02:00

无下划线, 字体颜色: 自动设置

页 64: [938] 带格式的 User 2018/6/30 17:02:00

无下划线, 字体颜色: 自动设置

页 64: [939] 带格式的 User 2018/6/30 17:02:00

无下划线, 字体颜色: 自动设置

页 64: [940] 带格式的 User 2018/6/30 17:02:00

无下划线, 字体颜色: 自动设置

页 64: [941] 带格式的 User 2018/6/30 17:15:00

定义网格后不调整右缩进, 不对齐到网格

页 64: [942] 带格式的 User 2018/6/30 17:02:00

无下划线, 字体颜色: 自动设置

页 64: [943] 带格式的 User 2018/6/30 17:02:00

无下划线, 字体颜色: 自动设置

页 64: [944] 带格式的 User 2018/6/30 17:02:00

无下划线, 字体颜色: 自动设置

页 64: [945] 带格式的 User 2018/6/30 17:02:00

无下划线, 字体颜色: 自动设置

页 64: [946] 带格式的 User 2018/6/30 17:02:00

无下划线, 字体颜色: 自动设置

页 64: [947] 带格式的 User 2018/6/30 17:02:00

无下划线, 字体颜色: 自动设置

页 64: [948] 带格式的 User 2018/6/30 17:02:00

无下划线, 字体颜色: 自动设置

页 64: [949] 带格式的 User 2018/6/30 17:15:00

定义网格后不调整右缩进, 不对齐到网格

页 64: [950] 带格式的 User 2018/6/30 17:02:00

无下划线, 字体颜色: 自动设置

页 64: [951] 带格式的 User 2018/6/30 17:02:00

无下划线, 字体颜色: 自动设置

页 64: [952] 带格式的 User 2018/6/30 17:02:00

无下划线, 字体颜色: 自动设置

页 64: [953] 带格式的 User 2018/6/30 17:02:00

无下划线, 字体颜色: 自动设置

页 64: [954] 带格式的 User 2018/6/30 17:02:00

无下划线, 字体颜色: 自动设置

页 64: [955] 带格式的 User 2018/6/30 17:02:00

无下划线, 字体颜色: 自动设置

页 64: [956] 带格式的 User 2018/6/30 17:02:00

无下划线, 字体颜色: 自动设置

页 64: [957] 带格式的 User 2018/6/30 17:15:00

定义网格后不调整右缩进, 不对齐到网格

页 64: [958] 带格式的 User 2018/6/30 17:02:00

无下划线, 字体颜色: 自动设置

页 64: [959] 带格式的 User 2018/6/30 17:02:00

无下划线, 字体颜色: 自动设置

页 64: [960] 带格式的 User 2018/6/30 17:02:00

无下划线, 字体颜色: 自动设置

页 64: [961] 带格式的 User 2018/6/30 17:02:00

无下划线, 字体颜色: 自动设置

页 64: [962] 带格式的 User 2018/6/30 17:02:00

无下划线, 字体颜色: 自动设置

页 64: [963] 带格式的 User 2018/6/30 17:02:00

无下划线, 字体颜色: 自动设置

页 64: [964] 带格式的 User 2018/6/30 17:02:00

无下划线, 字体颜色: 自动设置

页 64: [965] 带格式的 User 2018/6/30 17:15:00

定义网格后不调整右缩进, 不对齐到网格

页 64: [966] 带格式的 User 2018/6/30 17:02:00

无下划线, 字体颜色: 自动设置

页 64: [967] 带格式的 User 2018/6/30 17:02:00

无下划线, 字体颜色: 自动设置

页 64: [968] 带格式的 User 2018/6/30 17:02:00

无下划线, 字体颜色: 自动设置

页 64: [969] 带格式的 User 2018/6/30 17:02:00

无下划线, 字体颜色: 自动设置

页 64: [970] 带格式的 User 2018/6/30 17:02:00

无下划线, 字体颜色: 自动设置

页 64: [971] 带格式的 User 2018/6/30 17:02:00

无下划线, 字体颜色: 自动设置

页 64: [972] 带格式的 User 2018/6/30 17:02:00

无下划线, 字体颜色: 自动设置

页 64: [973] 带格式的 User 2018/6/30 17:15:00

定义网格后不调整右缩进, 不对齐到网格

页 64: [974] 带格式的 User 2018/6/30 17:02:00

无下划线, 字体颜色: 自动设置

页 64: [975] 带格式的 User 2018/6/30 17:02:00

无下划线, 字体颜色: 自动设置

页 64: [976] 带格式的 User 2018/6/30 17:02:00

无下划线, 字体颜色: 自动设置

页 64: [977] 带格式的 User 2018/6/30 17:02:00

无下划线, 字体颜色: 自动设置

页 64: [978] 带格式的 User 2018/6/30 17:02:00

无下划线, 字体颜色: 自动设置

页 64: [979] 带格式的 User 2018/6/30 17:02:00

无下划线, 字体颜色: 自动设置

页 64: [980] 带格式的 User 2018/6/30 17:02:00

无下划线, 字体颜色: 自动设置

页 64: [981] 带格式的 User 2018/6/30 17:15:00

定义网格后不调整右缩进, 不对齐到网格

页 64: [982] 带格式的 User 2018/6/30 17:02:00

无下划线, 字体颜色: 自动设置

页 64: [983] 带格式的 User 2018/6/30 17:02:00

无下划线, 字体颜色: 自动设置

页 64: [984] 带格式的 User 2018/6/30 17:02:00

无下划线, 字体颜色: 自动设置

页 64: [985] 带格式的 User 2018/6/30 17:02:00

无下划线, 字体颜色: 自动设置

页 64: [986] 带格式的 User 2018/6/30 17:02:00

无下划线, 字体颜色: 自动设置

页 64: [987] 带格式的 User 2018/6/30 17:02:00

无下划线, 字体颜色: 自动设置

页 64: [988] 带格式的 User 2018/6/30 17:02:00

无下划线, 字体颜色: 自动设置

页 64: [989] 带格式的 User 2018/6/30 17:15:00

定义网格后不调整右缩进, 不对齐到网格

页 64: [990] 带格式的 User 2018/6/30 17:02:00

无下划线, 字体颜色: 自动设置

页 64: [991] 带格式的 User 2018/6/30 17:02:00

无下划线, 字体颜色: 自动设置

页 64: [992] 带格式的 User 2018/6/30 17:02:00

无下划线, 字体颜色: 自动设置

页 64: [993] 带格式的 User 2018/6/30 17:02:00

无下划线, 字体颜色: 自动设置

页 64: [994] 带格式的 User 2018/6/30 17:02:00

无下划线, 字体颜色: 自动设置

页 64: [995] 带格式的 User 2018/6/30 17:02:00

无下划线, 字体颜色: 自动设置

页 64: [996] 带格式的 User 2018/6/30 17:02:00

无下划线, 字体颜色: 自动设置

页 64: [997] 带格式的 User 2018/6/30 17:15:00

定义网格后不调整右缩进, 不对齐到网格

页 64: [998] 带格式的 User 2018/6/30 17:02:00

无下划线, 字体颜色: 自动设置

页 64: [999] 带格式的 User 2018/6/30 17:02:00

无下划线, 字体颜色: 自动设置

页 64: [1000] 带格式的 User 2018/6/30 17:02:00

无下划线, 字体颜色: 自动设置

页 64: [1001] 带格式的 User 2018/6/30 17:02:00

无下划线, 字体颜色: 自动设置

页 64: [1002] 带格式的 User 2018/6/30 17:02:00

无下划线, 字体颜色: 自动设置

页 64: [1003] 带格式的 User 2018/6/30 17:02:00

无下划线, 字体颜色: 自动设置

页 64: [1004] 带格式的 User 2018/6/30 17:02:00

无下划线, 字体颜色: 自动设置

页 64: [1005] 带格式的 User 2018/6/30 17:15:00

定义网格后不调整右缩进, 不对齐到网格

页 64: [1006] 带格式的 User 2018/6/30 17:02:00

无下划线, 字体颜色: 自动设置

页 64: [1007] 带格式的 User 2018/6/30 17:02:00

无下划线, 字体颜色: 自动设置

页 64: [1008] 带格式的 User 2018/6/30 17:02:00

无下划线, 字体颜色: 自动设置

页 64: [1009] 带格式的 User 2018/6/30 17:02:00

无下划线, 字体颜色: 自动设置

页 64: [1010] 带格式的 User 2018/6/30 17:02:00

无下划线, 字体颜色: 自动设置

页 64: [1011] 带格式的 User 2018/6/30 17:02:00

无下划线, 字体颜色: 自动设置

页 65: [1012] 带格式的 User 2018/6/30 17:02:00

无下划线, 字体颜色: 自动设置

页 65: [1013] 带格式的 User 2018/6/30 17:02:00

无下划线, 字体颜色: 自动设置

页 65: [1014] 带格式的 User 2018/6/30 17:15:00

定义网格后不调整右缩进, 不对齐到网格

页 65: [1015] 带格式的 User 2018/6/30 17:02:00

无下划线, 字体颜色: 自动设置

页 65: [1015] 带格式的 User 2018/6/30 17:02:00

无下划线, 字体颜色: 自动设置

页 65: [1016] 带格式的 User 2018/6/30 17:02:00

无下划线, 字体颜色: 自动设置

页 65: [1016] 带格式的 User 2018/6/30 17:02:00

无下划线, 字体颜色: 自动设置

页 65: [1017] 带格式的 User 2018/6/30 17:02:00

无下划线, 字体颜色: 自动设置

页 65: [1017] 带格式的 User 2018/6/30 17:02:00

无下划线, 字体颜色: 自动设置

页 65: [1018] 带格式的 User 2018/6/30 17:02:00

无下划线, 字体颜色: 自动设置

页 65: [1018] 带格式的 User 2018/6/30 17:02:00

无下划线, 字体颜色: 自动设置

页 65: [1019] 带格式的 User 2018/6/30 17:02:00

无下划线, 字体颜色: 自动设置

页 65: [1019] 带格式的 User 2018/6/30 17:02:00

无下划线, 字体颜色: 自动设置

页 65: [1020] 带格式的 User 2018/6/30 17:02:00

无下划线, 字体颜色: 自动设置

页 65: [1020] 带格式的 User 2018/6/30 17:02:00

无下划线, 字体颜色: 自动设置

页 65: [1021] 带格式的 User 2018/6/30 17:02:00

无下划线, 字体颜色: 自动设置

页 65: [1021] 带格式的 User 2018/6/30 17:02:00

无下划线, 字体颜色: 自动设置

页 65: [1022] 带格式的 User 2018/6/30 17:02:00

无下划线, 字体颜色: 自动设置

页 65: [1022] 带格式的 User 2018/6/30 17:02:00

无下划线, 字体颜色: 自动设置

页 65: [1023] 带格式的 User 2018/6/30 17:02:00

无下划线, 字体颜色: 自动设置

页 65: [1023] 带格式的 User 2018/6/30 17:02:00

无下划线, 字体颜色: 自动设置

页 65: [1024] 带格式的 User 2018/6/30 17:02:00

无下划线, 字体颜色: 自动设置

页 65: [1024] 带格式的 User 2018/6/30 17:02:00

无下划线, 字体颜色: 自动设置

页 65: [1025] 带格式的 User 2018/6/30 17:02:00

无下划线, 字体颜色: 自动设置

页 65: [1025] 带格式的 User 2018/6/30 17:02:00

无下划线, 字体颜色: 自动设置

页 65: [1026] 带格式的 User 2018/6/30 17:02:00

无下划线, 字体颜色: 自动设置

页 65: [1026] 带格式的 User 2018/6/30 17:02:00

无下划线, 字体颜色: 自动设置

页 65: [1027] 带格式的 User 2018/6/30 17:02:00

无下划线, 字体颜色: 自动设置

页 65: [1027] 带格式的 User 2018/6/30 17:02:00

无下划线, 字体颜色: 自动设置

页 65: [1028] 带格式的 User 2018/6/30 17:02:00

无下划线, 字体颜色: 自动设置

页 65: [1028] 带格式的 User 2018/6/30 17:02:00

无下划线, 字体颜色: 自动设置

页 65: [1029] 带格式的 User 2018/6/30 17:02:00

无下划线, 字体颜色: 自动设置

页 65: [1029] 带格式的 User 2018/6/30 17:02:00

无下划线, 字体颜色: 自动设置

页 65: [1030] 带格式的 User 2018/6/30 17:02:00

无下划线, 字体颜色: 自动设置

页 65: [1030] 带格式的 User 2018/6/30 17:02:00

无下划线, 字体颜色: 自动设置

页 65: [1031] 带格式的 User 2018/6/30 17:02:00

无下划线, 字体颜色: 自动设置

页 65: [1032] 带格式的 User 2018/6/30 17:15:00

定义网格后不调整右缩进, 不对齐到网格

页 65: [1033] 带格式的 User 2018/6/30 17:02:00

无下划线, 字体颜色: 自动设置

页 65: [1033] 带格式的 User 2018/6/30 17:02:00

无下划线, 字体颜色: 自动设置

页 65: [1034] 带格式的 User 2018/6/30 17:02:00

无下划线, 字体颜色: 自动设置

页 65: [1034] 带格式的 User 2018/6/30 17:02:00

无下划线, 字体颜色: 自动设置

页 65: [1035] 带格式的 User 2018/6/30 17:02:00

无下划线, 字体颜色: 自动设置

页 65: [1035] 带格式的 User 2018/6/30 17:02:00

无下划线, 字体颜色: 自动设置

页 65: [1036] 带格式的 User 2018/6/30 17:02:00

无下划线, 字体颜色: 自动设置

页 65: [1036] 带格式的 User 2018/6/30 17:02:00

无下划线, 字体颜色: 自动设置

页 65: [1037] 带格式的 User 2018/6/30 17:02:00

无下划线, 字体颜色: 自动设置

页 65: [1037] 带格式的 User 2018/6/30 17:02:00

无下划线, 字体颜色: 自动设置

页 65: [1038] 带格式的 User 2018/6/30 17:02:00

无下划线, 字体颜色: 自动设置

页 65: [1038] 带格式的 User 2018/6/30 17:02:00

无下划线, 字体颜色: 自动设置

页 65: [1039] 带格式的 User 2018/6/30 17:02:00

无下划线, 字体颜色: 自动设置

页 65: [1039] 带格式的 User 2018/6/30 17:02:00

无下划线, 字体颜色: 自动设置

页 65: [1040] 带格式的 User 2018/6/30 17:02:00

无下划线, 字体颜色: 自动设置

页 65: [1040] 带格式的 User 2018/6/30 17:02:00

无下划线, 字体颜色: 自动设置

页 65: [1041] 带格式的 User 2018/6/30 17:02:00

无下划线, 字体颜色: 自动设置

页 65: [1042] 带格式的 User 2018/6/30 17:15:00

定义网格后不调整右缩进, 不对齐到网格

页 65: [1043] 带格式的 User 2018/6/30 17:02:00

无下划线, 字体颜色: 自动设置

页 65: [1043] 带格式的 User 2018/6/30 17:02:00

无下划线, 字体颜色: 自动设置

页 65: [1044] 带格式的 User 2018/6/30 17:02:00

无下划线, 字体颜色: 自动设置

页 65: [1044] 带格式的 User 2018/6/30 17:02:00

无下划线, 字体颜色: 自动设置

页 65: [1045] 带格式的 User 2018/6/30 17:02:00

无下划线, 字体颜色: 自动设置

页 65: [1045] 带格式的 User 2018/6/30 17:02:00

无下划线, 字体颜色: 自动设置

页 65: [1046] 带格式的 User 2018/6/30 17:02:00

无下划线, 字体颜色: 自动设置

页 65: [1046] 带格式的 User 2018/6/30 17:02:00

无下划线, 字体颜色: 自动设置

页 65: [1047] 带格式的 User 2018/6/30 17:02:00

无下划线, 字体颜色: 自动设置

页 65: [1047] 带格式的 User 2018/6/30 17:02:00

无下划线, 字体颜色: 自动设置

页 65: [1048] 带格式的 User 2018/6/30 17:02:00

无下划线, 字体颜色: 自动设置

页 65: [1048] 带格式的 User 2018/6/30 17:02:00

无下划线, 字体颜色: 自动设置

页 65: [1049] 带格式的 User 2018/6/30 17:02:00

无下划线, 字体颜色: 自动设置

页 65: [1049] 带格式的 User 2018/6/30 17:02:00

无下划线, 字体颜色: 自动设置

页 65: [1050] 带格式的 User 2018/6/30 17:02:00

无下划线, 字体颜色: 自动设置

页 65: [1050] 带格式的 User 2018/6/30 17:02:00

无下划线, 字体颜色: 自动设置

页 65: [1051] 带格式的 User 2018/6/30 17:02:00

无下划线, 字体颜色: 自动设置

页 65: [1052] 带格式的 User 2018/6/30 17:02:00

无下划线, 字体颜色: 自动设置

页 65: [1053] 带格式的 User 2018/6/30 17:15:00

定义网格后不调整右缩进, 不对齐到网格

页 65: [1054] 带格式的 User 2018/6/30 17:02:00

无下划线, 字体颜色: 自动设置

页 65: [1054] 带格式的 User 2018/6/30 17:02:00

无下划线, 字体颜色: 自动设置

页 65: [1055] 带格式的 User 2018/6/30 17:02:00

无下划线, 字体颜色: 自动设置

页 65: [1055] 带格式的 User 2018/6/30 17:02:00

无下划线, 字体颜色: 自动设置

页 65: [1056] 带格式的 User 2018/6/30 17:02:00

无下划线, 字体颜色: 自动设置

页 65: [1057] 带格式的 User 2018/6/30 17:15:00

定义网格后不调整右缩进, 不对齐到网格

页 65: [1058] 带格式的 User 2018/6/30 17:02:00

无下划线, 字体颜色: 自动设置

页 65: [1058] 带格式的 User 2018/6/30 17:02:00

无下划线, 字体颜色: 自动设置

页 65: [1059] 带格式的 User 2018/6/30 17:02:00

无下划线, 字体颜色: 自动设置

页 65: [1059] 带格式的 User 2018/6/30 17:02:00

无下划线, 字体颜色: 自动设置

页 65: [1060] 带格式的 User 2018/6/30 17:02:00

无下划线, 字体颜色: 自动设置

页 65: [1060] 带格式的 User 2018/6/30 17:02:00

无下划线, 字体颜色: 自动设置

页 65: [1061] 带格式的 User 2018/6/30 17:02:00

无下划线, 字体颜色: 自动设置

页 65: [1061] 带格式的 User 2018/6/30 17:02:00

无下划线, 字体颜色: 自动设置

页 65: [1062] 带格式的 User 2018/6/30 17:02:00

无下划线, 字体颜色: 自动设置

页 65: [1062] 带格式的 User 2018/6/30 17:02:00

无下划线, 字体颜色: 自动设置

页 65: [1063] 带格式的 User 2018/6/30 17:02:00

无下划线, 字体颜色: 自动设置

页 65: [1063] 带格式的 User 2018/6/30 17:02:00

无下划线, 字体颜色: 自动设置

页 65: [1064] 带格式的 User 2018/6/30 17:02:00

无下划线, 字体颜色: 自动设置

页 65: [1064] 带格式的 User 2018/6/30 17:02:00

无下划线, 字体颜色: 自动设置

页 65: [1065] 带格式的 User 2018/6/30 17:02:00

无下划线, 字体颜色: 自动设置

页 65: [1065] 带格式的 User 2018/6/30 17:02:00

无下划线, 字体颜色: 自动设置

页 65: [1066] 带格式的 User 2018/6/30 17:02:00

无下划线, 字体颜色: 自动设置

页 65: [1066] 带格式的 User 2018/6/30 17:02:00

无下划线, 字体颜色: 自动设置

页 65: [1067] 带格式的 User 2018/6/30 17:02:00

无下划线, 字体颜色: 自动设置

页 65: [1067] 带格式的 User 2018/6/30 17:02:00

无下划线, 字体颜色: 自动设置

页 65: [1068] 带格式的 User 2018/6/30 17:02:00

无下划线, 字体颜色: 自动设置

页 65: [1068] 带格式的 User 2018/6/30 17:02:00

无下划线, 字体颜色: 自动设置

页 65: [1069] 带格式的 User 2018/6/30 17:02:00

无下划线, 字体颜色: 自动设置

页 65: [1069] 带格式的 User 2018/6/30 17:02:00

无下划线, 字体颜色: 自动设置

页 65: [1070] 带格式的 User 2018/6/30 17:02:00

无下划线, 字体颜色: 自动设置

页 65: [1070] 带格式的 User 2018/6/30 17:02:00

无下划线, 字体颜色: 自动设置

页 65: [1071] 带格式的 User 2018/6/30 17:02:00

无下划线, 字体颜色: 自动设置

页 65: [1071] 带格式的 User 2018/6/30 17:02:00

无下划线, 字体颜色: 自动设置

页 65: [1072] 带格式的 User 2018/6/30 17:02:00

无下划线, 字体颜色: 自动设置

页 65: [1072] 带格式的 User 2018/6/30 17:02:00

无下划线, 字体颜色: 自动设置

页 65: [1073] 带格式的 User 2018/6/30 17:02:00

无下划线, 字体颜色: 自动设置

页 65: [1073] 带格式的 User 2018/6/30 17:02:00

无下划线, 字体颜色: 自动设置

页 65: [1074] 带格式的 User 2018/6/30 17:02:00

无下划线, 字体颜色: 自动设置

页 65: [1074] 带格式的 User 2018/6/30 17:02:00

无下划线, 字体颜色: 自动设置

页 65: [1075] 带格式的 User 2018/6/30 17:02:00

无下划线, 字体颜色: 自动设置

页 65: [1075] 带格式的 User 2018/6/30 17:02:00

无下划线, 字体颜色: 自动设置

页 65: [1076] 带格式的 User 2018/6/30 17:02:00

无下划线, 字体颜色: 自动设置

页 65: [1076] 带格式的 User 2018/6/30 17:02:00

无下划线, 字体颜色: 自动设置

页 65: [1077] 带格式的 User 2018/6/30 17:02:00

无下划线, 字体颜色: 自动设置

页 65: [1077] 带格式的 User 2018/6/30 17:02:00

无下划线, 字体颜色: 自动设置

页 65: [1078] 带格式的 User 2018/6/30 17:02:00

无下划线, 字体颜色: 自动设置

页 65: [1078] 带格式的 User 2018/6/30 17:02:00

无下划线, 字体颜色: 自动设置

页 65: [1079] 带格式的 User 2018/6/30 17:02:00

无下划线, 字体颜色: 自动设置

页 65: [1079] 带格式的 User 2018/6/30 17:02:00

无下划线, 字体颜色: 自动设置

页 65: [1080] 带格式的 User 2018/6/30 17:02:00

无下划线, 字体颜色: 自动设置

页 65: [1080] 带格式的 User 2018/6/30 17:02:00

无下划线, 字体颜色: 自动设置

页 65: [1081] 带格式的 User 2018/6/30 17:02:00

无下划线, 字体颜色: 自动设置

页 65: [1081] 带格式的 User 2018/6/30 17:02:00

无下划线, 字体颜色: 自动设置

页 65: [1082] 带格式的 User 2018/6/30 17:02:00

无下划线, 字体颜色: 自动设置

页 65: [1082] 带格式的 User 2018/6/30 17:02:00

无下划线, 字体颜色: 自动设置

页 65: [1083] 带格式的 User 2018/6/30 17:02:00

无下划线, 字体颜色: 自动设置

页 65: [1083] 带格式的 User 2018/6/30 17:02:00

无下划线, 字体颜色: 自动设置

页 65: [1084] 带格式的 User 2018/6/30 17:02:00

无下划线, 字体颜色: 自动设置

页 65: [1084] 带格式的 User 2018/6/30 17:02:00

无下划线, 字体颜色: 自动设置

页 65: [1085] 带格式的 User 2018/6/30 17:02:00

无下划线, 字体颜色: 自动设置

页 65: [1085] 带格式的 User 2018/6/30 17:02:00

无下划线, 字体颜色: 自动设置

页 65: [1086] 带格式的 User 2018/6/30 17:02:00

无下划线, 字体颜色: 自动设置

页 65: [1086] 带格式的 User 2018/6/30 17:02:00

无下划线, 字体颜色: 自动设置

页 65: [1087] 带格式的 User 2018/6/30 17:02:00

无下划线, 字体颜色: 自动设置

页 65: [1087] 带格式的 User 2018/6/30 17:02:00

无下划线, 字体颜色: 自动设置

页 65: [1088] 带格式的 User 2018/6/30 17:02:00

无下划线, 字体颜色: 自动设置

页 65: [1088] 带格式的 User 2018/6/30 17:02:00

无下划线, 字体颜色: 自动设置

页 65: [1089] 带格式的 User 2018/6/30 17:02:00

无下划线, 字体颜色: 自动设置

页 65: [1089] 带格式的 User 2018/6/30 17:02:00

无下划线, 字体颜色: 自动设置